Determination of the ligand pharmacophore required for secondary conformation activation of the human β_1-adrenoceptor

Emanuel Pinto de Sousa, MSc

University of Nottingham
UK | CHINA | MALAYSIA

MONASH University

Thesis submitted to the University of Nottingham and Monash University for the degree of Doctor of Philosophy

December 2019

ABSTRACT

The β_1-adrenergic receptor exists in at least two different agonist conformations: a primary conformation where endogenous catecholamines and β-blockers bind, and where agonist responses are blocked by low concentrations of antagonists and a secondary conformation, for which the precise nature is unknown, through which responses are more resistant to blockade by conventional primary conformation antagonists. Conventional agonists such as isoprenaline and cimaterol stimulate a response mainly through the primary conformation, while others such as alprenolol and oxprenolol can mediate a response through both conformations of the β_1-AR, though the response mediated through the secondary conformation requires a higher concentration of ligand. Other ligands, such as CGP12177, behave as non-conventional agonist and bind with high affinity to the primary conformation (blocking the response of conventional agonist) but then, at much higher concentrations, stimulate a response through the secondary conformation. Only ligands with higher affinity for the primary conformation than for the secondary have been identified so far.

This project aims to identify the molecular features required to bind and stimulate a response at the secondary conformation of the β_1-AR. This conformation has been studied so far with probes such as CGP12177 which bind the primary conformation at lower concentrations than the secondary conformation. The identification of a ligand with higher (if possible) or similar affinity for the secondary conformation would allow the better understanding of this conformation.

In this thesis, a set of alprenolol and oxprenolol *N*-alkyl analogues and alprenolol analogues bearing substituents in the aromatic ring were synthesised and pharmacologically characterised both through competitive radioligand binding assays and CRE-SPAP functional assays in CHO-β_1 and CHO-β_2 cells. Within these sets, *bis* alprenolol and *bis* oxprenolol ligands were identified as compounds able to bind to both conformations with similar affinities. The study of the individual enantiomers and meso compounds of this ligands and further modifications suggest the importance of the second aromatic core for the increase in affinity for the secondary conformation.

A potential photoreactive covalent antagonist was also synthesised to target the primary conformation and allow the better study of the secondary conformation of the β_1-AR.

Contents

Nomenclature

GPCRs	G protein-coupled receptors
cryo-EM	Cryogenic electron microscopy
NMR	Nuclear magnetic resonance
TM	Transmembrane domains
ECLs	Extracellular loops
ICLs	Intracellular loops
ARs	Adrenergic receptors
GTP	Guanosine triphosphate
ATP	Adenosine triphosphate
cAMP	Cyclic adenosine monophosphate
AC	Adenylyl cyclase
PKA	Protein kinase A
AKAP	PKA-A-kinase anchoring proteins
Epac	Exchange protein activated directly by cAMP
CNG	Cyclic nucleotide-gated
MAPK	Mitogen-activated protein kinase
PDE	Phosphodiesterases
EGFR	Epidermal growth factor receptor
ETC	Extended ternary complex
CTC	Cubic ternary complex
Boc	*tert*-butyloxycarbonyl
Bn	Benzyl
DCM	Dichloromethane
DMF	*N,N* - Dimethylformamide
DMSO	Dimethyl sulphoxide
eq	molar equivalents
ES	electrospray
Et_2O	Diethyl ether
EtOAc	Ethyl acetate

EtOH	Ethanol
FCC	Flash column chromatography

Acknowledgements

I would like to thank my supervisors Dr. Shailesh Mistry and Dr. Jillian Baker for the opportunity, the guidance and the support along my PhD. I would also like to thank Dr. Peter Scammells for welcoming me at Monash University.

The chemical synthesis work would not have been the same without everyone from C25 lab and the daily chat during column purifications. A special mention goes to Dr. Sarah Mistry and Dr. Sarah Cully for the guidance in the lab. I would also like to thank everyone from C floor for offering their knowledge and experience, especially Dr. Barry Kellam and Dr. Michael Stocks for the value insights during the meetings. This work would not have been possible without the daily technical assistance provided by the team of technicians at C floor, with a special thanks to Lee Hibbett which was always promptly available to solve any problem.

The *in vitro* pharmacological assays carried out in this project were particularly new to me so I would like to thank Richard Proudman and all the team of technicians at the cell signaling group for their time and valuable help along the way.

During my time at Monash University I was warmly welcomed and for that I would like to thank my colleagues at Monash, particularly Raymond Lam, Tim Fyfe, Dr. and Dr. Manuela Jorg for the valuable insights in the lab and during the weekly GPCR group meetings.

Finally, I would like to thank to my parents and my girlfriend, Vanda, for the daily encouragement and support provided, even though from far away, this would not have been possible without you.

Chapter 1

Introduction

1.1 G Protein-Coupled Receptors: History and structure

G protein-coupled receptors (GPCRs) are the largest family of membrane-bound receptors of the human genome and are encoded by more than 800 genes. More than 25% of marketed drugs target GPCRs which cover a wide range of therapeutic indications from diseases ranging from cancer to asthma or migraines.[1] In recent years, GPCR-related drug discovery has improved and more GPCR-targeting drugs have been approved. [2] New techniques available to obtain new high-resolution x-ray crystal structures, NMR and cryogenic electron microscopy (cryo-EM) studies have facilitated to this improvement that has allowed a better understanding of ligand-protein interactions, allosteric modulation and biased signaling.[2, 3, 4]

All GPCRs have a similar structure that consists in a single polypeptide chain in the cell membrane with an amino and carboxy termini exposed to extracellular environment and cytosol, respectively. GPCRs are also known as 7-transmembrane domains receptors (7-TM) due to their conserved structure of seven transmembrane α-helical domains joined by three extracellular loops (ECLs) and three intracellular loops (ICLs). ICL2 and ICL3 are thought to have an important role in the selectivity, binding and activation of G proteins.[5] Though all GPCRs are similar in overall structure, they are classified into three main families: the rhodopsin-like family A, which is the largest and most-studied, characterised by highly conserved amino acids in the 7TM bundle and a disulfide bridge between the ECL1 and ECL2; the secretin-like receptor family B that are characterised by a long NH_2 terminus which is implicated in ligand binding; and the metabotropic glutamate receptor-like family C, characterised by long NH_2 and COOH-terminal tails and a disulfide bridge between ECL1 and ECL2. The adrenergic receptors (ARs) belong to the rhodopsin-like family A (Fig. 1.1).[6, 2, 1]

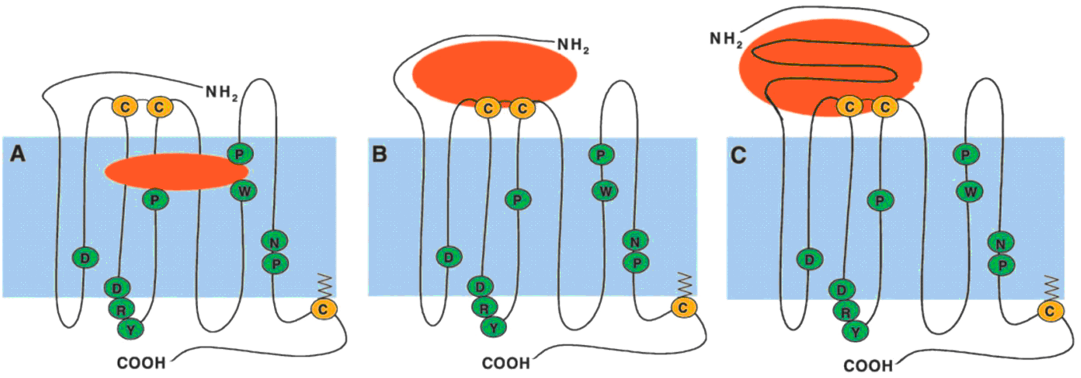

FIGURE 1.1: Classification of the human GPCRs. Historically these were classified into three families: A (Rhodopsin-like family), B (secretin-like family) and C (glutamate receptor-like family);[1]

Adrenergic receptors were discovered and classified in 1948, by Raymond Ahlquist, 73 years after receptor theory was proposed for the first time.[6] Ahlquist established the idea that a single mediator could produce both excitatory and inhibitory responses. Before that, in 1897, adrenaline **(1)** was isolated for the first time and in 1933 the "fight-or-flight" theory was formulated by W. B. Cannon which also identified noradrenaline **(2)** as a chemical transmitter (Fig. 1.2).[6] Shortly after the discovery of adrenergic receptors the first β-blocker (a β-adrenergic receptor antagonist), dichloroisoproterenol **(3)**, was synthesised by Eli Lilly Laboratories. Later, Sir James Black found that β-blockers could be useful for the treatment of angina pectoris, and reported a study with propranolol **(4)**.[7]

After the synthesis of dichloroisoproterenol (**3**) and propranolol (**4**) (which belong to the first generation of β-blockers) many other compounds were synthesised (**see section 1.3**).[6] From the discovery of the first β-blocker in 1958 to more recent years, many clinical studies have been conducted in order to find the best β-blocker for the treatment of both heart failure and angina pectoris (Fig 1.3). Even though this field has been extensively studied, it is still unclear as to why not all β-blockers class does not offer a beneficial effect in the treatment of heart failure.

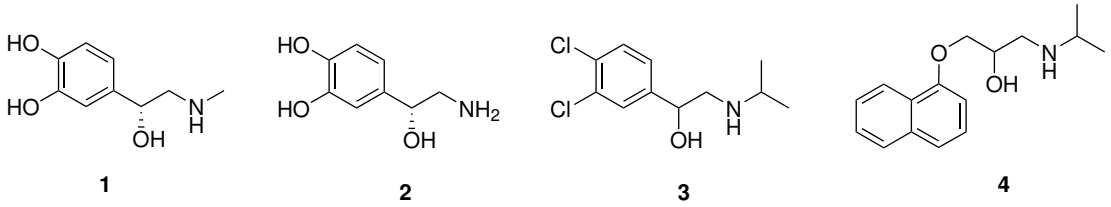

FIGURE 1.2: β-AR endogenous ligands: Adrenaline (**1**), Noradrenaline (**2**); and first generation compounds: Dichloroisoproterenol (**3**), Propranolol (**4**).

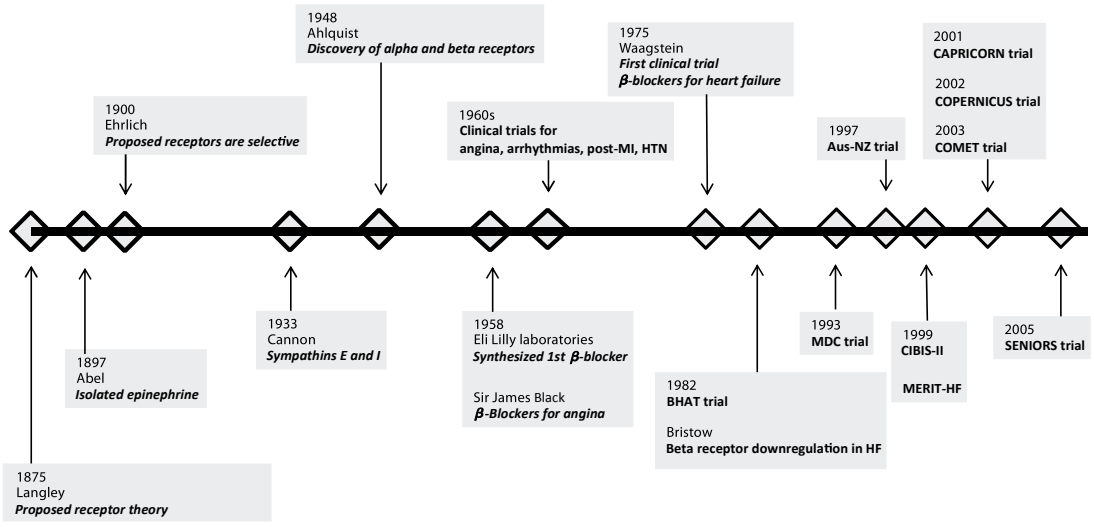

FIGURE 1.3: Timeline of events from the discovery to the application and clinical investigation of β-blockers.[6]

Adrenergic receptors are rhodopsin-like GPCRs and are divided into two types: α and β adrenoceptors. The α-adrenergic receptors are further divided into α_1-AR and α_2-AR. These receptors can cause a different range of effects when activated by agonist binding. The α_1-AR can cause glycogenolysis in the liver and vasoconstriction and relaxation of smooth muscle in the gut, while the α_2-AR mediates synaptic transmission in post- and presynaptic nerve terminals and inhibits lipolysis and insulin release in adipose tissue and the pancreas, respectively.[1, 2]

The β-adrenoceptors can be further divided into β_1, β_2 and β_3 adrenergic receptors. The β_1-AR, once activated by agonist binding, causes an increase in the heart rate, known as chronotropy, and in the force of contraction (positive inotropy). The adult human heart tissue expresses both β_1 and β_2-ARs in a proportion of approximately 4:1 but in the failing heart, the β_1-AR undergoes selective downregulation at mRNA and protein levels, resulting in a shift in β_1:β_2 subtype proportions to approximately 1:1. The extent of this downregulation of β_1-AR is thought to be related with the severity of heart disease but can only be evaluated through heart biopsy. The β_1-AR also acts in the kidneys where it increases blood pressure through the renin-angiontensin-aldosterone system.[6, 8] The β_2-AR is important in the treatment of asthma and other respiratory diseases. Its activation causes vasodilation and opening of the airways. The last cloned β_3-AR is found mainly in adipose tissue where it promotes lipolysis and thermogenesis, particulary in rodents. The endogenous cathecolamines **1** and **2** can bind and activate all the receptors but display a 10-30 fold selectivity towards β_1-AR compared to β_2-AR.[6]

1.2 Signal transduction

1.2.1 Receptor activation and cAMP pathway

The sympathetic and parasympathetic nervous systems tightly regulate cardiac performance. They are able to transmit input to the heart in order to match the cardiac output to meet the body demands. On one hand, activation of the parasympathetic system decreases heart rate through the action of acetylcholine on sinoatrial cells. Conversely, the action of the sympathetic system increases heart rate, through release of the endogenous catecholamines adrenaline (**1**) and noradrenaline (**2**), and increases myocardial contractility.[9] Endogenous catecholamines bind to β-adrenergic receptors present in the cardiomyocytes and activate them. These members of the GPCR family, as described in the last section, are 7TM receptors coupled to an intracellular heterotrimeric G protein (guanine nucleotide-binding regulatory protein) complex ($G_{\alpha\beta\gamma}$). [10]

Upon interaction with an agonist the receptor undergoes distinct conformational changes promoting GDP (guanosine diphosphate) release from G_α. This results in a high-affinity ternary complex with G_α guanine nucleotide-free. Upon binding of GTP (guanosine triphosphate) to G_α, both G_α and $G_{\beta\gamma}$ dissociate from the receptor and cause a complex cascade of events, transferring and amplifying the original signal. The efficacy of an agonist measures its capacity to activate this complex cascade. This activation cycle is terminated when G_α hydrolyses the GTP bound to this subunit back to GDP through its inherent GTPase activity. The deactivated G_α subunit re-associates with $G_{\beta\gamma}$ and with the receptor to form the initial inactive GPCR complex.[8]

The cascade of events and the downstream effect depends upon the type of $G_\alpha$subunit that is coupled to the receptor. There are four types of $G_\alpha$units: $G_{\alpha.s}$, $G_{\alpha.i}$, $G_{\alpha.q}$ and $G_{\alpha.12}$.[9, 11] Even though it was initially believed that the β-adrenoceptor family were only able to couple to $G_{\alpha.S}$ (stimulatory) protein, both β_2 and β_3 adrenoceptors have been found to also couple with $G_{\alpha.i}$ (inhibitory) protein in numerous studies involving cardiac and skeletal muscle.[12, 13] Kompa and Mallen also proposed that the secondary conformation of the β_1-AR could couple to $G_{\alpha.i}$ proteins in rat heart and blood vessels, however this is not seen in the many recombinant cell system used to evaluate signaling through this conformation.[14, 15, 16, 17]

The most studied and well characterized pathway is the $G_{\alpha.s}$-AC-cAMP signaling pathway (Fig 1.4). When $G_{\alpha.s}$-AC-cAMP is activated, $G_{\alpha.s}$ causes activation of adenylyl cyclase that catalyses the conversion of adenosine triphosphate (ATP) to cyclic adenosine monophosphate (cAMP). Each adenylyl cyclase can catalyse several conversions, resulting in multiple cAMP molecules, as well as each $G_{\alpha.s}$ can activate multiple adenylyl

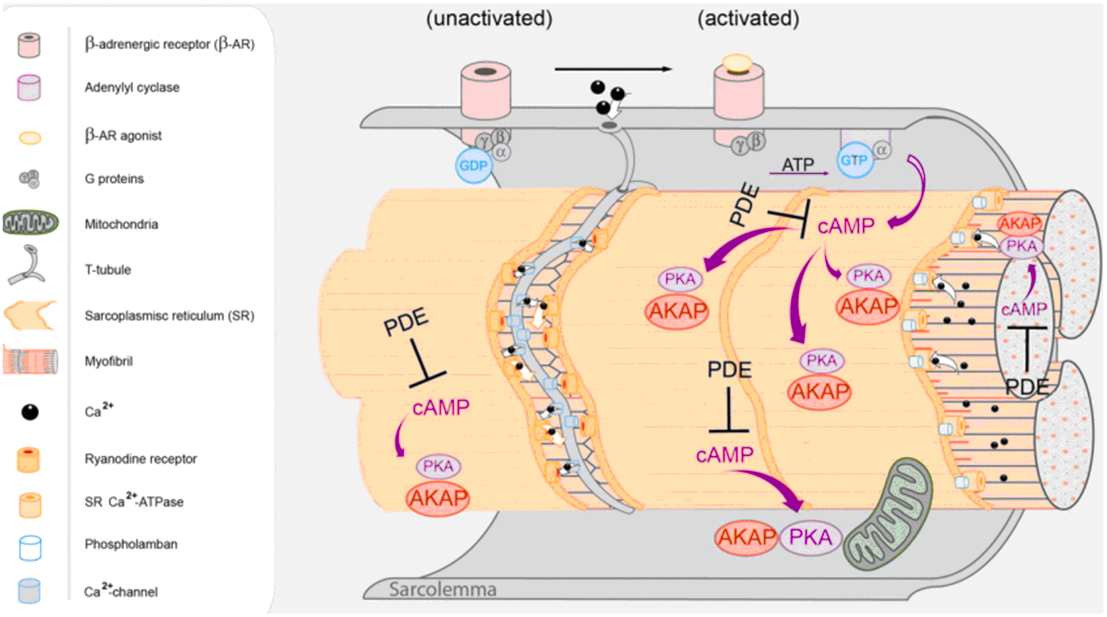

FIGURE 1.4: Activation cascade of a β-adrenergic receptor. Binding of an agonist promotes exchange of guanosine diphosphate (GDP) for guanosine triphosphate (GTP), which leads to the dissociation of the G protein into G_α and $G_{\beta\gamma}$.[9, 5]

cyclases.[9] In turn, the secondary messenger cAMP can activate numerous downstream signaling pathways, including: protein kinase A (PKA), that is distributed in multiple compartments of the cell through PKA-A-kinase anchoring proteins (AKAP) complexes; exchange protein activated directly by cAMP (Epac); and cyclic nucleotide-gated (CNG) cation channels. [11]

The Epac, a guanine nucleotide exchange factor that facilitates the exchange of GDP for GTP of the Ras-like small GTPases Rap1 and Rap2, can also be activated upon binding of cAMP. The GTPase Rap1 is able to alter the mitogen-activated protein kinase (MAPK) signaling pathway.[11] cAMP can also activate CNG cation channels. However, this activation is thought to be limited to specialized cells and it does not appear to influence cardiac output.[11]

cAMP also binds to the regulatory subunits of PKA and activates it. The activation of PKA leads to phosphorylation of several regulatory proteins present in the cardiac muscle cells that lead to positive ionotropy (increase in contractility) and increase lusitropy (increase relaxation). These effects occur within 30 seconds from the exposure of β-AR to agonists through several mechanism including: the phosphorylation of myofilament proteins (eg. cardiac troponin I) resulting in a decrease in Ca^{+2} sensitivity; and the phosphorylation of L-type Ca^{+2} channels increasing the probability of an open state, and therefore an increase in Ca^{+2} influx and cardiac muscle cell contraction. [11, 9, 6] The PKA activation is regulated by phosphodiesterases (PDE) via breakdown of cAMP.

There are different types of PDEs, even though PDE4 appears to be the major cAMP hydrolyser. Interestingly, Vargas *et al*, stated that different PDEs can hydrolise cAMP generated through different agonist conformations of the β_1-adrenoceptor.[11] Whereas, the cAMP generated through the interaction of noradrenaline (**2**) with the primary conformation of the β_1-adrenergic receptor was hydrolysed only by PDE4 in rat ventricles, the cAMP generated through binding of CGP12177 (**16**) to the secondary conformation was hydrolysed by both PDE3 and PDE4. [18, 19]

It is also possible to turn off G protein signal through a process known as desensitization where G protein-coupled receptor kinase (GRK) phosphorylates the receptor and recruitment of β-arrestin. β-arrestin mediates β_1-AR transactivation of EGFR which is cardioprotective under conditions of chronic catecholamine stimulation.[20]

1.2.2 Ligand efficacy and biased agonists

As stated previously not every β-blocker seems to have a beneficial effect in the treatment of heart failure. This seems to be due to the degree of efficacy of each compound. As a few β-blockers are known to activate more than one signaling pathway, all the compounds should be evaluated in different functional paradigms and ligand efficacy should be carefully interpreted. Each ligand has different strength of signaling intrinsic to itself or a receptor complex, commonly known as efficacy, and are classified as full agonists, partial agonists, antagonists or inverse agonists, however the paradigm on how to evaluate ligand efficacy is changing.[21, 22] Galandrin and Bouvier clarified the importance of analysing each signaling pathway individually.[22] Propranolol **(4)**, for example, displays an inverse agonism towards the AC pathway but acts as an agonist towards ERK1/2 (extracellular signal-regulated kinase) pathways in both β_1-AR and β_2-AR.[22] Bucindolol **(14)** was also reported to act as a partial agonist toward AC pathway while it activates MAPK pathway through a G_s-independent pathway.[23] Alprenolol **(6)** and carvedilol (**13**) were also found to mediate β-arrestin-mediated EGFR transactivation using cells expressing β_1-AR and EGFRs.[20] This pathway have shown to be cardioprotective with important therapeutic implications and could represent a new generation of β-blockers. Sun *et al*, proposed that this activity could be associated with receptor dimerisation, while Soriano-Ursua *et al* proposed that it could be mediated through a secondary binding region in the same crevice as the catecholamine binding pocket.[24, 25] It is also known that this activity is not mediated through the secondary agonist conformation of the β_1-AR that will be analysed in detail in the next sections.[20]

Recently, compartmentalised GPCR signalling has also been studied.[26] The β_1-ARs expressed at the Golgi apparatus are able to couple with G protein and mediate an

internal G_s-cAMP signal when stimulated by a cell permeant agonist in HeLa cells.[27] Dobutamine, a cell permeant agonist, and the endogenous ligands adrenaline (**1**) and noradrenaline (**2**), presumably transported across the cell membrane by Oct3 (an organic cation transporter), were able to increase cAMP levels internally. The responses mediated by these ligands were antagonised in a more effective manner by the cell permeant antagonist metoprolol than the impermeant antagonist sotalol.[27]

All this together implies that distinct ligands can promote selectively different receptor conformations that interact with different pathways. This also illustrates the level of complexity seen in β-AR signaling efficacy and selectivity. The efficacy of a ligand should be evaluated individually due to the pluridimensionality of the ligands. A dynamic evaluation of the ligand-receptor interaction could be important to identify other agonist conformations and rationalise the activation of different pathways. Some initial steps have been taken in this direction by Isogai *et al* that evaluated the backbone of the receptor through NMR and were able to correlate the $[^{15}N]$valine shifts in TM5 with the ligand efficacy towards the G protein pathway.[28]

1.2.2.1 GPCR pharmacology principles

GPCRs can exist in an equilibrium between several conformational states, inactive states (R) or activated states (R*). The extended ternary complex model (ETC model described by Samama *et al.*, Fig 1.5 left) describes the complexes and interactions between a ligand (A), a receptor (R) and a G-protein (G). [30] In this model, L represents the isomerisation constant describing the equilibrium between the R and R* receptor states while K_a represents the equilibrium constant between the receptor (R) and ligand-bound receptor (AR) complexes. The cooperativity factor α represents the proportion of the affinity of a

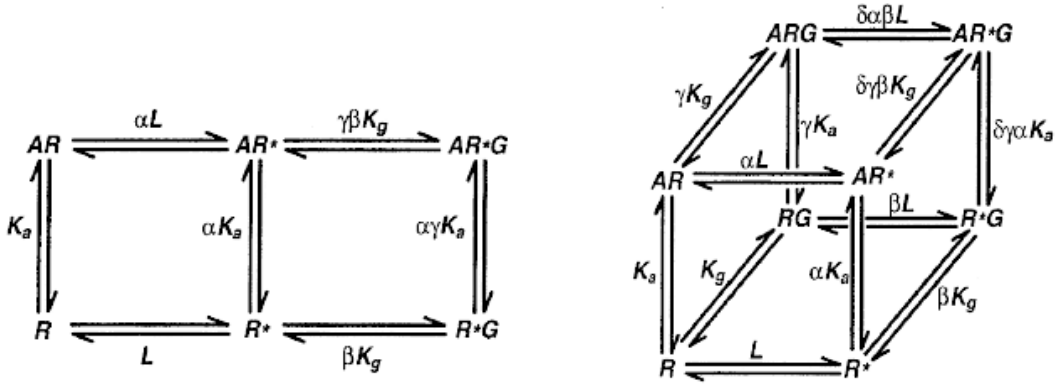

FIGURE 1.5: Left: the extended ternary complex model (ETC model); Right: the cubic ternary complex model (CTC model). Taken from Christopoulos *et al.* [29]

ligand for the active (R*) versus the inactive state (R) of the receptor while γ represents the cooperativity factor for the G-protein.[29] This ETC model accounts for constitutive GPCR activity, the spontaneous coupling of R* receptors to G-proteins in the absence of a ligand (R*G). β-ARs, especially the β_1-AR, exhibit low levels of constitutite activity (R*G), which means that only a small proportion of the receptor is an activated state in the absence of ligand.[5]. A more complex model, the cubic ternary complex model (CTC model, described by Weiss *et al*, Fig 1.5 right) was developed to complete the ETC model termodinamically. [31, 32, 33] The CTC models accounts for the existence of inactive receptor G-protein complexes in the presence (ARG) and absence (RG) of a ligand bound to the receptor. More complex extended models have been created in the past few years to accommodate different receptor active conformations. These receptor models account for biased signalling in which different active receptor conformations may be able to signal via differing signalling cascades or allosteric interactions (quarternary complex model).[29] Both the β_1-AR and β_3-AR are known to exist in at least two agonist conformations, for which different ligands have varying affinity, and will be discussed in further detail in the next section.[34, 35, 36]

1.3 β-Blockers

As described in the previous sections, β-blockers are a heterogeneous group of ligands and even though all show an antagonistic action at β-ARs they differ in their beneficial utility in clinic. β-Blockers are still used in clinic for the treatment of heart failure, ischemia, and arrhythmias, among other diseases. They can differ in receptor selectivity,

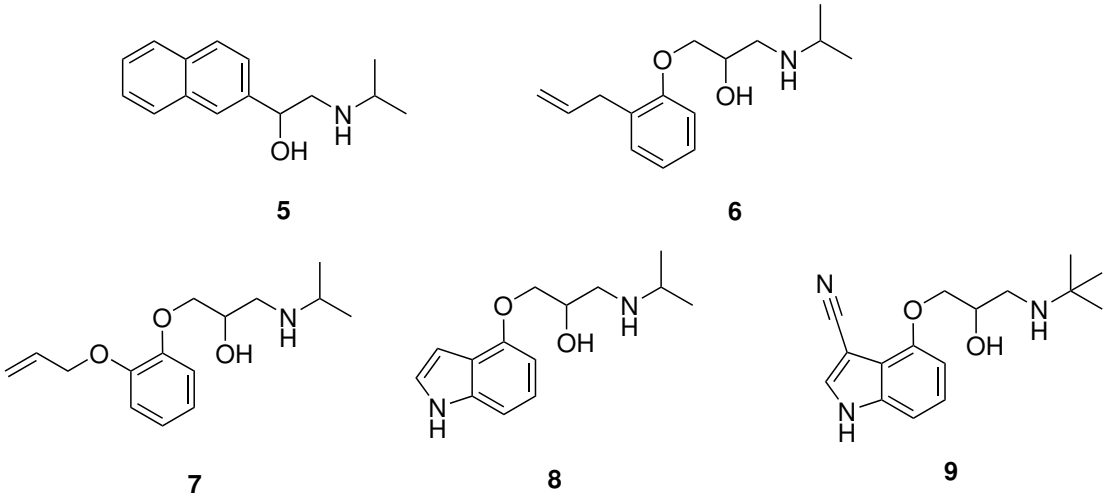

FIGURE 1.6: First generation β-blockers: pronethalol (**5**), alprenolol (**6**), oxprenolol (**7**), pindolol (**8**) and cyanopindolol (**9**)

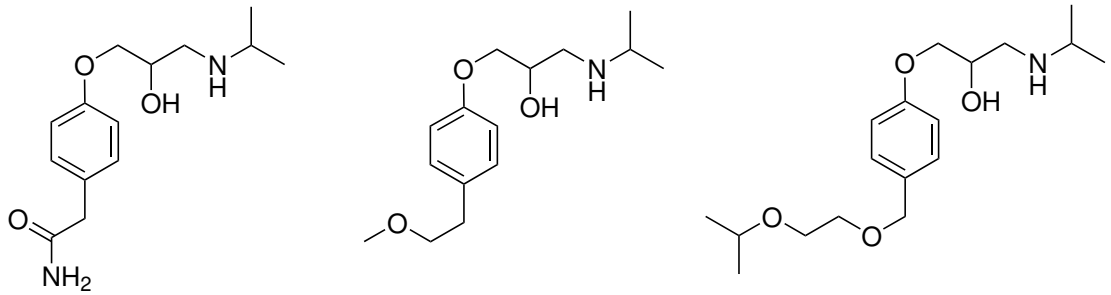

10 **11** **12**

FIGURE 1.7: Second generation β-blockers: atenolol (**10**), metoprolol (**11**) and bisoprolol (**12**).

vasodilating properties, intrinsic sympathomimetic activity and pathways which mediate their responses.[37]

As stated previously, dichloroisoproterenol **(3)**, an isoprenaline analogue, was the first synthetic β-blocker. This compound showed undesirable partial agonism and poor affinity. In order to reduce this partial agonism, the dichlorophenyl group was replaced by a napthyl group, leading to the discovery of pronethalol **(5)**. Even though this compound had reduced partial agonism, it was found to be carcinogenic in rats. Pronethalol was the lead compound in the discovery of propranolol **(4)**. The insertion of a oxymethylene chain connecting the aromatic core to the ethanolamine moiety removed the side effects and increased the affinity. Propranolol (**4**) is still used nowadays, mainly to treat anxiety due to its short action. Nevertheless, propranolol (**4**) is a non-selective antagonist which limits its use for treatment of patients suffering from chronic obstructive airways disorders. A considerable amount of non-selective β-blockers also showed intrinsic sympathomimetic activity such as alprenolol **(6)**, oxprenolol **(7)**, pindolol **(8)** and cyanopindolol **(9)** (Fig 1.6).

In order to decrease the selectivity for the β_2-AR, several ligands were synthesised. Among these second-generation β-blockers, atenolol **(10)**, metoprolol **(11)** and bisoprolol (**12**) have showed some cardioselectivity (β_1-AR selectivity over β_2-AR).(Fig 1.7) Although cardioselectivity is important to avoid several side effects through the blockade of other β-ARs, other non-selective ligands were more beneficial in clinical trials.[37]

Carvedilol (**13**), a third-generation β-blocker, can preserve the activity of nitric oxide synthase, due to its antioxidant properties, increasing the bioavailability of nitric oxide and subsequently increasing vasodilatation.[38]

Nebivolol (**15**) also displays this nitric oxide-mediated action through direct activation of nitric oxide synthase. Both of these compounds reduced mortality in heart failure

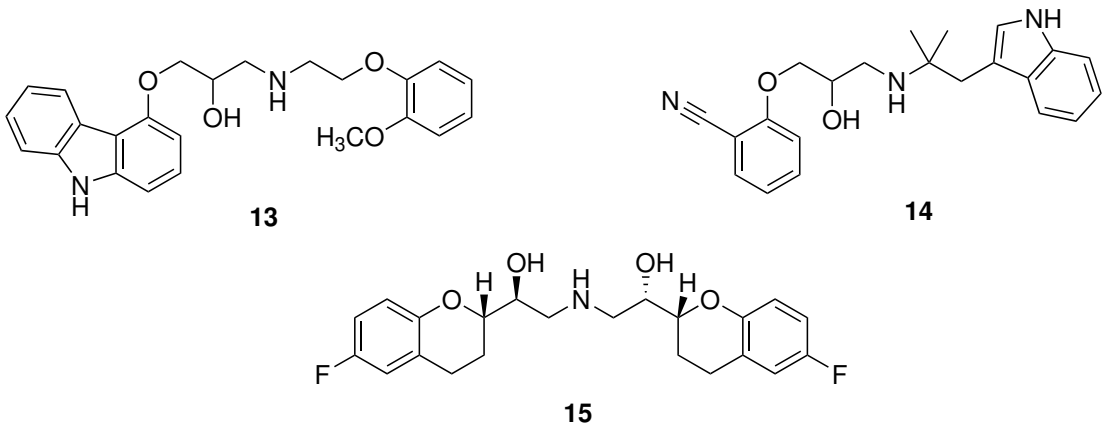

FIGURE 1.8: Third generation β-blockers: carvedilol (**13**), bucindolol (**14**) and nebivolol (**15**).

patients, and have been shown to be superior to metoprolol (**11**) for primary and secondary end points in clinical trials and are approved in many countries for the treatment of heart failure.[42]

1.4 Structural insights on β_1-AR activation

The structural differences of active and inactive structures of GPCRs have been studied by x-ray crystallography. The crystallisation of GPCRs is particulary challenging due to their instability in detergent, the unstructured loop regions and the ease they cycle

Ligand	$LogK_D\beta_1$	$LogK_D\beta_2$	*Selectivity ratio* β_1/β_2
Nebivolol	-9.06	-7.92	13.8
Propranolol	-8.16	-9.08	-8.3
Carvedilol	-8.75	-9.40	-4.5
Metoprolol	-7.26	-6.89	2.3
Atenolol	-6.66	-5.99	4.7
Alprenolol	-7.83	-9.04	-16.2
Oxprenolol	-7.96	-8.97	-10.2
Pronethalol	-6.44	-7.36	-8.3

TABLE 1.1: Binding affinities and selectivity for human β-adrenergic receptors of several β-blockers from a competitive binding assay with the radioligand (-)[^3H] CGP12177 in CHO cells with the human recombinant β_1-AR or β_2-AR. The affinity is represented by the logK_D value in a logarithmic scale while the selectivity represents the number of folds that a ligand in more selective for the β_1-AR. A value with a negative sign represents selectivity towards the β_2-AR. [39, 40, 41]

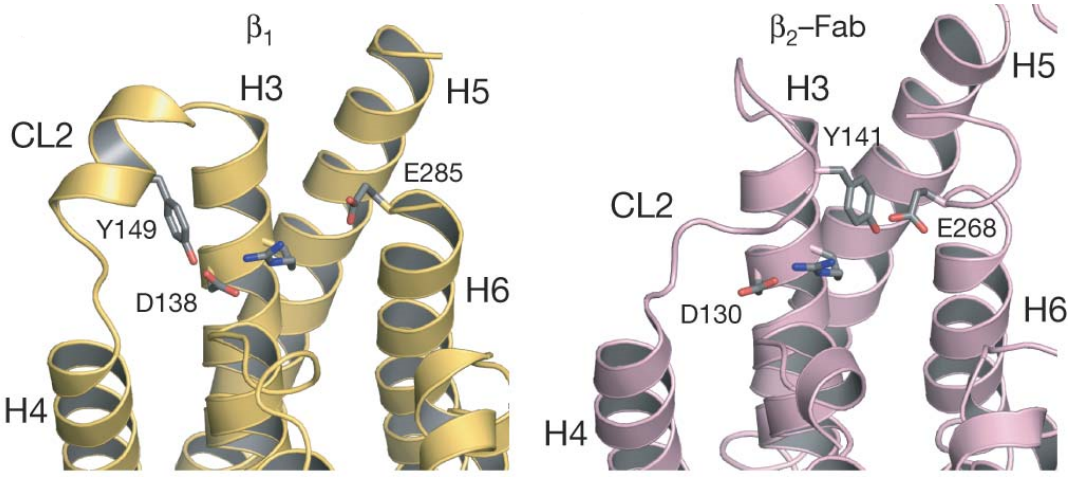

FIGURE 1.9: Comparison of the ICL2 loop region for the turkey β_1-AR and the human β_2-AR in complex with an antibody fragment.[5]

spontaneously from inactive antagonist state to active agonist states. The publication of the crystal structure of the human β_2-AR in complex with an antibody fragment was one of the most important milestones in β-AR drug discovery and contributed extensively to our knowledge regarding the binding pocket of β-AR.[5, 43] In 2008, Warne *et al*, published the first β_1-AR x-ray structure, a modified turkey β_1-AR (β_1-AR.m23), in complex with the antagonist cyanopindolol (**9**).[5] This mutated turkey receptor has higher thermostability over the wild-type and a lower basally activated receptor population. Even though the structure of this receptor is similar to the β_2-AR there is a small difference in the cytoplasmic loop 2 (ICL2) that can be observed in figure 1.9.[5, 44] The β_1-AR seems to have a small α-helix in ICL2 not observed in the β_2-AR that might be involved in the receptor activation as a switch enabling G protein activation.[5] The crystal structure of β_1-AR-m23 has shown two different conformations of the transmembrane α-helix 6 (referred as H6), one where H6 is straight and another one where it is bent. The H6-straight conformation shows a larger distance between H3 and H6 and no ionic lock (a salt bridge between $Arg^{3.50}$ and $Glu^{6.30}$ linking H3 to H6).[45, 46] On the other hand, the H6-bent conformation has an ionic lock between H3 and H6, even though the distance between them is larger than in rhodopsin. The straight conformation, without the salt bridge, increases the probability of activation and can explain the basal activity of β_1-AR.[45]

The ligand pose of cyanopindolol (**9**) in the β_1-AR and the binding mode in the binding pocket were similar to that of carvedilol in the β_2-AR (Fig 1.10).[5, 47, 48] The binding pocket comprises 15 side-chain aminoacids localised in four different TMs and the ECL2. This loop is stabilised by a sodium ion and two disulphide bridges and defines the ligand entrance to the binding pocket.[5] A further sodium ion was found in the hydrophobic core

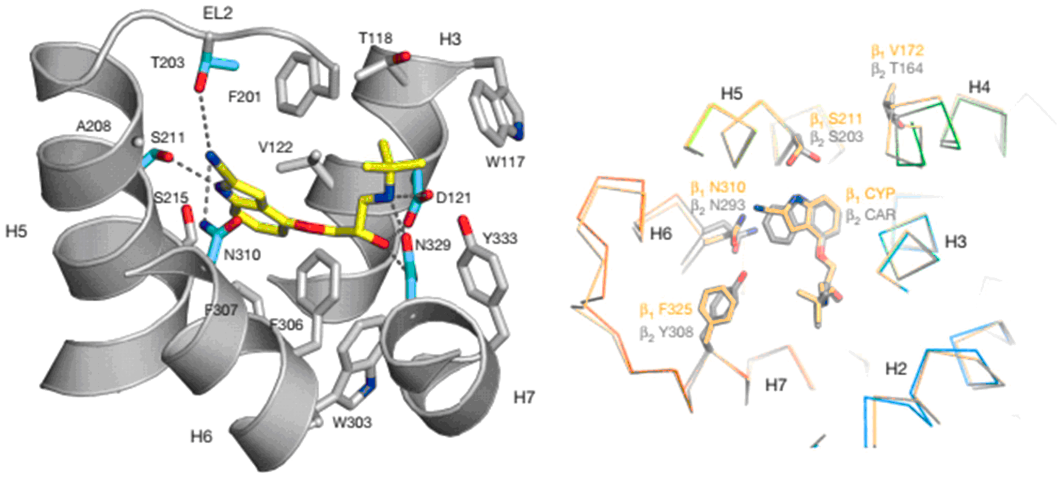

FIGURE 1.10: **Left:** interaction of cyanopindolol with binding-pocket residues in the turkey β_1-AR by polar interactions (light blue) or non-polar interactions (grey); **Right:** Superposition of cyanopindolol in the turkey β_1-AR binding pocket with carvedilol (**13**) in the β_2-AR binding pocket. [5]

of the receptor. This intramembrane sodium ion stabilises the ligand-free conformation of the β_1-AR but it is not essential for receptor activation, which involves the collapse of the sodium ion interaction with the receptor.[49] Cyanopindolol interacts with the residues from the binding pocket of β_1-AR in a similar way to those of β_2-AR. As expected, the amine and hydroxyl moiety from the oxypropanolamine side chain form polar interactions with $Asp^{3.32}$ and $Asn^{7.39}$, respectively. The indolic NH of cyanopindolol (**9**) forms an hydrogen bond with $Ser^{5.42}$, which seems important for agonist efficacy (Fig 1.10) Besides this interaction, cyanopindolol also interacts with $Thr203^{ECL2}$ through a weak hydrogen bond of the nitrogen in the cyano-moiety. Further conformations of the β_1-AR-m23 were crystallised later in complex with the full agonists (isoprenaline), partial agonists (dobutamine and salbutamol) and partial biased agonists (carvedilol and bucindolol).[5, 47, 48, 50]

Several differences between the interaction of partial and full agonists in the β_1-AR binding pocket were found in these inactive x-ray conformations of the β_1-AR and not in complex with G protein. Full agonists interacted with two serine side-chains in the TM5 ($Ser^{5.42}$ and $Ser^{5.46}$), while partial agonists like cyanopindolol only interacted with $Ser^{5.42}$.[47] Agonist binding also induces a 1 Åcontraction of the binding pocket in comparison with the antagonist bound and changed the rotamer conformation of both $Ser^{5.42}$ and $Ser^{5.46}$. This might increase the probability of activation state formation due to the disruption of the Van-der-Waals interaction between $Val^{4.56}$ and $Ser^{5.46}$, reducing the interactions between H4 and H5 (Fig 1.11).[47] Through evaluation of all these structures it is plausible to assume that $Ser^{5.42}$ and $Ser^{5.46}$ play an important role in ligand efficacy through the G protein pathway, while $Asp^{3.32}$ and $Asn^{7.39}$ play a part in determining

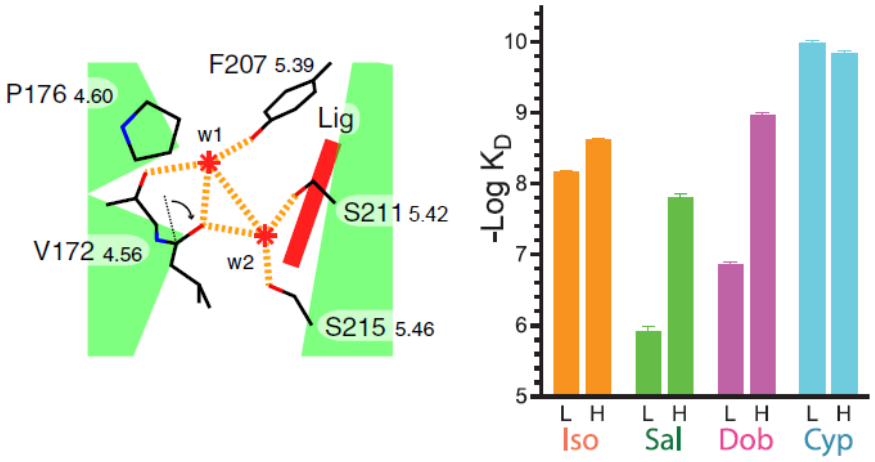

FIGURE 1.11: **Left:** Hydrogen bond network between TM5 and TM4 and two water molecules (w1 and w2), involving $Ser^{5.42}$, $Ser^{5.46}$, $Val^{4.52}$, $Pro^{4.60}$ and $Phe^{5.39}$. Taken from Isogai *et al.* [28] **Right:** Affinity values (-LogK_D) for isoprenaline (Iso), salbutamol (Sal), dobutamine (Dob) and cyanopindolol (Cyp) at the inactive state (L) and active state (H, coupled to mini-G_s) of the β_1-AR. Taken from Tate *et al.* [50]

ligand affinity for the β_1-AR . If the efficacy is indeed governed by the interaction with $Ser^{5.42}$ and $Ser^{5.46}$, a compound that could prevent the rotamer change of $Ser^{5.46}$ would have reduced efficacy. Recently, Sato *et al*, synthesised 7-methylcyanopindolol which has a methyl group preventing the interaction with $Ser^{5.46}$ seen in cyanopindolol complex with β_1-AR.[**?**] The crystallised structure of 7-methylcyanopindolol with β_1-AR showed an enlargement of the binding pocket and a different position of $Ser^{5.46}$ residue but it still acted as an extremely weak partial agonist. This means that different residues could also play a smaller part in ligand efficacy and still need to be taken in account. [**?** 5] It is also interesting to notice that carvedilol (**13**) and bucindolol (**14**), biased agonists (which stimulate a response through G protein pathways and G protein-independent cascades), interacted with additional residues in H7 and ECL2 that might be related to their ability to activate G protein-independent pathways [48, 51]

Recently, Tate *et al*, determined the x-ray crystal structure of several ligands bound the receptor in the fully activated terniary state, in complex with mini-G_s proteins. [50] As previously mentioned, GPCRs are known to exist in active (when coupled to G proteins) and inactive states, but also in a plethora of substates between these two extremes. Pardon *et al* previously determined the affinity of several ligands for both β_2-AR basal-state conformation and a nanobody-fused active state conformation, mimicking a fully active state coupled to G protein. [52] These nanobody-enabled reverse pharmacology studies enable the prediction of the ability or inability of the ligands to activate the receptor and mediate a response since agonists showed a much higher affinity for the active than inactive state of the receptor. [52] Tate *et al* demonstrated that this higher

affinity in agonists seen for the active state of the receptor is due to the contraction of the binding pocket, therefore reducing the distance and strenghtening the hydrogen bonds in the active state compared to the inactive state.[50] This decrease in volume is mainly obtained by the pincer-like movement of Phe^{ECL2} and $Phe^{7.35}$ and the inward movement of extracellular ends of H7 and H6.[50] Interestingly, a similar decrease in volume is obtained when the receptor is submitted to high pressure (2500 bar), moving the receptor to an active state even in the absence of G protein. [53]

These numerous X-ray structures are highly relevant and have contributed a lot to the better understanding of protein-ligand interaction in the β_1-AR. However, the m23 thermostabilising mutations and the β36 deletions of β_1-AR-m23 receptor seem to change the pharmacological behaviour of several ligands. [54] The β36 deletions alone made no difference in the ability of agonists, partial agonist and neutral antagonists to bind the receptor (when compared to the initial turkey tβtrunc construct). [54, 39] The tβtrunc receptor, the turkey β-adrenergic receptor, exhibits a high homology (82%) with the human β_1-AR. [39] m23-Thermostabilising mutation alone resulted in a ten fold lower affinity for the ligands tested, while the β_1-AR-m23 (β36–m23 mutant) receptor used in the x-ray crystallography showed a striking reduction in affinity and identically a reduction in potency, consistent with the stabilisation of the receptor and therefore the increase in the energy required for receptor activation. For these reasons, all the information should be carefully analysed and used in drug discovery due to the differences between turkey and human β_1-AR.

1.5 Secondary conformation of the β_1-AR

1.5.1 History and discovery

In the 1970s Kaumann, while comparing the intrinsic agonist activities and therapeutic ratio of several β-blockers on feline isolated tissues, identified DCI (**3**), pindolol (**8**) and other β-blockers as partial agonists. These compounds produced smaller cardiovascular effects than the maximal effects of isoprenaline. Partial agonists, unlike full agonists, are considered to exert their maximum effects when the receptor population is saturated. For this reason, the K_D (concentration required to occupy half of the receptors) of a partial ligand is expected to be the same as the EC_{50} (concentration that produces the half maximum effect). This was found to be true for several β-blockers in this study, except for pindolol **8**. The concentrations of pindolol required to achieve the

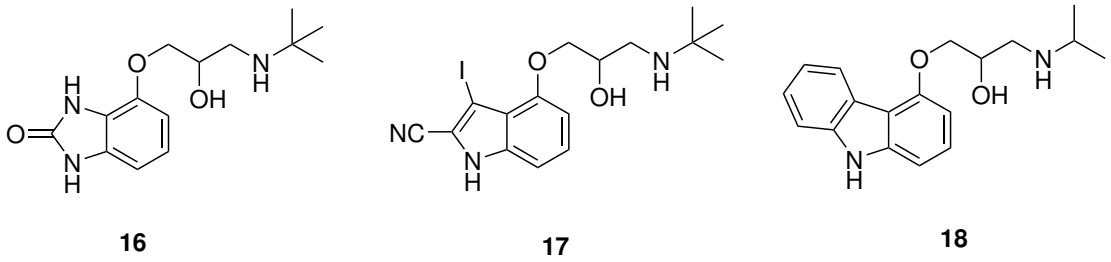

FIGURE 1.12: Ligands that posses a partial agonist response at the secondary conformation: CGP12177 (**16**), Iodocyanopindolol (**17**) and carazolol (**18**).

half maximal agonist effect were more than ten-fold greater than the experimentally determined K_D. Besides pindolol (**8**), the chemically related hydroxybenzylpindolol, *tert*-butylpindolol, iodohydroxybenzylpindolol, iodocyanopindolol **(17)** and carazolol **(18)** were also found to have the same behavior (Fig 1.12).[36] These unusual and unexplained results led to the classification of pindolol and its analogues as non-conventional partial agonists. In 1972, Kaumann, defined a non-conventional partial agonist as "an agonist that causes receptor activation only at high receptor occupancies".[36] In the following studies, alprenolol and oxprenolol were also found to possess the same pharmacological behavior.[55] In 1983, Staehelin synthesised and radiolabeled [^{3}H] CGP12177 (4-(3-*tert*-butylamino-2-hydroxyproppxy)-[5,7-^{3}H]benzimidazole-2-one), a radioligand that is still used nowadays for competitive whole cells binding assays due to its low non-specific binding.[56] This study showed that CGP12177 (**16**) blocked (LogK_D= -9) the isoproterenol-induced cAMP response in rat C6 glioma cells but also displayed a weak partial agonist effect at higher concentrations. This partial agonist effect was about 15% of the cAMP response achieved by isoproterenol with an EC_{50} two orders of magnitude higher than the K_D. At the time, this partial agonist effect was attributed to the amine moiety, present both in CGP12177 (**16**) and pindolol (**8**), that was thought to weakly mimic the hydroxyl moiety of cathecol.[56]

In order to understand if the non-conventional partial agonist response was mediated throught the β-adrenergic receptors, Walter *et al*, used several β-blockers to antagonise the partial agonist response generated by pindolol. [57] Both enantiomers, (-) pindolol and (+) pindolol, showed cardiostimulant effects on guinea pig atrium. (-) Pindolol showed a biphasic concentration-effect curve with a high-sensitivity and a low-sensitivity component. Even though most of the β-blockers (eg. the β_1-AR antagonist (-)bisoprolol, **12**) were only able to antagonise the high-sensitivity component, (-) bupranolol antagonised, with moderate potency, the low-sensitivity component. (-) Bupranolol was previously shown to have high affinity for both cardiac β_1- and β_2-ARs. Neither of components were affected by the β_2-AR- selective antagonist ICI118551, suggesting that, at least, the high-sensitivity component could be mediated through the β_1-AR.[58] At this point, the

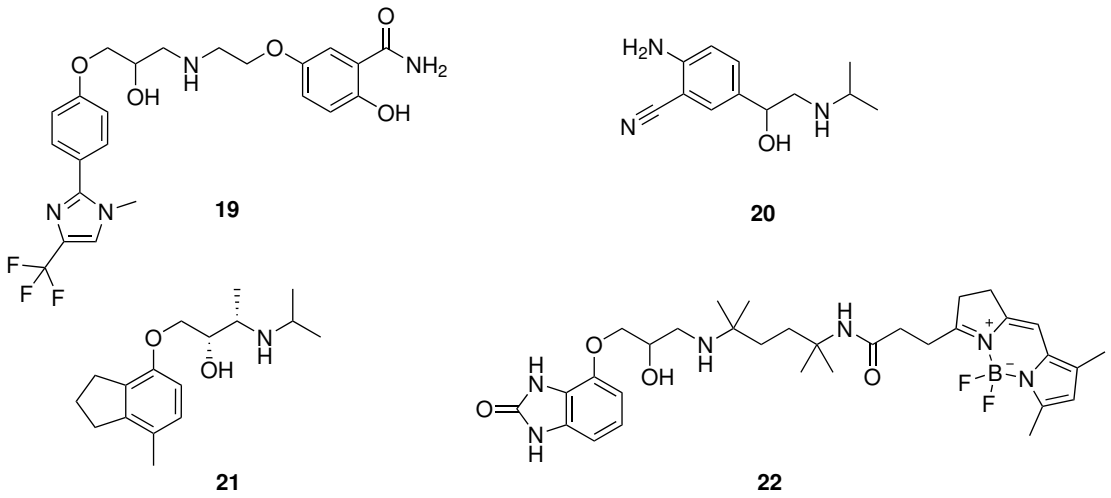

FIGURE 1.13: Ligand structures of CGP20712A (**19**), β_1-selective antagonist; Cimaterol (**20**), a primary conformation agonist; ICI118551 (**21**), a β_2-selective antagonist; BODIPY-TMR-CGP (**22**), a fluorescent analog of CGP12177.

low-sensitivity component was suggested to be mediated in cardiac tissue through a β-adrenergic receptor distinct from β_1- and β_2-AR. This hypothetical β-AR was known as "a putative β_4-adrenoceptor". Later on, the β_1-selective antagonist CGP20712A (**19**) was also found to antagonise the cardiostimulant effects of non-conventional partial agonists, even though it required higher concentrations.[14]

Pak and Fishman suggested that this "putative β_4-aderenoceptor" was a low-affinity site/conformation of the β_1-adrenergic receptor, which was confirmed later when studies showed that the cardiostimulant effects of CGP12177 (**16**) were absent in β_1-adrenoceptor knockout mice.[15, 14] During their work, Pak and Fishman, used recombinant rat and human β_1-AR transfected into chinese hamster ovary (CHO) cells as a cardiovascular model and concluded that the agonist response of CGP12177 was proportional to β_1-AR density and that this response was caused through the low-affinity conformation coupled to Gs protein.[14]

For these reasons, it was suggested that the β_1-AR exists in, at least, two distinct agonist conformations: a high-affinity conformation where responses are readily inhibited by antagonists and a low-affinity conformation, of which the precise nature is unknown, where agonist responses are relatively resistant to antagonism by the well-studied β_1 antagonists (eg. propranolol **4**). These high-affinity and low affinity conformations will be referenced throughout this report as the primary and secondary conformation, respectively.

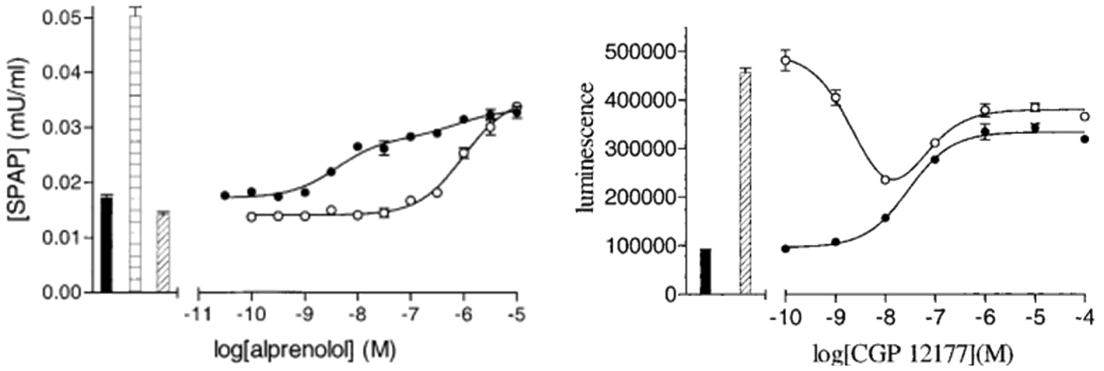

FIGURE 1.14: **Left:** SPAP production induced by alprenolol in the absence (black dots) and in the presence (white dots) of 100 nM CGP20712A. **Right:** Bars show basal luciferase activity (black) and the response to 100 nM isoprenaline (stripes). Black dots represent CGP12177 alone and white dots in the presence of 100 nM isoprenaline.[34]

1.5.2 Pharmacology

As stated in the previous section, the first evidence for this pharmacological phenomenon, emerged in the 1970s, when Kaumann identified pindolol as a non-conventional partial agonist. Pindolol possesses a biphasic concentration-effect curve and an EC_{50} value higher than its K_D, suggesting that it has an agonist response through both the β_1-AR conformations. This was later confirmed using recombinant β_1-AR, Konkar *et al*, demonstrated that CGP12177 stimulation of adenyl cyclase in the adipocytes is mediated through both this secondary conformation and, at higher concentration, through the β_3-AR.[59]

In 2003, Baker *et al.*, used the same model as Pak and Fishman to evaluate if a range of clinically used β-blockers can stimulate gene transcription via primary, secondary or both conformations of the β_1-AR (Fig 1.15).[34] These results confirmed the results obtained by Pak and Fishman and provide four pieces of evidence that support the existence of a secondary conformation of the β_1-adrenergic receptor:

1. Blockade of the CGP12177 agonist response required concentrations of β_1-antagonists that were at least one order of magnitude larger than those required to antagonise the isoprenaline agonist response. If these responses were mediated through the same conformation it would be expected that the same concentration of antagonists inhibit both of them to the same degree. Baker *et al*, using a CHO-β_1-SPAP cell line with high receptor expression, showed that this CGP12177 agonist response is relatively resistant to antagonism by other classic β_1-antagonists. Atenolol (**10**), propranolol (**4**) and CGP20712A (**19**) log K_D values for antagonism of isoprenaline-stimulated response ($logK_D\beta_{1ISO} = -7.43$ for atenolol **10**; $logK_D\beta_{1ISO} = -9.10$ for propanolol **4**; $logK_D\beta_{1ISO} = -9.19$

for CGP20712A (**19**)) were higher than for antagonism of CGP12177-stimulated response ($logK_D\beta_{1CGP} = -4.43$ for atenolol **10**; $logK_D\beta_{1CGP} = -7.02$ for propanolol **4**; $logK_D\beta_{1ISO} = -7.09$ for CGP20712A). (Tab 1.3) The discrepancies between the logK_D values for antagonism were also found in cells with low receptor expression and, therefore, are not likely to be a function of a overexpressed system;[34]

2. As stated in the previous section, the EC_{50} value for the CGP12177 agonist response, as well as pindolol stimulatory response, is higher than the K_D values obtained for these ligands. This means that these ligands require a much higher concentration to stimulate a response than that required to bind the orthosteric binding site of receptor and thus suggesting that the response is not being mediated through that site/conformation; [34, 60]

3. Several ligands have biphasic agonist response curves, containing more than one component (eg. pindolol, bucindolol, alprenolol, carazolol). An example is shown in figure 1.14 where the concentration response curve of alprenolol is fitted best by a two-component analysis. Alprenolol achieved 52.9% of the total response of isoprenaline through primary conformation with a calculated logEC_{50} of approximately -8.66 for primary conformation and -6.13 for the secondary conformation. However, when in the presence of 100 nM CGP 20712A, the agonist response through primary conformation was inhibited and alprenolol showed a single component agonist response with a logEC_{50} of -6.03.[34] These results resemble the biphasic concentration-effect curves also found for pindolol on the guinea pig and feline sinoatrial node.[57, 55]

4. If the β_1-AR exists in at least two agonist conformations and CGP12177 (**16**) is able to bind both then it would be expected that CGP12177 inhibited the agonist response of isoprenaline through primary conformation and, at higher concentrations, stimulated a agonist response, per si, through the secondary conformation. That is indeed what is shown in figure 1.14: the response of isoprenaline (fixed at 100 nM) is, at first, potently inhibited by increasing concentrations of CGP12177 and, as this concentration increased further, the agonist effects of CGP12177 could be seen. This figure clearly demonstrates the antagonism of CGP12177 (**16**) at lower concentrations through the primary conformation followed by an agonist response through the secondary conformation at higher concentrations.[34, 14]

The recombinant human β_1-AR transfected into CHO cells turned out to be a good experimental model for the evaluation of pharmacology at the two conformations of the β_1-AR since the results obtained by Baker *et al.* correlated well with the logK_D values obtained in human atrium studies.[36] These two β_1-AR conformations are also seen in rat, mouse, ferret and human heart and in whole animals where its activation produced an increase in atrial and ventricular force and sinoatrial tachycardia.[61, 62, 63] This

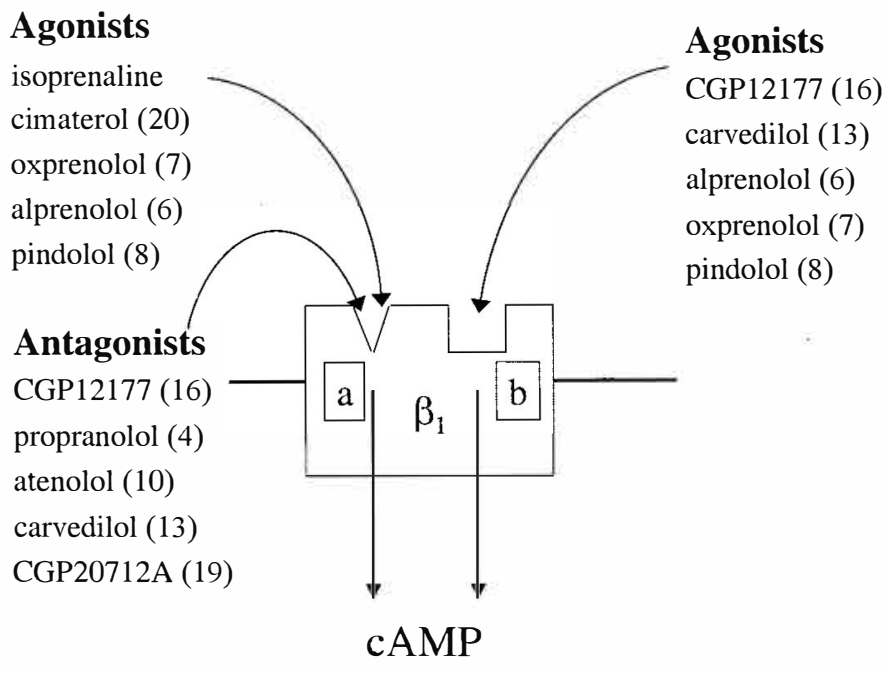

FIGURE 1.15: Schematic representation of the primary (a) and secondary (b) conformation of the β_1-AR. Several ligands are able to stimulate a response through both conformations (eg. alprenolol **6** and oxprenolol **7**) or only through the secondary conformation (eg. CGP12177 **16** and carvedilol **13**). Taken from Baker *et al.*[34, 35]

is consistent with the activation of the cAMP pathway and with the results obtained through *in vitro* testing.

The existence of a secondary conformation of the β_1-AR is supported by pharmacological data whether through *in vitro* or *in vivo* testing. Even though these distinct pharmacological models come to the same conclusion, there are still some problems in comparing the data mainly to the lack of a compound with higher affinity for this secondary conformation than for the primary. The development of a selective compound, with a higher affinity for this secondary conformation, is a urgent need and could contribute to the unveiling of the structure of this agonist conformation, the possible effects mediated by it and the activation of signaling pathways.

1.5.3 Structure and conformation

Many key questions still remain to be answered. The molecular basis for this non-conventional partial agonism is still unknown. It is also not known either the ligands that present this peculiar pharmacological response bind to a different binding site other than the regular catecholamine binding site in order to induce a secondary conformation

of the β_1-AR (Fig 1.10). Other possibilities have been proposed and will be discussed further on this subsection.

As stated previously, until recently our knowledge concerning the binding sites of β-adrenergic receptors came from site-directed mutagenesis studies of the β_2-adrenergic receptor. In order to understand the importance of each transmembrane domain in this non-convential partial agonist response Baker *et al* made a series of point mutations in the human β_1-adrenoceptor and examined the effects of swapping transmembrane domains of the human β_1-AR and β_2-AR .[64] During these studies, the amino acid residues essential for the binding to the catecholamine site were also mutated, and their effect on the binding of antagonists, such as CGP20712A (**19**) and propranolol (**4**), was evaluated.[64] An analysis of the residues will be made during this subsection.

The interaction of catecholamines was found to be similar to the one in the β_2-AR in the catecholamine binding pocket. Residue $Asp^{3.49}$ in TM3 is likely to be the anchor point for the amine group of isoprenaline and cimaterol (**20**), whereas the hydroxyl groups in the aromatic core were found to interact with three serine residues in TM5 ($Ser^{5.42}$, $Ser^{5.43}$ and $Ser^{5.46}$).[65] Mutations at the residue $Asp^{3.49}$ ($D138A^{3.49}$ and $D138S^{3.49}$) in TM3 abolished all binding and functional responses at both primary and secondary conformation, showing that it is essential for both the responses. On the other hand, the mutation $S228A^{5.42}$ and $S229A^{5.43}$ did not abolish the agonist response of CGP12177 mediated through the secondary conformation but slightly rightshifted this response while also decreased the affinity for the primary conformation. This response mediated by CGP12177 still showed more resistance to antagonism by known β-blockers, suggesting that the secondary conformation is still present. These mutations also affected the affinity of other compounds: propranolol (**4**) affinity for the primary conformation decreased and cimaterol (**20**) affinity increased. The $S232A^{5.46}$ mutation did not influence the binding affinity of CGP12177 but reduced the affinity of isoprenaline. These three serine residues in the TM5 are important for the binding of catecholamines to the primary conformation of the β_1-AR but only $S228A^{5.42}$ and $S229A^{5.43}$ seem to decrease the affinity of CGP12177 for the primary conformation and also for the secondary conformation (reduces the EC_50 value and therefore the potency obtained). $Asn^{7.39}$ mutation to either alanine, cysteine, tyrosine, or phenylalanine in the TM7 abolished all specific binding of aryloxypropanolamines, showing its importance for the binding of both agonists and antagonists to the β_1-AR. This residue is known to interact with the chiral hydroxyl group of aryloxypropanolamines and it is vital both for binding to the primary as for the secondary conformations in this receptor.[64]

In the β_2-AR, $Phe^{6.52}$ has been proposed to be involved in the receptor activation as a rotamer "toggle switch". The mutation of the equivalent phenylalanine ($F341A^{6.52}$) in

the β_1-AR did not affect the affinity of isoprenaline, cimaterol or propranolol (**4**) but decreased the affinity of CGP12177 for the primary conformation. Surprisingly, this point mutation abolished the ability of CGP20712A (**19**) to differentiate between the two distinct conformations of the β_1-AR, even though other antagonists (eg. propranolol **4**) still required higher concentrations to inhibit CGP12177 mediated response in this mutated receptor. N344A$^{6.55}$ mutation also had an identical effect on CGP20712A affinity for both conformations.[64]

Besides these residues that are important within the catecholamine binding pocket both in β_1- and β_2-AR, Baker *et al*, found several residues in the TM4 of β_1-adrenoceptor that completely abolished the pharmacology associated with the secondary conformation.[64, 66] In the chimeric β_1-TM4 (containing the TM4 domain of the β_2-AR) antagonists inhibited CGP12177 (**16**) and cimaterol (**20**) responses with similar logK_D values. The EC_{50} and the K_D found for CGP12177 were also similar, suggesting that these responses are mediated through the same conformation. The residues Leu$^{4.62}$ and Trp$^{4.66}$ present in the TM4 were found to be crucial in the secondary conformation, while Val$^{4.56}$ was also found to influence lightly this conformation. The mutation of L195Q$^{4.62}$ and W199D$^{4.66}$ was found to change the two-component concentration-response curve of pindolol to a single-component, creating a β_1 adrenoceptor with only one agonist conformation.[64] W199D$^{4.66}$ mutation alone was also able to abolish the secondary conformation of the β_1-AR yielding identical EC_{50} and K_D for CGP12177, as expected for a conventional partial agonist.

Abdelkrim *et al* suggested that the ECL2 could have a different function in the two distinct agonist conformations, autoantibodies directed against this extracellular loop could recognise and stabilise the primary conformation but not the secondary.[67] Similarly, a monoclonal antibody (mAb3) raised against the turkey β_1-AR, which binds a region in the ECL2 of this receptor, elicited a negative allosteric effect on agonist-mediated cAMP responses for conventional agonist but did not affect the CGP12177 mediated response. [68]

Analysing these structural data it is still not possible to state if the non-conventional partial agonism of some compounds is due to the binding to another binding pocket within the same receptor or through a different secondary conformation. The fact that Asp$^{3.49}$ and Asn$^{7.39}$ residues are essential for both pharmacological responses could suggest that there are two binding sites partially overlapping. However, this cannot explain why the binding of CGP12177 to one of the binding sites does not block its binding to the other one. It is plausible to assume that a first binding event of CGP12177 to the orthosteric catecholamine binding pocket could induce structural changes and lead to an extension of the binding pocket. Joseph *et al*, suggested that the coupling of G_s protein to β_1-AR

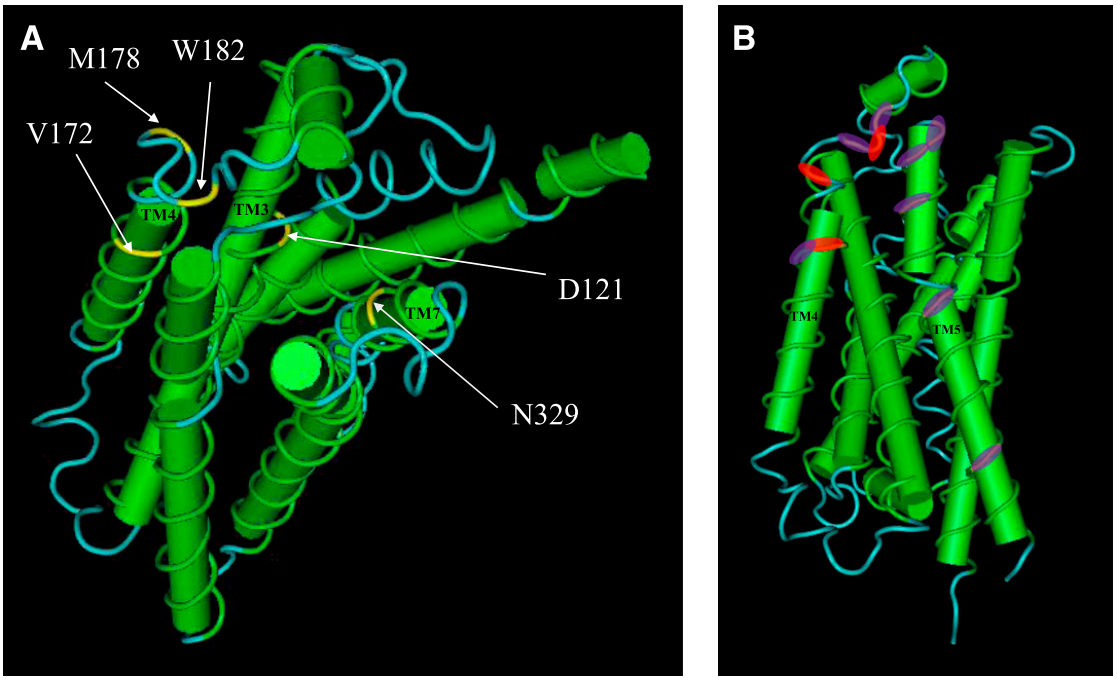

FIGURE 1.16: Location of equivalent residues which mutation impacts the secondary conformation ($Val^{4.56}$/V172, $Leu^{4.62}$/M178, $Trp^{4.66}$/W182) but also key residues for both conformations ($Asp^{3.32}$/D121, $Asn^{7.39}$/N329) in the crystal structure of the turkey β_1-AR described by Huang *et al.* [69] TM4 and TM5 are suggested to be involved in an homodimer interface in this ligand-free state structure. Residues suggested to be involved in this homodimerisation are highlighted in purple, while the three key residues for the secondary conformation are highlighted in red. Taken from Baker *et al.*[66]

activated by catecholamines is different than for receptors activated by CGP12177 and other non-conventional agonists. The well-known Gly389 mutation in β_1-AR reduced considerably less the agonist response of CGP12177 than that of isoprenaline, suggesting that CGP12177 might interact with a different residue to promote the coupling of the β_1-AR to Gs proteins.[70] In contrast, Baker *et al*, argued that there is no change in the stimulation of $G_{\alpha.S}$-cAMP pathway in either of the agonist conformations with the polymorphic variant.[71]

It is also proposed that these pharmacological phenomena might be associated with receptor dimerisation or oligomerisation, a conformation dependent on the extent of receptor phosphorylation or association with other scaffold proteins.[72, 10] It is indeed suggested by Baker *et al*, and Gherbi *et al*, that the agonist response of CGP12177 might be related with the dimerisation of the β_1-AR and negative cooperativity across the two orthosteric binding sites of a homodimer.[66, 73] Baker *et al* state that the residues $Leu^{4.62}$ and $Trp^{4.66}$, crucial for the secondary conformation, are within the TM4/TM5 dimer interface in the turkey β_1-AR crystal structure published by Huang (Fig 1.16).[64, 69] Gherbi *et al* showed negative cooperativity between two distinct β_1-AR conformations

using a fluorescent analog of CGP12177 (BODIPY-TMR-CGP, **22**).[74, 75] The presence of CGP12177 and propranolol (**4**) in micromolar concentration enhanced the dissociation rate of the fluorescent CGP12177, an effect even more noticeable when the population of homodimers was increased. These effects were abolished when using the chimeric β_1-AR with point mutations in TM4 within the dimer interface. [73]

Overall, these mutation studies identified two residues within the orthosteric binding pocket ($Asp^{3.49}$ and $Asn^{7.39}$) that have a striking effect on the affinity for both conformations and three residues ($Leu^{4.62}$ and $Val^{4.56}$ but especially $Trp^{4.66}$) that only influence the secondary conformation of the β_1-AR. Unfortunately, either CGP12177 or pindolol are not able to stimulate a response in the β_1-AR-m23, the thermostabilised turkey receptor used in x-ray crystallography, either due to disruption of the secondary conformation in this heavily mutated receptor or due to the reduced ability to mediate a response through this receptor seen for different ligands. This might limit the relevant information for this secondary conformation obtained from the crystal structure determined for the β_1-AR-m23. It is therefore of the utmost importance to synthesise ligands able to bind to the secondary conformation with higher affinity than to the primary conformation which could be used as important pharmacological tools.

1.5.4 Ligands

In order to understand the origin of the secondary conformation of the β_1-AR it is important to gather information about the affinities of several known β-blockers used in the clinic for each conformations. It is also important and extremely necessary to find how these molecules interact with the receptor in this secondary conformation. Even though the affinities at each conformation have been determined for several known β-blockers in the last few years, no structure-activity relationships studies have been conducted. Structure-activity relationship studies would provide useful data to understand the differences between these two distinct conformations and to possibly identify chemical features that confer selectivity for either the primary or the secondary conformation. To date, no ligand has been identified with a higher affinity for the secondary conformation of the β_1-AR than for the primary conformation. Interestingly, the rank order of ligand affinities is different at each conformation, where ICI118551, bupranolol and other ligands rank higher for the secondary conformation than for the primary while atenolol (**10**) ranks lower.[60]

As stated in the previous section, CGP12177 (**16**) has been an important tool in the study of this secondary conformation mainly because it acts as an antagonist through the primary conformation of the β_1-AR and as an agonist through the secondary conformation.

Ligand	System	Log EC_{50}	Log $K_D\beta_1$ ISO	Log EC_{50} - Log $K_D\beta_1$ ISO
(-)CGP12177	Human recombinant β_1-AR	-7.6	-9.3	1.7
(±)Alprenolol	Right atrium	-6.8	-8.6	1.8
(±)Tert-butylcarazolol	Rat right atrium	-7.4	-9.8	2.4
(-)Pindolol	Right atrium	-7.0	-9.6	2.6
(±)Bucindolol	Atrial trabecuale	-6.3	-9.0	2.7
(±)Carteolol	Right atrium	-6.1	-9.0	2.9
(±)Carazolol	Rat right atrium	-7.0	-9.9	2.9
(±)Iodocyanopindolol	Left atrium	-7.4	-10.8	3.4

TABLE 1.2: Affinity estimates (Log$K\beta_1$ ISO), determined through the inhibition of isoprenaline response, and agonist potencies (LogEC_{50}) of several non-conventional partial agonists.[36]

Ligand	Stimulation	Log $K_D\beta_1$ ISO	Log $K_D\beta_1$ CGP	Log $K_D\beta_1$ ISO - Log $K_D\beta_1$ CGP
(-) ICI118551	CRE-luciferase (b)	-6.77	-5.80	0.97
(-) Bupranolol	cAMP (a)	-9.38	-7.63	1.75
(±) Nadolol	cAMP (a)	-8.07	-6.24	1.83
(±) Alprenolol	cAMP (a)	-8.61	-6.71	1.90
(±) Bisoprolol	cAMP (a)	-7.68	-5.70	1.98
(-) Propranolol	cAMP (a)	-9.10	-7.02	2.08
(±) CGP20712A	CRE-luciferase (b)	-9.19	-7.09	2.10
(±) Sotalol	cAMP (a)	-6.01	-3.89	2.12
(±) Oxprenolol	cAMP (a)	-8.19	-6.05	2.14
(±) Carvedilol	cAMP (a)	-9.87	-7.56	2.31
(-) Timolol	cAMP (a)	-9.15	-6.38	2.77
(-) Pindolol	cAMP (a)	-9.30	-6.50	2.80
(±) Metoprolol	cAMP (a)	-8.24	-5.41	2.83
(-) Atenolol	cAMP (a)	-7.43	-4.43	3.00

TABLE 1.3: Affinity of several known ligands at both the primary and the secondary conformation. Log $K_D\beta_1$ISO is determined by inhibition of (-) isoprenaline response and Log $K_D\beta_1$ CGP is determined by inhibition of racemic CGP12177 response in CHO β_1 cells. The agonist response of the ligands are measured either through CRE luciferase (b, Baker *et al*) or cAMP stimulation (a, Joseph *et al*). [60, 65]

Other ligands, such as alprenolol and pindolol, have been found to act as agonists at both conformations, whilst bupranolol and CGP20712A (**19**) act as antagonist at both conformations. Sarsero also reported that isoprenaline, adrenaline (**1**) and noradrenaline (**2**) might interact with the secondary conformation in rat atrial membranes with millimolar affinity.[76]

Kaumann *et al* and Baker *et al* contributed greatly to the identification of β-blockers

that possess a non-conventional agonism.[36, 34, 60] The affinity of a ligand for each conformation could be determined using an *in vitro* system with the transfected β_1-AR by comparing its K_D value for the inhibition of isoprenaline (or other conventional β_1-AR agonist) and CGP12177, which purely activate the primary and the secondary conformation, respectively.[60] Table 1.2 compares the $\log EC_{50}$ values of several ligands with their $\log K_D$ value for the primary conformation ($\log K\beta_{1ISO}$) of the β_1-AR determined by both *in vitro* and *ex vivo* methods. All these compounds show a higher value for $\log EC_{50}$ than for $\log K_D$ which means that they possess an agonist response mediated through the secondary conformation of the β_1-AR.[36] CGP12177 possesses a higher agonist response at this secondary conformation than than pindolol, which in turn, possesses a higher agonist response than alprenolol.[63] Lowe *et al* tried to rationalise the interaction of several compounds with the secondary conformation. The hydrophilicity of CGP12177 was not regarded as an important factor because other hydrophilic phenoxypropanolamines were not found to activate this secondary conformation. The ability to stabilise the secondary conformation was attributed to the high electron density of the aromatic core of CGP12177 which was higher than pindolol and alprenolol.[63]

The affinity of several compounds for each conformation of the β_1-AR is described in table 1.3. These data have been collected from *in vitro* studies in CHO cells with human recombinantβ_1-AR through the inhibition of the stimulation of an agonist response for (-)isoprenaline ($\text{Log}K\beta_{1ISO}$) and (-) or (±)CGP12177, as indicated, ($\text{Log}K\beta_{1CGP}$) and measurement of cAMP or CRE luciferase levels.[60, 41] The $\log K\beta_{1ISO}$ determined through CRE luciferase stimulation was consistently slightly lower than the one obtained through cAMP stimulation.[60, 41] The compounds are ranked by the difference between the $\log K\beta_{1ISO}$ and $\log K\beta_{1CGP}$ and all of them bind to the primary conformation of the β_1-AR with higher affinity than to the secondary conformation. Phenethanolamines like sotalol, even though with a small affinity, can also bind to both conformations, which means that is not a conformation exclusive to phenoxypropanolamines interaction.

Bupranolol, an antagonist at both conformations, was one the compounds with the highest affinity for the secondary conformation and with less of a difference between $\log K\beta_{1H}$ and $\log K\beta_{1L}$. For these reasons, the affinities of several bupranolol analogues were evaluated in pithed rat models. (Fig 1.17)[62, 61, 78] To measure the affinity of each compound the heart rate was measured and CGP12177 and xamoterol were used to activate the secondary and the primary conformation, respectively, and induce an increase in the heart rate. The potency of each compounds to antagonise the increase in the heart rate by xamoterol addition is represented as $\log K(\beta_{1H})$ and as $\log K(\beta_{1L})$ by CGP12177 addition. (-) Bupranolol ($\log K(\beta_{1H})$= - 7.9 and $\log K(\beta_{1L})$= - 6.1) showed a similar difference in this study between the affinity for the primary and secondary conformation as the one seen in human recombinant β_1-AR (1.8 vs 1.75) (Table 1.3).

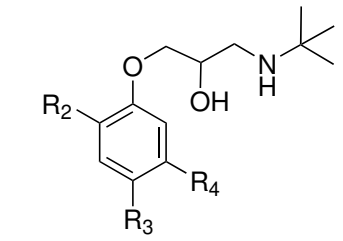

23 Bupranolol	**R2:** Cl	**R3:** H	**R4:** CH_3
24 Desmethylbupranolol	**R2:** Cl	**R3:** H	**R4:** H
25 GD-7	**R2:** Cl	**R3:** Cl	**R4:** H
26 GD-6	**R2:** F	**R3:** H	**R4:** CH3
27 BK-22	**R2:** CH_3	**R3:** H	**R4:** H
28 DZ-51	**R2:** CH3	**R3:** H	**R4:** CH3
29 BK-25	**R2:** H	**R3:** H	**R4:** H
30 BK-26	**R2:** H	**R3:** Cl	**R4:** CH_3
31 DZ-28*	**R2:** F	**R3:** H	**R4:** CH_3

*Isopropylamine substituent

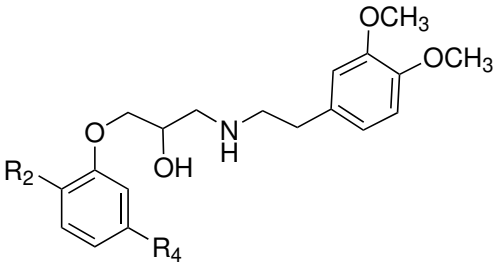

32 Bevantolol	**R2:** Cl	**R4:** CH_3
33 DZ-53	**R2:** CH_3	**R4:** CH_3
34 BK-23	**R2:** CH_3	**R4:** H
35 DZ-43	**R2:** H	**R4:** CF3

FIGURE 1.17: A set of bupranolol and bevantolol analogues, some of which are antagonist at the secondary conformation.[61, 77]

The removal of the CH_3 group in bupranolol (desmethylbupranolol) led to an increase in heart rate through the primary conformation. BK-22, BK-23, BK-25 and GD-7, that also lack the CH_3 group in the R_4 position, increased the heart rate as well. Interestingly, BK-26 only antagonised the response mediated through the primary conformation, which shows the importance of the substituent at R_2. GD-6, that has a fluor substituent instead of a chloro, had the same affinity for the secondary conformation (logK(β_{1L})= - 6.1) but a slightly higher affinity for the primary conformation (logK(β_{1H})= - 8.1) than bupranolol. DZ-28 that possesses the same aromatic core as GD-6 but an isopropylamine substituent in the phenoxypropanolamine chain showed a decrease in affinity for both conformations logK(β_{1H})= - 6.9 and logK(β_{1L})= - 5.2). DZ-51 can also antagonise the responses at both conformations with lower affinity (logK(β_{1H})= - 7.3 and logK(β_{1L})= - 5.1). Interestingly, bevantolol, which possesses the same aromatic core as bupranolol but replaces the *N-tert*-butyl moiety with an *N*-2-(3,4-dimethoxyphenyl)ethyl group, can only antagonise the CGP12177 mediated response stereoselectively as a (-) enantiomer. The use of the bioisoster CF_3 group instead of CH_3 also yield a compound that could antagonise the responses at both conformations (logK(β_{1H})= - 6.3 and logK(β_{1L})= - 5.2).

Even though the information is not sufficient to draw definitive conclusions, in the bupranolol analogues, the CH_3 group seems to play an important part in the antagonism at both conformations while the R_2 and the amine group seems to modulate the potency and selectivity of the antagonism.[78, 62]

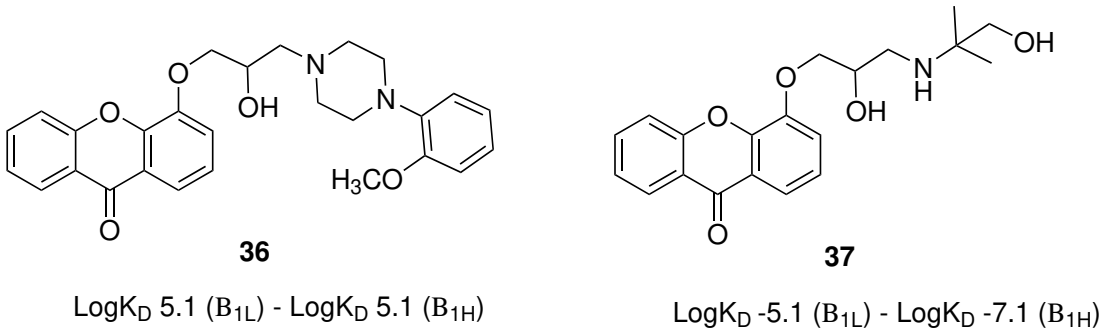

FIGURE 1.18: Structure of Xanthone **36** and **37** which can bind to both conformations of the β_1-AR.

Schlicker *et al* also reported the identification of two xanthones **(36** and **37)** with two different amino substituents. The xanthone **36** was the first compound to ever show a similar affinity for both conformations, even though that it has quite poor affinity for both conformations. The introduction of a different amino group (**37**) increased the affinity for the primary conformation but did not affect the affinity for the secondary conformation.[78]

1.5.5 Clinical relevance of the secondary conformation of the β_1-AR

So far, the effects mediated through the secondary conformation of the β_1-AR have been demonstrated *in vitro* and *in vivo*.[62] The activation of this conformation induces sinoatrial tachycardia, increases contractile force, shortens ventricular action potential and elicits arrhythmias in ventricular and atrial myocytes in rats and mice.[62, 76] All the compounds that present a non-conventional partial agonism have a lower affinity to this secondary conformation of the β_1-AR that translates into a small cAMP accumulation but in a substantial gene transcription effect after five hours of exposure *in vitro*. Several of these compounds are used in prolonged treatments so it is extremely pertinent to interrogate if this effect would be seen in patients and would have an impact in clinic.[34]

Concentrations of bucindolol (**14**) up to 1 μM have been measured in plasma of patients that were treated for hypertension with 50-200 mg of bucindolol.[36] At this concentration bucindolol can bind to the secondary conformation of the β_1-AR and increase contractility of ventricular trabeculae *in vitro*.[51] It is therefore possible that this interaction with the secondary conformation might produce cardiac arrhythmias and might be related with the failure shown by bucindolol in increasing survival in patients after myocardial infarction.[63] The activation of this conformation might also contribute to the intrinsic sympathomimetic activity (ISA) of alprenolol and pindolol which is harmful in the prolonged treatment of chronic heart failure.[79, 63] However, some studies suggest

that pindolol might be beneficial for the treatment of orthostatic hypotension (drop of blood pressure when suddenly standing up) and neurocardiogenic syncope (inappropriate activation of the vagus nerve) and that this effect might be mediated through the secondary conformation.[36]

These findings suggest that activation of the secondary conformation of the β_1-AR might have more harmful effects than plausible beneficial effects. However, further investigations and pharmacological tools are needed in order to come to any strong conclusion.

1.6 Research aims

As explained during this introduction, there is not much known about the secondary conformation of β_1-AR from a clinical to a biological point of view but specially from a chemical and structural point of view. The main goal of this project is the identification of the chemical features that can confer selectivity and increase the affinity for the secondary conformation. The better understanding of the chemical moieties that promote a higher affinity, could help to understand the interaction between a ligand and this particular conformation of the receptor. This study also aims to identify the chemical features responsible for mediating a response via the secondary conformation of the β_1-AR since some ligands are known to mediate a response only through the primary conformation (eg. cimaterol), only via the secondary conformation (eg. CGP12177 **16**) or via both of the conformations (eg. alprenolol **6** and oxprenolol **7**). This could be an important help for the identification of the residues involved in the activation of this secondary conformation and could help revealing the clinical effects that the activation of this receptor conformation might have. Since no compound is known to have higher affinity for the secondary conformation than the primary conformation of the β_1-AR, a pharmacological tool capable of blocking irreversibly the primary conformation could also be of great use. This would enable the study of the secondary conformation while the same fixed ligand is occupying the primary conformation in an irreversible manner.

The first step towards this goal should consist in the synthesis of a set of compounds with several modifications both in the amine-end and in the aromatic core groups of the compounds. Alprenolol **6** and oxprenolol **7** were chosen as the lead compounds. As previously explained, alprenolol and oxprenolol can bind and activate both the primary and the secondary conformation of the β_1-AR, even though they possess a much lower affinity for the secondary conformation. Initially, the thorough validation of the cell lines expressing either the human β_1 or β_2-AR along with CRE-SPAP (secreted placental alkaline phosphatase under the control of a cAMP response element) used during these

experiments with well-charaterised literature compounds is of highly importance. Validation of the cell lines used in the experiments will be described in chapter 2. Three distinct sets of analogues will be presented in chapters 3-5 and fully characterised for both the β_1 and β_2-AR. An iterative plan was put in place to fully characterise these compounds and described in the following workflow:

1) A set of ligands is synthesised.

2) Following the synthesis, this set of compounds is tested in the validated CHO-β_1 and CHO-β_2 cells in several assays. Initially, these compounds are characterised in radioligand competitive binding assays for both receptors. In these assays, a fixed concentration of a fully characterised radioligand ((-)[^{3}H] CGP12177) is added to increasing concentration of compound. Compounds might be able to bind to the receptor and displace (-)[^{3}H] CGP12177 with a certain $logIC_{50}$ value taken from the displacement curve. $LogK_D$ values can then be derived from the $logIC_{50}$ values using Cheng-Prusof equation detailed in the methods chapter. It is noteworthy to mention that the concentration of radioligand used is only enough for (-)[^{3}H] CGP12177 to bind mainly to the primary conformation but not to the secondary conformation of the β_1-AR. For this reason, it is correct to assume that $logK_D\beta_1$ values obtained through these radioligand competitive binding experiments in CHO-β_1 cells represent the affinity of these compounds for the primary conformation of the β_1-AR.

3) Independently of whether the compound is able to bind to the receptors or not a CRE-SPAP functional study is performed. In this assay, increasing concentrations of the compound are added to the cells and the concentration of SPAP, a cAMP reporter gene, is measured. This assay allows the determination of $logEC_{50}$ values, corresponding to the logarithm of the concentration required to elicit half of the maximal response. A $\%isop$ is also obtained, corresponding to the percentage of the response elicited by 10μM isoprenaline mediated by the compound. Compounds that fail to elicit an increase in SPAP concentration are deemed as antagonists for the system used. Compounds able to elicit a response similar to 100% of the response mediated by 10μM isoprenaline (the maximum response cells are able to mediate) are deemed as full agonist. If the compounds are only able to mediate a lower response than 10μM isoprenaline they are considered partial agonists. As previously mentioned, for a partial agonist the concentration required to elicit half of the maximal response should be the same as the concentration required to occupy half of the receptors ($logEC_{50} = logK_D$). While this is true for the β_2-AR, some ligands (eg. CGP12177) only mediate a response at higher concentrations than they require to bind the receptor. This assay will therefore allow the detection of anomalous behaviour by comparing the $logEC_{50}$ value with the $logK_D$ previously obtained from the radioligand assays, which may indicate if the response is mediated through the primary

or secondary conformation of the β_1-AR. Compounds may also mediate a response best described by a biphasic curve (eg. alprenolol **6**, Fig 1.14) which suggests that one of the components is mediated through the primary conformation ($logEC_{50}\beta_1 1$) and the other via the secondary conformation of the β_1-AR ($logEC_{50}\beta_1 2$).

4) $logK_D$ values for a certain ligand can also be obtained by inhibition of an agonist response. $logK_D$ values for the ligand can be derived from the parallel rightwards shift of the agonist response caused by the addition of a fixed concentration of ligand using the equation presented in the methods chapter. These $logK_D$ should always be the same independently of the agonist used to mediate the response. This is true for the β_2-AR as no secondary conformation is observed for this receptor, but not for the β_1 where CGP12177-mediated response via the secondary conformation was found more resistant to antagonism by every literature ligand previously tested. That being said, fixed concentrations of ligand can be added to increasing concentrations of a secondary conformation agonist (eg. CGP12177) to obtain a $logK_D$ for this conformation (referred to as $logK\beta_{1L}$ in the literature and $logK_{DCGP}$ in this thesis). Likewise, $logK_D$ values for the primary conformation can be obtained by the righshifting the response mediated by a primary conformation agonist (eg. cimaterol (**20**) - referred to as $logK\beta_{1H}$ in the literature and $logK_{Dcim}$ in this thesis), which should equal the $logK_D$ values obtained from binding.

5) For those compounds from the set which are able to elicit a response through the receptor, a fixed concentration of an antagonist (eg. CGP20712A (**19**) for β_1-AR; ICI118551 (**21**) for β_2-AR) can be added, and their ability to righshift the response can be measured. This will help to distinguish responses mediated through the primary and secondary conformation of the β_1-AR as responses mediated via the secondary conformation are known to be more resistant to CGP20712A, requiring higher concentration of the antagonist to produce a shift in the response and therefore yielding higher $logK_DCGP20712A$ values.

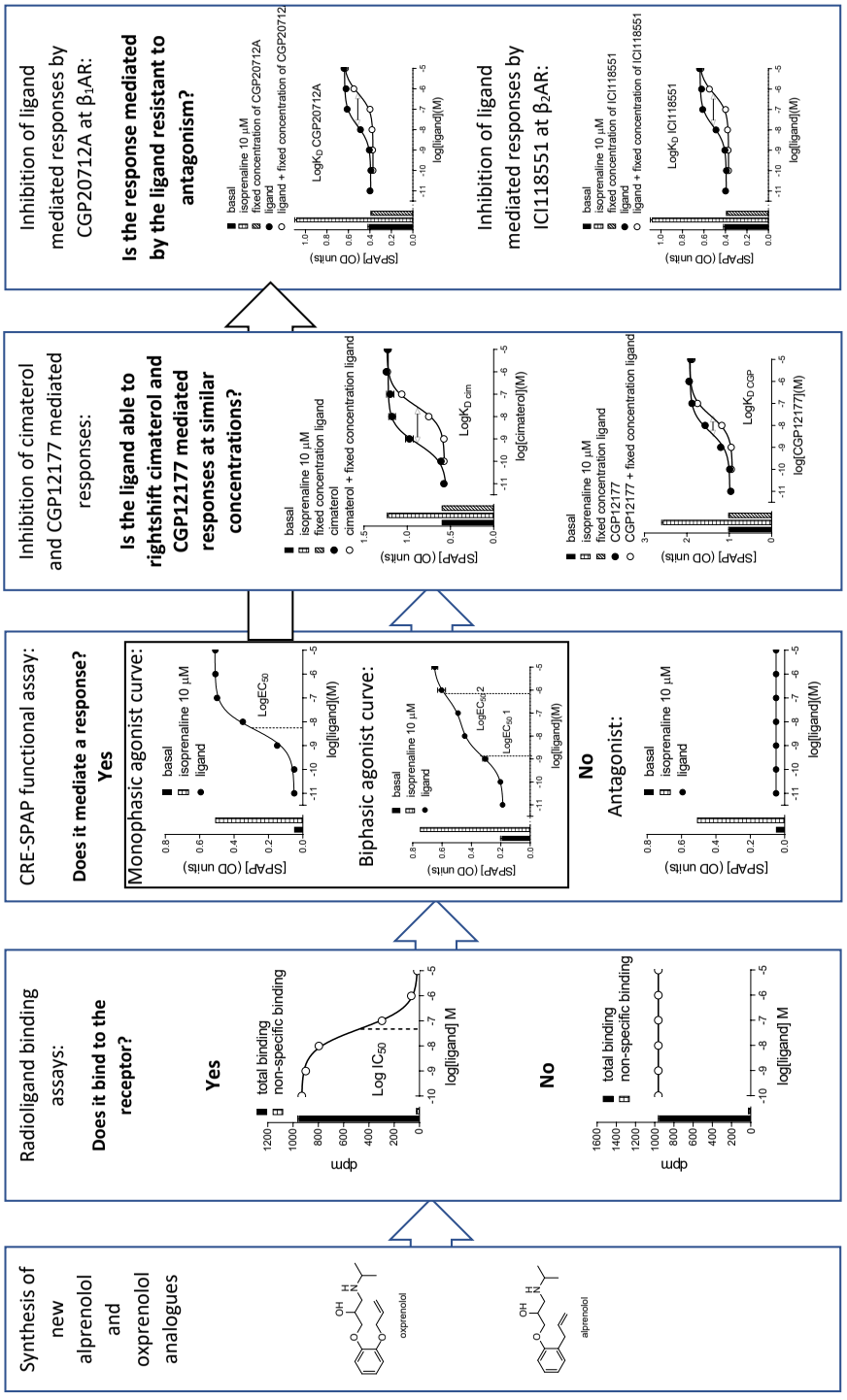
Synthesis of new alprenolol and oxprenolol analogues
oxprenolol
alprenolol
Radioligand binding assays:
Does it bind to the receptor?
Yes
total binding
non-specific binding
Log IC50
log[ligand] M
dpm
No
CRE-SPAP functional assay:
Does it mediate a response?
Yes
Monophasic agonist curve:
basal
isoprenaline 10 µM
ligand
LogEC50
log[ligand](M)
[SPAP] (OD units)
Biphasic agonist curve:
LogEC50/2
LogEC50/1
No
Antagonist:
Inhibition of cimaterol and CGP12177 mediated responses:
Is the ligand able to rightshift cimaterol and CGP12177 mediated responses at similar concentrations?
fixed concentration ligand
cimaterol
cimaterol + fixed concentration ligand
LogKD cim
log[cimaterol](M)
CGP12177
CGP12177 + fixed concentration ligand
LogKD CGP
log[CGP12177](M)
Inhibition of ligand mediated responses by CGP20712A at β1AR:
Is the response mediated by the ligand resistant to antagonism?
CGP20712A
ligand + fixed concentration of CGP20712A
LogKD CGP20712A
Inhibition of ligand mediated responses by ICI118551 at β2AR:
ICI118551
ligand + fixed concentration of ICI118551
LogKD ICI118551

Chapter 2

Pharmacological characterisation of literature compounds in CHO-β_1 and CHO-β_2 cells

2.1 Introduction

In this chapter, a thorough validation of CHO cells expressing either the human β_1 or β_2-AR and a CRE-SPAP reporter gene is described. Several literature compounds were characterised in this system in order to validate the cell lines used in the following experiments. Initially, [^{3}H]-CGP12177 affinity was determined for both receptors by saturation binding assays. This ligand was used afterwards to obtain the affinity for several β_1 (eg. CGP20712A **19** and bisoprolol **12**) and β_2-selective (eg. salbutamol, salmeterol) ligands in radioligand competitive binding assays. Pharmacological characterisation of these ligand in functional assays is presented. Herein, the phenomenon of the secondary conformation is also described and reproduced in CHO-β_1 cells. CHO-β_2 cells were used as a control cell line for this phenomenon to demonstrate that the phenomenon observed is not an artefact of the experimental conditions used. The behaviour of alprenolol (**6**) and oxprenolol (**7**) at both β_1 and β_2-AR is also reproduced in this chapter.

2.1.1 Pharmacology

2.1.2 Radioligand competitive binding assay

Initially, K_D values for [^{3}H] CGP12177 in both CHO-β_1 and β_2 cell lines were determined by saturation binding. This is necessary in order to calculate $logK_D$ values for all ligands through radioligand competitive binding assays using the Cheng-Prusoff equation and [^{3}H] CGP12177 as radiolabeled ligand.[80] Figure 2.1 shows the total binding of the radioligand, in the presence of serum-free media, (which increases for increasing concentrations of radioligand) and the non-specific binding in the presence of 10 μM propranolol (**4**), which prevents the binding of the radioligand to the receptor. The specific binding function is determined by subtracting the total binding, which represents the binding of the radioligand to the receptor plus binding to other materials, and the nonspecific binding, which represents the binding of the radioligand only to other materials. The K_D values for β-AR binding of [^{3}H] CGP12177 were 0.26 ± 0.02 nM (n=10) for CHO-β_1 cell line and 0.20 ± 0.01 nM (n=10) for CHO-β_2.

Following the determination of the K_D values for [^{3}H] CGP12177, several literature ligands were used to displace this radioligand. In order to validate the CHO-cells expressing the human β_1 and β_2-AR, β_1 (eg. CGP20712A **19**, bisoprolol **12**) and β_2-selective ligands (eg. ICI118551 **21** and salmeterol) were used. Figure 2.2 shows the inhibition of [^{3}H] CGP12177 binding to whole cells by CGP20712A (**19**), salmeterol and ICI118551 (**21**). This figure represents the amount of radioactivity bound to the CHO-β_1 and CHO-β_2

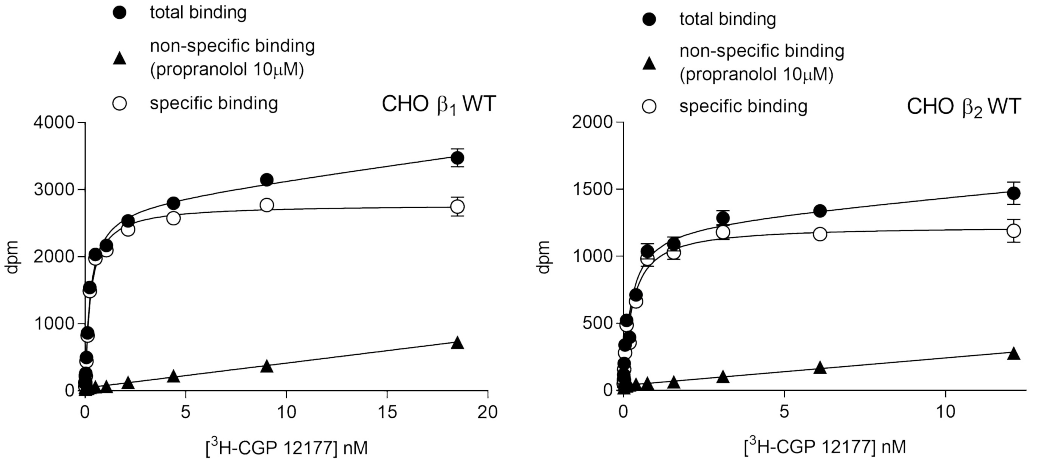

FIGURE 2.1: Saturation binding curves for the radioligand [^{3}H] CGP12177 in CHO-β_1 (left) and -β_2 (right) cells. Non-specific binding was determined in the presence of 10μM propranolol and was then subtracted to total binding to obtain the specific binding curve. Data points represent mean $\pm$ s.e.m. of quadriplicate determinations.

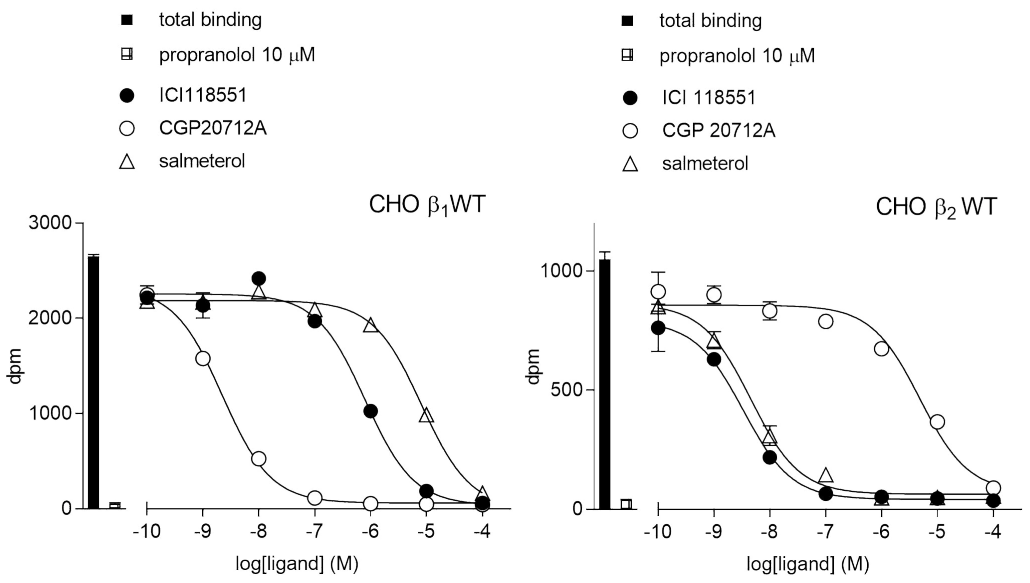

FIGURE 2.2: Inhibition of [^{3}H] CGP12177 binding to whole cells in CHO-β_1 and -β_2 by CGP20712A (**19**), ICI118551 (**21**) and salmeterol. Left bar represents total [^{3}H] CGP12177 binding for a concentration of 0.82 nM and the right one nonspecific binding which was determined in the presence of 10 μM propranolol. Data points represent mean $\pm$ s.e.m. of triplicate determinations.

cells at different concentration of ligand when a fixed concentration of 0.82 nM of radiolabeled [^{3}H] CGP12177 is added. CGP20712A (**19**) required much lower concentration to displace [^{3}H] CGP12177 in CHO-β_1 than CHO-β_2 cells, which is in accordance with its reported β_1 selectivity.[81] On the contrary, ICI118551 (**21**) and salmeterol required much lower concentrations to displace the radiolabeled ligand [^{3}H] CGP12177 from CHO-β_2 than CHO-β_1 cells, also in agreement with their previously described β_2 selectivity. [81]

Observed IC_{50} values were then converted in K_D values using the Cheng-Prusoff equation and represented in table 2.1 as $logK_D$ values. Selectivity is also presented in table 2.1 in a logarithmic scale in which a positive signal represents selectivity towards the β_2-AR while a negative signal represents selectivity towards the β_1-AR. As expected CGP20712A (**19**) and bisoprolol (**12**) showed a much higher affinity for the β_1-AR (lower $logK_D\beta_1$ value) than for the β_2-AR (3.11 log units higher for CGP20712A and 1.66 log units higher for bisoprolol), while, on the contrary, salmeterol and ICI118551 (**21**) exhibited a marked β_2-selectivity (3.21 log units for salmeterol and 2.42 log units for ICI118551). All the $logK_D$ values and selectivities obtained are in accordance with the values expected from cell lines expressing the β_1 or β_2-AR. [40]

Compound	$LogK_D\beta_1$	n	$LogK_D\beta_2$	n	$LogK_D(\beta_2/\beta_1)$
Salmeterol	-5.79 ± 0.06	7	-9.00 ± 0.04	7	3.21
ICI118551 (21)	-6.82 ± 0.04	12	-9.24 ± 0.05	11	2.42
Salbutamol	-4.72 ± 0.05	5	-5.89 ± 0.05	5	1.17
Alprenolol (6)	-7.94 ± 0.02	6	-9.01 ± 0.04	6	1.07
Propranolol (4)	-8.20 ± 0.04	5	-9.22 ± 0.06	5	1.02
Oxprenolol (7)	-7.89 ± 0.02	6	-8.77 ± 0.03	6	0.88
Bucindolol (14)	-9.35 ± 0.09	13	-10.18 ± 0.02	9	0.83
Bisoprolol (12)	-7.99 ± 0.07	6	-6.33 ± 0.10	6	-1.66
CGP20712A (19)	-8.97 ± 0.07	16	-5.86 ± 0.04	15	-3.11

TABLE 2.1: Binding affinities and selectivity for human β-adrenergic receptors of known ligands. Values represent mean of data obtained and ± the standard error of the mean (s.e.m) for n separate experiments

2.1.3 CRE-SPAP production

Following the characterisation of these literature compounds through radioligand binding assays, their ability to mediate an increase in CRE-SPAP production in these cell lines was evaluated. As mentioned before, CHO cells expressing either the human β_1 or β_2-AR and a CRE-SPAP reporter gene were used throughout these experiments. In this system, transcription of secreted placental alkaline phosphatase (SPAP) is facilitated in the presence of cAMP and is used as an amplified downstream measurement of cAMP production upon receptor activation. [82, 83]. Although full and partial agonists are expected to stimulate an increase in SPAP concentration, antagonists should fail to mediate any response. Full agonists are expected to mediate a full response (maximal response identical to the positive control of of 10μM of isoprenaline used) with a $logEC_{50}$ value equal or lower to the $logK_D$, while partial agonists should require a similar concentration to occupy and activate the receptor as they require full receptor occupation to stimulate their maximal response ($logEC_{50}$ should be identical to $logK_D$).

CRE-SPAP production in response to salmeterol, CGP20712A (**19**) and ICI118551 (**21**) is represented in figure 2.3. As previously observed in the literature, salmeterol is able to increase CRE-SPAP production in both CHO-β_1 and β_2 cells, with a maximum response similar to the response of 10μM of isoprenaline (% isop), therefore behaving as a full agonist at both receptors. [84] This compound required a much higher concentration to mediate a response through the β_1 than β_2-AR as displayed in figure 2.3, consistent with its β_2-selectivity.

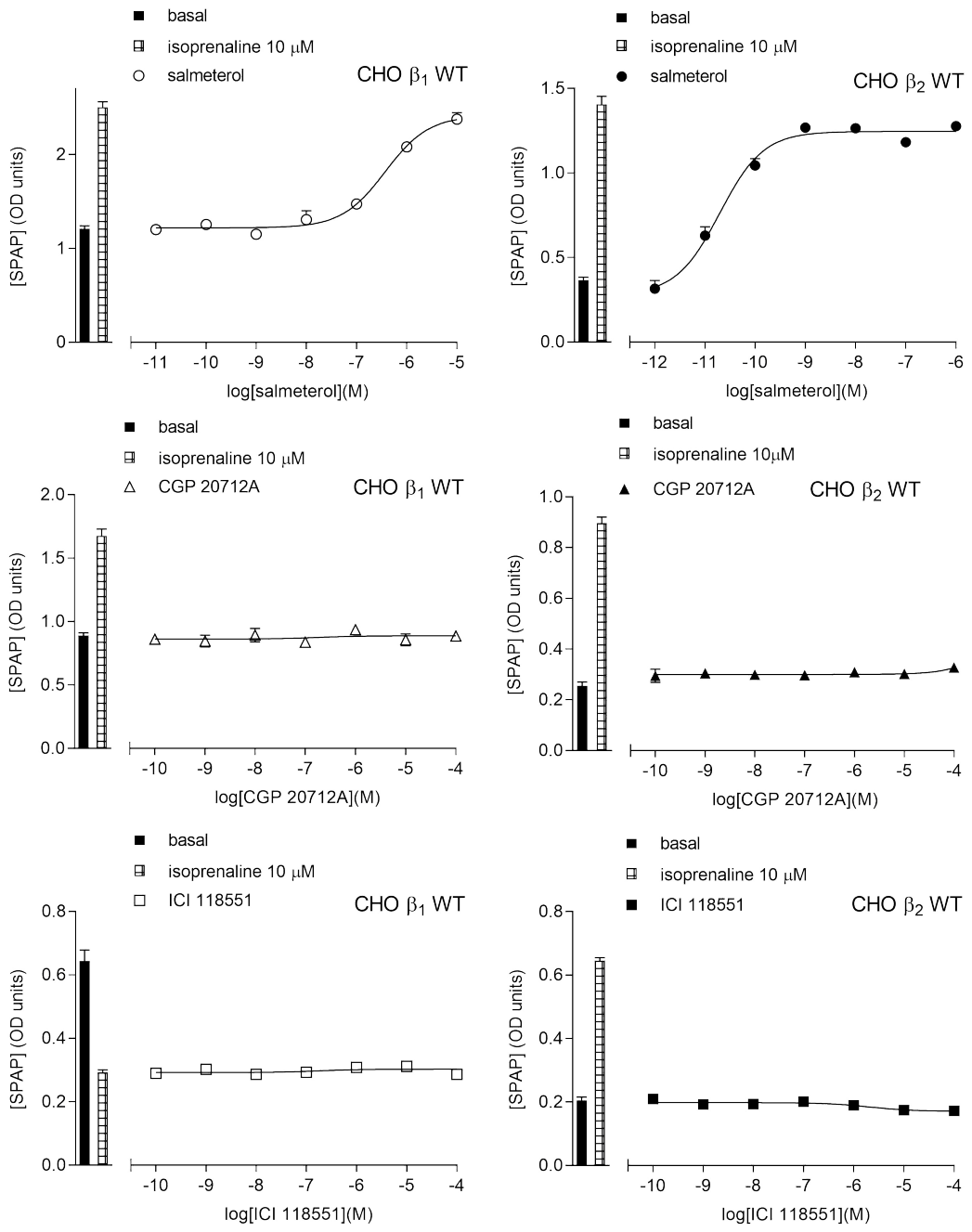

FIGURE 2.3: CRE-SPAP production in response to salmeterol (top), CGP20712A (**19**, middle) and ICI118551 (**21**, bottom) in CHO-β_1 and β_2 cells. Basal bar represents the SPAP accumulation in the presence of serum free media, while isoprenaline 10μM bar represents SPAP accumulation in the presence of 10μM of isoprenaline. Data points represent mean $\pm$ s.e.m. of triplicate determinations.

CGP20712A (**19**) and ICI118551 (**21**) failed to mediate a response in both CHO-β_1 and

Compound	$LogK_D\beta_1$	n	$LogEC_{50}\beta_1$	%isop	n
ICI118551 (21)	-6.82 ± 0.04	12	-	No response	6
Propranolol (4)	-8.20 ± 0.04	5	-	No response	3
Salmeterol	-5.79 ± 0.06	7	-6.36 ± 0.04	109 ± 8	3
CGP20712A (19)	-8.97 ± 0.07	16	-	No response	6
Salbutamol	-4.72 ± 0.05	5	-6.53 ± 0.18	99 ± 5	7
Fenoterol	-5.04 [a]		-7.38 ± 0.03	111 ± 4	3
Cimaterol (20)	-6.57 [a]		-8.72 ± 0.06	90 ± 2	27
CGP12177 (16)	-9.58		-7.99 ± 0.07	67 ± 3	27

TABLE 2.2: $LogK_D$, $logEC_{50}$ and $\%isop$ maximum responses for several literature compounds are presented in the table for β_1-AR. $LogK_D$ values were derived from IC_{50} values obtained through radioligand competitive binding assays (figure 2.2). $LogEC_{50}$ were obtained from CRE-SPAP functional assays (figure 2.3) and $\%isop$ represents the percentage of the response generated by 10μM isoprenaline which is the maximum response the cells is able to generate. Values represent mean of data obtained and ± the standard error of the mean (s.e.m) for n separate experiments. [a] values taken from Baker *et al* [84].

CHO-β_2 cells even though they bind to the receptors as shown by radioligand competitive binding assays, behaving, therefore, as antagonists at both receptors (figure 1.3). $LogEC_{50}$ values and the percentage of maximum isoprenaline response are presented in tables 2.2 and 2.3 for the β_1 and β_2-AR, respectively. Propranolol (**4**), CGP20712A (**19**) and ICI118551 (**21**), well described β_1 and β_2-AR antagonists, failed to mediate a response at either receptor. Salmeterol, as shown in figure 2.3, stimulated an increase of CRE-SPAP production at CHO-β_1 cells with a $logEC_{50}\beta_1 = -6.36 \pm 0.04$ and a $\%isop = 109 \pm 8$ and at CHO-β_2 cells with a $logEC_{50}\beta_2 = -9.75 \pm 0.02$ and a $\%isop = 104 \pm 8$. Salbutamol, fenoterol and cimaterol (**20**) were able to stimulate a response in both receptors, yielding a much lower $logEC_{50}$ than the respective $logK_D$ derived from radioligand binding assays. CGP12177 (**16**) behaved as a weak partial agonist at the β_2-AR with a $logEC_{50}\beta_2 = -9.69 \pm 0.04$ ($logK_D = -9.70$ from saturation binding assays) and a $\%isop = 37 \pm 4$. As mentioned during the introduction, CGP12177 (**16**) yielded a $LogEC_{50}\beta_1 = -7.99 \pm 0.07$ ($\%isop = 67 \pm 3$) higher than the $logK_D = -9.58$. This behaviour of CGP12177 (**16**) at the β_1-AR will be described in further detail later on this chapter.

Addition of a fixed concentration of antagonist to increasing concentrations of agonist constitutes an alternative way to determine the binding affinity of the antagonist. These affinity values are derived from the ability of the antagonist to parallel rightward shift the dose response of the agonist. In figure 2.3, the concentration response of cimaterol (**20**) in the presence and absence of either CGP20712A (**19**) and ICI118551 (**21**) in both

Compound	$LogK_D\beta_2$	n	$LogEC_{50}\beta_2$	%isop	n
ICI118551 (21)	-9.24 ± 0.05	11	-	No response	6
Propranolol (4)	-9.22 ± 0.06	5	-	No response	3
Salmeterol	-9.00 ± 0.04	7	-9.75 ± 0.02	104 ± 8	3
CGP20712A (19)	-5.86 ± 0.04	15	-	No response	6
Salbutamol	-5.89 ± 0.05	5	-7.91 ± 0.16	99 ± 6	3
Fenoterol	-7.03 [a]		-9.10 ± 0.04	106 ± 10	3
Cimaterol (20)	-7.26 [a]		-9.85 ± 0.04	90 ± 1	21
CGP12177 (16)	-9.70		-9.69 ± 0.04	37 ± 4	18

TABLE 2.3: $LogK_D$, $logEC_{50}$ and $\%isop$ maximum responses for several literature compounds are presented in the table for β_2-AR. $LogK_D$ values were derived from IC_{50} values obtained through radioligand competitive binding assays (figure 2.2). $LogEC_{50}$ were obtained from CRE-SPAP functional assays (figure 2.3) and $\%isop$ represents the percentage of the response generated by 10μM isoprenaline which is the maximum response the cells is able to generate. Values represent mean of data obtained and ± the standard error of the mean (s.e.m) for n separate experiments. values taken from Baker *et al* [84].

CHO-β_1 and β_2 cells is represented. Basal accumulation, in the presence of the serum free media, is identical to SPAP accumulation of the fixed concentration of CGP20712A (**19**) or ICI118551 (**21**) used, yielded similar SPAP which is consistent with the antagonist activity of these ligands previously demonstrated in both β_1 and β-ARs. CGP20712A (**19**) was able to rightshift the cimaterol concentration response in both receptors, even though this required a much higher concentration to rightshift this response at the β_2-AR, consistent with its β_1 selectivity. $logK_D$ values obtained for CGP20712A (**19**) through this assay were comparable to $logK_D$ values obtained from radioligand binding assays for both β_1-AR ($logK_D\beta_1 = -9.23 \pm 0.11$, n=6 vs $logK_D\beta_1 = -8.97$, respectively) and β_2-AR ($logK_D\beta_2 = -6.12 \pm 0.07$, n=7 vs $logK_D\beta_2 = -5.86$. Similarly, $logK_D$ values obtained for ICI118551 (**21**) through these functional assays were consistent with the values obtained from radioligand binding assays ($logK_D\beta_1 = -7.21 \pm 0.08$, n=9 vs $logK_D\beta_1 = -6.82$) ($logK_D\beta_2 = -9.84 \pm 0.06$, n=8 vs $logK_D\beta_2 = -9.24$). Overall, this similarity observed in the K_D values obtained for both CGP20712A (**19**) and ICI118551 (**21**) from radioligand binding assays and functional assays show that these ligands are able to compete and block cimaterol response with an affinity similar to the one they require to bind the receptors. This therefore demonstrates that cimaterol (**20**) is stimulating a response through the well-known catecholamine binding site of both receptors.

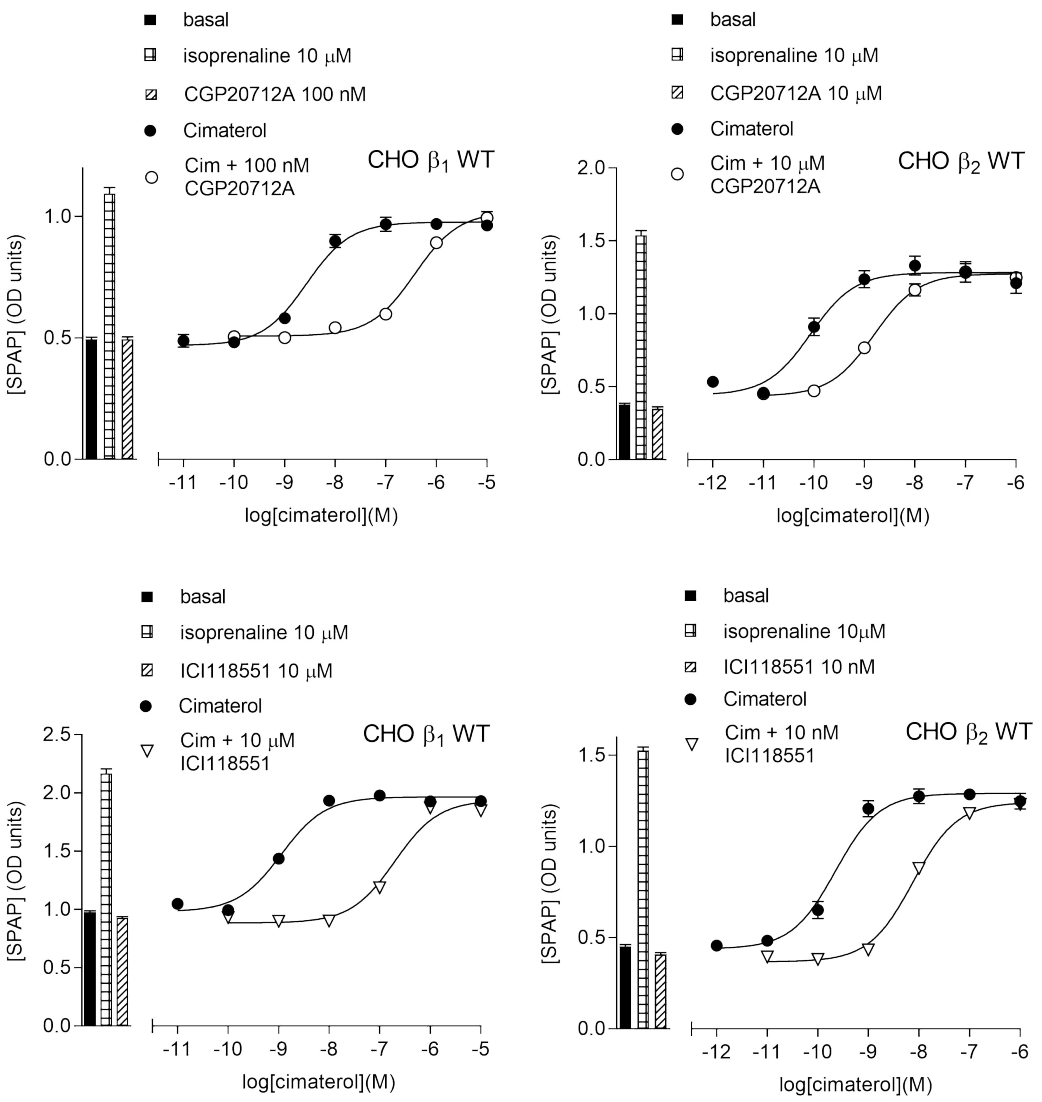

FIGURE 2.4: Left: CRE-SPAP production in response to cimaterol (**20**) in the absence and presence of CGP20712A (**19**) and ICI118551 (**21**) in CHO-β_1 cells; Right: CRE-SPAP production in response to cimaterol in the absence and presence of CGP20712A and ICI118551 in CHO-β_2 cells. Data points represent mean ± s.e.m. of triplicate determinations.

2.1.4 Pharmacology of CGP12177 (16)

2.1.4.1 CGP12177 (16) behaviour at β_2-AR

CGP12177 (**16**) binds with high affinity to the β_2-AR ($logK_D\beta_2 = -9.70$) and mediates a response with a $logEC_{50}\beta_2 = -9.69$ and a $\%isop = 37\%$, an identical value to the $logK_D$ obtained for this receptor from the radioligand binding assays (table 2.3). This is consistent with a partial agonistic behaviour, in which the ligand is expected to

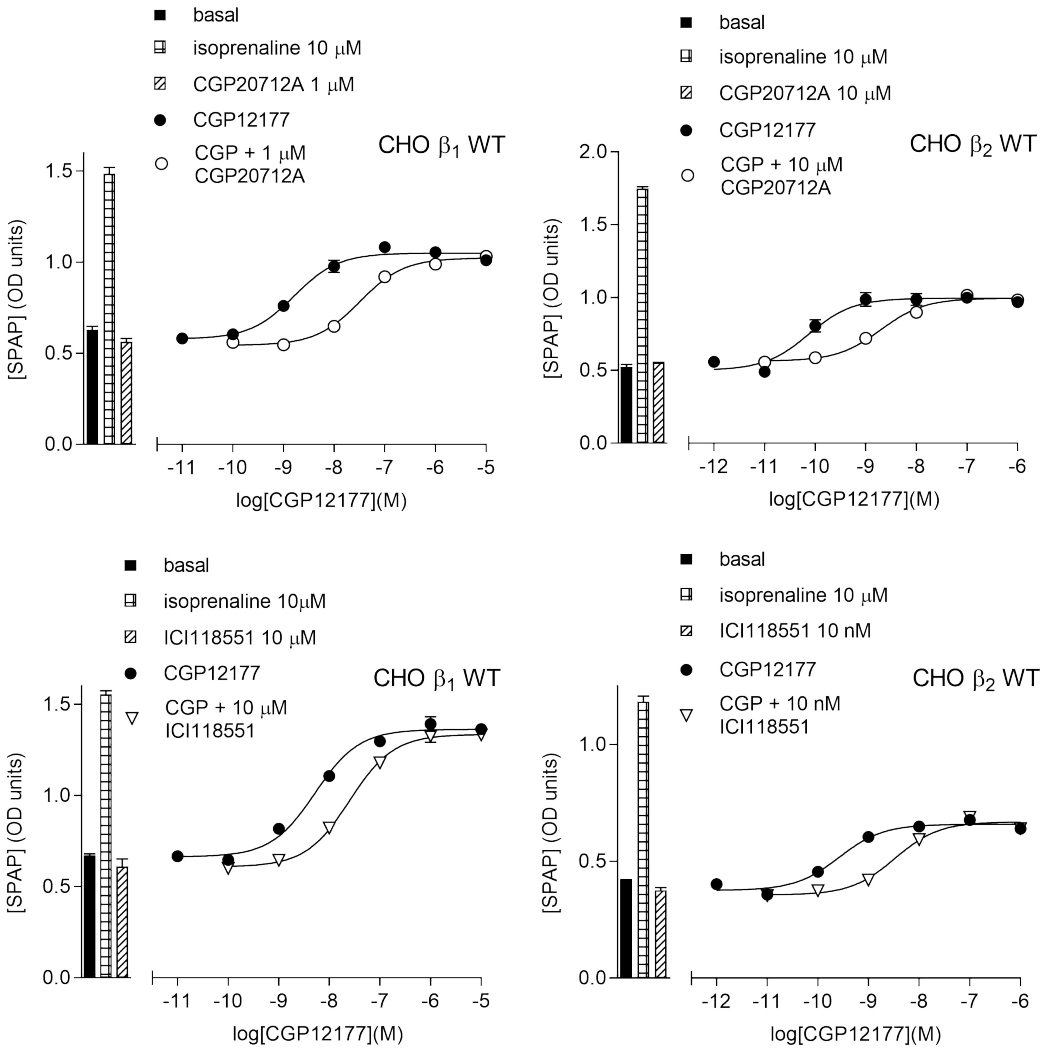

FIGURE 2.5: Left: CRE-SPAP production in response to CGP12177 (**16**) in the absence and presence of CGP20712A (**19**) and ICI118551 (**21**) in CHO-β_1 cells; Right: CRE-SPAP production in response to CGP12177 in the absence and presence of CGP20712A and ICI118551 in CHO-β_2 cells. Data points represent mean ± s.e.m. of triplicate determinations.

stimulate half of its maximal response when occupying half of the receptors. Figure 2.5 right displays CGP12177 concentration response curve in CHO-β_2 cells in the absence or presence of a fixed concentration of CGP20712A (**19**) or ICI118551 (**21**). Both of these antagonists were able to block CGP12177 (**16**) and rightshift its concentration response curve similarly to observed for cimaterol response in figure 2.4. $LogK_D$ values for CGP20712A (**19**) and ICI118551 (**21**) derived from this method are presented in table 2.4 along with the $logK_D$ values obtained for these antagonists using cimaterol (**20**) as an agonist and the $logK_D$ values obtained from radioligand binding assays. $LogK_D$ values derived from this method using CGP12177 (**16**) as an agonist are identical to the $logK_D$

values obtained when using cimaterol (**20**) as an agonist for both CGP20712A ($logK_D$ of -6.23 vs -6.12, respectively) and ICI118551 ($logK_D$ of -9.48 vs -9.84, respectively). These $logK_D$ values are slightly lower than the values obtained from radioligand binding assays.

Overall, CGP12177 (**16**) acts as a partial agonist at the β_2-AR mediating a response with a $logEC_{50}\beta_2$ value identical to the $logK_D\beta_2$ obtained from radioligand binding assays, meaning this response is mediated through the catecholamine site where CGP12177 competed with [^{3}H] CGP12177 in radioligand binding assays. The response mediated by CGP12177 (**16**) is also inhibited by CGP20712A (**19**) and ICI118551 (**21**) at the binding site in a manner consistent with the affinities of this antagonists which proves once again that this response is mediated through the orthosteric catecholamine binding site.

2.1.4.2 CGP12177 behaviour at β_1-AR

CGP12177 (**16**) is also able to bind with high affinity to the β_1-AR with a $logK_D\beta_1 = -9.58$. However, unlike for the β_2-AR, CGP12177 is only able to mediate a response through the β_1-AR at much higher concentration ($logEC_{50}\beta_1 = -7.99$, $\%isop = 67\%$) than it requires to bind the receptor (table 2.2). As mentioned in chapter 1, this CGP12177 anomalous behaviour at the β_1-AR was initially described by Pak and Fishman and observed in several systems both *in vitro* and *in vivo*. [14] This has also been observed in the system used in these experiments as displayed in table 2.2, $logEC_{50}\beta_1$ obtained for CGP12177 was greater by 1.59 log units to the $logK_D\beta_1$ determined by radioligand binding assays.

The response elicited by CGP12177 (**16**) at the β_1-AR is more resistant to antagonism by both CGP20712A (**19**) and ICI118551 (**21**) (figure 2.5). Addition of a fixed concentration of either CGP20712A (**19**) or ICI118551 (**21**) to increasing concentrations of CGP12177 (**16**) produced a strikingly less parallel rightshift than previously observed for cimaterol response in figure 2.4. This is indeed noticeable in the derived $logK_D$ values for CGP20712A (**19**) and ICI118551 (**21**) obtained from the inhibition of CGP12177 response (table 2.4). A $logK_D = -7.23$ was obtained for CGP20712A (**19**) when using CGP12177 (**16**) as an agonist which differs from both the $logK_D$ obtained when using cimaterol (**20**) as an agonist ($logK_D = -9.23$) and the $logK_D$ obtained from radioligand binding assays ($logK_D\beta_1 = -8.97$). Similarly, a higher $logK_D$ is obtained for ICI118551 (**21**) when using CGP12177 (**16**) as an agonist ($logK_D = -5.76$) (table 2.4). As previously referred, this anomolous behaviour is not observed at the β_2-AR where the $logK_D$ obtained for these antagonists were identical whether cimaterol (**20**) or CGP12177 (**16**) were used as agonists.

CHO-β_1 cells							
Compound	$LogK_D\beta_1$	$LogEC_{50}\beta_1$	% isop	CGP20712A $LogK_D$	n	ICI118551 $LogK_D$	n
Cimaterol (20)	-6.57 [a]	-8.72	90	-9.23 ± 0.11	6	-7.21 ± 0.08	9
CGP12177 (16)	-9.58	-7.99	67	-7.23 ± 0.07	7	-5.76 ± 0.09	9
CHO- β_2 cells							
Compound	$LogK_D\beta_2$	$LogEC_{50}\beta_2$	% isop	CGP20712A $LogK_D$	n	ICI118551 $LogK_D$	n
Cimaterol (20)	-7.26 [a]	-9.85	90	-6.12 ± 0.07	7	-9.84 ± 0.06	8
CGP12177 (16)	-9.70	-9.69	37	-6.23 ± 0.19	4	-9.48 ± 0.07	8

TABLE 2.4: $LogK_D$, $logEC_{50}$ and $\%isop$ maximum responses for CGP12177 (**16**) and cimaterol (**20**) are presented in the table for β_1 and β_2-AR. $LogK_D$ values were derived from IC_{50} values obtained through radioligand competitive binding assays (figure 2.2). $LogEC_{50}$ were obtained from CRE-SPAP functional assays (figure 2.3, 2.4 and 2.5) and $\%isop$ represents the percentage of the response generated by 10μM isoprenaline. CGP20712A $logK_D$ and ICI118551 $logK_D$ represents the affinity derived from the inhibition of the ligand CRE-SPAP production using fixed concentrations of either CGP20712A or ICI118551 in whole cell assays (figure 2.4 and 2.5). Values represent mean of data obtained and ± the standard error of the mean (s.e.m) for n separate experiments. [a] values taken from Baker *et al* [84].

The discrepancy between the $logK_D$ value obtained from radioligand competitive binding assays and the $logEC_{50}$ obtained from functional assays at the β_1-AR, together with the resistance to antagonism by known β-blockers suggest that CGP12177 (**16**) is mediating a response through a different conformation of the β_1-AR. A possible explanation for this phemonemon is the existence of a primary conformation of the β_1-AR where CGP12177 (**16**) binds with high affinity to the orthosteric binding site ($logK_D = -9.58$) and behaves as an antagonist at low concentrations and a secondary conformation where CGP12177 (**16**) binds at much higher concentrations (and, therefore with lower affinity) and elicits a response ($logEC_{50} = -7.99$) more resistant to antagonism. The fact that these CGP12177 responses are more resistant to antagonism by both CGP20712A (**19**) and ICI118551 (**21**) suggests that these ligands bind with lower affinity to this secondary conformation and so does CGP12177 (**16**). This can be observed in figure 2.6. Addition of a fixed concentration of cimaterol (**20**), able to increase CRE-SPAP gene transcription, to increasing concentrations of CGP12177 (**16**) result in high affinity inhibition of cimaterol response by CGP12177 followed by stimulation by CGP12177 at much higher concentrations in CHO-β_1 cells. This supports the idea that CGP12177 acts as a high affinity antagonist at the primary conformation of the β_1-AR, blocking cimaterol response, and then, at higher concentrations, elicits a response through the secondary conformation of the β_1-AR. Once again this phenomenon is not observed in

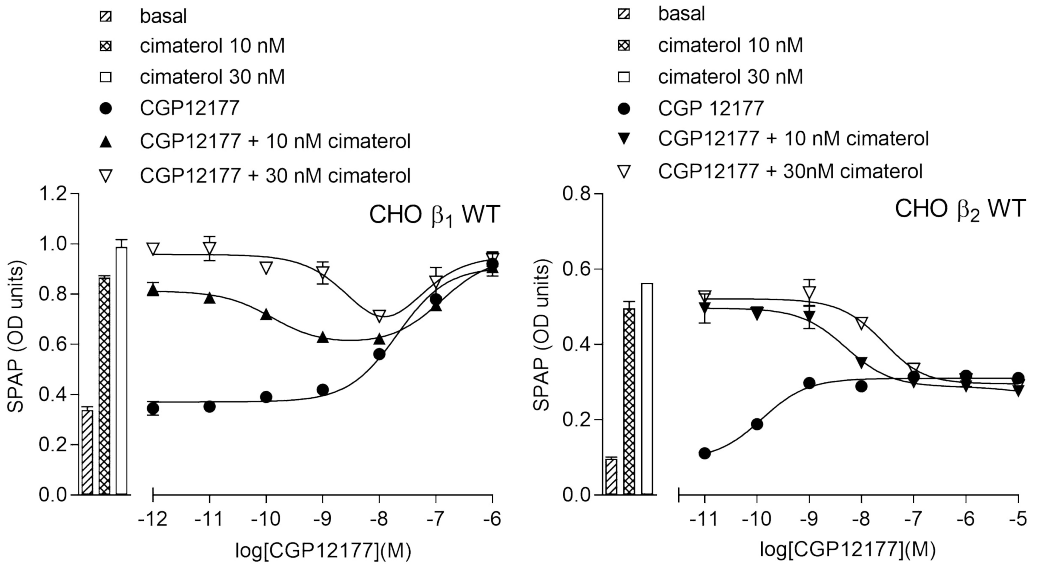

FIGURE 2.6: CRE-SPAP production in CHO-β_1 (left) and CHO-β_2 (right) whole cells in response to CGP12177 (**16**) in the absence and presence of 10 and 30 nM of cimaterol (**20**). Bars represent basal CRE-SPAP production and isoprenaline response at 10μM. Data points represent mean ± s.e.m. of triplicate determinations.

CHO-β_2 cells. Addition of a fixed concentration of cimaterol (**20**) to increasing concentrations of CGP12177 resulted in an inhibition of cimaterol response coherent with the response mediated by CGP12177 (**16**, figure 2.6 *right*).

2.1.5 Pharmacology of alprenolol (6) and oxprenolol (7) at β_1 and β_2-AR

Pharmacological characterisation of alprenolol (**6**) and oxprenolol (**7**) in CHO-β_1 and -β_2 cells is described here. The affinity of these compounds was initially evaluated through radioligand competitive binding assays using [^{3}H] CGP12177 as radioligand. Both alprenolol (**6**) and oxprenolol (**7**) displaced [^{3}H] CGP12177 in CHO-β_1 and -β_2 cells (figure 2.7). $LogK_D$ values derived from these inhibition curves are presented in table 2.5. Alprenolol (**6**) displayed a $logK_D\beta_1 = -7.94 \pm 0.02$ and a $logK_D\beta_2 = -9.01 \pm 0.04$, showing a slight selectivity towards the β_2-AR. Similarly, oxprenolol (**7**) demonstrates a slight selectivity towards the β_2-AR with a $logK_D\beta_2 = -8.77 \pm 0.03$ and $logK_D\beta_1 = -7.89 \pm 0.02$.

In CRE-SPAP functional assays, both alprenolol (**6**) and oxprenolol (**7**) are able to stimulate a response through the β_2-AR (figure 2.8 *right*). Alprenolol (**6**) elicited a partial agonistic response in CHO-β_2 cells with a $logEC_{50}\beta_2 = -9.45 \pm 0.05$ corresponding to 37% of the response elicited by 10μM of isoprenaline. Oxprenolol (**7**) also led to an

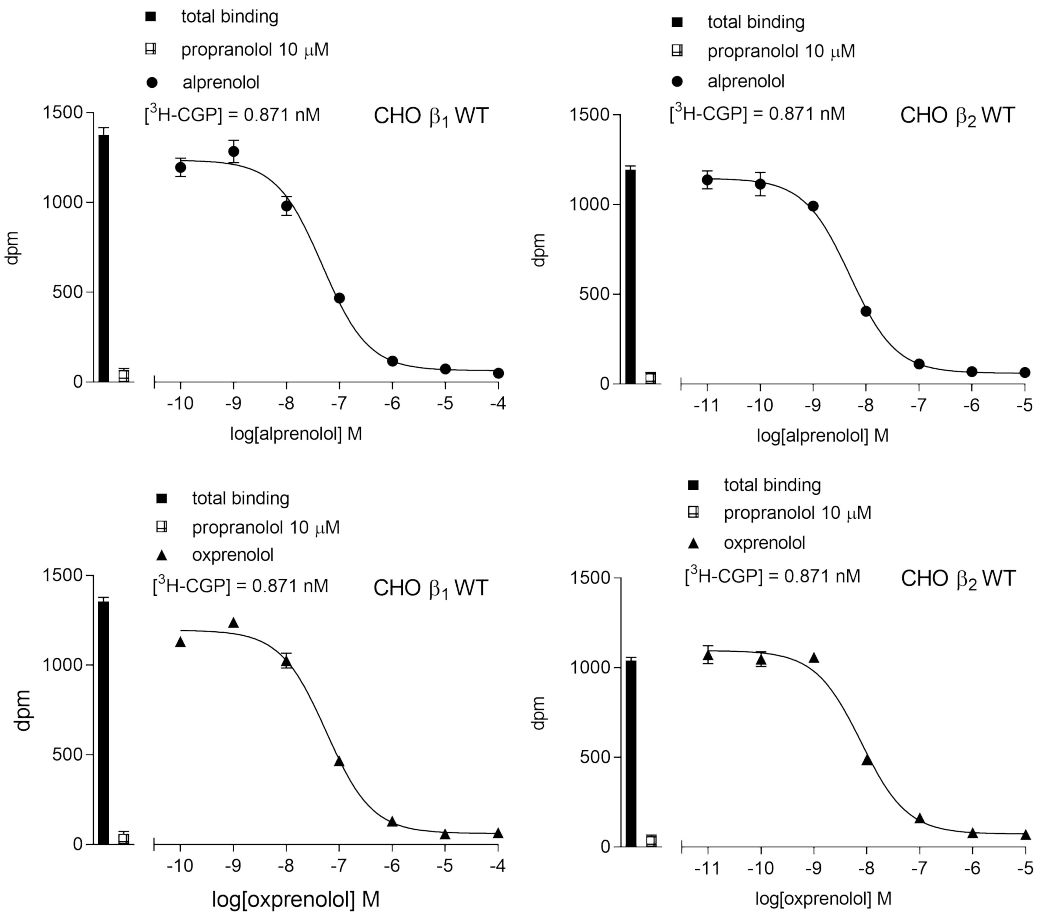

FIGURE 2.7: Inhibition of [^{3}H] CGP12177 binding to whole cells in CHO-β_1 and -β_2 by alprenolol (**6**) and oxprenolol (**7**). Left bar represents total [^{3}H] CGP12177 binding for a concentration of 0.871 nM and the right one nonspecific binding determined in the presence of 10 μM propranolol. Data points represent mean $\pm$ s.e.m. of triplicate determinations.

increase of SPAP accumulation with a $logEC_{50}\beta_2 = -9.15 \pm 0.07$ corresponding to 27% of isoprenaline response. Both ligands behaved as typical partial agonists at the β_2-AR with a $logEC_{50}$ similar to the $logK_D$ obtained from radioligand binding assays (-9.49 vs -9.01, respectively, for alprenolol; -9.15 vs -8.77, respectively, for oxprenolol). These responses elicited by alprenolol (**6**) and oxprenolol (**7**) at the β_2-AR are easily antagonised by ICI118551 (**21**, figure 2.9 *right*). $logK_D\beta_2$ determined for ICI118551 through this method using alprenolol (**6**) and oxprenolol (**7**) as agonists were identical to the $logK_D\beta_2$ obtained using cimaterol (**20**) and CGP12177 as agonists and to the $logK_D$ obtained from radioligand binding assays and are displayed in table 2.5 ($logK_D\beta_2$ for ICI118551 of -9.69 using alprenolol as agonist; -9.72 using oxprenolol as agonist; -9.84 using cimaterol as agonist; -9.48 using CGP12177 as agonist; -9.24 from radioligand competitive binding assays). The $logK_D$ values obtained for ICI118551 (**21**) through

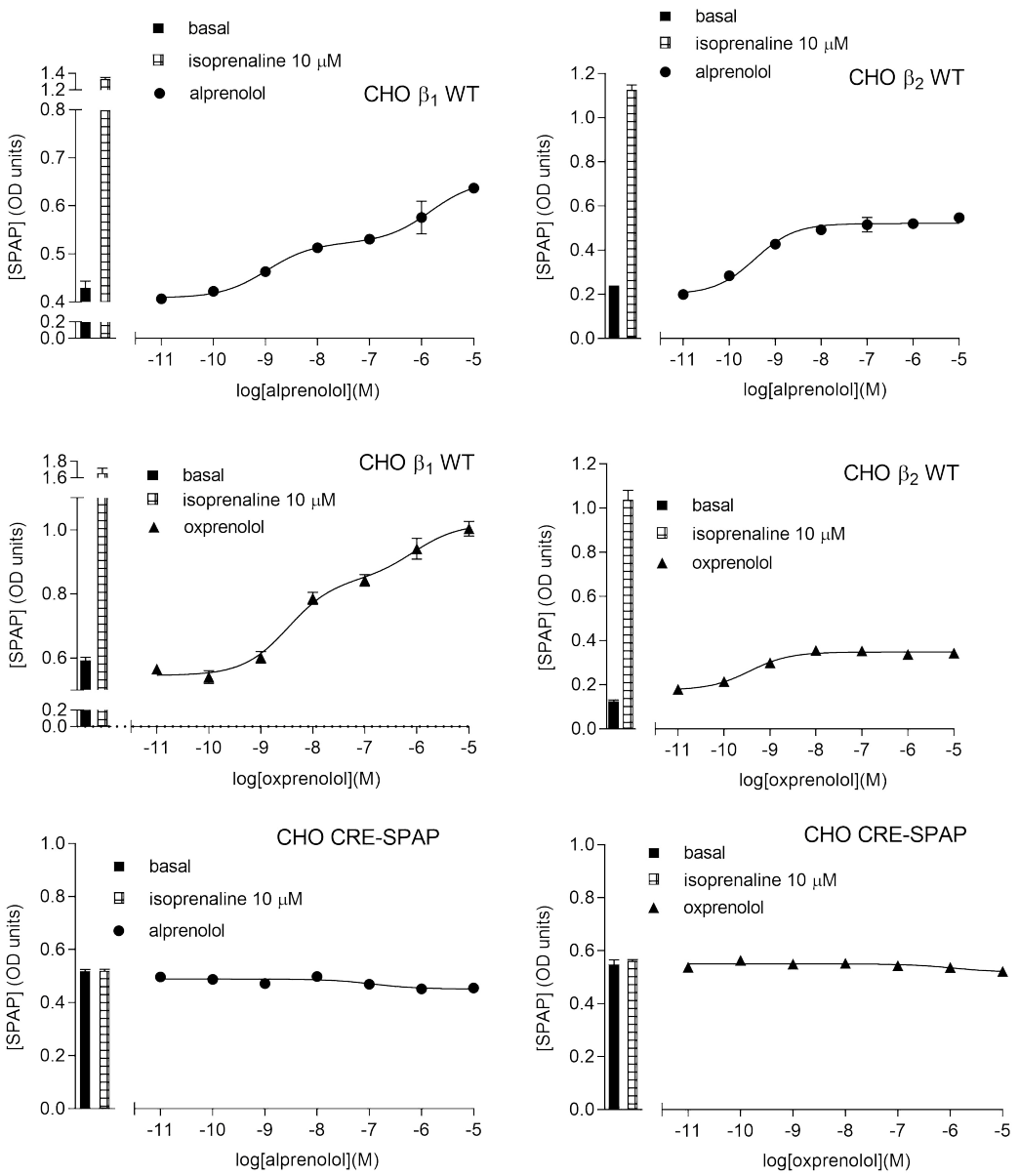

FIGURE 2.8: CRE-SPAP production in response to alprenolol (**6**) and oxprenolol (**7**) in CHO-β_1, CHO-β_2 and CHO CRE-SPAP (without receptor expression) cells. Basal bar represents the SPAP accumulation in the presence of serum free media, while isoprenaline 10μM bar represents SPAP accumulation in the presence of 10μM of isoprenaline. Data points represent mean $\pm$ s.e.m. of triplicate determinations.

this method are independent of the agonist used, as expected.

Similarly, a fixed concentration of a partial agonist can also be added to increasing concentrations of agonist to determine their $logK_D$ values using the derived equation reported by Stephenson *et al.* [85] Addition of 30 nM of alprenolol (**6**) to increasing

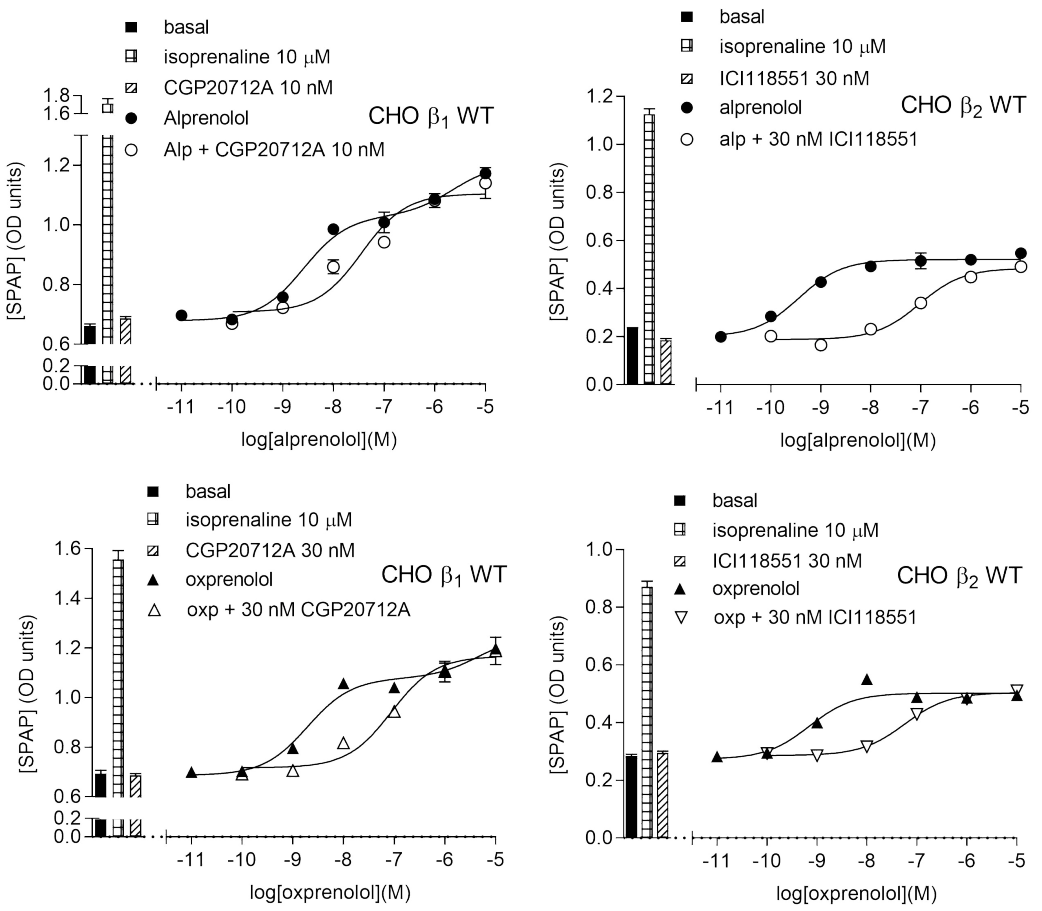

FIGURE 2.9: Top: CRE-SPAP production in response to alprenolol (**6**) in the absence and presence of CGP20712A (**19**) and ICI118551 (**21**) in CHO-β_1 and CHO-β_2 cells; Bottom: CRE-SPAP production in response to oxprenolol (**7**) in the absence and presence of CGP20712A and ICI118551 in CHO-β_1 and CHO-β_2 cells. Data points represent mean $\pm$ s.e.m. of triplicate determinations.

concentrations of cimaterol increases the basal level of SPAP in accordance with alprenolol partial agonist activity and is able to rightshift cimaterol response (figure 2.10). A $logK_D\beta_2 = -9.18 \pm 0.13$ was obtained for alprenolol (**6**) when using cimaterol as agonist, a value similar to $logK_D\beta_2 = -9.01$ from binding. A $logK_D\beta_2$ value for alprenolol (**6**) could not be obtained through this method using CGP12177 as an agonist since the response mediated by alprenolol is higher than the maximal response of CGP12177 at the β_2-AR as observed in figure 2.10 *right bottom*. $LogK_D$ values obtained from oxprenolol (**7**) through the righshifting of cimaterol ($logK_D = -9.13 \pm 0.07$) and CGP12177 ($logK_D\beta_2 = -8.87 \pm 0.15$) response were similar to the binding affinity obtained from radioligand binding assays ($logK_D\beta_2 = -8.77$).

CHO-β_1 cells										
Compound	Log$K_D\beta_1$	n	Log$EC_{50}\beta_1$1	Log$EC_{50}\beta_1$2	% site 1	n	% isop	n	CGP20712A LogK_D	n
Alprenolol (6)	-7.94 ± 0.02	6	-8.57 ± 0.15	-6.14 ± 0.13	43 ± 7	8	29 ± 4	12	-8.78 ± 0.11	3
Oxprenolol (7)	-7.89 ± 0.02	6	-8.59 ± 0.08	-5.94 ± 0.16	58 ± 4	10	38 ± 2	14	-8.70 ± 0.13	3
Cimaterol (20)	-6.57 [a]		-8.72 ± 0.06	-	-	27	90 ± 2	27	-9.23 ± 0.11	6
CGP12177 (16)	-9.58		-7.99 ± 0.07	-	-	27	67 ± 3	27	-7.23 ± 0.07	7
CHO-β_2 cells										
Compound	Log$K_D\beta_2$	n	Log$EC_{50}\beta_2$			n	% isop	n	ICI118551 LogK_D	n
Alprenolol (6)	-9.01 ± 0.04	6	-9.49 ± 0.05			11	37 ± 2	11	-9.69 ± 0.08	6
Oxprenolol (7)	-8.77 ± 0.03	6	-9.15 ± 0.07			12	27 ± 2	12	-9.72 ± 0.16	6
Cimaterol (20)	-7.26 [a]		-9.85 ± 0.04			21	90 ± 1	21	-9.84 ± 0.06	8
CGP12177 (16)	-9.70		-9.69 ± 0.04			18	37 ± 4	18	-9.48 ± 0.07	8

TABLE 2.5: $LogK_D$, $logEC_{50}$ and $\%isop$ maximum responses for alprenolol (**6**), oxprenolol (**7**), CGP12177 (**16**) and cimaterol (**20**) are presented in the table for β_1 and β_2-AR. $LogK_D$ values were derived from IC_{50} values obtained through radioligand competitive binding assays (figure 2.7). $LogEC_{50}$ were obtained from CRE-SPAP functional assays (figure 2.8) and $\%isop$ represents the percentage of the response generated by 10μM isoprenaline. $LogEC_{50}\beta_1 1$ represents the $logEC_{50}$ determined for the first (high affinity) component of a biphasic response curve while $LogEC_{50}\beta_1 2$ represents the value for the second component. $\%site1$ represents the percentage of total response accounted for the first component of a biphasic response curve. CGP20712A $logK_D$ and ICI118551 $logK_D$ represents the affinity derived from the shift of the first component response using fixed concentrations of either CGP20712A or ICI118551 in whole cell assays (figure 2.9). Values represent mean of data obtained and ± the standard error of the mean (s.e.m) for n separate experiments. [a] values taken from Baker *et al* [84]

In CHO-β_1 cells, both alprenolol (**6**) and oxprenolol (**7**) stimulated a biphasic response with two components (figure 2.8 *left*). Alprenolol (**6**) elicited a biphasic dose response curve with a $logEC_{50} = -8.57 \pm 0.15$ for the first component and a $logEC_{50} = -6.14 \pm 0.13$ for the second component, with the first component accounting for 43% of the maximal response (alprenolol total response 29±4% of isoprenaline maximum). Similarly, oxprenolol response at CHO-β_1 cells was best fitted in a two conformation model with a $logEC_{50} = -8.59 \pm 0.08$ for the first component and a $logEC_{50} = -5.94 \pm 0.16$ for the second component. First component response accounted for 58±4% of the total response and oxprenolol total response corresponded to 38±2% of isoprenaline maximum. $logEC_{50}$ values obtained for the first component of alprenolol (**6**) and oxprenolol (**7**) mediated response were around 0.6 log units higher than the $logK_D$ obtained from radioligand binding assays for these compounds (-8.57 vs -7.94, respectively, for alprenolol; -8.59 vs -7.89, respectively, for oxprenolol) (table 2.5).

It is notewhorty to mention that over cell passages the $\%iso$ responses declined, which most likely represent a reduction in receptor expression levels, therefore earlier passage cells were obtained periodically. This likely reduction in receptor expression level also seems to reduce the assay window leading to an apparent decrease of the percentage of response accounted for the first component of the response and will be mention and described later on chapter 4. CRE-SPAP production assays were also performed in cells only expressing CRE-SPAP alone without receptor expression in order to demonstrate that the biphasic response is receptor-dependent. As expected both alprenolol (**6**) and oxprenolol (**7**) failed to mediate an increase in SPAP accumulation in cells lacking receptor expression (figure 2.8 *bottom*).

In order to confirm that the first component of the biphasic response is mediated via the catecholamine site in the primary conformation the ability of CGP20712A (**19**) to parallel rightshift these responses was measured (figure 2.9 *left*). Addition of a 10 nM or 30 nM CGP20712A (**19**) fixed concentration led to an observable rightshift of the first component of the response while the second component remained unaltered (figure 2.9 *left*). This is consistent with the resistance to antagonism seen by this second component of the response, identically to CGP12177 mediated response. Addition of a higher CGP20712A (**19**) fixed concentration to these biphasic responses would result in a larger shift for the first component and a small shift for the second component of the response as described in the literature by Baker *et al.* [35] $LogK_D$ values obtained for CGP20712A from these assays are displayed in table 2.5. A $logK_D = -8.78 \pm 0.11$ was obtained for CGP20712A (**19**) when using alprenolol (**6**) as agonist, while a $logK_D = -8.70 \pm 0.13$ was determined when oxprenolol (**7**) was used as agonist. These values are similar to the $logK_D$ obtained for CGP20712A (**19**) from radioligand binding assays ($logK_D = -8.97$, table 2.1) but inferior to the $logK_D$ obtained when using cimaterol as agonist ($logK_D = -9.23$,

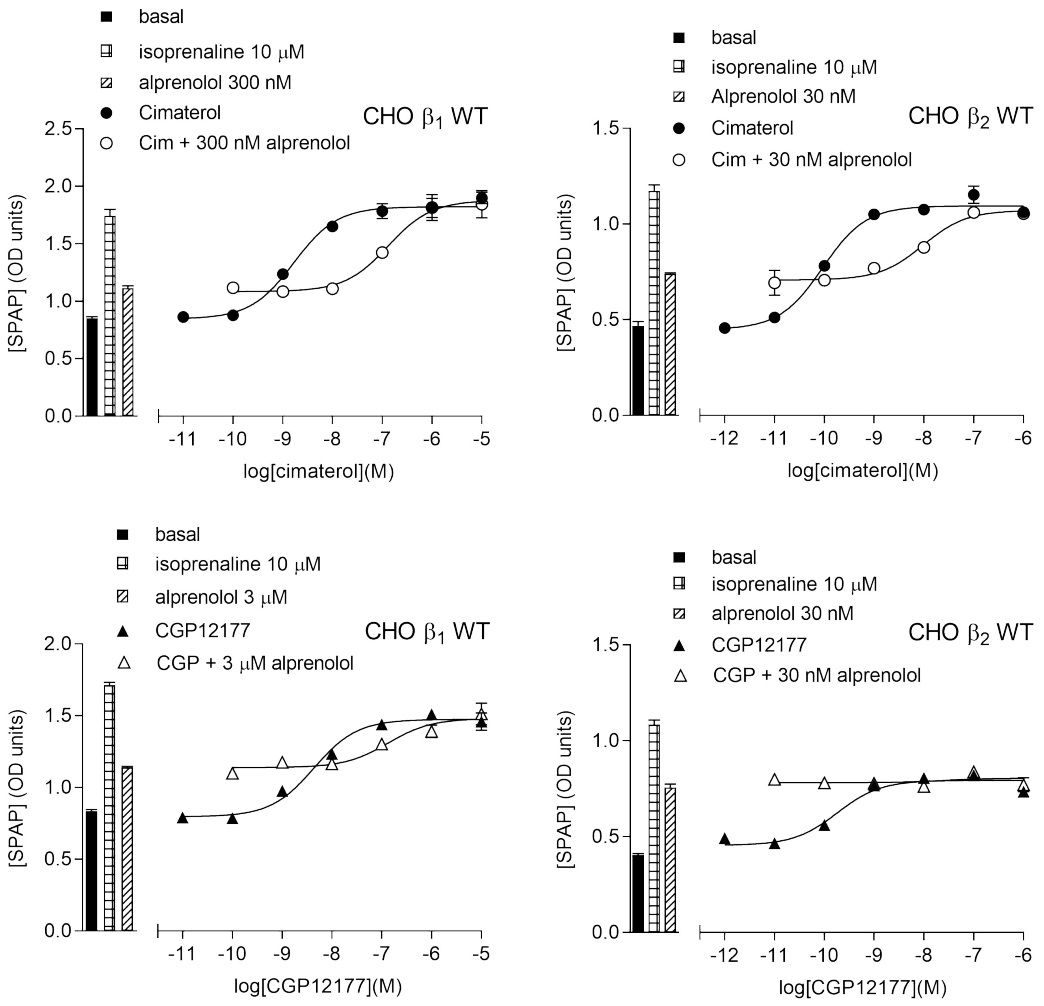

FIGURE 2.10: Top: CRE-SPAP production in response to cimaterol (**20**) in the absence and presence of alprenolol (**6**) in CHO-β_1 and CHO-β_2 cells; Bottom: CRE-SPAP production in response to CGP12177 in the absence and presence of alprenolol in CHO-β_1 and CHO-β_2 cells. Bars represent basal activity, SPAP production in the presence of 10μM and SPAP production in the presence of a fixed concentration of alprenolol. Data points represent mean $\pm$ s.e.m. of triplicate determinations.

table 2.4). Overall, this suggests that both alprenolol (**6**) and oxprenolol (**7**) are able to increase CRE-SPAP transcription at low concentrations through the primary conformation of the β_1-AR (first component of the biphasic response) and then increase the transcription further at higher concentrations through the secondary conformation of the β_1-AR (second component of the biphasic response). Furthermore, the first component of alprenolol and oxprenolol responses is easily antagonised by CGP20712A (**19**), in agreement with the high affinity of CGP20712A for the β_1-AR, again suggesting that this first component is mediated through the primary conformation of the β_1-AR.

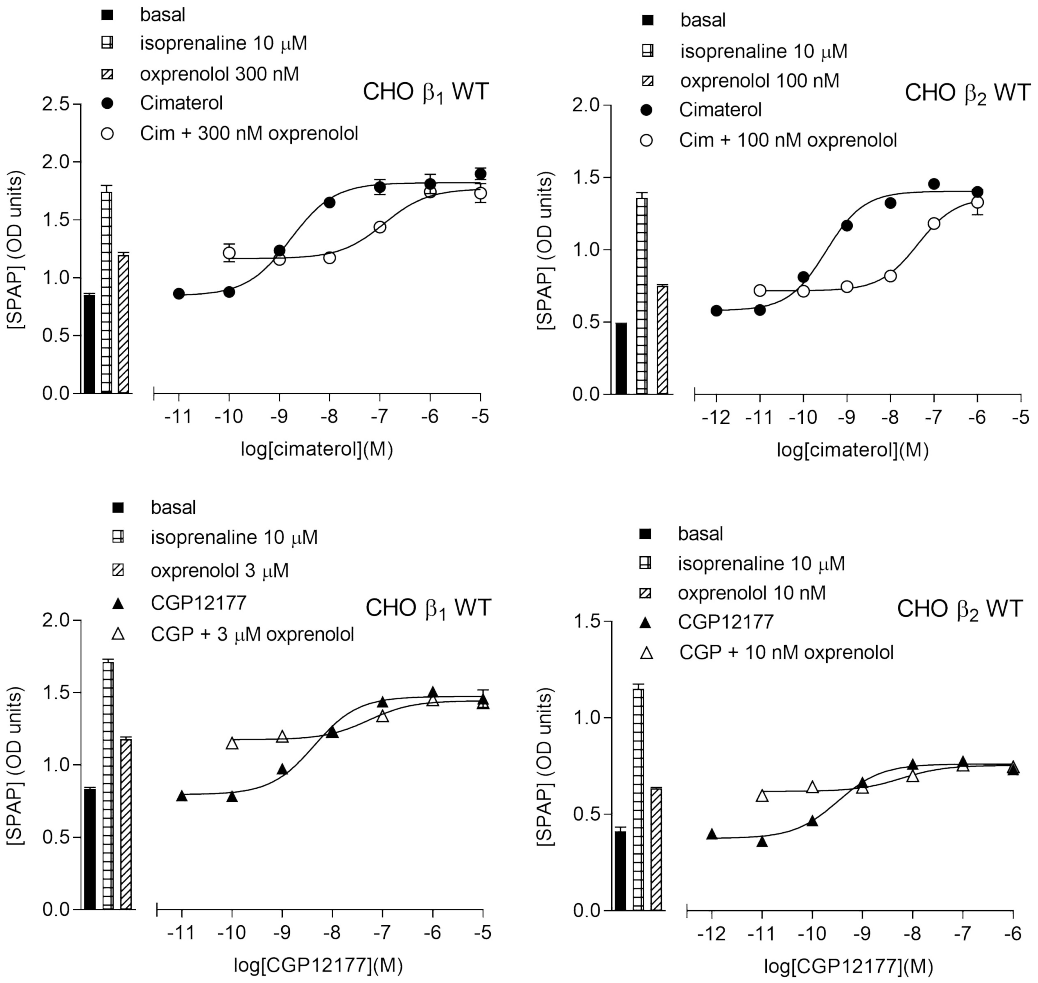

FIGURE 2.11: Top: CRE-SPAP production in response to cimaterol (**20**) in the absence and presence of oxprenolol (**7**) in CHO-β_1 and CHO-β_2 cells; Bottom: CRE-SPAP production in response to CGP12177 in the absence and presence of oxprenolol in CHO-β_1 and CHO-β_2 cells. Bars represent basal activity, SPAP production in the presence of 10μM and SPAP production in the presence of a fixed concentration of oxprenolol. Data points represent mean $\pm$ s.e.m. of triplicate determinations.

To confirm this second component of the responses is mediated through the same conformation secondary conformation via which CGP12177 elicits a response, alprenolol or oxprenolol fixed concentrations were used to inhibit CGP12177 response (figure 2.10 and 2.11). Addition of a 3μM concentration of alprenolol (**6**) to increasing concentrations of CGP12177 caused an increase in SPAP basal levels coherent with alprenolol (**6**) partial agonism and pushed CGP12177 response to the right (figure 2.10 *bottom left*). Addition of a lower concentration of alprenolol (30nM) to increasing concentrations of cimaterol (**20**) resulted in a much larger shift than observed for CGP12177 response (figure 2.10 *top left*). It is therefore clear that the response mediated by CGP12177 is also more

CHO-β_1 cells						
Compound	$LogK_D\ \beta_1$	$LogK_D\ \beta_{1\ cim}$ cimaterol as agonist	n	$LogK_D\ \beta_{1\ CGP}$ CGP12177 as agonist	n	$LogK_{D\ Cim} - LogK_{D\ CGP}$
Alprenolol (6)	-7.94	-8.19 ± 0.05	4	-6.40 ± 0.15	4	1.79
Oxprenolol (7)	-7.89	-8.18 ± 0.08	3	-6.15 ± 0.15	3	2.03
ICI118551 (21)	-6.82	-7.21 ± 0.08	9	-5.76 ± 0.09	9	1.45
CGP20712A (19)	-8.97	-9.23 ± 0.11	6	-7.23 ± 0.07	7	2.00
CHO- β_2 cells						
Compound	$LogK_D\ \beta_2$	$LogK_D\ \beta_{2\ cim}$ cimaterol as agonist	n	$LogK_D\ \beta_{2\ CGP}$ CGP12177 as agonist	n	$LogK_{D\ Cim} - LogK_{D\ CGP}$
Alprenolol (6)	-9.01	-9.18 ± 0.13	3	-	-	-
Oxprenolol (7)	-8.77	-9.13 ± 0.07	3	-8.87 ± 0.15	3	0.26
ICI118551 (21)	-9.24	-9.84 ± 0.06	8	-9.48 ± 0.07	8	0.36
CGP20712A (19)	-5.86	-6.12 ± 0.07	7	-6.23 ± 0.19	4	-0.11

TABLE 2.6: $LogK_D$ for alprenolol (**6**), oxprenolol (**7**), CGP20712A (**19**) and ICI118551 (**21**) are presented in the table for β_1 and β_2-AR. $LogK_D$ values were derived from IC_{50} values obtained through radioligand competitive binding assays (figure 2.7). $LogK_D$ were also determined through the inhibition of either cimaterol (**20**) or CGP12177 CRE-SPAP production using fixed concentrations of ligand in whole cell assays (figure 2.10 and 2.11). Values represent mean of data obtained and ± the standard error of the mean (s.e.m) for n separate experiments.

resistant to inhibition by alprenolol (**6**) in CHO-β_1 cells. $LogK_D$ obtained for alprenolol when using CGP12177 as agonist was consistent with the $logEC_{50}$ obtained for the second component of alprenolol (**6**) biphasic response (-6.40 vs -6.14, respectively; table 2.5 and 2.6). Similarly, oxprenolol (**7**) was able to inhibit CGP12177 elicited response with a $logK_D = -6.15$ similar to the $logEC_{50}$ obtained for the second component of its response ($logEC_{50} = 5.94$; figure 2.11, table 2.5 and 2.6). Altogether this strengthens the idea that alprenolol (**6**) and oxprenolol (**7**) are able to mediate a response through the primary conformation of the β_1-AR at low concentration and then further mediate a second response, corresponding to the second component, mediated through the secondary conformation of the β_1-AR.

2.2 Conclusion

In this chapter, a thorough validation of CHO cells expressing either the human β_1 or β_2-AR and a CRE-SPAP reporter gene was described in detail. Cell lines expressing either human β_1 or β_2-AR are able to differentiate between β_1 (eg. CGP20712A **19**) and β_2

selective (eg. ICI118551 **21**) compounds, yielding $logK_D$ and selectivity values identical to the literature.[81] In functional assays, agonists (eg. cimaterol, salmeterol) mediated responses with $logEC_{50}$ similar to the values referred in the literature while antagonists (eg. CGP20712A (**19**) and propranolol (**4**)) failed to increase SPAP accumulation. [81, 84]

Herein, the three main pieces of evidence that contributed to the hypothesis of the secondary conformation of the β_1-AR were presented in detail for the cell lines used throughout the experiments:

1) CGP12177 binds with high affinity to the β_1-AR ($logK_D\beta_1 = -9.58$) but only elicits a response at much higher concentrations ($logEC_{50}\beta_1 = -7.99$). This discrepancy between $logK_D\beta_1$ and $logEC_{50}\beta_1$ suggests that CGP12177 is mediating these responses via a conformation other than the primary conformation where CGP12177 competed and displaced [^{3}H] CGP12177. This is quite clear in figure 2.6 in which CGP12177 (**16**) behaves as a high affinity antagonist at low concentrations inhibiting cimaterol response and then, at higher concentrations, stimulates a response. This phenomenon is not observed in CHO-β_2 cells as demonstrated in figure 2.5 and 2.6. CGP12177 (**16**) behaves as a partial agonist at the β_2-AR with a $logK_D\beta_2 = logEC_{50}\beta_2$ which demonstrates that the discrepancy observed at the β_1-AR is receptor dependent and not an artefact of the system used.

2) Agonist activity elicit by CGP12177 (**16**) in CHO-β_1 cells is quite resistant to antagonism by well-known β-blockers (eg. CGP20712A **19** and ICI118551 **21** in figure 2.5). A much higher concentration of antagonist is required to right-shift CGP12177 response curve than cimaterol response curve (figure 2.4 and figure 2.5). This strengthens the existence of a secondary conformation for which these compounds show a lower affinity similarly to CGP12177 (**16**). Once again, this is not observed in CHO-β_2 cells where antagonists are able to rightshift both cimaterol (**20**) and CGP12177 (**16**) at similar concentrations (figure 2.4 and figure 2.5)

3) Alprenolol (**6**) and oxprenolol (**7**) show a biphasic concentration response curve at the β_1-AR. The first component of these responses is mediated through the primary conformation with a $logK_D\beta_1 = logEC_{50}\beta_1$ and is easily antagonised by β-blockers (figure 2.10 and 2.11). The second component is more resistant to antagonism suggesting that is mediated through the same secondary conformation as CGP12177 elicited response. Indeed, when using fixed concentrations of alprenolol or oxprenolol to rightshift CGP12177 mediated response a $logK_D\beta_1$ similar to the $logEC_{50}\beta_1$ of the second component is obtained (figure 2.10 and 2.11). This therefore suggests that alprenolol (**6**) and oxprenolol (**7**) are able to bind and activate both conformations of the β_1-AR even though they require much higher concentrations to activate the secondary conformation of the β_1-AR.

For these reasons, alprenolol (**6**) and oxprenolol (**7**) were chosen as the starting point for the synthesis of new analogues that might contribute to the better understanding of the secondary conformation of the β_1-AR and will be described in detail in the following chapters.

Chapter 3

Synthesis and pharmacological evaluation of *N*-alkyl alprenolol and oxprenolol analogues

3.1 Introduction

Alprenolol and oxprenolol were chosen as lead compounds for the first set of compounds. As previously explained, alprenolol and oxprenolol can bind and activate both the primary and the secondary conformation of the β_1-AR. Even though they can bind to both conformations, they require a hundred fold (a difference of two log units in the $logK_D$) higher concentration to bind (K_D) and activate (EC_{50}) the secondary conformation. A set of alprenolol (**6**) and oxprenolol (**7**) analogues were synthesised with a range of different amine groups in the phenoxypropanolamine chain. The amino group of the phenoxypropanolamines forms a salt-bridge interaction with an acidic aspartate residue ($Asp^{3.32}$) that is essential for ligand binding to the primary conformation of the β_1 and the β_2 adrenergic receptors.[5, 47, 48] Firstly, the affinity of these compounds was evaluated for both primary conformation of β_1-AR and β_2-AR through radioligand binding assays along with several literature compounds. Next, the CRE-mediated secretion of SPAP (a cAMP reporter gene) was measured in CHO-β_1 and CHO- β_2 cells to determine the potency and efficacy of these compounds. In this assay the parent compounds, alprenolol and oxprenolol, show a biphasic dose-response curve as both are able to activate the primary and secondary conformation, even though they require a much higher concentration to activate the secondary conformation (see chapter 2, figure 2.9). Partial agonists and antagonists were then used to rightward shift the concentration-response curve of cimaterol (**20**) (known to mediate a response through the primary conformation)

and CGP12177 (**16**) (known to mediate a response only through the secondary conformation) to access their affinity for the primary and secondary conformations of the β_1-AR, respectively. CGP20712A (**19**) was also used to right-shift the concentration-response curve of the agonists found in this set of ligands in order to access if their response is mediated through the primary or secondary conformation (responses mediated through the secondary conformation are more resistant to antagonism by known antagonists, which translates in a much lower derived CGP20712A affinity).

3.2 Results and discussion

3.2.1 Chemistry

Commercially available pyrocatechol (**38**) was converted to 2-(allyloxy)phenol (**40**) through a known procedure (Scheme 3.1). The addition of base and one equivalent of allyl bromide (**39**) afforded the desired phenol that was further purified by column chromatography. 2-(allyloxy)phenol was then alkylated with racemic epichlorohydrin (**41**) to yield the 2-((2-(allyloxy)phenoxy)methyl)oxirane (**42**). This alkylation was made at room temperature, using sodium hydride as a base, to avoid the undesirable claisen rearrangement of compound 40 to the corresponding diol.

Oxirane 42 was then submitted to nucleophilic ring-opening of the epoxide with a range of amines (**43a-k**) to afford the corresponding phenoxypropanolamines and oxprenolol analogues (**44b-k** and **7**). Amines were used in excess as a solvent in the microwave

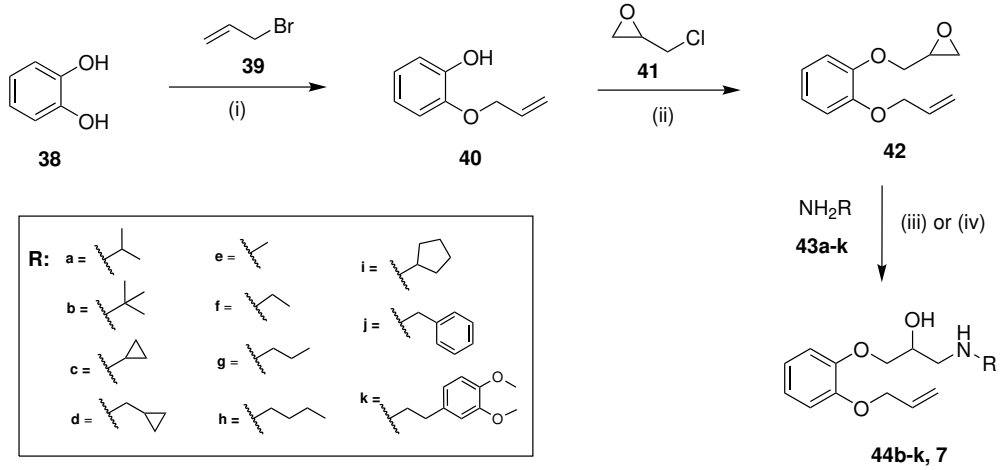

SCHEME 3.1: Synthesis of N-alkyl oxprenolol analogues. Reagents and conditions: (i) allyl bromide, K_2CO_3, acetone, reflux, 48h, 78%; (ii) epichlorohydrin, NaH, DMF, 0 °C -> r.t., 48h, 89%; (iii) NH_2R **(43a-k)**, MW, 60 °C, 1h, 64-92%; (iv) NH_2R, hexafluoroisopropanol, MW, 60 °C, 1h, 61-76%.

reaction to avoid a second epoxide opening by the initial product formed, even though it is not a problem when using bulkier amines such as *iso*-propylamine and *tert*-butylamine. The basic conditions of this reaction also increase the selectivity towards opening of epoxide via the least hindered carbon to yield the secondary alcohol. The excess of amine was easily removed afterward due to the low boiling point of the used amines.

The synthesis of alprenolol analogues was made in a similar fashion to oxprenolol analogues. The commercially available 2-allylphenol (**45**) yielded the oxirane 46 in the presence of racemic epichlorohydrin and potassium carbonate in dry acetone (Scheme 3.2). Even though epichlorohydrin was added in a 1.5 equivalents excess, it was possible to identify the presence of a undesired product resulting from nucleophilic attack of the initial phenol to the epoxide present in the product. The mixture was then purified by column chromatography originating compound 46 in a 62% yield. The same set of amines (**43a-k**) was also used to open the epoxide as described for the synthesis of oxprenolol analogues. Most of these reactions were microwave assisted using the amine, in a high excess, as a solvent at 70 °C during 1 hour.

However, for the synthesis of analogues 44i, 44k, 44i and 44k, due to the higher boiling point of the amines, the oxirane 40 and 46, respectively, were dissolved in hexafluoroisopropanol and only 2 equivalents of the correspondent amine were added. Analogues 44e, 47e, 44f and 47f were synthesised at room temperature with the addition of a 40% solution of methylamine in water or a 2M solution of ethylamine in THF to the oxirane 40 or 46. The addition of a 1N solution of ammonia in methanol to either oxirane 40 or 46 yielded two products for each starting material (Sch. 3.3). This reaction took place at room temperature for 48 hours using 1 equivalent of amine and afforded the compounds

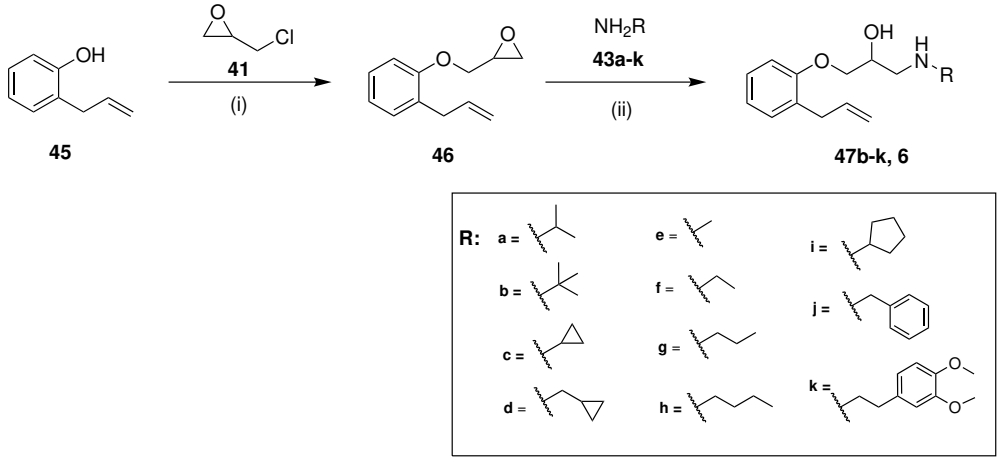

SCHEME 3.2: Synthesis of N-alkyl alprenolol analogues. Reagents and conditions: (i) epichlorohydrin, K_2CO_3, acetone, reflux, 48h, 62%; (ii) NH_2R **(43a-k)**, MW, 70 °C, 1h, 12-96%.

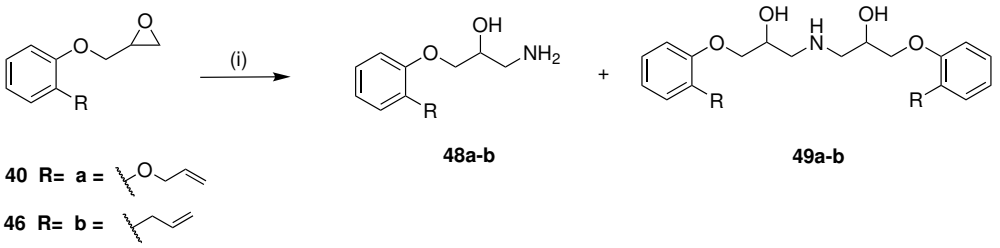

SCHEME 3.3: Synthesis of unsubstituted amine and *bis* analogues of oxprenolol and alprenolol. Reagents and conditions: (i) 7N solution of NH_3 in MeOH, r.t., 48h.

49a-b in higher yields than compounds 48a-b. The yield for compound 48b increased when using a 7N solution of ammonia in methanol instead of a 1N solution. The *bis* products 49a-b result from a second nucleophilic epoxide opening of the product 48a-b to the oxiranes. These products were easily separated by flash column chromatography. All compounds were synthesised as racemates because, even though the *S*-enantiomer would most likely yield higher affinities for both β_1 and β_2-AR, most of the beta-blockers are administrated in clinic as racemic mixtures.

3.2.2 Pharmacology

3.2.2.1 Radioligand binding assays

Initially, the affinity of several known β-blockers were determined and compared with the literature values, using chinese hamster ovary cells (CHO) stably expressing the human β_1-AR or β_2-AR. The $logIC_{50}$ values for these compounds were determined in a competitive whole-cell binding study using the radioligand [^{3}H] CGP12177 and then used to determine $logK_D$ values using the Cheng-Prusoff equation. The K_D value for [^{3}H] CGP 12177 in these two cell lines was determined by saturation binding and used to calculate the $LogK_D$ values of all the ligands, as explained in the previous chapter. The affinities for all of the alprenolol and oxprenolol analogues were determined by whole-cell competitive binding studies using [^{3}H] CGP12177 as radioligand. Figure 3.1 represents the amount of radioactivity bound to the CHO-β_1 and CHO-β_2 cells at different concentrations of either oxprenolol (**7**), analogue 44j and 47k when a fixed concentration of the radiolabeled [^{3}H] CGP12177 is added. These ligands are able to fully displace the radioligand from the receptor. Total binding and non-specific binding in the presence of a 10μM of propranolol are also represented.

Substituent (**R**)	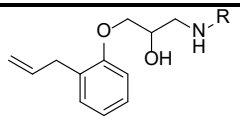					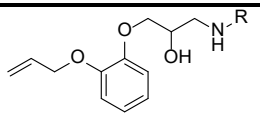					
		LogK$_D$β$_1$	n	LogK$_D$β$_2$	n	LogK$_D$(β$_2$/β$_1$)		LogK$_D$β$_1$	n	LogK$_D$β$_2$	n	LogK$_D$(β$_2$/β$_1$)
	Alprenolol	-7.94 ± 0.02	6	-9.01 ± 0.04	6	1.07	Oxprenolol	-7.89 ± 0.02	6	-8.77 ± 0.03	6	0.88
	47d	-7.04 ± 0.02	6	-8.04 ± 0.02	6	1.00	44d	-6.78 ± 0.06	5	-7.91 ± 0.05	5	1.13
	47c	-7.36 ± 0.03	6	-8.35 ± 0.06	6	0.99	44c	-7.50 ± 0.05	5	-8.53 ± 0.04	6	1.03
	47i	-7.66 ± 0.03	6	-8.69 ± 0.03	6	1.03	44i	-7.46 ± 0.03	5	-8.52 ± 0.08	6	1.06
	47e	-6.58 ± 0.03	6	-7.66 ± 0.02	6	1.08	44e	-6.44 ±0.05	6	-7.48 ± 0.04	5	1.04
	47f	-7.23 ± 0.02	6	-8.23 ± 0.04	6	1.00	44f	-7.31 ± 0.04	6	-8.20 ± 0.05	5	0.89
	47g	-7.07 ± 0.04	6	-8.09 ± 0.11	5	1.02	44g	-6.93 ± 0.03	6	-7.83 ± 0.04	6	0.90
	47h	-6.86 ± 0.02	6	-7.75 ± 0.04	6	0.89	44h	-6.75 ± 0.03	6	-7.70 ± 0.03	5	0.95
	47b	-8.51 ± 0.05	6	-9.74 ± 0.09	5	1.23	44b	-8.37 ± 0.03	5	-9.51 ± 0.06	6	1.14
H	48b	-6.56 ± 0.03	6	-7.18 ± 0.03	6	0.62	48a	-6.41 ± 0.01	6	-7.07 ± 0.02	5	0.66
	47j	-6.61 ± 0.04	5	-7.55 ± 0.06	5	0.94	44j	-6.44 ± 0.04	6	-7.77 ± 0.03	6	1.33
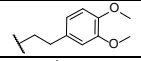	47k	-8.14 ± 0.03	6	-8.24 ± 0.04	6	0.10	44k	-8.22 ± 0.04	6	-8.15 ± 0.04	6	-0.07
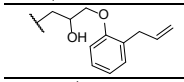	49b	-7.12 ± 0.02	6	-8.16 ± 0.04	6	1.04		-	-	-	-	-
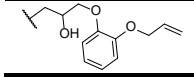		-	-	-	-	-	49a	-7.42 ± 0.01	6	-9.01 ± 0.08	5	1.59

TABLE 3.1: Binding affinities (logK_D values) and selectivity for the human β_1 and β_2-adrenergic receptors of alprenolol and oxprenolol N-alkyl analogues. Values represent mean of data obtained and ± the standard error of the mean (s.e.m) for n separate experiments

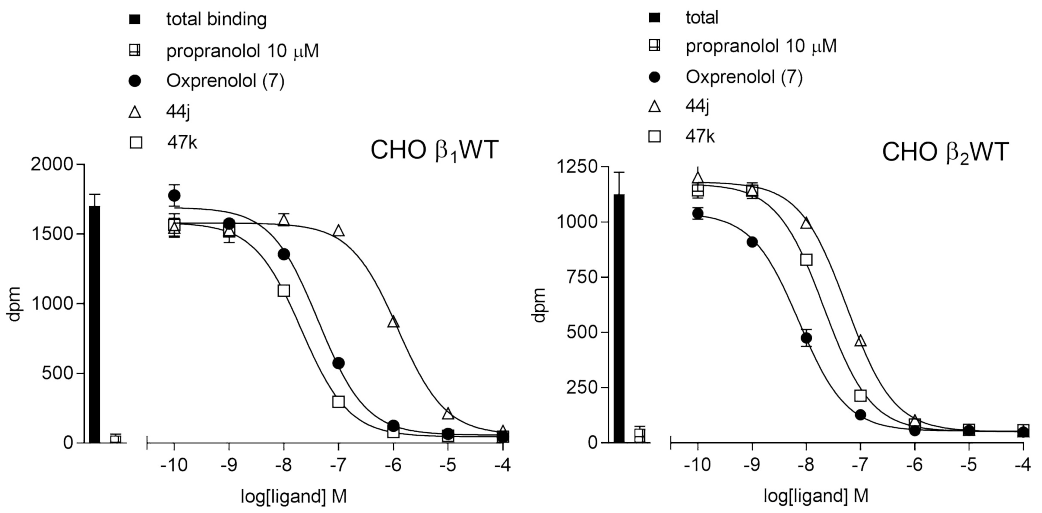

FIGURE 3.1: Inhibition of [^{3}H] CGP12177 binding to whole cells in CHO-β_1 and -β_2 by compounds 7 (oxprenolol), 44j and 47k. A fixed concentration of 0.67 nM of [^{3}H] CGP12177 was used. Left bar represents total [^{3}H] CGP12177 binding and the right one nonspecific binding which was determined in the presence of 10 μM propranolol.

The $logK_D$ values for each of the *N*-alkyl analogues of alprenolol and oxprenolol are presented in Table 3.1. The $logK_D$ values obtained for oxprenolol (**7**) and alprenolol (**6**) are in accordance with literature values ($logK_D\beta_1$= -7.83 and $logK_D\beta_2$= -9.04 for alprenolol; $logK_D\beta_1$= -7.96 and $logK_D\beta_2$= -8.97) [40]. Alprenolol analogues, in general, showed a slightly higher affinity than the equivalent analogue from the oxprenolol series. Analogues bearing a *tert*-butyl amine (44b and 47a) yielded the highest affinity within the alprenolol and oxprenolol analogues for both β_1 and β_2 adrenergic receptor while the primary amine group (48a and 48b), lacking a substituent, yielded the worst affinity. Introduction of an hydrophobic benzylamino group (44j and 47j) also yielded a low affinity for both receptors. Comparing the homologation of the linear chain, the ethylamino group (44f and 47f) seems to be the ideal size to yield a better affinity followed by the propyl (44g and 47g) and butylamino (44h and 47h) groups, whereas the methylamino (44e and 47e) group substituent yielded the lowest affinity of the extended chain for both β_1 and β_2-AR. Analogues containing a cyclic substituent, either cyclopentyl or cyclobutyl, showed a higher affinity than the extended equivalents at both receptors. Analogues containing a (3,4-dimethoxyphenethyl)amino group (44k and 47k) showed one of the highest affinities for both receptors. *Bis* compounds, containing two alprenolol aryloxypropanolamine units connected to a single central amino group (49a and 49b), presented a surprisingly high affinity even though they bear an extended chain in the amino end. The *bis* analogue of oxprenolol **49a** showed the second highest affinity from this set for the β_2-AR.

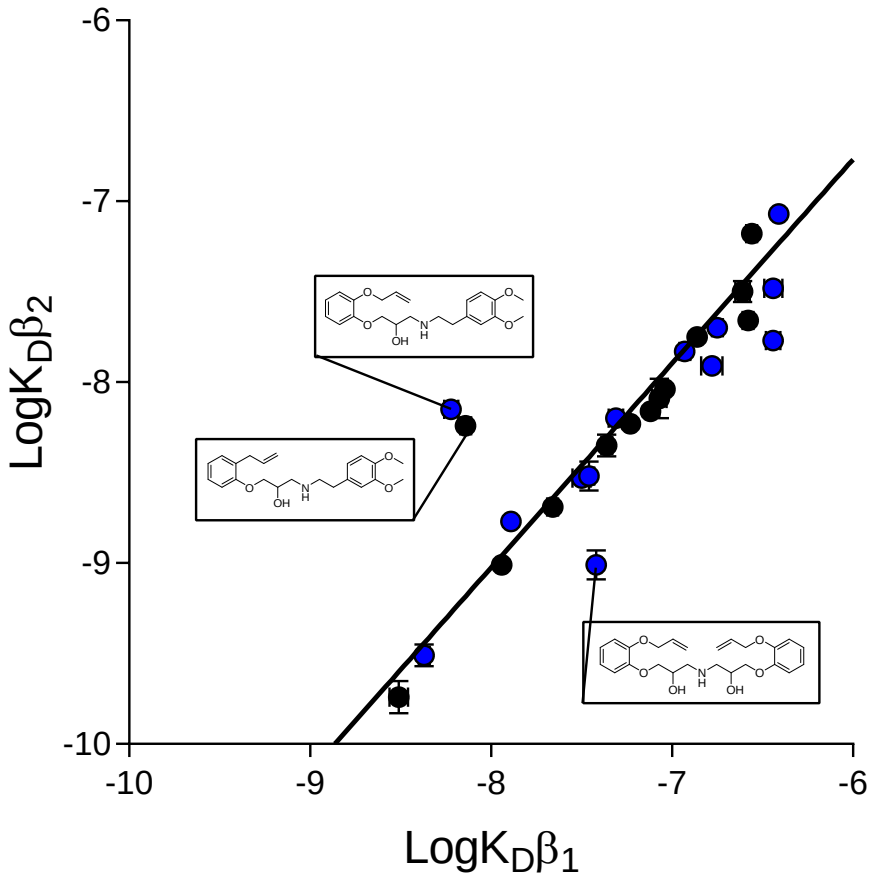

FIGURE 3.2: Correlation between $logK_D\beta_1$ and $logK_D\beta_2$ obtained for alprenolol and oxprenolol *N*-alkyl analogues ($r^2 = 0.867$, $y = 0.9x - 1.667$) Alprenolol analogues are displayed in black, while oxprenolol analogues are displayed in blue with s.e.m. represented. Analogues 44k, 47k and 49a are highlighted in this figure.

In general fashion, most oxprenolol and alprenolol analogues showed around 10 fold selectivity (around 1 log unit difference between $logK_D\beta_1$ and $logK_D\beta_2$) for the β_2-AR in the system used. This is highlighted in figure 3.2, where $logK_D\beta_2$ shows a strong linear correlation with $logK_D\beta_1$ ($r^2 = 0.87$). Introduction of a (3,4-dimethoxyphenethyl) amino group is known to increase the β_1-selectivity which is consistent with the results presented here. [86] Both alprenolol and oxprenolol analogues containing a (3,4-dimethoxyphenethyl)amino group lost the slight selectivity for the β_2-AR seen in the other analogues and showed identical affinity values for both receptors. Interestingly, oxprenolol *bis* analogue 49a showed the highest selectivity value towards β_2 ($\log K_D(\beta_2/\beta_1) = 1.59$, around 39-fold selectivity). This is not seen in the alprenolol *bis* ligand which shows identical selectivity to the other analogues.

This set of analogues demonstrates the importance of the amino group to determine

the affinity of compounds at both the primary conformation of β_1 and at the β_2-AR. Oxprenolol and alprenolol analogues containing the same amine substituent ranked in a very similar way for the two identical aromatic cores with distinct 2-substituent.

3.2.2.2 CRE-SPAP production

Following the characterisation of this set of compounds through radioligand binding assays, CHO cells expressing a CRE-SPAP reporter gene were used to evaluate the potency and efficacy of these compounds. In this system, transcription of SPAP (secreted placental alkaline phosphatase) is facilitated in the presence of cAMP. This can, therefore, be used as an amplified downstream measurement of cAMP production upon receptor activation. [35, 83]

As explained during chapter 1, ligands can activate (agonists), block (antagonists) or even reduce basal activity of the receptor (inverse agonists). Surprisingly, in the β_1-AR some ligands have been shown to behave as antagonists at lower concentrations and then activate the receptor at higher concentrations (eg. CGP 12177, an antagonist at primary conformation but an agonist at the secondary conformation of the β_1-AR). Other ligands (eg. alprenolol and oxprenolol), the parent compounds of this set, activate both conformations of β_1-AR and therefore showed a biphasic dose response curve in CRE-SPAP assays but also in several different systems. As previously mentioned, this phenomenon is not seen at β_2-AR even though these compounds might be able to activate the receptor and show a dose dependent SPAP accumulation in CHO-β_2 cells. For this reason, the activation of the β_2-AR by these compounds was also examined, as a negative control, in order to confirm that the results obtained were not an artefact of the system and experimental conditions used.

Tables 3.2 and 3.3 represent the binding affinity ($logK_D$), potency ($logEC_{50}$) and efficacy ($\%isop$) of alprenolol and oxprenolol analogues, respectively in CHO-β_1 cells. CGP20712A was used to inhibit the response mediated by the partial agonists of this set, and the calculated LogK_D is represented as CGP20712A LogK_D and will be discussed in a later subsection. Tables 3.4 and 3.5 display the binding affinity, potency and efficacy of this set of ligands for the β_2-AR. Predominantly, analogues behaved as partial agonist with low efficacy. Analogue 47h, the most efficacious analogue of the set for β_1-AR, reached only $55\% \pm 4$ (n=3, table 3.2) of the maximum isoprenaline response. In CHO-β_2 cells, alprenolol analogues consistently presented higher efficacy than equivalent oxprenolol analogue and alprenolol *tert*-butylated analogue (47b) presented the highest efficacy of the set ($\%isop = 42 \pm 3$; Table 3.4).

Substituent (**R**)	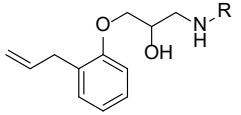										
		$LogK_D\beta_1$	n	$LogEC_{50}\beta_1 1$	$LogEC_{50}\beta_1 2$	% 1st component	n	% isop	n	CGP20712A $LogK_D$	n
Alprenolol		-7.94 ± 0.02	6	-8.57 ± 0.15	-6.14 ± 0.13	43 ± 7	8	29 ± 4	12	-8.78 ± 0.11	3
47d		-7.04 ± 0.02	6	-7.46 ± 0.09	-*	-	7	44 ± 2	7	-8.67 ± 0.07	3
47c		-7.36 ± 0.03	6	-	-	-	-	< 10	7	-	-
47i		-7.66 ± 0.03	6	-8.04 ± 0.12	-6.06 ± 0.13	42 ± 5	6	32 ± 4	14	-8.92 ± 0.05	3
47e		-6.58 ± 0.03	6	-	-	-	-	< 10	5	-	-
47f		-7.23 ± 0.02	6	-	-	-	-	< 10	7	-	-
47g		-7.07 ± 0.04	6	-7.40 ± 0.21	-	-	6	29 ± 4	6	-9.26 ± 0.11	3
47h		-6.86 ± 0.02	6	-7.22 ± 0.06	-*	-	3	55 ± 4	3	-8.90 ± 0.09	3
47b		-8.51 ± 0.05	6	-9.08 ± 0.10	-6.84 ± 0.15	42 ± 7	11	43 ± 3	12	-8.55 ± 0.11	3
48a	H	-6.56 ± 0.03	6	-	-	-	-	< 10	3	-	-
47j		-6.61 ± 0.04	5	-6.63 ± 0.15	-	-	8	41 ± 2	8	-7.82 ± 0.06	3
47k	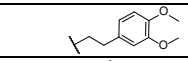	-8.14 ± 0.03	6	-8.41 ± 0.09	-5.80 ± 0.13	59 ± 6	6	36 ± 2	11	-8.62 ± 0.13	4
49b	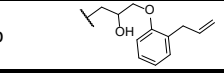	-7.12 ± 0.02	6	-7.13 ± 0.12	-	-	5	47 ± 6	5	-7.93 ± 0.15	3

TABLE 3.2: Binding affinity, potency and efficacy for β_1-AR of alprenolol analogues in CHO cells stably expressing the human β_1-AR. Data are mean ± SEM for n experiments. $logK_D\beta_1$ represents the binding affinity assessed using [^{3}H]-CGP12177 whole cell binding assays; $logEC_{50}\beta_1 1$ represents potency derived from the first component of a biphasic concentration-response curve or single component in monophasic responses. $logEC_{50}\beta_1 2$ represents the potency value for the second component in a biphasic response; $\%1^{st}$ component represents the percentage of the overall response mediated through the first component; $\%isop$ represents the efficacy (percentage of isoprenaline response) evaluated through CRE-SPAP assays; CGP20712A $logK_D$ represents the affinity derived from the inhibition of the ligand CRE-SPAP production using fixed concentrations of CGP20712A in whole cell assays; *compound seems to activate both conformations even though the value is out of range for this assay.

Substituent (**R**)	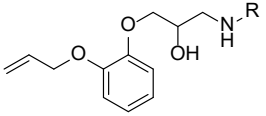									
		$LogK_D\beta_1$	n	$LogEC_{50}\beta_1 1$	$LogEC_{50}\beta_1 2$	% 1st component	n	% isop	n	CGP20712A $LogK_D$	n
Oxprenolol		-7.89 ± 0.02	6	-8.59 ± 0.08	-5.94 ± 0.16	58 ± 4	10	38 ± 2	14	-8.70 ± 0.13	3
44d		-6.78 ± 0.06	5	-7.16 ± 0.13	-	-	9	34 ± 3	8	-8.71 ± 0.11	3
44c		-7.50 ± 0.05	5	-8.02 ± 0.15	-	-	8	23 ± 3	11	-9.13 ± 0.15	3
44i		-7.46 ± 0.03	5	-7.97 ± 0.09	-*	-	11	34 ± 4	11	-8.59 ± 0.17	3
44e		-6.44 ±0.05	6	-6.95 ± 0.07	-	-	8	37 ± 5	8	-8.99 ± 0.16	3
44f		-7.31 ± 0.04	6	-7.61 ± 0.14	-	-	13	26 ± 2	13	-8.77 ± 0.02	3
44g		-6.93 ± 0.03	6	-7.58 ± 0.21	-	-	8	34 ± 4	8	-8.86 ± 0.04	3
44h		-6.75 ± 0.03	6	-7.20 ± 0.13	-	-	5	31 ± 4	5	-8.50 ± 0.20	3
44b		-8.37 ± 0.03	5	-8.80 ± 0.09	-6.39 ± 0.14	55 ± 5	11	41 ± 3	11	- 8.51 ± 0.08	3
48a	H	-6.41 ± 0.01	6	-	-	-	-	< 10	3	-	-
44j		-6.44 ± 0.04	6	-7.03 ± 0.23	-	-	6	39 ± 3	3	-8.80 ± 0.14	3
44k	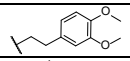	-8.22 ± 0.04	6	-8.66 ± 0.05	-*	-	13	46 ± 2	13	-8.98 ± 0.07	5
49a	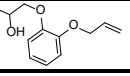	-7.42 ± 0.01	6	-7.50 ± 0.15	-	-	6	32 ± 3	6	-8.03 ± 0.23	3

TABLE 3.3: Binding affinity, potency and efficacy for β_1-AR of oxprenolol analogues in CHO cells stably expressing the human β_1-AR. Data are mean ± SEM for n experiments. $logK_D\beta_1$ represents the binding affinity assessed using [^{3}H]-CGP12177 whole cell binding assays; $logEC_{50}\beta_1 1$ represents potency derived from the first component of a biphasic concentration-response curve or single component in monophasic responses. $logEC_{50}\beta_1 2$ represents the potency value for the second component in a biphasic response; $\%1^{st}$ component represents the percentage of the overall response mediated through the first component; $\%isop$ represents the efficacy (percentage of isoprenaline response) evaluated through CRE-SPAP assays; CGP20712A $logK_D$ represents the affinity derived from the inhibition of the ligand CRE-SPAP production using fixed concentrations of CGP20712A in whole cell assays; *compound seems to activate both conformations even though the value is out of range for this assay.

Substituent (**R**)	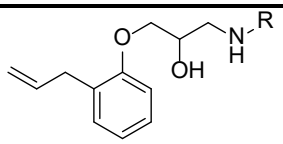						
		$LogK_D\beta_2$	n	$LogEC_{50}\beta_2$	% isop	n	ICI118551 $LogK_D$	n
Alprenolol		-9.01 ± 0.04	6	-9.49 ± 0.05	37 ± 2	11	-9.69 ± 0.08	6
47d		-8.04 ± 0.02	6	-8.71 ± 0.10	28 ± 2	8	-9.79 ± 0.11	3
47c		-8.35 ± 0.06	6	-8.79 ± 0.04	28 ± 2	10	-9.64 ± 0.13	5
47i		-8.69 ± 0.03	6	-9.15 ± 0.10	38 ± 2	13	-9.67 ± 0.06	5
47e		-7.66 ± 0.02	6	-8.32 ± 0.07	32 ± 4	10	-9.85 ± 0.04	4
47f		-8.23 ± 0.04	6	-8.77 ± 0.06	34 ± 3	10	-9.79 ± 0.10	4
47g		-8.09 ± 0.11	5	-8.44 ± 0.11	28 ± 2	8	-9.67 ± 0.10	3
47h		-7.75 ± 0.04	6	-8.29 ± 0.09	30 ± 3	10	-10.00 ± 0.15	3
47b		-9.74 ± 0.09	5	-9.65 ± 0.07	42 ± 3	12	-9.29 ± 0.11	5
48a	H	-7.18 ± 0.03	6	-	< 10	3	-	-
47j	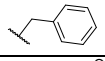	-7.55 ± 0.06	5	-7.70 ± 0.11	22 ± 3	9	-9.64 ± 0.06	3
47k	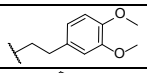	-8.24 ± 0.04	6	-	No response	3	-	-
49b	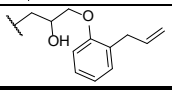	-8.16 ± 0.04	6	-	No response	3	-	-

TABLE 3.4: Binding affinity, potency and efficacy for β_2-AR of alprenolol analogues in CHO cells stably expressing the human β_2-AR. Data are mean ± SEM for n experiments. $logK_D\beta_2$ represents the binding affinity assessed using [^{3}H]-CGP12177 whole cell binding assays; $logEC_{50}\beta_2$ represents potency derived from the concentration-response curve in CRE-SPAP assays. $\%isop$ represents the efficacy (percentage of isoprenaline response); ICI118551 $logK_D$ represents the affinity derived from the inhibition of the ligand CRE-SPAP production using fixed concentrations of ICI118551 in whole cell assays.

Compounds which mediated a response lower than ten percent of the maximum isoprenaline response ($\%isop$ <10 %) have been treated as antagonists, due to the system signal amplification and difficulty to accurately measure a logEC_{50} value. Alprenolol *N*-methyl (47e), *N*-ethyl (47f) and *N*-cyclopropylamino (47c) analogues behaved as such, eliciting a response inferior to <10 % of the maximum isoprenaline response for β_1-AR. Non-substituted analogues 48a and 48b also showed a small response at β_1-AR.

Similarly, analogues containing a primary amine elicited a lower response for β_2-AR. Bis analogues 49a, 49b and analogues 44k and 47k behaved as antagonists at this receptor. Interestingly, oxprenolol benzylamino analogue 44j did not increase CRE-SPAP accumulation in CHO-β_2 cells contrary to alprenolol analogue 47j which elicited a response with

Substituent (**R**)	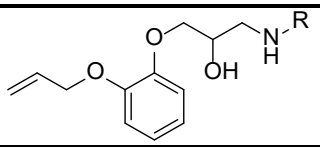						
		$LogK_D\beta_2$	n	$LogEC_{50}\beta_2$	% isop	n	ICI118551 $LogK_D$	n
Oxprenolol		-8.77 ± 0.03	6	-9.15 ± 0.07	27 ± 2	12	-9.72 ± 0.16	6
44d		-7.91 ± 0.05	5	-8.37 ± 0.11	16 ± 2	6	-9.90 ± 0.13	3
44c		-8.53 ± 0.04	6	-8.89 ± 0.07	20 ± 1	10	-9.53 ± 0.06	3
44i		-8.52 ± 0.08	6	-8.94 ± 0.10	23 ± 1	11	-9.69 ± 0.17	3
44e		-7.48 ± 0.04	5	-8.24 ± 0.06	15 ± 2	9	-10.02 ± 0.08	3
44f		-8.20 ± 0.05	5	-8.68 ± 0.13	24 ± 1	13	-9.66 ± 0.14	4
44g		-7.83 ± 0.04	6	-	< 10	3	-	-
44h		-7.70 ± 0.03	5	-	< 10	3	-	-
44b		-9.51 ± 0.06	6	-9.46 ± 0.03	30 ± 2	10	-9.18 ± 0.16	4
48a	H	-7.07 ± 0.02	5	-	< 10	3	-	-
44j		-7.77 ± 0.03	6	-	No response	3	-	-
44k	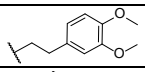	-8.15 ± 0.04	6	-	No response	3	-	-
49a	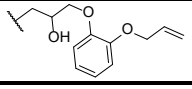	-9.01 ± 0.08	5	-	No response	3	-	-

TABLE 3.5: Binding affinity, potency and efficacy for β_2-AR of oxprenolol analogues in CHO cells stably expressing the human β_2-AR. Data are mean ± SEM for n experiments. $logK_D\beta_2$ represents the binding affinity assessed using [^{3}H]-CGP12177 whole cell binding assays; $logEC_{50}\beta_2$ represents potency derived from the concentration-response curve in CRE-SPAP assays. $\%isop$ represents the efficacy (percentage of isoprenaline response); ICI118551 $logK_D$ represents the affinity derived from the inhibition of the ligand CRE-SPAP production using fixed concentrations of ICI118551 in whole cell assays.

an $\%isop$ of $22 \pm 3\%$ (n=9; Table 3.4).

Alprenolol (**6**) showed a biphasic dose response curve with a $\log EC_{50}\beta_1 1$ of -8.57 ± 0.15 and a second $\log EC_{50}\beta_1 2$ of -6.14 ± 0.13 (n=8) with an $\%isop$ of $29 \pm 4\%$ (n=12) of the maximum isoprenaline response for β_1-AR. Response mediated through the primary conformation accounted for $43 \pm 7\%$ (n=8) of the response seen. In CHO-β_2 cells, alprenolol stimulated a response in a single component-dose response curve with a $\log EC_{50}\beta_2$ of -9.49 ± 0.05 (n=11) and an $\%isop$ of $37 \pm 2\%$ (n=11). In CHO-β_1 cells, oxprenolol also stimulated SPAP transcription in a biphasic concentration response manner with a $\log EC_{50}\beta_1 1$ of -8.59 ± 0.08 and a second $\log EC_{50}\beta_1 2$ of -5.94 ± 0.16 (n=10) with an

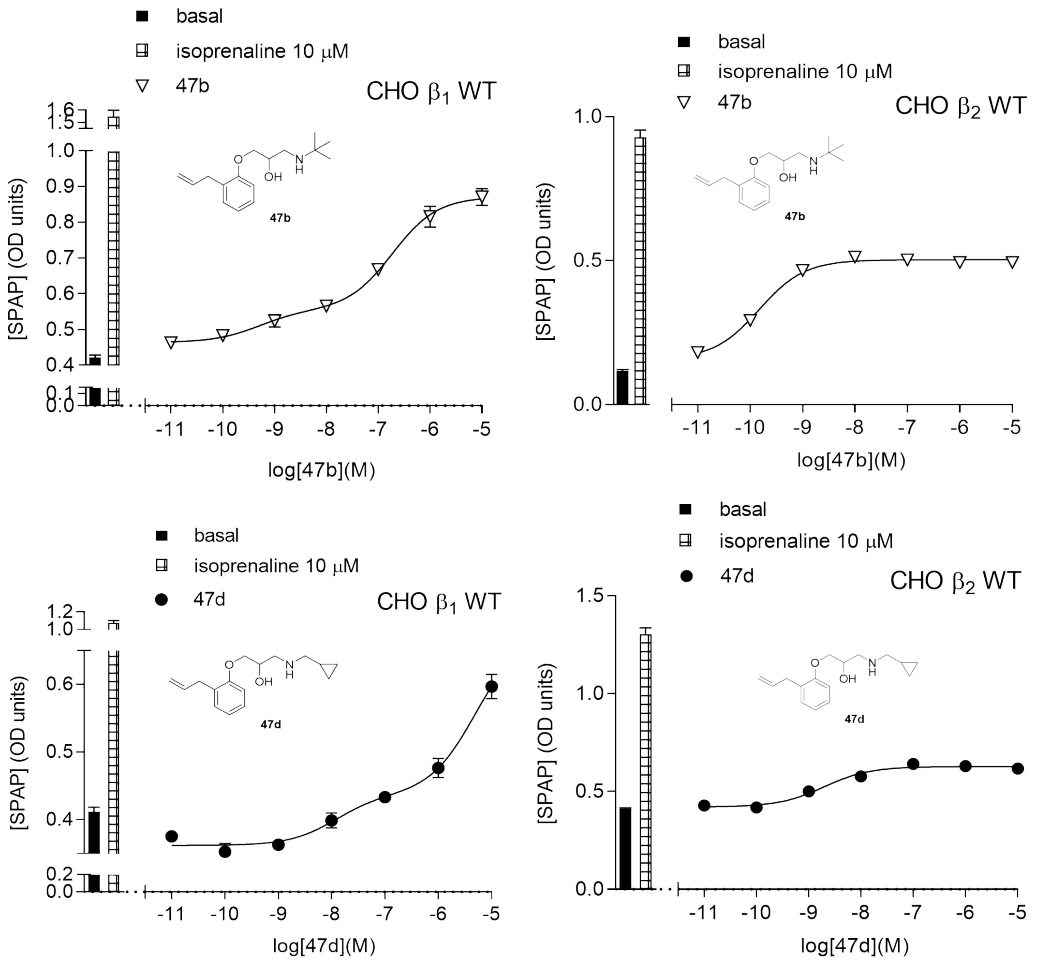

FIGURE 3.3: CRE-SPAP activity in response to analogues 47a (top) and 47d (bottom) in CHO-β_1 and -β_2 cells.

$\%isop$ of $38 \pm 2\%$ (n=14) of the maximum isoprenaline response in which the first component accounted for 58% (n=10) of the response. Oxprenolol stimulated a response in CHO-β_2 cells with a log$EC_{50}\beta_2$ of -9.15 ± 0.07 and a $\%isop$ of $27 \pm 2\%$. These values are consistent with the literature. [34] The first component of the response curve (log$EC_{50}1$) at CHO-β_1 cells and the $logEC_{50}$ for CHO-β_2 cells are around 0.5 log units higher than the logK_D obtained from radioligand competitive binding assays, which is common in CRE-SPAP assays for partial agonists and might be due to the signal amplification in this system. [34]

Overall, most logEC_{50} values are consistent with a response mediated through the primary conformation of the β_1-AR. As previously mentioned, for partial agonists, the ligand is expected to mediate half of the maximal response when it occupies half of the receptors (logK_D should equal logEC_{50}). Analogues containing a *tert*-butylamino

group (44b and 47b), instead of the *iso*-propylamino group seen in both alprenolol and oxprenolol, behaved in a similar manner to the parent compounds causing a biphasic concentration-dependent secretion of SPAP. The *tert*-butylated alprenolol analogue showed the highest potency of the set for both the primary and secondary conformation of the β_1-AR with a $\log EC_{50}\beta_1 1$ of -9.08 ± 0.10 and a $\log EC_{50}\beta_1 2$ of -6.84 ± 0.15 with an $\%isop$ of $42 \pm 7\%$ (n=11) (fig. 3.3 top). This compound was also the most potent for the β_2-AR with a $\log EC_{50}\beta_2$ of -9.65 ± 0.07 and an $\%isop$ of $42 \pm 3\%$ (n=12). (3,4-dimethoxyphenethyl)amino alprenolol analogue 47k also mediated a response in a biphasic fashion with 2.61 log units difference between the $\log EC_{50}$ of the two components of the curve. The corresponding oxprenolol analogue 44k mediated a single-component response in the CRE-SPAP assay, however this might be due to a lower affinity for the secondary conformation and therefore out of the range of this assay. In fact, several compounds (eg. 47d, fig. 3.3 bottom) seem to elicit a second response component at the maximum concentration used for the assay ($10\mu M$) which hinders the accurate determination of a $\log EC_{50}$ for the second component. While most of compounds displayed a difference of around 0.5 log units between $\log EC_{50}$ and $\log K_D$, compounds 49a, 49b and 47j showed identical values of potency and affinity. Interestingly, analogue 49a exhibited cytotoxicity at $10\mu M$ in both CHO-β_1 and -β_2 cells represented by an abrupt drop in the response of the partial agonist at this concentration.

3.2.2.3 Affinity at primary and secondary conformation of the β_1-AR

Following the determination of the activity of this set of ligands, a CRE-SPAP assay was used to examine the affinity for both the primary and secondary conformation of the β_1-AR. As represented in figure 3.4, to determine the affinity of these compounds at the secondary conformation, a fixed concentration of either antagonists or partial agonists from this set was added to increasing concentrations of CGP12177 (an agonist at the secondary conformation of the β_1-AR). By obtaining the CGP12177 concentration-response curves both in the absence and presence of a fixed concentration of these compounds, their affinity for the secondary conformation can be determined by their ability to shift the curve. The same method was used to determine the affinity for the primary conformation by adding a fixed concentration of the desired compound to increasing concentrations of cimaterol (an agonist at the primary conformation of the β_1-AR). The same method was done for β_2-AR as a negative control, to confirm that the differences seen are not due to any artefact.

Results are presented in table 3.6 and 3.7, where $logK_D\beta_{1cim}$ and $logK_D\beta_{1CGP}$ represent the affinity for the primary and secondary conformations of the β_1-AR, respectively.

Substituent (**R**)	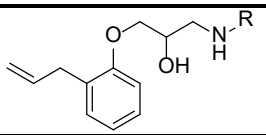						
	$LogK_D\ \beta_1$	n	$LogK_D\ \beta_{1cim}$	n	$LogK_D\ \beta_{1CGP}$	n	$LogK_D\ \beta_{1cim} - LogK_D\ \beta_{1CGP}$
Alprenolol	-7.94 ± 0.02	6	-8.19 ± 0.05	4	-6.40 ± 0.15	4	1.79
47d	-7.04 ± 0.02	6	-7.45 ± 0.08	4	-5.76 ± 0.04	4	1.69
47c	-7.36 ± 0.03	6	-7.78 ± 0.06	4	-5.56 ± 0.02	4	2.22
47i	-7.66 ± 0.03	6	-8.10 ± 0.10	4	-6.08 ± 0.09	4	2.02
47e	-6.58 ± 0.03	6	-6.72 ± 0.07	3	-5.13 ± 0.09	3	1.59
47f	-7.23 ± 0.02	6	-7.63 ± 0.09	3	-5.65 ± 0.09	3	1.98
47g	-7.07 ± 0.04	6	-7.53 ± 0.05	4	-5.49 ± 0.08	4	2.04
47h	-6.86 ± 0.02	6	-7.06 ± 0.08	4	-5.23 ± 0.00	3	1.83
47b	-8.51 ± 0.05	6	-8.91 ± 0.03	4	-7.31 ± 0.07	4	1.60
48b	-6.56 ± 0.03	6	-6.52 ± 0.11	3	-5.60 ± 0.02	3	0.92
47j	-6.61 ± 0.04	5	-6.83 ± 0.08	4	-6.32 ± 0.12	4	0.51
47k	-8.14 ± 0.03	6	-8.67 ± 0.05	4	-6.53 ± 0.13	4	2.14
49b	-7.12 ± 0.02	6	-7.45 ± 0.11	4	-7.11 ± 0.03	5	0.34

TABLE 3.6: Affinity values of alprenolol analogues for the primary and secondary conformation of the β_1-AR. $LogK_D\beta_1$ represents the affinity obtained through radioligand binding assays, previously discussed; $LogK_D\beta_{1cim}$ represents the inhibition of cimaterol, a primary conformation agonist, CRE-SPAP production in whole cell assays (fig. 3.4 right). $LogK_D\beta_{1CGP}$ represents the affinity for the secondary conformation obtained through the inhibition of CGP12177, a secondary conformation agonist, CRE-SPAP production (fig. 3.4 left). $LogK_D\beta_{1cim}$-$LogK_D\beta_{1CGP}$ represents the logaritmical selectivity values towards the primary conformation.

Substituent (**R**)		LogK$_D$ β_1	n	LogK$_D$ β_{1cim}	n	LogK$_D$ β_{1CGP}	n	LogK$_D$ β_{1cim} – LogK$_D$ β_{1CGP}
Oxprenolol		-7.89 ± 0.02	6	-8.18 ± 0.08	3	-6.15 ± 0.15	3	2.03
44d		-6.78 ± 0.06	5	-6.82 ± 0.09	3	-5.49 ± 0.05	3	1.33
44c		-7.50 ± 0.05	5	-7.58 ± 0.02	3	-5.62 ± 0.19	3	1.96
44i		-7.46 ± 0.03	5	-7.57 ± 0.05	3	-5.51 ± 0.04	4	2.06
44e		-6.44 ±0.05	6	-6.44 ± 0.07	3	≈ -5	4	≈1.44
44f		-7.31 ± 0.04	6	-7.38 ± 0.05	4	-5.43 ± 0.06	3	1.95
44g		-6.93 ± 0.03	6	-7.21 ± 0.07	3	-5.45 ± 0.07	3	1.76
44h		-6.75 ± 0.03	6	-6.93 ± 0.07	3	> -5	3	-
44b		-8.37 ± 0.03	5	-8.51 ± 0.11	3	-6.51 ± 0.19	3	2.00
48a	H	-6.41 ± 0.01	6	-6.56 ± 0.08	3	> -5	3	-
44j		-6.44 ± 0.04	6	-6.61 ± 0.12	4	-5.92 ± 0.06	4	0.69
44k	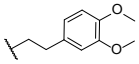	-8.22 ± 0.04	6	-8.31 ± 0.03	4	-5.82 ± 0.09	3	2.49
49a	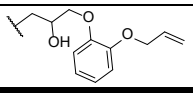	-7.42 ± 0.01	6	-7.73 ± 0.07	3	-6.86 ± 0.09	3	0.87

TABLE 3.7: Affinity values of oxprenolol analogues for the primary and secondary conformation of the β_1-AR. $LogK_D\beta_1$ represents the affinity obtained through radioligand binding assays, previously discussed; $LogK_D\beta_{1cim}$ represents the inhibition of cimaterol, a primary conformation agonist, CRE-SPAP production in whole cell assays (fig. 3.4 right). $LogK_D\beta_{1CGP}$ represents the affinity for the secondary conformation obtained through the inhibition of CGP12177, a secondary conformation agonist, CRE-SPAP production (fig. 3.4 left). $LogK_D\beta_{1cim}$-$LogK_D\beta_{1CGP}$ represents the logaritmical selectivity values towards the primary conformation.

Substituent (**R**)	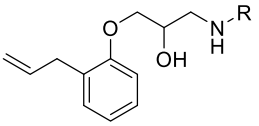							
		$LogK_D\ \beta_2$[a]	n	$LogK_{DCim}$[b]	n	$LogK_{DCGP}$[c]	n	$LogK_{DCim} - LogK_{DCGP}$
Alprenolol		-9.01 ± 0.04	6	-9.18 ± 0.13	3	-	-	-
47d		-8.04 ± 0.02	6	-8.74 ± 0.01	3	-	-	-
47c		-8.35 ± 0.06	6	-8.99 ± 0.10	3	-	-	-
47i		-8.69 ± 0.03	6	-9.32 ± 0.02	3	-	-	-
47e		-7.66 ± 0.02	6	-7.79 ± 0.11	3	-	-	-
47f		-8.23 ± 0.04	6	-8.82 ± 0.05	3	-	-	-
47g		-8.09 ± 0.11	5	-8.72 ± 0.10	3	-	-	-
47h		-7.75 ± 0.04	6	-8.43 ± 0.11	3	-	-	-
47b		-9.74 ± 0.09	5	-10.41 ± 0.03	3	-	-	-
48b	H	-7.18 ± 0.03	6	-7.46 ± 0.06	4	-7.00 ± 0.15	4	0.46
47j		-7.55 ± 0.06	5	-7.95 ± 0.12	4	-7.42 ± 0.14	4	0.53
47k	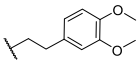	-8.24 ± 0.04	6	-8.64± 0.12	6	-8.21 ± 0.08	3	0.43
49b	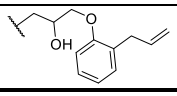	-8.16 ± 0.04	6	-8.39 ± 0.14	7	-7.87 ± 0.12	3	0.52

TABLE 3.8: Affinity values of alprenolol analogues for the β_2-AR. $LogK_D\beta_2$ represents the affinity obtained through radioligand competitive binding assays; $LogK_D\beta_{2Cim}$ represents the affinity derived from the rightward shift of cimaterol concentration-response curve in CRE-SPAP assays.; $LogK_D\beta_{2CGP}$ represents the affinity derived from the rightward shift of CGP12177 concentration-response curve in CRE-SPAP assays.

Substituent (**R**)	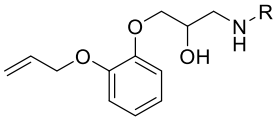						
	$LogK_D\beta_2$[a]	n	$LogK_{DCim}$[b]	n	$LogK_{DCGP}$[c]	n	$LogK_{DCim} - LogK_{DCGP}$
Oxprenolol		-8.77 ± 0.03	6	-9.13 ± 0.07	3	-8.87 ± 0.15	3	0.26
44d		-7.91 ± 0.05	5	-8.37 ± 0.05	4	-8.12 ± 0.07	3	0.25
44c		-8.53 ± 0.04	6	-8.69 ± 0.02	3	-8.51 ± 0.06	3	0.18
44i		-8.52 ± 0.08	6	-8.77 ± 0.02	3	-8.40 ± 0.09	4	0.37
44e		-7.48 ± 0.04	5	-7.75 ± 0.10	3	-7.41 ± 0.08	4	0.34
44f		-8.20 ± 0.05	5	-8.59 ± 0.10	3	-7.99 ± 0.11	4	0.60
44g		-7.83 ± 0.04	6	-8.28 ± 0.09	3	-7.90 ± 0.11	3	0.38
44h		-7.70 ± 0.03	5	-8.17 ± 0.09	4	-7.49 ± 0.09	4	0.68
44b		-9.51 ± 0.06	6	-9.86 ± 0.02	3	-9.49 ± 0.02	3	0.37
48a	H	-7.07 ± 0.02	5	-7.49 ± 0.08	4	-7.07 ± 0.06	4	0.42
44j		-7.77 ± 0.03	6	-8.03 ± 0.07	4	-7.59 ± 0.09	4	0.44
44k	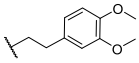	-8.15 ± 0.04	6	-8.51 ± 0.04	4	-8.18 ± 0.08	4	0.33
49a	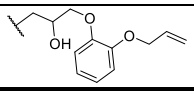	-9.01 ± 0.08	5	-9.49 ± 0.10	6	-9.16 ± 0.11	4	0.33

TABLE 3.9: Affinity values of oxprenolol analogues for the β_2-AR. $LogK_D\beta_2$ represents the affinity obtained through radioligand competitive binding assays; $LogK_D\beta_{2Cim}$ represents the affinity derived from the rightward shift of cimaterol concentration-response curve in CRE-SPAP assays.; $LogK_D\beta_{2CGP}$ represents the affinity derived from the rightward shift of CGP12177 concentration-response curve in CRE-SPAP assays.

$\text{Log}K_D\beta_{2Cim}$ and $\log K_D\beta_{2GCP}$ represent the affinity for β_2-AR determined through parallel rightward shifts of cimaterol and CGP12177 concentration-response curves in CHO-β_2 cells, highlighted in tables 3.8 and 3.9. $\text{Log}K_D\beta_1$ values previously obtained from

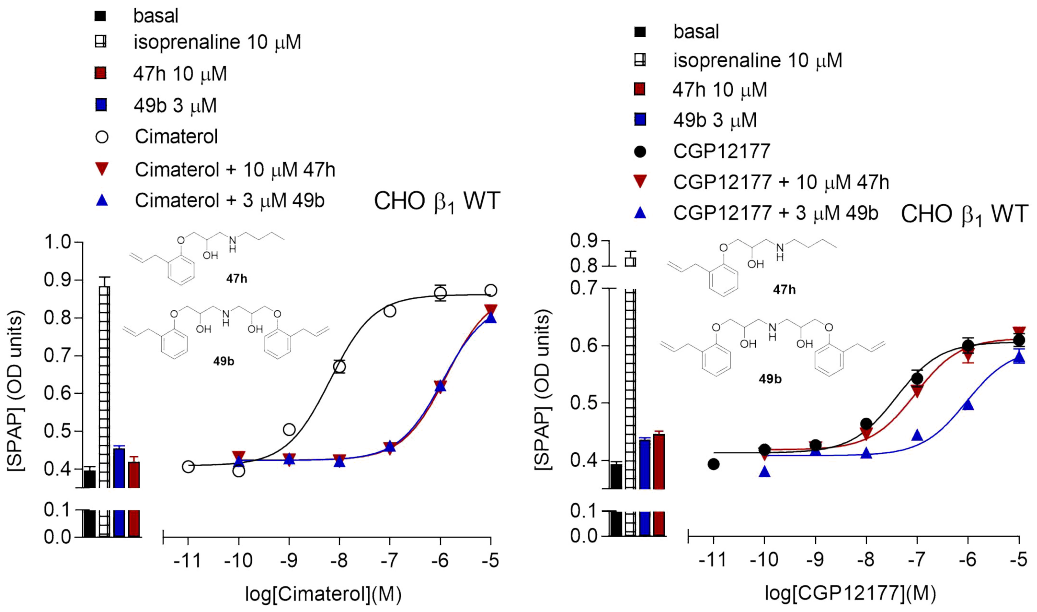

FIGURE 3.4: Left: CRE-SPAP production in response to cimaterol in the absence and presence of 49b and 47h; Right: CRE-SPAP production in response to CGP12177 in the absence and presence of 49b and 47h.

radioligand binding assays, correlate well with log$K_D\beta_{1cim}$ values as shown in figure 3.5 ($r^2 = 0.96$). These $logK_D\beta_{1cim}$ values are, consistently, slightly higher than those obtained by radioligand binding assays. Similarly, $logK_D$ values obtained from radioligand binding assays for the β_2-AR correlate well with $logK_D\beta_{2Cim}$ ($r^2 = 0.94$) but also with log$K_D\beta_{2CGP}$ ($r^2 = 0.96$). Generally, $logK_D\beta_{2CGP}$ values seem to differ around 0.5 log units from those obtained using cimaterol as an agonist. In the presence of partial agonists, the baseline of cimaterol and CGP12177 responses increased and the $logK_D$ values were derived from these curves using the Stephenson method (fig. 3.4). [85]

This hindered the determination of $logK_D\beta_{2GCP}$ for multiple analogues as CGP12177 behaves as a partial agonist at β_2-AR and these analogues displayed higher efficacy than CGP12177 in the system used.

Overall, alprenolol and oxprenolol analogues show around 2 orders of magnitude higher affinity for the primary conformation over the secondary conformation of the β_1-AR. $LogK_D\beta_{1CGP}$ values were not determined for some compounds as, at the maximum concentration of 10 μM, no shift in the CGP12177 concentration-response curve was observed (represented as <-5). Figure 3.6 displays the relationship between the affinity for the primary and secondary conformation. As expected from the literature, no compound is selective for the secondary conformation and a cluster of compounds with around 2 log

units difference between affinities can be observed, which is consistent with the primary and secondary conformation hypothesis.

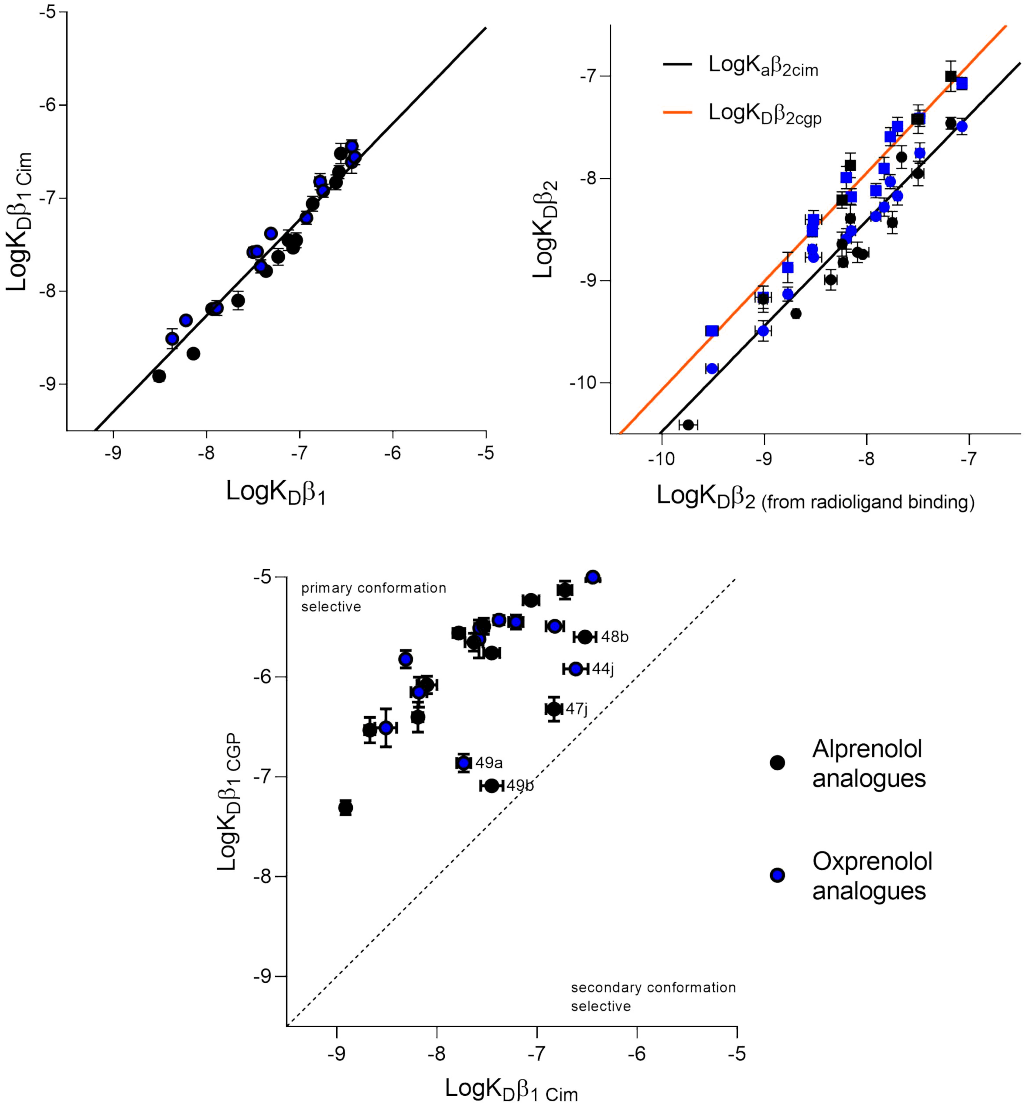

FIGURE 3.5: Left, top: correlation between $logK_D\beta_1$ obtained from radioligand competitive binding assays in β_1-CHO cells and $logK_D\beta_{1cim}$ derived from the rightward shift of cimaterol response curve in CRE-SPAP assays ($r^2 = 0.958$, $y = 1.092x + 0.437$); Right top: correlation between $logK_D\beta_2$ obtained from radioligand competitive binding assays and $logK_D\beta_{2Cim}$ and $logK_D\beta_{2CGP}$ obtained from the rightward shift of cimaterol or CGP12177 response curves in CRE-SPAP assays (Cim: $r^2 = 0.940$, $y = 1.032x - 0.1598$; CGP: $r^2 = 0.964$, $y = 1.061x + 0.5437$); Bottom: Relantionship between $logK_D\beta_{1cim}$ and $logK_D\beta_{1CGP}$ data is displayed in the plot along with an identation line allowing the visualisation of primary conformation selectivity.

Alprenolol shows a $logK_D\beta_{1cim}$ of -8.19 ± 0.05 and a $\log K_D\beta_{1CGP}$ of -6.40 ± 0.15, which translates in a difference of 1.79 log units between the affinity of both conformations. This is in good agreement with the affinity values found in the literature.[65] *tert*-Butylated analogue of alprenolol, 47b, showed an increase in the affinity for the primary conformation as also seen in the radioligand binding assays, but also an increase in the affinity for the secondary conformation. In general, the affinitiy for the secondary conformation seems to decrease or increase in a similar fashion to the affinity for the primary conformation with a few exceptions (figure 3.6; table 3.6). The same trend can also be found on the affinity values for most of oxprenolol analogues (figure 3.6; table 3.7). Compounds highlighted with compound numbering in figure 3.6, exhibit the lowest difference in affinity for both conformations. Bis compounds 49b and 49a, the benzylamino analogues 44j and 47j and the non-substituted alprenolol analogue 48b do not seem to follow the same trend as the majority of the set. Alprenolol analogue 48b shows a small difference between the affinity for both conformations ($logK_D\beta_{1cim}$ - $logK_D\beta_{1CGP}$ = 0.92). Introduction of methyl, propyl, butyl and cyclopropyl groups seems to decrease the affinity for the secondary conformation, even though an increase in affinity for the primary conformation is observed. Also, introduction of (3,4 dimethoxyphenethyl)amino group leads to one of the highest differences in affinity between both conformations, both in the alprenolol analogue ($logK_D\beta_{1cim}$ - $logK_D\beta_{1CGP}$ = 2.14) and the oxprenolol analogue ($logK_D\beta_{1cim}$ - $logK_D\beta_{1CGP}$ = 2.49). In contrast, alprenolol bis analogue 49b shows only a slight difference between the affinity for both conformations ($logK_D\beta_{1cim}$-$logK_D\beta_{1CGP}$ = 0.34) and the second highest affinity of the set for the secondary conformation, higher than alprenolol which has 30 fold (1.46 log units) higher affinity for the primary conformation. Oxprenolol bis analogue 49a also presents a marked decrease in selectivity between conformations. Interestingly, benzylamino analogues possess more than 6-fold (0.8 log units) lower affinity than the methylamino analogues for the primary conformation but 4-fold (0.6 log units) higher affinity for the secondary conformation which highlights the importance of a phenyl ring in that position. These ligands are, to our knowledge, the first sub-μM compounds to possess similar affinity for both conformations.

3.2.2.4 CGP20712A affinity

In order to confirm in a second assay which conformation mediated the response of these compounds, a fixed concentration of CGP20712A (an antagonist at both conformations) was added to increasing concentration of ligand. CGP20712A was able to shift rightwards the concentration-response curve of cimaterol, mediated through the primary conformation, with a $\log K_D\beta_{1cim}$ of -9.23 ± 0.11 while it required 100 fold (2 log units) higher concentration to righshift CGP12177 concentration-response curve the same amount ($\log K_D\beta_{1CGP} = -7.23 \pm 0.07$) (See table 2.5 in the previous chapter).

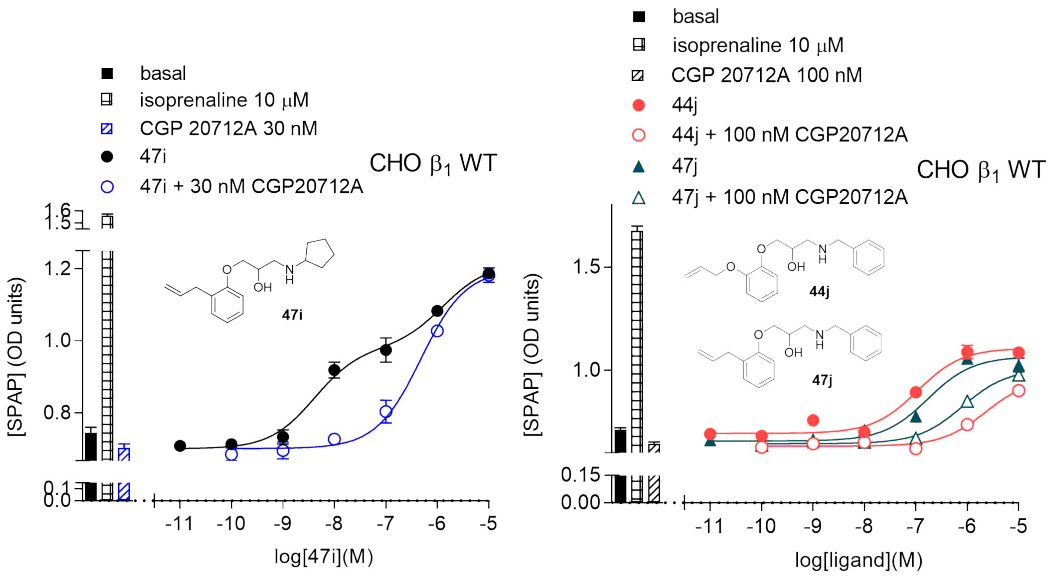

FIGURE 3.6: Left: CRE-SPAP production in response to analogue 47i in the presence and absence of 30 nM CGP20712A; Right: CRE-SPAP production in response to either analogue 44j or 47j in the presence and absence of 100 nM CGP20712A.

The logK_D value for CGP20712A calculated through the rightshifting of the ligands concentration-response curve is represented in tables 3.2 and 3.3 as CGP20712A logK_D. ICI118551, a selective β_2-AR antagonist which binds to the receptor with a logK_D of -9.24 ± 0.05 (See table 2.1 in the previous chapter), was used as a negative control experiment for this assay in CHO-β_2 cells.

Overall, CGP20712A was able to inhibit the response of most ligands at low concentration, which indicates that the response of these ligands is mediated through the primary conformation through binding to the well-known cathecolamine site. This is consistent with the $logEC_{50}$ values for those responses, which are similar to the $logK_D$ values determined through competitive radioligand binding assays for the respective ligand. In compounds that are able to mediate a response in a biphasic manner the $logK_D$ for CGP20712A represents the affinity for the conformation in which the first component is mediated (eg. 47i, figure 3.6). Analogue 47i increases CRE-SPAP accumulation in a biphasic fashion but, in the presence of 30 nM CGP 20712A, the response seems to contain only a single component. This concentration of antagonist, as can be seen in figure 3.6 (left) rightshifts the first component of the response but is not able to rightward shift the second component, which is consistent with a first response component mediated through the primary conformation and a second component, more resistant to antagonism, mediated through the secondary conformation of the β_1-AR.

Interestingly, responses mediated by the bis analogues 49a and 49b seem to be more resistant to antagonism. CGP20712A was able to inhibit these response with a logK_D of -7.93 ± 0.15 for alprenolol bis analogue 49b and -8.03 ± 0.23 for oxprenolol bis analogue 49a. These responses are not as resistant to antagonism as CGP12177 mediated response, which might indicate that these compounds are able to mediate a response through both conformations with a similar $logEC_{50}$ and not purely through the secondary conformation due to the small difference between the affinity for both conformations. Even though the $logEC_{50}$ values for alprenolol bis analogue is in agreement with the $logK_D$ obtained from radioligand binding assays, it is also in agreement with the log$K_D\beta_{1CGP}$ value (-7.13 vs -7.11, respectively).

Identically, benzylamino alprenolol analogue 47j also activates the receptor with a $logEC_{50}$ value similar to the log$K_D\beta_{1CGP}$ (-6.63 vs -6.32), which does not happen in the oxprenolol analogue 44j (-7.03 vs -5.92). Response mediated by analogue 47j is also more resistant to antagonism by CGP20712A ($logK_D = -7.82 \pm 0.06$, n=3, table 3.2) while response mediated by analogue 44j (CGP20712A $logK_D = -8.80 \pm 0.14$, n=3, table 3.3) is in agreement with a response mediated through the primary conformation of the β_1-AR. This is highlighted in figure 3.6 (right), which depicts the CRE-SPAP accumulation in response to these analogues in the presence and absence of a fixed concentration of 100 nM of CGP20712A. As can be seen in the figure, this concentration of antagonist leads to the parallel rightward shift of both curves but produces a larger shift for 44j mediated response.

Affinity values obtained for ICI118551 in β_2-CHO cells through the rightward shifting of the ligands concentration-response were slighlty higher than those obtained from radioligand competitive binding assays (table 3.4 and 3.5). Lastly, this demonstrates the importance of confirming the conformation of action for these ligands in a second assay even if logEC_{50} values are identical to the logK_D obtained from competitive ligand binding assays.

3.3 Conclusion

A set of 26 alprenolol and oxprenolol N-akyl analogues was synthesised. All compounds bound to both β_1- and β_2-AR in a competitive radioligand binding assay in CHO cells expressing either the human β_1- or β_2-AR. Overall, the compounds in this set of alprenolol and oxprenolol N-alkyl analogues seem to possess some degree of selectivity for the β_2-AR, as the parent compounds. Introduction of a (3,4-dimethoxyphenethyl)amino group converts the compounds in non-selective ligands with similar affinities for both receptors,

while oxprenolol bis analogue 49a possesses the highest selectivity for the β_2-AR. *tert*-Butylated analogues (44b and 47b) exhibit the highest affinity for both receptors, showing that branched analogues have overall higher affinity than the counterpart extended chain or ring-constrained analogues.

Most of these ligands are able to elicit a response in CRE-SPAP assays, behaving as partial agonists as the parent compounds. Alprenolol, oxprenolol and analogues 47b, 44b, 47i and 47k display a biphasic concentration-response curve with two components: a first component mediated through the primary conformation of the β_1-AR with a $logEC_{50}$ consistent with the $logK_D$ data; a second component, presumably mediated through the secondary conformation, which requires two order of magnitude higher concentration in agreement with the $\log K_D \beta_{1CGP}$ determined through the rightward shifting of CGP12177 mediated response. Some ligands emerge from this set of compounds. Bis analogues 49a and 49b and benzylamino analogues 44j and 47j yielded a surprisingly low selectivity for the primary conformation over the secondary conformation of the β_1-AR. Bis analogues 49a and 49b seem to mediate a response through the secondary conformation, even though it may not be purely mediated through this conformation as CGP20712A requires a higher concentration to antagonise these responses than cimaterol, but a lower concentration than the one needed to antagonise CGP12177 response. Benzylamino analogue 44j also mediates a response through the secondary conformation which is relatively resistant to antagonism, contrary to benzylamino analogue 47j that mediates a response through the primary conformation and is easily inhibited by CGP20712A.

Overall, N-alkyl substitution seems to have a pronunced influence on the affinity for the secondary conformation demonstrated by the introduction of the benzylamine and the bis ligands. Aromatic core also seems to influence the affinity and activity at the secondary conformation as alprenolol benzylamino analogue is able to activate the secondary conformation contrary to the oxprenolol benzylamino analogue which mediates a response through the primary conformation. Alprenolol analogues also show consistently higher affinity for the secondary conformation, but also for the primary conformation, than the equivalent oxprenolol analogues. No compound selective for the secondary conformation has been identified yet. It cannot be excluded that selectivity for the secondary conformation of the β_1-AR cannot be obtained and might be somehow dependent on a first binding event to orthosteric site of the receptor.

Chapter 4

Synthesis and pharmacological evaluation of aromatic core alprenolol analogues

4.1 Introduction

In this chapter the synthesis and pharmacological evaluation of several alprenolol analogues containing different substituents in the aromatic ring will be described. Alprenolol aromatic core was chosen over oxprenolol as starting point due to several reasons: (1) it has higher affinity for the secondary conformation of β_1-AR which facilitates its determination through CRE-SPAP assays; (2) it shows a lower difference in affinities between the primary conformation and secondary conformation ($logK_D\beta_{1cim}$-$logK_D\beta_{1CGP}$) across all *N*-alkyl analogues described in the previous chapter (see table 3.6); (3) Analogues can be obtained through a simpler synthetic route leading to faster generation of new analogues. *N-tert* butylated compounds were prefered over *N-iso*-propylated compounds and other *N*-alkyl substituents due to their, generally, higher affinity. As shown in the flowchart in the introduction, the affinity of these analogues was firstly evaluated through radioligand binding assays in CHO-cells expressing the human β_1 or β_2 adrenergic receptor. From these values (represented as $logK_D$) it was possible to calculate selectivity values for each receptor. If the compounds were able to bind to the receptor, they were evaluated in CRE-SPAP assays to determine their potency and efficacy. Affinities for the primary and secondary conformation of the β_1-AR were then derived from the ability of the antagonists or weak partial agonists of the set to parallel rightward shift the response of either cimaterol (**20**), an agonist at the primary conformation of the β_1-AR, or CGP12177 (**16**), an agonist at the secondary conformation of the β_1-AR, respectively. Fixed concentration

of CGP20712A, an antagonist at both conformation, was also added to increasing concentrations of agonists present in the set in order to determine the conformation through which the response is mediated.

4.2 Results and discussion

4.2.1 Chemistry

Firstly, a synthetic pathway with a common intermediate to all analogues was chosen in order to introduce the aromatic core in one of the final steps of the synthetic pathway (Scheme 4.1). The *N*-alkyl-2,3-epoxyamine **53** was synthesised through a known procedure in the literature. [87] The desired phenols were generally synthesised through the alkylation of the hydroxyl group with allyl bromide followed by a Claisen rearrangement as shown in scheme 4.1 using naphthol (**50**) as starting material. However, the

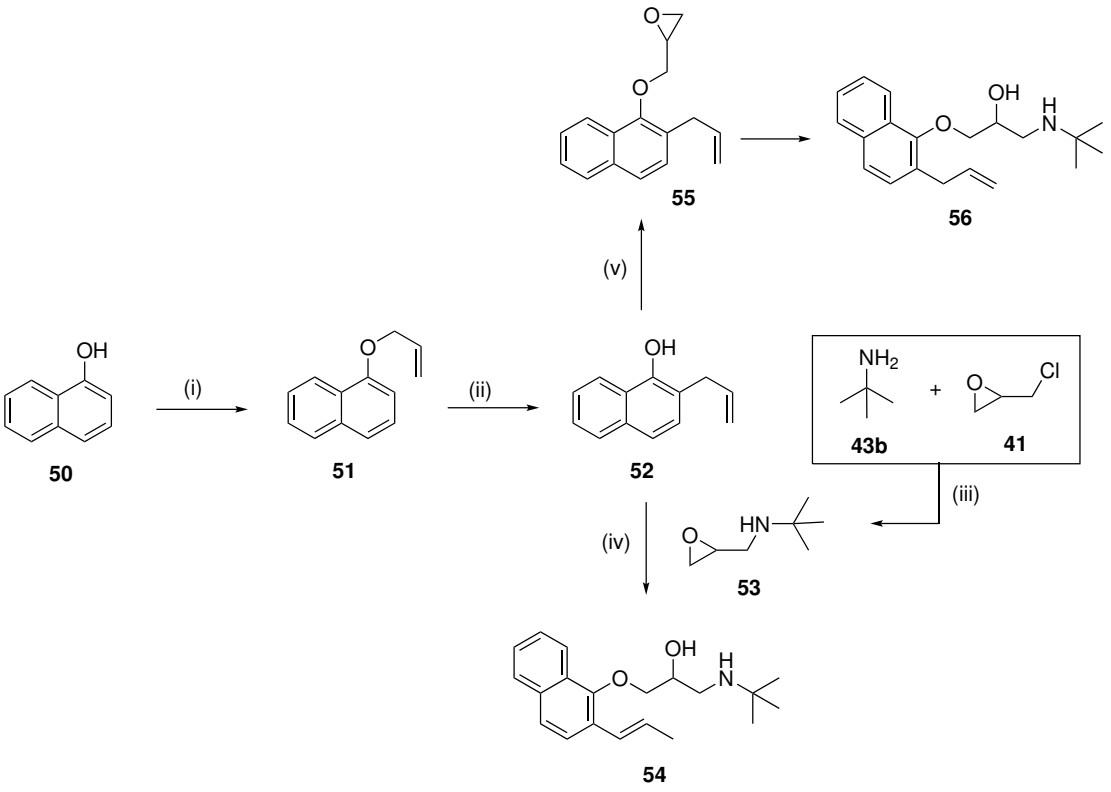

SCHEME 4.1: Synthesis of 1-((2-allylnaphthalen-1-yl)oxy)-3-(*tert*-butylamino)propan-2-ol **(56)**. Conditions and reagents: (i) allyl bromide, K_2CO_3, DMF, r.t., 24h, 85%; (ii) DMF, MW, 200 °C, 40 min., 66%; (iii) tert-butylamine, epichlorohydrin, isopropyl alcohol, 0 °C -> r.t., 24h followed by KOH, diethyl ether, r.t., 1.5h, 56%; (iv) NaOH, isopropyl alcohol, 95 °C, 12h, 4%; (v) epichlorohydrin, NaOH, MW, 120 °C, 30 min., 60%; (v) *tert*-butylamine, MW, 70 °C, 1h., 72%

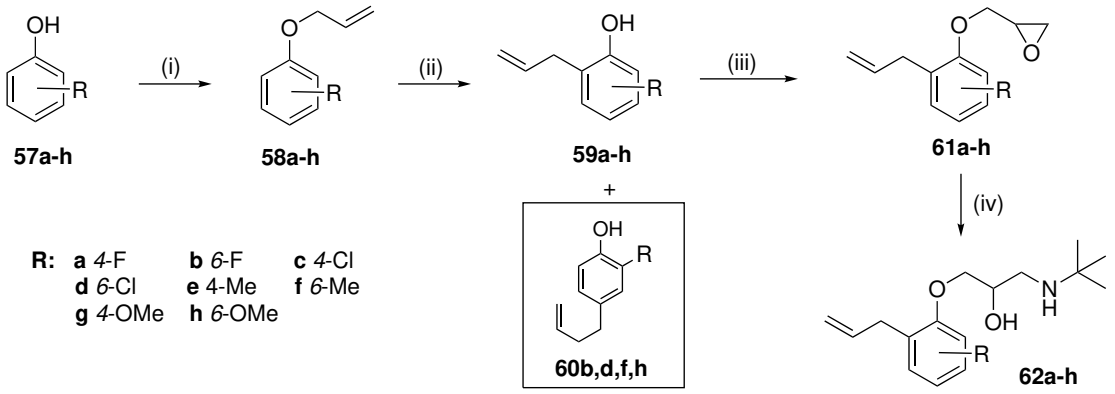

SCHEME 4.2: Synthesis of alprenolol analogues bearing ortho- and para- substituents. Conditions and reagents: (i) allyl bromide, K_2CO_3, DMF, r.t., 24h, 80-93%; (ii) DMF, MW, 200 °C, 40 min., 45-89%;(iii) epichlorohydrin, NaOH, MW, 120 °C, 30 min., 39-75%; (iv) *tert*-butylamine, MW, 70 °C, 1h., 78-90%.

reaction of the desired phenol **52** with the epoxide **53** in the presence of NaOH yielded the phenoxypropanolamine **54** rather than the desired phenoxypropanolamine **56**. The use of a strong base may have led to the isomerisation seen in the allyl side chain. The use of weaker bases, as K_2CO_3 or Et_3N, yielded the desired compounds only in residual amounts.

N-alkyl-2,3-epoxyamine **53** is known to have a higher stability than other oxiranes bearing secondary and primary amines due to the hindering *tert*-butyl group, however, its degradation in solution and autocatalytic oligomerisation might have contributed to the residual yields obtained. [88] As the desired compounds could not be obtained through this synthetic route, the general synthetic pathway for the synthesis of phenoxypropanolamines was used. Phenol **52** was coupled with epichlorohydrin followed by nucleophilic epoxide opening with *tert*-butyl amine to obtain the desired final compound **56** in good yields.

The same procedure was used for phenols containing substituents in the *ortho* and *para* positions (**57a-h**, Scheme 4.2). Alkylation with allyl bromide afforded the alkylated phenols in good yields. Phenols **59a-h** were obtained through a Claisen rearrangement of the allylated phenols. Several different methods have been used for the Claisen rearrangement. [87] Heating the allylated phenols in DMF in a microwave vial for 45 minutes at 200°C was found to be the fastest and most efficient method. Reaction rates are known to increase with polar solvents and with formation of the phenolic product, working as an autocatalyst. Phenols **60** were formed as a side product of the Claisen rearrangement of the *ortho*-substituted allylated phenols. In the Claisen rearrangement of an allyl aryl ether a thermal [3,3] sigmatropic rearrangement occurs, affording an *ortho*-dienone that promptly enolizes into an *ortho*-allylphenol. The reaction is considered to be concerted

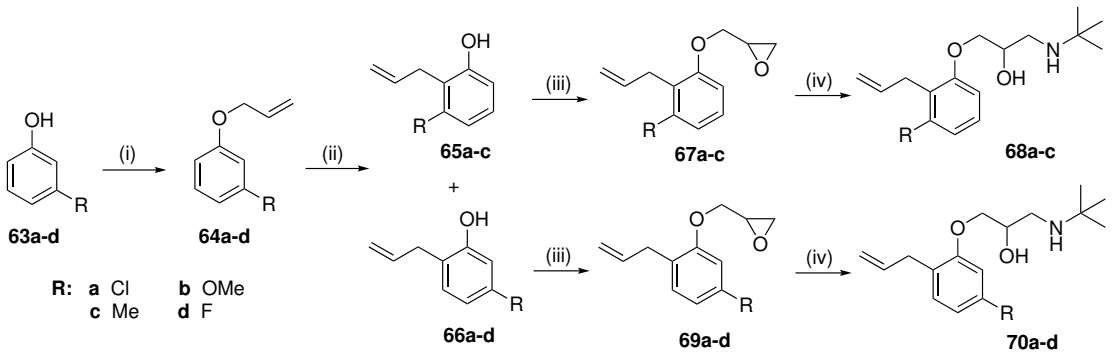

SCHEME 4.3: Synthesis of alprenolol analogues bearing meta-substituents. Conditions and reagents: (i) allyl bromide, K_2CO_3, DMF, r.t., 24h, 82-93%; (ii) DMF, MW, 200 °C, 50 min., 32-47%; (iii) epichlorohydrin, NaOH, MW, 120 °C, 30 min., 47-68%; (iv) *tert*-butylamine, MW, 70 °C, 1h., 80-91%.

through a favorable chair-like transition state. As 1-(allyloxy)-2-methylbenzene bears a substituent in the *ortho*-position subsequent [3,3] sigmatropic rearrangement (Cope rearrangement) occurs as side reaction leading to the formation of the *para*-allyl phenols **60**. [89]

Phenols **63a-d** containing *meta*-substituents were also alkylated with allyl bromide originating the alkylated phenols **64a-d** (Scheme 4.3). However, in this case, as the phenols are assymetrical, the Claisen rearrangement yielded two products (**65a-c** and **66a-d**). Claisen rearrangements of *meta*-substituted compounds were found to occur at slightly slower rate, which is in accordance with the literature, therefore the time of reaction was increased. [87] Claisen rearrangements containing substrates in the meta position are not highly regioselective although this roughly depends on the electronic nature of the substituent. The thermal [3,3] sigmatropic rearrangement of the chloro analogue **64a** yielded the phenol **65a** as major product, while the rearrangement of the methoxy analogue **64b**, containing an electron-donating group, promoted the rearragement to the less hindered position, originating the phenol **66b** in higher quantity, which is also in accordance with the literature.[89]

The two *meta*-methyl adducts **65c** and **66c** were obtained as an inseparable mixture which was then coupled with epichlorohydrin yielding the oxiranes **67c** and **69c**. The oxiranes were then submitted to epoxide-opening in the presence of *tert*-butyl amine leading to the formation of the final phenoxypropanolamines **68c** and **70c**. The mixture of phenoxypropanolamines was separated through preparative HPLC, resulting in the isolation of compound **68c** with good purity. Due to the similar retention times of both compounds, compound **70c** was collected with a purity around 90%, below purity standards required for biological testing. For this reason an alternative route was designed to obtain phenol **66c** (Scheme 4.4).[90] Phenol **71** was acetylated, in order to improve both

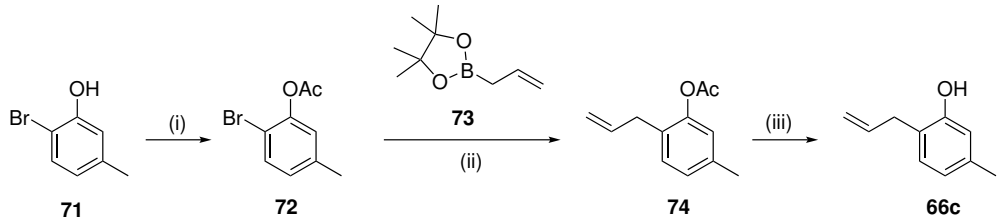

SCHEME 4.4: Alternative route for the synthesis of *meta*-substituted phenols. Conditions and reagents: (i) Ac_2O, Pyridine, r.t., 24h, 79%; (ii) $Pd(PPh_3)_4$, K_2CO_3, THF, 100 °C, 50 min., MW (no purification); (iii) $LiAlH_4$, THF, r.t., 24h., 85%.

stability and reactivity, to give compound **72**. The Suzuki-Miyaura reaction of **72** in the presence of pinacol boronic ester **73** afforded the desired product **74**. The crude of this reaction, without further purification, was treated with $LiAlH_4$ to originate the deacetylated phenol **66c** which was then purified through column chromatography. The desired final phenoxypropanolamine was synthesised through the path shown on the previous schemes. Phenol **66c** was alkylated with epichlorohydrin, unreacted phenol was removed through a base wash, and the crude was then reacted with *tert*-butylamine yielding final compound **70c**.

4.2.2 Pharmacology

4.2.2.1 Competitive radioligand binding assays

Alprenolol analogues containing different substituents in the aromatic ring were initially evaluated in chinese hamster ovary cells (CHO) stably expressing the human β_1-AR or β_2-AR. Their ligand affinity was determined in a competitive whole-cell binding study using the radioligand [^{3}H] CGP12177. [^{3}H] CGP12177 was used in concentrations such that it mostly occupies the primary conformation of the β_1, therefore affinity values for analogues obtained from this method are regarded as affinity values for the primary conformation of the β_1.

Figure 4.1 represents the amount of radioactivity bound to the CHO-β_1 and CHO-β_2 cells at different concentrations of ligand when a fixed concentration of radiolabeled [^{3}H] CGP12177 is added. Total binding and non-specific binding in the presence of a 10 μM of propranolol are also represented. The IC_{50} values taken from the dose-response curve were then converted into K_D values through the Cheng-Prusoff equation presented in the experimental section.

Substituent (**R**)		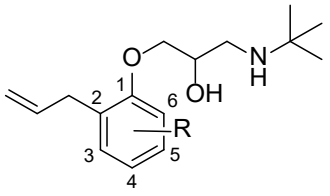				
		$LogK_D\beta_1$	n	$LogK_D\beta_2$	n	$LogK_D(\beta_2/\beta_1)$
47b	H	-8.51 ± 0.05	6	-9.74 ± 0.09	5	1.23
62a	4-F	-7.24 ± 0.06	6	-8.47 ± 0.05	6	1.23
70d	5-F	-8.53 ± 0.03	6	-9.64 ± 0.05	6	1.11
62b	6-F	-7.92 ± 0.04	6	-9.43 ± 0.09	6	1.51
68a	3-Cl	-8.21 ± 0.06	6	-9.67 ± 0.05	6	1.46
62c	4-Cl	-7.63 ± 0.05	6	-9.09 ± 0.05	7	1.46
70a	5-Cl	-8.48 ± 0.05	6	-10.17 ± 0.07	5	1.69
62d	6-Cl	-5.89± 0.08	6	-7.02 ± 0.04	7	1.13
68b	3-OMe	-7.60 ± 0.05	6	-8.68 ± 0.04	6	1.08
62g	4-OMe	-7.09 ± 0.03	6	-8.08 ± 0.04	5	0.99
70b	5-OMe	-7.91 ± 0.03	6	-9.54 ± 0.06	6	1.63
62h	6-OMe	-5.72 ± 0.02	5	-6.94 ± 0.05	6	1.22
68c	3-Me	-8.44 ± 0.04	7	-9.67 ± 0.03	5	1.23
62e	4-Me	-7.86 ± 0.04	6	-9.43 ± 0.05	7	1.57
70c	5-Me	-8.66 ± 0.04	6	-10.19 ± 0.05	6	1.53
62f	6-Me	-5.35 ± 0.05	5	-6.53 ± 0.06	6	1.18

TABLE 4.1: Binding affinities for human β_1- and β_2-AR of alprenolol analogues bearing aromatic substituents assessed using [^{3}H] CGP12177 whole cell binding assays. Values represent mean and ± the standard error of the mean (s.e.m) for n separate experiments.

The $logK_D$ values for each alprenolol analogue are presented in table 4.1. All analogues bound to both β_1- and β_2-adrenergic receptors. Affinity values obtained for the β_1-AR correlate well with the values for β_2-AR ($r^2 = 0.972$, fig. 4.2) which emphasizes the similarities between the two orthosteric binding pockets. Parent compound 47b showed a higher affinity than alprenolol for both receptors as presented in table 3.2 in the previous chapter.

Analogues containing substituents at the position 5 of the aromatic ring showed the highest affinity for both receptors within the same substituent, followed by 3-R analogues, 4-R analogues and then 6-R analogues (fig. 4.2). Methoxy analogues generally afforded the lowest affinity for each position, followed by fluoro, chloro and then methyl analogues for both receptors. 5-F, 5-Cl and 5-Me analogues yielded similar affinities to the parent compound 47b for the β_1-AR. In β_2-CHO cells, the 5-Cl and 5-Me analogues displayed

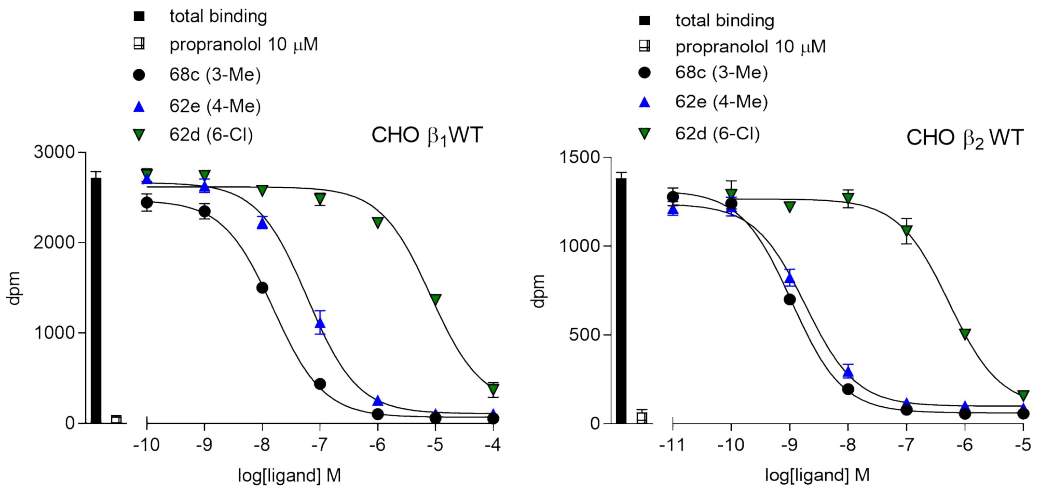

FIGURE 4.1: Inhibition of [^{3}H] CGP12177 binding to whole cells CHO-β_1 and CHO-β_2 by compounds **68c**, **62e** and **62d**. A fixed concentration of 0.82 nM of [^{3}H] CGP12177 was used. Data points were obtained in triplicate. Black bar represents total [^{3}H] CGP12177 binding, while the white bar represents nonspecific binding determined in the presence of 10 μM propranolol.

higher affinity than the parent compound. Introduction of a substituent in the 3-position of the aromatic ring led to a slight decrease in affinity for both receptores, while this decrease in affinity was more pronounced for 4-R analogues. 6-R analogues, except 6-F analogue 62b, showed a striking decline in affinity (around 1400-fold decrease, 3.16 log units, for 6-Me analogue 62f for β_1-AR) for both receptors, yielding the lowest affinities of the set. The difference in affinities between 3-Me and 6-Cl is quite noticeable in figure 4.1. Analogue 62d is only able to displace the radiolabeled CGP12177 at high concentrations. This striking decline in affinity seen in the 6-R analogues might be due to a steric clash in the well-known cathecolamine binding site at both the primary conformation of the β_1 and the β_2 leading to a rotation of the aromatic core.

No noticeable pattern was found regarding selectivity for any of the receptors. Parent compound, 47b, is slightly β_2 selective and exhibits a difference between $logK_D\beta_2$ and $logK_D\beta_1$ of 1.23 log units. Introduction of a chloro subtituent does increase this selectivity, except for 6-Cl analogue (62d), while introduction of a methoxy group in the *meta*- position of the aromatic ring can reduce the β_2 selectivity down to 10-fold (0.99 log units).

Overall, introduction of a larger subtituent as chloro, methoxy or methyl in the 5-position of the aromatic core increased the affinity for the β_2-AR and mantained similar affinity for the primary conformation of the β_1-AR.

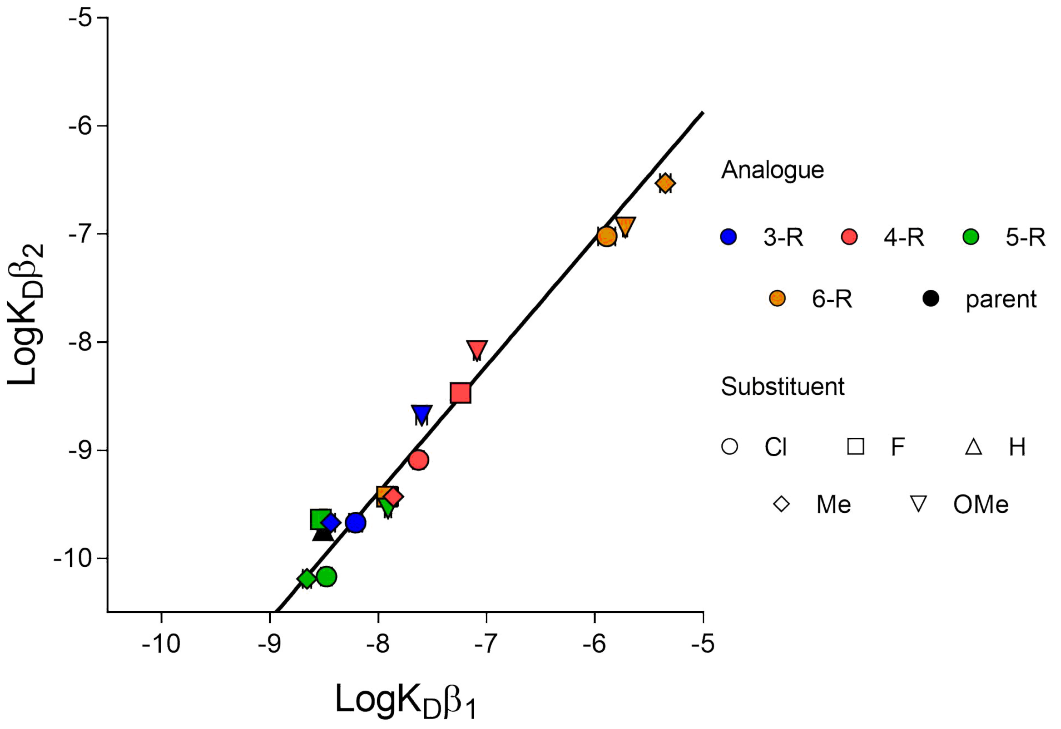

FIGURE 4.2: Correlation between $logK_D\beta_1$ and $logK_D\beta_2$ obtained for alprenolol aromatic core analogues ($r^2 = 0.972$; $y = 1.092x - 0.636$). Points are represented with different colours according to the position of the substituent in the aromatic ring and different shapes according to the substituent group.

4.2.2.2 CRE-SPAP production

Potency and efficacy for alprenolol aromatic core analogues were determined through CRE-SPAP production, a reporter gene for cAMP, in CHO-cells expressing either the human β_1- or β_2- receptors. $logEC_{50}$ values for the β_1 and β_2 are presented for all analogues in table 4.2 and table 4.3, respectively.

Overall, most ligands of this set behaved as antagonists both in β_1- and β_2-AR. Parent compound 47b behaved as a partial agonist at β_1-AR and increased CRE-SPAP production in a biphasic fashion with a $\log EC_{50}\beta_1 1$ of -9.08 ± 0.10 and a $\log EC_{50}\beta_1 2$ of -6.84 ± 0.15 with an $\%isop$ of $42 \pm 7\%$ (n=11). Methyl analogues bound to the receptors but failed to mediated any response. Methyl groups in the position 4 of the aromatic ring are known to prevent the rotamer change of $Ser^{5.46}$ by steric hindrance in the orthosteric binding pocket of the β_1-AR and therefore decrease efficacy.[91]

Substituent (**R**)		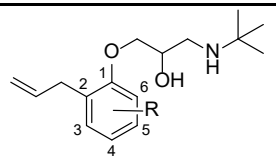									
		$LogK_D$ β_1	n	$LogEC_{50}$ $\beta_1$1	$LogEC_{50}$ $\beta_1$2	% 1st component	n	% isop	n	CGP20712A log K_D	n
47b	H	-8.51 ± 0.05	6	-8.57 ± 0.15	-6.14 ± 0.13	43 ± 7	8	29 ± 3	12	-8.78 ± 0.11	3
62a[L]	4-F	-7.24 ± 0.06	6	-5.91 ± 0.13	-	-	8	11 ± 1	6	-7.39 ± 0.08	3
62a				-7.46 ± 0.19	-*	-	4	11 ± 1	3	-	-
70d	5-F	-8.53 ± 0.03	6	-8.52 ± 0.09	-6.45 ± 0.30	56 ± 8	5	42 ± 5	5	-8.34 ± 0.14	4
62b[L]	6-F	-7.92 ± 0.04	6	-6.84 ± 0.06	-	-	4	18 ± 2	4	-7.46 ± 0.09	3
62b				-8.05 ± 0.25	-6.06 ± 0.26	50 ± 3	5	25 ± 5	5	-8.78 ± 0.22	4
68a	3-Cl	-8.21 ± 0.06	6	-	-	-	-	No response	6	-	-
62c	4-Cl	-7.63 ± 0.05	6	-7.55 ± 0.07	-	-	6	32 ± 6	6	-8.76 ± 0.11	4
70a	5-Cl	-8.48 ± 0.05	6	-	-	-	-	No response	8	-	-
62d	6-Cl	-5.89± 0.08	6	-	-	-	-	No response	3	-	-
68b	3-OMe	-7.60 ± 0.05	6	-	-	-	-	No response	8	-	-
62g	4-OMe	-7.09 ± 0.03	6	-7.26 ± 0.09	-	-	8	16 ± 3	5	-8.59 ± 0.09	3
70b	5-OMe	-7.91 ± 0.03	6	-	-	-	-	No response	8	-	-
62h	6-OMe	-5.72 ± 0.02	5	-	-	-	-	No response	3	-	-
68c	3-Me	-8.44 ± 0.04	7	-	-	-	-	No response	3	-	-
62e	4-Me	-7.86 ± 0.04	6	-	-	-	-	No response	3	-	-
70c	5-Me	-8.66 ± 0.04	6	-	-	-	-	No response	3	-	-
62f	6-Me	-5.35 ± 0.05	5	-	-	-	-	No response	3	-	-

TABLE 4.2: Binding affinity, potency and efficacy for β_1-AR of aromatic core alprenolol analogues in CHO cells stably expressing the human β_1-AR. Data are mean ± SEM for n experiments. $logK_D\beta_1$ represents the binding affinity assessed using [^{3}H]-CGP12177 whole cell binding assays; $logEC_{50}\beta_1 1$ represents potency derived from the first component of a biphasic concentration-response curve or single component in monophasic responses. $logEC_{50}\beta_1 2$ represents the potency value for the second component in a biphasic response; % 1^{st} component represents the percentage of the overall response mediated through the first component; $\%isop$ represents the efficacy (percentage of isoprenaline response) evaluated through CRE-SPAP assays; CGP20712A $logK_D$ represents the affinity derived from the inhibition of the ligand CRE-SPAP production using fixed concentrations of CGP20712A in whole cell assays; *compound seems to activate both conformations even though the value is out of range for this assay; ^{L} represents values obtained in cells with low expression levels of β_1-AR.

Substituent (**R**)		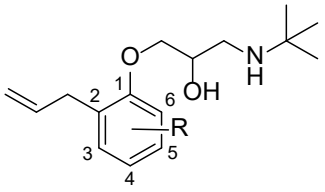							
		$LogK_D\ \beta_2$	n	$LogEC_{50}\ \beta_2$	n	% isop	n	ICI118551 $LogK_D$	n
47b	H	-9.74 ± 0.09	5	-9.65 ± 0.07	12	42 ± 3	12	-9.29 ± 0.11	5
62a	4-F	-8.47 ± 0.05	6	-8.92 ± 0.14	9	19 ± 2	6	-9.91 ± 0.03	3
70d	5-F	-9.64 ± 0.05	6	-9.60 ± 0.05	7	25 ± 2	7	-9.51 ± 0.06	4
62b	6-F	-9.43 ± 0.09	6	-9.48 ± 0.05	10	23 ± 2	6	-9.84 ± 0.13	4
68a	3-Cl	-9.67 ± 0.05	6	-	-	No response	3	-	-
62c	4-Cl	-9.09 ± 0.05	7	-	-	No response	3	-	-
70a	5-Cl	-10.17 ± 0.07	5	-	-	No response	3	-	-
62d	6-Cl	-7.02 ± 0.04	7	-	-	No response	3	-	-
68b	3-OMe	-8.68 ± 0.04	6	-	-	No response	3	-	-
62g	4-OMe	-8.08 ± 0.04	5	-	-	No response	3	-	-
70b	5-OMe	-9.54 ± 0.06	6	-	-	No response	3	-	-
62h	6-OMe	-6.94 ± 0.05	6	-	-	No response	3	-	-
68c	3-Me	-9.67 ± 0.03	5	-	-	No response	3	-	-
62e	4-Me	-9.43 ± 0.05	7	-	-	No response	3	-	-
70c	5-Me	-10.19 ± 0.05	6	-	-	No response	3	-	-
62f	6-Me	-6.53 ± 0.06	6	-	-	No response	3	-	-

TABLE 4.3: Binding affinity, potency and efficacy for β_2-AR of alprenolol aromatic core analogues in CHO cells stably expressing the human β_2-AR. Data are mean ± SEM for n experiments. $logK_D\beta_2$ represents the binding affinity assessed using [^{3}H]-CGP12177 whole cell binding assays; $logEC_{50}\beta_2$ represents potency derived from the concentration-response curve in CRE-SPAP assays. $\%isop$ represents the efficacy (percentage of isoprenaline response); ICI118551 $logK_D$ represents the affinity derived from the inhibition of the ligand CRE-SPAP production using fixed concentrations of ICI118551 in whole cell assays.

4-Chloro 62c and 4-methoxy 62g analogues, on the other hand, behave as weak β_1 partial agonists activating the receptor with a $logEC_{50}\beta_1 1$ of -7.55 ± 0.07 ($\%isop = 32 \pm 6\%$, n=6) and $logEC_{50}\beta_1 1$ of -7.26 ± 0.09 ($\%isop = 16 \pm 3\%$, n=5), respectively. Potencies values exhibited by these analogues are identical to the affinity values derived from the radioligand competitive binding experiments which suggest that these responses are mediated through the primary conformation of the β_1-AR. These weak responses also suggest a possible rotamer change of $Ser^{5.46}$ due to hydrogen bound formation but no rotamer change of $Ser^{5.42}$ or binding pocket contraction.[47, 91]

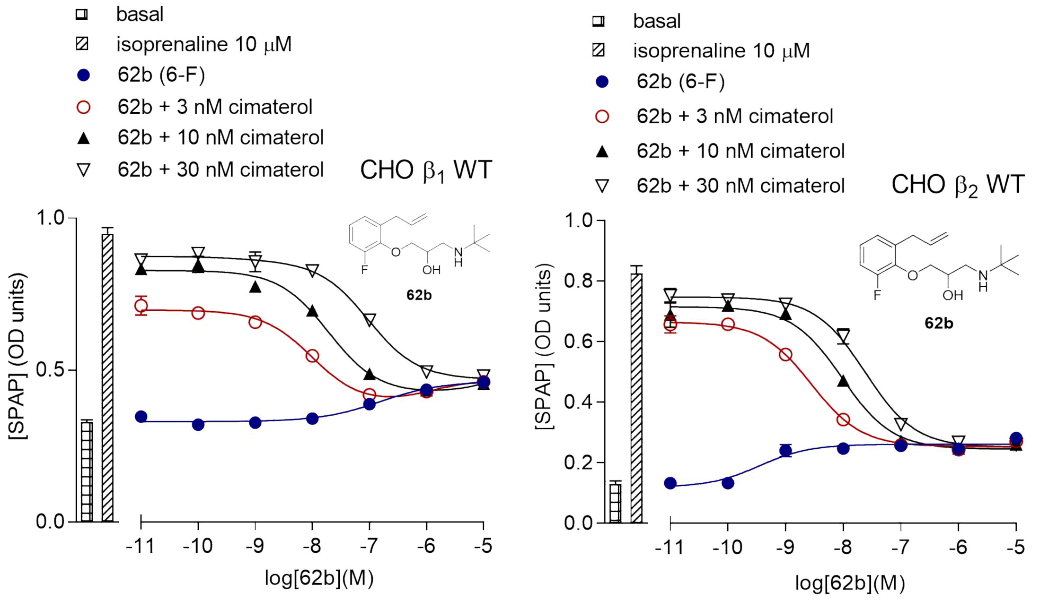

FIGURE 4.3: CRE-SPAP production in low expression CHO-β_1 (left) and CHO-β_2 (right) whole cells in response to analogue 62b in the absence and presence of fixed concentrations of 3, 10 and 30 nM of cimaterol. Bars represent basal CRE-SPAP production and isoprenaline (full agonist) response at 10 μM. Data points were obtained in triplicate.

Fluoro analogues were able to activate both receptors in CRE-SPAP assays. All fluoro analogues behaved in a similar fashion to the parent compounds, mediating a biphasic response at the β_1-AR. $logEC50\beta_1 1$ values obtained for the first component of the response are identical to $logK_D\beta_1$ values obtained indicating that these responses are mediated through the primary conformation. 5-Fluoro analogue (70d) exhibited a two component response with a first $logEC_{50}\beta_1 1$ of -8.52 ± 0.09 and a second $logEC_{50}\beta_1 2$ of -6.45 ± 0.30 with an $\%isop$ of $42 \pm 5\%$ (n=5, table 4.2). Interestingly, when using CHO-β_1 cells with low expression levels of protein, which reduces the assay window, only the second component of the response was detected for analogues 62a and 62b. This is highlighted in figure 4.3, where increasing concentrations of analogue 62b are added to several fixed concentrations of the primary conformation agonist cimaterol. In CHO-β_1 cells, analogue 62b only mediates a response at much higher concentrations than it requires to inhibit cimaterol response. On the other hand, in CHO-β_2 cells, the analogue is able to increase CRE-SPAP production in agreement with the inhibition of the cimaterol response seen. In CHO-β_2 cells these fluoro analogues were also able to activate the receptor, with potency values identical to affinity values obtained, even though they showed lower efficacy than the parent compound.

Overall, fluoro analogues were are able to activate both receptors and behaved in a

similar fashion to the parent compound. Methyl analogues behaved as antagonists at both receptors independently of the position of the substituent in the aromatic ring, while chloro and methoxy analogues were only able to mediate a response through the primary conformation of the β_1-AR only at position 4 of the aromatic core.

4.2.2.3 Affinity at primary and secondary conformation of the β_1-AR

Affinities for the primary ($logK_D\beta_{1cim}$) and secondary conformation ($logK_D\beta_{1CGP}$) of the β_1-AR are presented in table 4.4. These $logK_D$ values have been derived from the

Substituent (**R**)		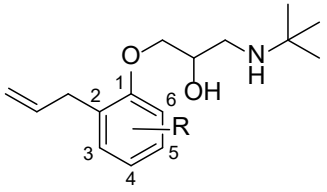						
		$LogK_D\ \beta_1$	n	$LogK_D\ \beta_{1\ cim}$	n	$LogK_D\ \beta_{1\ CGP}$	n	$LogK_{Dcim} - LogK_{DCGP}$
47b	H	-8.51 ± 0.05	6	-8.91 ± 0.03	4	-7.31 ± 0.07	4	1.60
62a	4-F	-7.24 ± 0.06	6	-7.50 ± 0.12	5	-5.58 ± 0.05	5	1.92
70d	5-F	-8.53 ± 0.03	6	-8.90 ± 0.08	6	-6.93 ± 0.08	6	1.97
62b	6-F	-7.92 ± 0.04	6	-8.18 ± 0.11	5	-6.47 ± 0.06	5	1.71
68a	3-Cl	-8.21 ± 0.06	6	-8.49 ± 0.15	5	-6.93 ± 0.14	5	1.56
62c	4-Cl	-7.63 ± 0.05	6	-7.78 ± 0.08	7	-6.53 ± 0.10	6	1.25
70a	5-Cl	-8.48 ± 0.05	6	-8.99 ± 0.06	7	-7.22 ± 0.05	7	1.77
62d	6-Cl	-5.89± 0.08	6	-5.96 ± 0.09	4	> -5	3	-
68b	3-OMe	-7.60 ± 0.05	6	-7.94 ± 0.05	7	-6.05 ± 0.15	7	1.89
62g	4-OMe	-7.09 ± 0.03	6	-7.34 ± 0.08	5	-5.50 ± 0.08	5	1.84
70b	5-OMe	-7.91 ± 0.03	6	-8.41 ± 0.07	7	-6.61 ± 0.13	6	1.8
62h	6-OMe	-5.72 ± 0.02	5	-5.88 ± 0.15	4	> -5	3	-
68c	3-Me	-8.44 ± 0.04	7	-8.61 ± 0.06	7	-6.77 ± 0.04	6	1.84
62e	4-Me	-7.86 ± 0.04	6	-7.93 ± 0.06	6	-6.71 ± 0.08	7	1.22
70c	5-Me	-8.66 ± 0.04	6	-8.97 ± 0.08	3	-7.16 ± 0.04	3	1.81
62f	6-Me	-5.35 ± 0.05	5	-5.29 ± 0.19	4	> -5	3	-

TABLE 4.4: Affinity values of alprenolol aromatic core analogues for the primary and secondary conformation of the β_1-AR. $LogK_D\beta_1$ represents the affinity obtained through radioligand binding assays; $LogK_D\beta_{1cim}$ represents the inhibition of cimaterol, a primary conformation agonist, CRE-SPAP production in whole cell assays; $LogK_D\beta_{1CGP}$ represents the affinity for the secondary conformation obtained through the inhibition of CGP12177, a secondary conformation agonist.; $LogK_D\beta_{1cim}$-$LogK_D\beta_{1CGP}$ represents the logaritmical selectivity values towards the primary conformation.

Substituent (**R**)		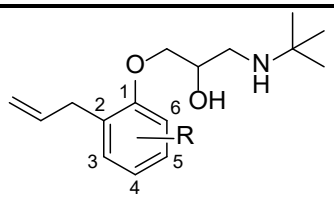						
		$LogK_D\ \beta_2$	n	$LogK_D\ \beta_{2\ cim}$	n	$LogK_D\ \beta_{2\ CGP}$	n	$LogK_{Dcim} - LogK_{DCGP}$
47b	H	-9.74 ± 0.09	5	-10.41 ± 0.03	3	-	3	-
62a	4-F	-8.47 ± 0.05	6	-8.97 ± 0.08	4	-8.50 ± 0.09	5	0.47
70d	5-F	-9.64 ± 0.05	6	-10.09 ± 0.10	8	-	3	-
62b	6-F	-9.43 ± 0.09	6	-10.02 ± 0.09	4	-9.60 ± 0.15	5	0.42
68a	3-Cl	-9.67 ± 0.05	6	-9.98 ± 0.09	4	-9.87 ± 0.10	6	0.11
62c	4-Cl	-9.09 ± 0.05	7	-9.41 ± 0.11	6	-9.18 ± 0.13	7	0.23
70a	5-Cl	-10.17 ± 0.07	5	-10.57 ± 0.10	6	-10.24 ± 0.12	3	0.33
62d	6-Cl	-7.02 ± 0.04	7	-7.08 ± 0.11	4	-7.03 ± 0.02	3	0.05
68b	3-OMe	-8.68 ± 0.04	6	-9.24 ± 0.07	5	-9.11 ± 0.06	3	0.13
62g	4-OMe	-8.08 ± 0.04	5	-8.53 ± 0.08	4	-8.17 ± 0.12	5	0.36
70b	5-OMe	-9.54 ± 0.06	6	-9.99 ± 0.09	4	-9.96 ± 0.10	3	0.03
62h	6-OMe	-6.94 ± 0.05	6	-7.05 ± 0.12	4	-6.97 ± 0.10	3	0.08
68c	3-Me	-9.67 ± 0.03	5	-9.86 ± 0.07	7	-9.95 ± 0.04	6	-0.09
62e	4-Me	-9.43 ± 0.05	7	-9.63 ± 0.05	7	-9.75 ± 0.08	6	-0.12
70c	5-Me	-10.19 ± 0.05	6	-10.50 ± 0.09	3	-10.33 ± 0.05	3	0.17
62f	6-Me	-6.53 ± 0.06	6	-6.36 ± 0.11	5	-6.35 ± 0.09	3	0.01

TABLE 4.5: Affinity values of alprenolol aromatic core analogues for the β_2-AR. $LogK_D\beta_2$ represents the affinity obtained through radioligand competitive binding assays; $LogK_D\beta_{2Cim}$ represents the affinity derived from the rightward shift of cimaterol concentration-response curve in CRE-SPAP assays.; $LogK_D\beta_{2CGP}$ represents the affinity derived from the rightward shift of CGP12177 concentration-response curve.

rightward shift of cimaterol, a primary conformation agonist, or CGP12177, a secondary conformation agonist, concentration-response curves by a fixed concentration of ligand. All the affinity values obtained for the primary conformation of the β_1-AR through this method strongly correlate with the affinity values obtained from competitive radioligand binding ($r^2 = 0.991$, fig. 4.5 top left). Similarly, $logK_D\beta_{2Cim}$ values also correlate well with values obtained from radioligand binding for β_2-AR ($r^2 = 0.983$), however this is also seen for $logK_D\beta_{2CGP}$ values obtained ($r^2 = 0.990$) which are identical to the values obtained from binding assays (fig. 4.5 top right).

Parent compound, 47b, showed a 1.60 log unit difference between affinity values obtained for primary and secondary conformation. All the compounds from this set, similarly

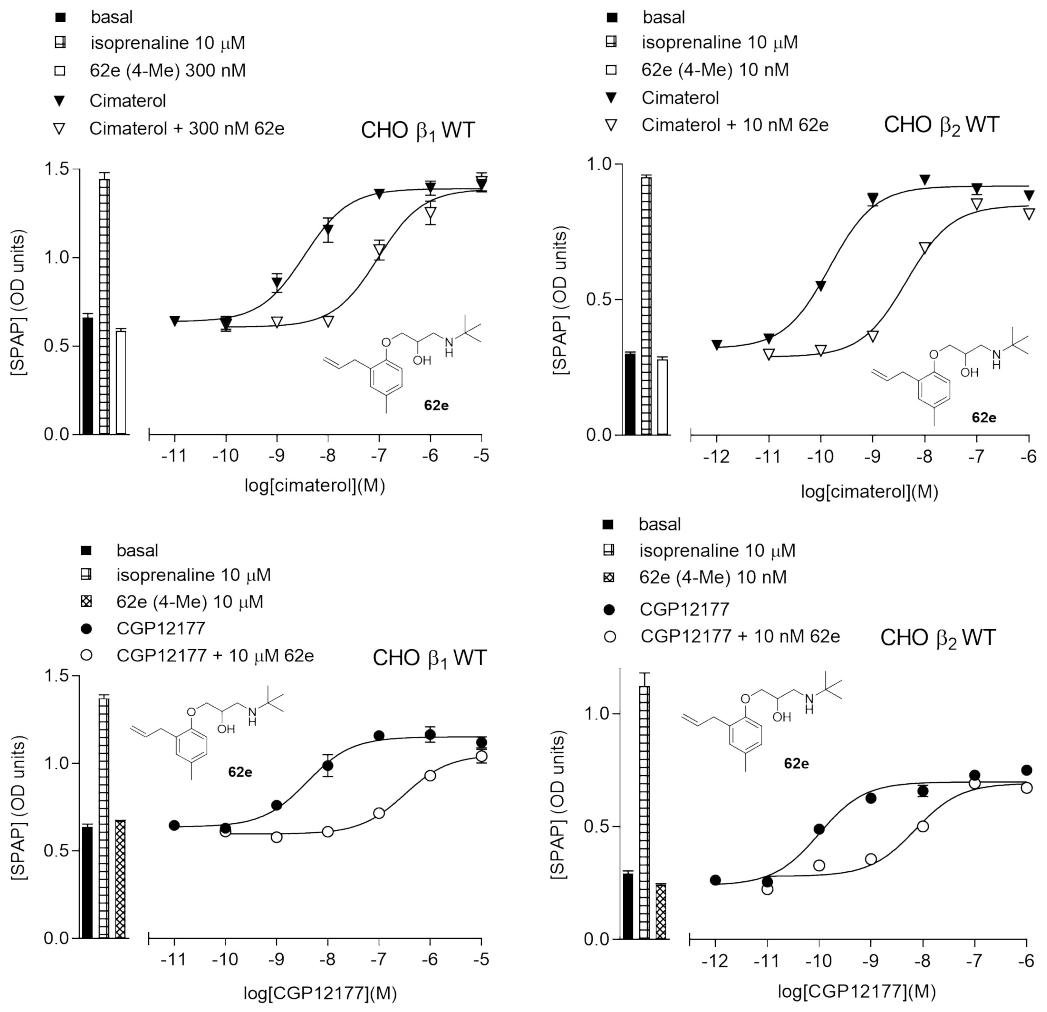

FIGURE 4.4: CRE-SPAP production in response to cimaterol in the absence and presence of a fixed concentration of analogue 62e (4-Me) in CHO-β_1 (top left) and -β_2 cells (bottom left); CRE-SPAP production in response to CGP12177 in the absence and presence of a fixed concentration of analogue 62e (4-Me) in CHO-β_1 (top right) and -β_2 cells (bottom right)

to the parent compound, required a higher concentration to rightward shift CGP12177 concentration-response curve than cimaterol. This is highlighted in figure 4.4, compound 62e is able to parallel rightwards shift cimaterol dose response at a fixed concentration of 300 nM but requires a higher concentration to shift CGP12177 response ,while in CHO-β_2 cells, a 10 nM fixed concentration of 62e, produces the same shift to both cimaterol and CGP12177 SPAP production curve.

Affinities for the secondary conformation of the β_1-AR seem to increase or decrease in agreement with the affinity for the primary conformation. This can be seen in figure 4.5 which demonstrates the linear correlation relationship between these two affinities

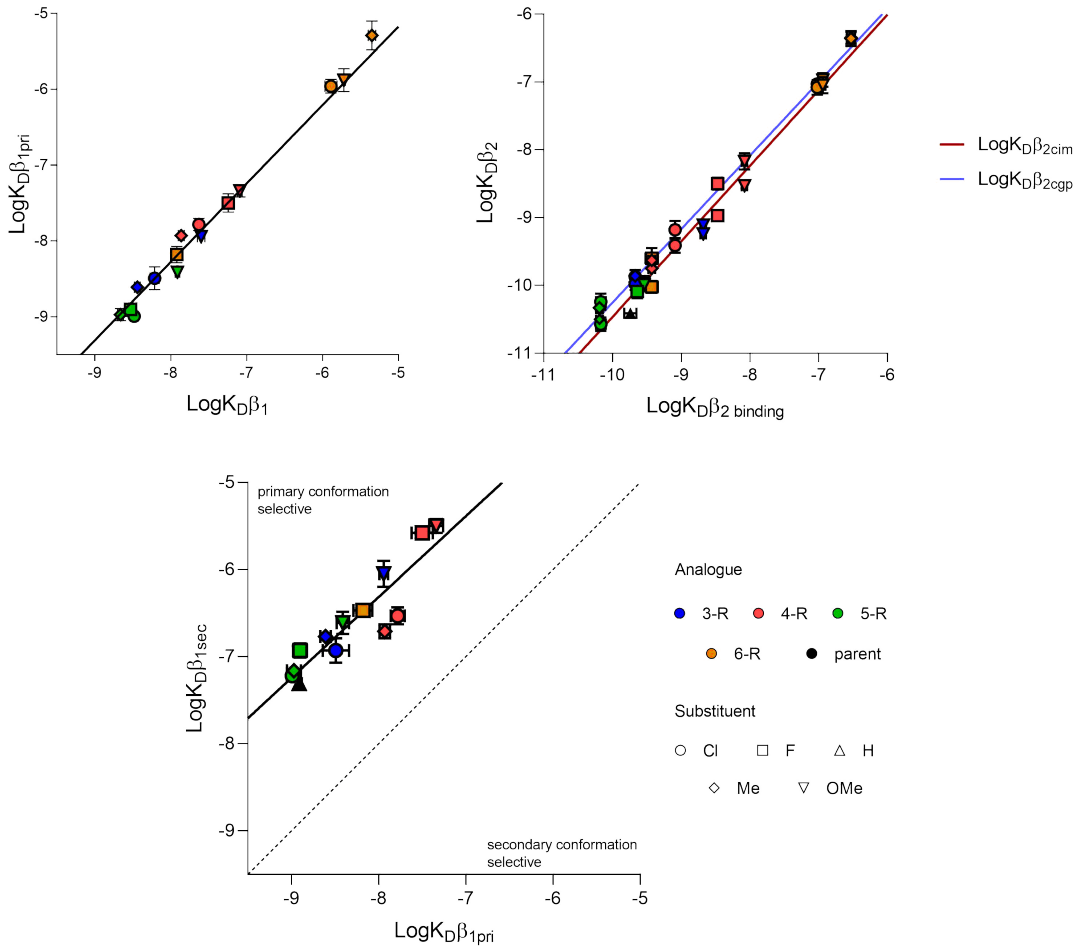

FIGURE 4.5: Top left: correlation between $logK_D\beta_1$ obtained from radioligand competitive binding assays in β_1-CHO cells and $logK_D\beta_{1cim}$ derived from the rightward shift of cimaterol response curve in CRE-SPAP assays ($r^2 = 0.991$, $y = 1.101x + 0.509$); Top right: correlation between $logK_D\beta_2$ obtained from radioligand competitive binding assays and $logK_D\beta_{2Cim}$ and $logK_D\beta_{2CGP}$ obtained from the rightward shift of cimaterol or CGP12177 response curves in CRE-SPAP assays (Cim: $r^2 = 0.983$, $y = 1.114x + 0.681$; CGP: $r^2 = 0.990$, $y = 1.084x + 0.586$); Bottom: Relationship between $logK_D\beta_{1cim}$ and $logK_D\beta_{1CGP}$ data is displayed in the plot along with an identation line allowing the visualisation of primary conformation selectivity ($r^2 = 0.835$, $y = 0.928x + 1.108$).

($r^2 = 0.835$). 6-R analogues 62d, 62f and 62h were not able to rightshift CGP12177 at the maximum concentration used (10 μM) hindering the determination of their affinity for the secondary conformation. Changes in the differences between the affinities for the primary and secondary conformation are not as pronounced as in the previous set. Methoxy analogues present a (log$K_D\beta_{1Cim}$ - log$K_D\beta_{1CGP}$) around 1.85 log units, higher than the parent compound. Likewise, fluoro analogues show a higher selectivity for the primary conformation than the parent compound. Interestingly, both in methyl and chloro series, the 4-R analogues showed a lower selectivity (log$K_D\beta_{1Cim}$ - log$K_D\beta_{1CGP}$

= 1.25 for 4-Cl analogue; $\log K_D\beta_{1Cim}$ - $\log K_D\beta_{1CGP}$ = 1.22 for 4-Me analogue.) towards the primary conformation (tab. 4.4).

4.2.2.4 CGP20712A affinity

In order to identify if a CRE-SPAP response is mediated through the primary or the secondary conformation of the β_1-AR a fixed concentration of the antagonist CGP20712A was added to increasing concentrations of ligand. CGP20712A is able to inhibit cimaterol response with a $logK_D$ of -9.23 ± 0.11, while it requires a higher concentration to inhibit CGP12177 response ($logK_D = -7.23 \pm 0.07$). Similarly, ICI118551, a β_2 antagonist was added to increasing concentrations of ligand as a control assay ($logK_D = -9.24 \pm 0.05$, obtained from competitive binding assays). These $logK_D$ values for CGP20712A and ICI118551 obtained are presented in tables 4.2 and 4.3, respectively.

Responses elicited by analogue 4-chloro and 4-methoxy seem to be mediated through the primary conformation as CGP20712A was able to antagonise these response at lower concentration. The first component of 5-fluoro and 6-fluoro analogues sigmoidal response curve was also easily inhibited by CGP20712A, as observed for the parent compound. In CHO cells with a low expression level of β_1-AR, 6-fluoro analogue presented a single component response, consistent with the second component found in CHO cells with higher expression levels of protein. Figure 4.6 shows these responses in the presence of

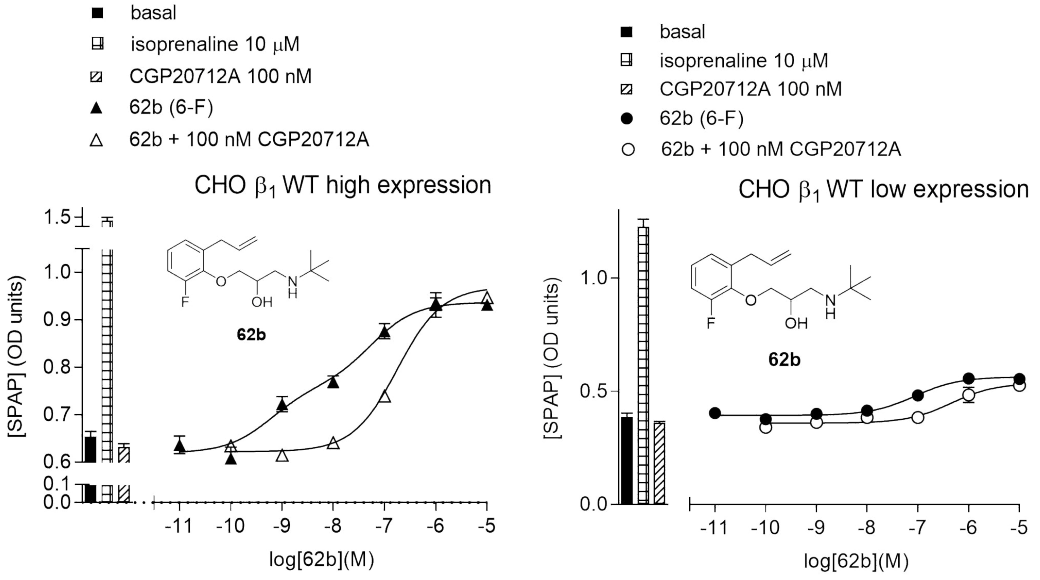

FIGURE 4.6: CRE-SPAP production in response to analogue 62b (6-fluoro) in the presence and absence of 100 nM CGP20712A in CHO-β_1 cells with high (left) and low (right) receptor expression.

100 nM of CGP20712A in both cells, obtained as a single component response. The antagonist was able to readily inhibited the first component of the response, while the second component was more resistant to antagonism producing a parallel rightward shift identical to the one seen for the response for the low expression cell line. This suggests that, in the low expression cell line, only the second component of the response is visible and demonstrates the importance of assay window in an experiment. 4-fluoro response in low expression CHO-β_1 cells was also resistant to antagonism which is consistent with a response mediated through the secondary conformation (CGP20712A $logK_D = -7.39 \pm 0.08$, table 4.2).

In CHO-β_2 cells, the antagonist ICI118551 was able to easily antagonise the responses elicited by fluoro analogues (table 4.3).

4.3 Conclusion

A set of aromatic core alprenolol analogues was synthesised. The first route using epoxide **53** as a common intermediate failed to yield the desired compounds. A second route was designed involving the addition of epichlorohydrin to every phenol followed by epoxide opening with *tert*-butyl amine. This route failed to produce the final 5-Me analogue due to the impossibility of separating the starting phenol from the regioisomer during the claisen reaction and following steps. A third route, using a Suzuki-Miyaura reaction, was used to obtain the desired phenol and then the desired 5-Me analogue.

All aromatic core analogues bound to both β_1- and β_2-AR. In a general fashion, affinity for both receptors was strongly affected by the position of the substituent within each substituent series ($5-R > 3-R > 4-R \gg 6-R$, with the exception of 6-F) and by the nature of the substituent ($Me > Cl > F > OMe$, except 6-R analogues). All fluoro analogues were able to activate both receptors, as seen for the *tert*-butylated alprenolol parent compound. These analogues mediated a biphasic concentration-response curve, in CHO-β_1 cells, which first component was mediated through the primary conformation and easily antagonised by CGP20712A. In CHO-β_1 cells with low expression levels of receptor, 4-F and 6-F analogues mediated a single component sigmoidal response, more resistant to antagonism with similar potencies to the second component of the response obtained previously. Analogues 4-OMe and 4-Cl showed weak partial agonism and mediated a response through the primary conformation of the β_1-AR.

All these analogues bound with higher affinity to the primary conformation than to the secondary conformation. Affinities for the secondary conformation seem to change accordingly with the changes seen for the primary conformation for this set. Analogues 62c

(4-Cl) and 62g (4-Me) stand out as the compounds with lower selectivity for the primary conformation with a $logK_D\beta_{1cim} - logK_D\beta_{1CGP}$ inferior to the parent compound.

Chapter 5

Synthesis and pharmacological evaluation of bis alprenolol analogues

5.1 Introduction

In this chapter, the synthesis, isolation and pharmacological characterisation of individual enantiomers and meso compounds for both the bis alprenolol analogue 49b (3,3'-azanediylbis(1-(2-allylphenoxy)propan-2-ol)) and the bis oxprenolol analogue 49a (3,3'-azanediylbis(1-(2-(allyloxy)phenoxy)propan-2-ol)) described in chapter 3 is reported.[40] Individual enantiomers for non-substituted analogues 48a and 48b, previously synthesised and pharmacologically characterised as a racemate, were also synthesised and purified. Bis analogue 49a and 49b emerged from the first set described in chapter 3. Alprenolol bis analogue 49b showed the lowest difference between the affinity obtained for the primary and secondary conformation of the β_1-AR ($logK_D\beta_{1cim} - logK_D\beta_{1CGP} = 0.34$, table 3.6) while retaining good affinity for the secondary conformation ($logK_D\beta_{1CGP} = -7.11 \pm 0.03$, n=5, table 3.6). This difference in affinity values is identical to the difference seen for the β_2-AR when using cimaterol and CGP12177 as agonists and it is quite striking when compared with the parent compound ($logK_D\beta_{1cim} - logK_D\beta_{1CGP} = 1.79$, table 3.6) and literature compounds.[65] Oxprenolol bis analogue 49a exhibits a similar behaviour with a $logK_D\beta_{1cim} - logK_D\beta_{1CGP}$ of 0.87. These bis analogues behave as partial agonists mediating a response that is more resistant to antagonism by CGP20712A suggesting it is mainly mediated through the secondary conformation of the β_1-AR. For these reasons the isolation and pharmacological characterisation of the individual isomers and meso compound seems of high importance to elucidate the role of each of the

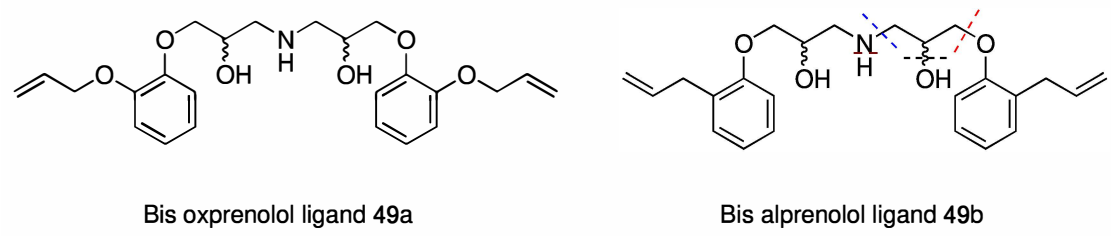

FIGURE 5.1: Oxprenolol bis ligand **49a** and alprenolol bis ligand **49b** with the representation of possible truncation points.

two stereocenters. *(S)*-aryloxypropanolamines are known to generally bind with higher affinity than the corresponding *(R)* enantiomer to both the primary conformation of the β_1-AR and β_2-AR, but also to the secondary conformation of the β_1-AR. The importance of the second stereocenter is unknown as little information regarding the synthesis and pharmacologically characterisation of bis aryloxypropanolamine compounds has been described in the literature. A ligand truncation study was also carried out for alprenolol bis analogue 49b to identify the chemical features responsible for the decrease in selectivity seen for the primary conformation of the β_1-AR (figure 5.1).

5.2 Results and discussion

5.2.1 Chemistry

In order to synthesise the enantiomerically pure epoxides **76a-b**, the chiral reagent *(S)*-glycidyl nosylate (75) was added to the corresponding phenol (40 or 45) in the presence of potassium carbonate (scheme 5.1). Epoxide opening of these epoxides was then performed in the presence of a 7N solution of ammonia in methanol at room temperature for 48 hours as described in chapter 3 to yield a mixture of *(S)*-non substituted analogues 77a-b and the bis *(S,S')* analogues **78a-b** which were then isolated through flash column chromatography. Similar procedure was used to obtain the *(R)*-enantiomers using *(R)*-glycidyl nosylate to introduce the chiral epoxide moiety.

Meso analogues **83a-b** have been synthesised through the addition of *(S)*-non substituted analogues **77a-b** to the corresponding *(R)*-epoxide under microwave irradiation using hexafluoro-2-propanol (HFIP) as a solvent at 70 °C (scheme 5.2). The enantiopurity of the final isomers obtained through these methods was then analysed through analytical chiral high-performance liquid chromatography (HPLC). Undesirably, these methods yielded only enriched fractions of the desired enantiomer but without the required enantiomeric purity for *in-vitro* testing (enantiomeric excess (ee) of 80-90% for analogues **77a-b**, **78a-b**, **81a-b** and **82a-b** and an even lower ee of 60-80% for meso

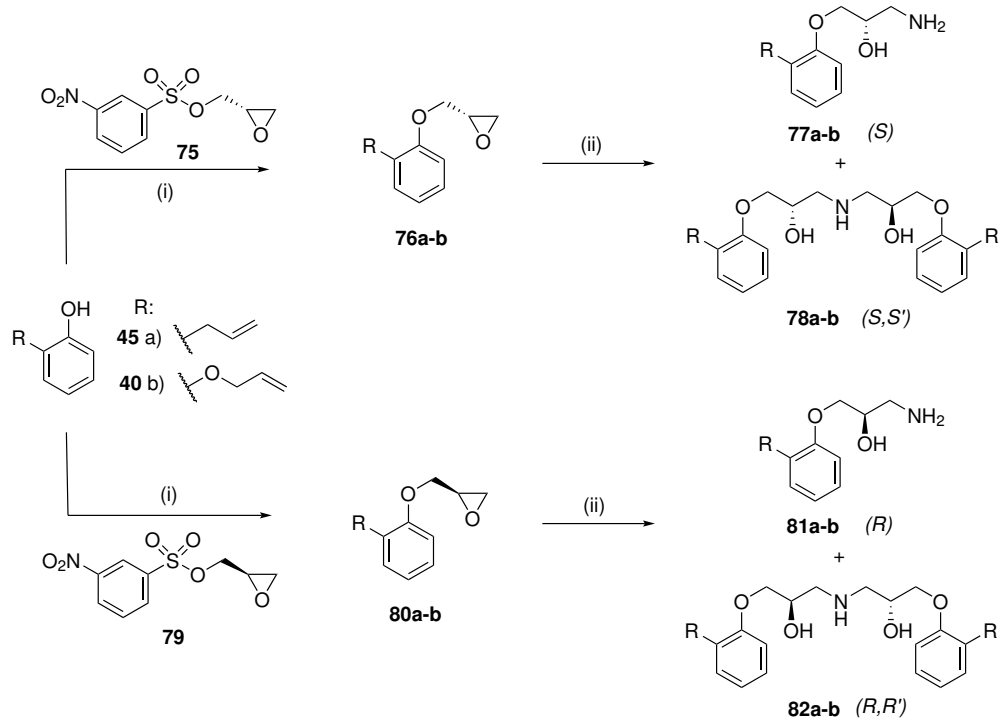

SCHEME 5.1: Synthesis of single enantiomers. Conditions and reagents: (i) **75**, K_2CO_3, acetone, reflux, 12h; (ii) 7N solution of NH_3 in MeOH, r.t., 48h.

compounds **83a-b**). Even though these methods did not afford the isomers with the desired enantiopurity, the enriched fractions allowed the assignment of the isomer to the correspondent peak and retention time. These isomers were then isolated through a semi-preparative chiral HPLC purification of the mixtures previously obtained in chapter 3 (48a-b and 49a-b) and purified to an ee of 99%. A chromatogram of the separation of mixtures **49b** and **48b** is presented in figure 5.2. Alprenolol bis analogue **49b** was previously obtained and tested as a mixture of 23% of the *(R,R')* enantiomer, 23% of the *(S,S')* enantiomer and 54% of the meso ligand as expected. Non-substituted alprenolol analogue **48b** was obtained as a racemic mixture of 52% of the *(R)*-enantiomer and 48% of the *(S)*-enantiomer.

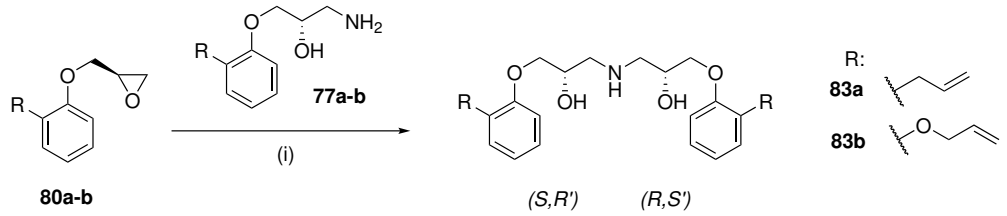

SCHEME 5.2: Synthesis of meso compounds **83a** and **83b**. Conditions and reagents: (i) HFIP, MW, 70°C, 1h.

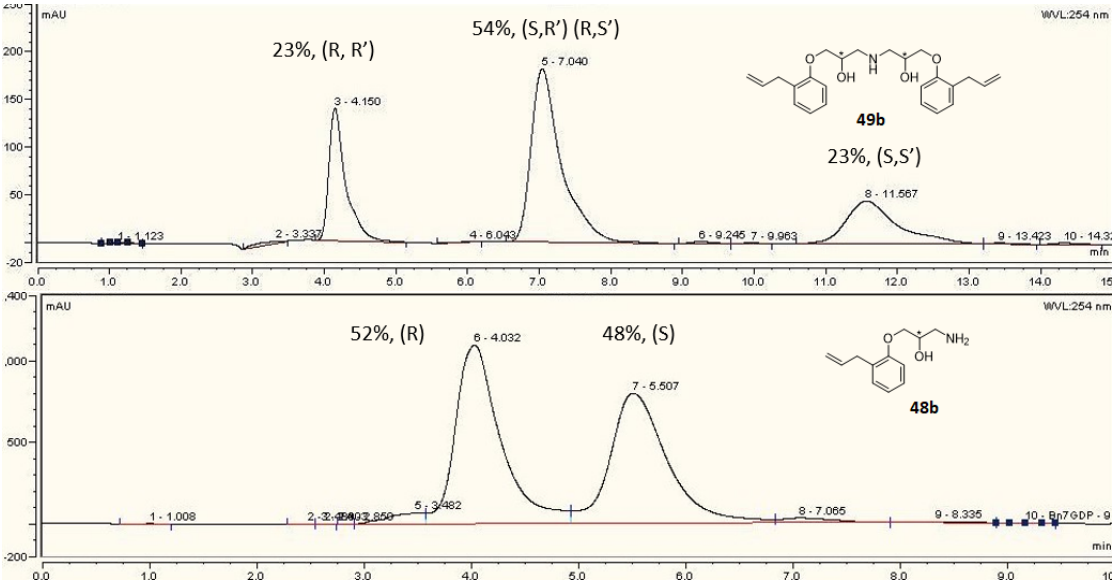

FIGURE 5.2: Chromatograms obtained from the separation of mixture **49b** (top) and racemic mixture **48b** (bottom) by chiral semi-preparative HPLC using a Lux Cellulose-2 chiral column.

Analogues lacking the 2-allylphenoxy group (**85**) or the second hydroxyl group (analogue **90** that also resulted in the removal of the second chirality centre) were synthesised in order to understand the importance of these groups in the binding and activation of the secondary conformation of the β_1-AR observed in parent compound **49b**. A *N*-alkyated analogue of compound **49b** was also obtained to understand the importance of the central secondary amine in the secondary conformation. Alkylation of this secondary amine to a tertiary amine generally results in a decrease in affinity when compared with their secondary amine counterparts for the primary conformation of the β_1-AR and β_2-AR. Truncated analogue **85**, without the second 2-allylphenoxy group present in the alprenolol bis analogue 49b, was obtained through the alkylation of 2-allyphenol with epichlorohydrin under microwave irradiation in the presence of sodium hydroxide followed by the addition of amine **84** to epoxide **46** (Scheme 5.3). Similarly, synthesis of the *N*-alkyated bis analogue **86** was obtained through the addition of a 2M solution of methylamine in methanol to the previously synthesised epoxide **46** yielding compound **47e** (Scheme 5.3). This reaction required harsher conditions in order to progress to compound **86**, therefore compound **47e** was isolated and heated under microwave radiation, for 1h at 70 °C in HFIP, in the presence of 2 equivalents of epoxide **46**. Synthesis of analogue **90** required the initial boc protection of amine **87** to **88** using a slight excess of boc anhydride in the presence of 4 equivalents of triethylamine. The boc protected amine was then added to an excess of phenol **45**, which was removed through a base wash, in the presence of potassium carbonate in DMF. Without further purification, the resulting amine was deprotected using trifluoroacetic acid (TFA) in DCM to yield compound **89**.

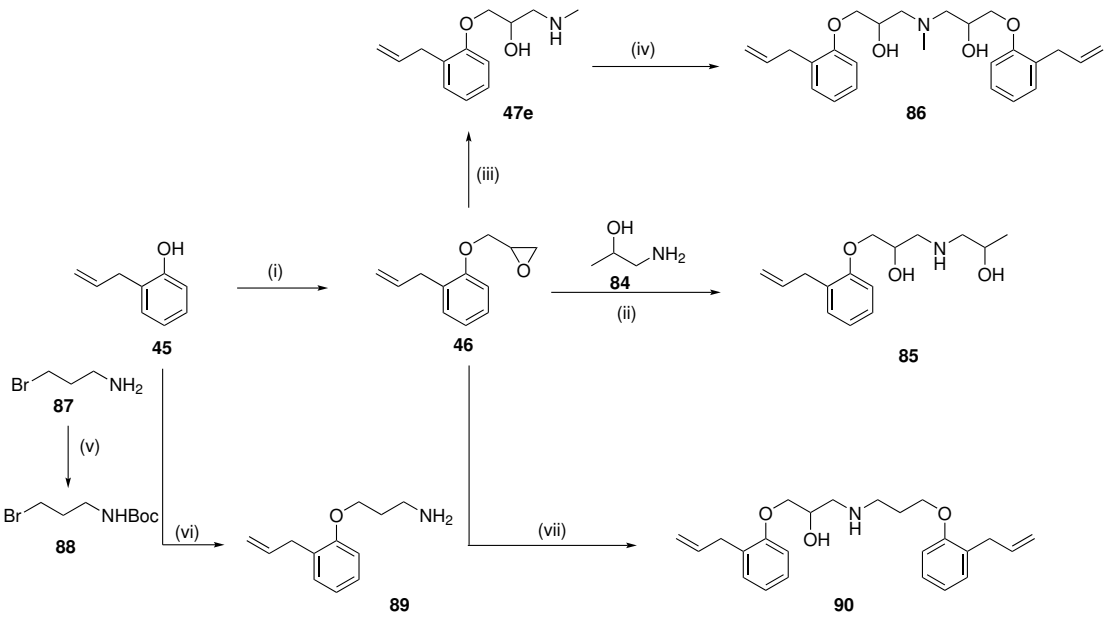

SCHEME 5.3: Synthesis of analogues **85**, **86** and **90**. Conditions and reagents: (i) Epichlorohydrin, NaOH, MW, 120 °C, 40 min, 62%; (ii) Methanol, r.t., 48h, 45%; (iii) 2.0M methylamine solution in methanol, r.t. 48h; (iv) **46**, HFIP, MW, 70 °C, 1.5h, 72%; (v) Boc anhydride, TEA, DCM, r.t., 24h, 92%; (vi) 1. K_2CO_3, r.t., 24h; 2. TFA, DCM, 4h, 82%; (vii) HFIP, MW, 70 °C, 1h, 51%.

Amine **89** was used to open epoxide **46** using the general method in HFIP and yield final analogue **90**.

Introduction of a linear carbon linker between two aryloxypropanolamine alprenolol

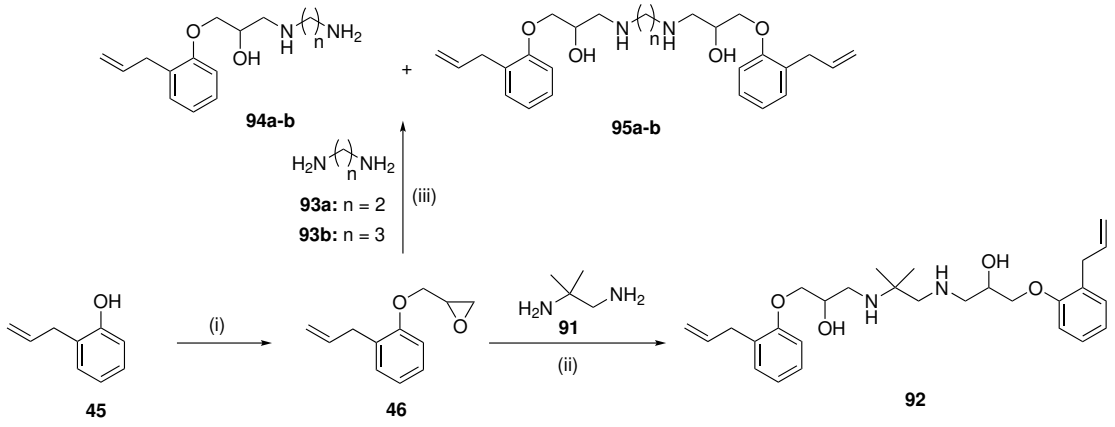

SCHEME 5.4: Synthesis of analogues **92**, **94a-b** and **95a-b**. Conditions and reagents: (i) Epichlorohydrin, NaOH, MW, 120 °C, 40 min, 62%; (ii) **91**, HFIP, MW, 70 °C, 1h; (iii) **93a** or **93b**, MeOH, r.t., 12h.

units (**95a-b**) was achieved through addition of either ethylenediamine (**93a**) or 1,3-diaminopropane (**93b**) to 2 equivalents of epoxide **46** (scheme 5.4) at room temperature. Side products containing only the linker moiety (**94a-b**) were also isolated through preparative HPLC. Likewise, amine **91** was used as a linker and added to epoxide **46** to obtain compound **92** as a mixture of four enantiomers. Analogue **92** bears a bulkier group adjacent to one of the amine groups which is expected to result in improved affinity for the primary conformation of the β_1-AR and β_2-AR as observed for *N*-tert-butylated analogues in chapter 3.

5.2.2 Pharmacology

5.2.2.1 Radioligand binding assays

Ligand affinity of this set of compounds was initially evaluated for the primary conformation of the β_1-AR and for the β_2-AR through whole-cell radioligand competitive assay using [^{3}H]-CGP12177 as radioligand for both receptors. $logK_D$ values obtained through this assay are presented in table 5.1 and table 5.2. *(S,S')* bis oxprenolol ligand **78b** and meso bis oxprenolol ligand **83b** exhibited higher affinity for both β_1- and β_2-AR than the mixture of isomers **48a**, as generally expected for enantiomers containing a *(S)* chirality centre, while retaining the selectivity seen for the β_2-AR. *(R,R')*-enantiomer **82b** showed a much lower affinity for both receptors and a slightly lower selectivity towards the β_2-AR

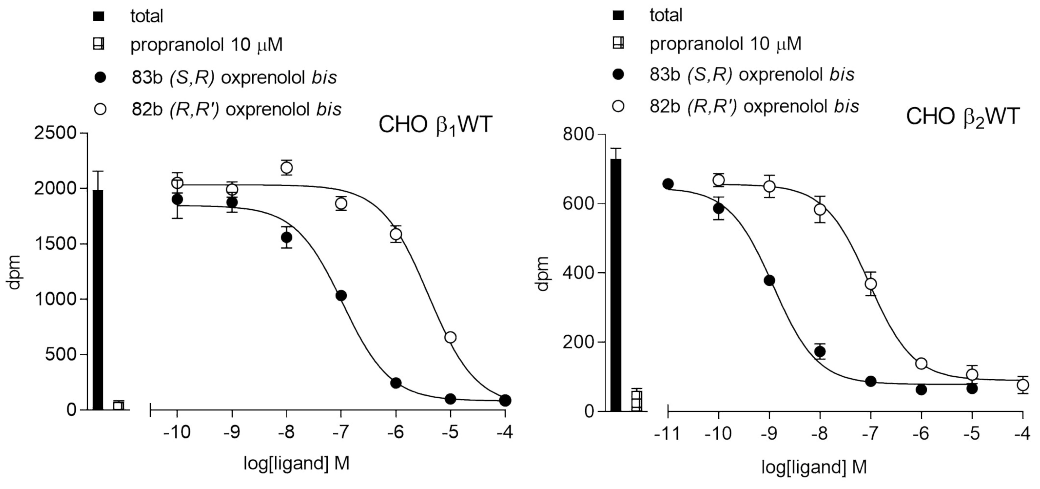

FIGURE 5.3: Inhibition of [^{3}H] CGP12177 binding to whole cells in CHO-β_1 and -β_2 cells by oxprenolol *(R,R')* bis ligand 82b and meso oxprenolol bis ligand 83b. Left bar represents total binding for a concentration of 1.417 nM and the right one nonspecific binding which was determined in the presence of 10 μM propranolol. Data points represent mean $\pm$ s.e.m. of triplicate determinations.

	Structure	$LogK_D\beta_1$	n	$LogK_D\beta_2$	n	$LogK_D(\beta_2/\beta_1)$
49a	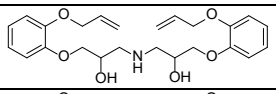	-7.42 ± 0.01	6	-9.01 ± 0.08	5	1.59
78b	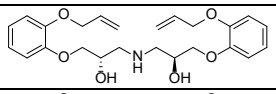	-7.68 ± 0.06	5	-9.30 ± 0.04	4	1.62
82b	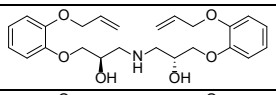	-6.33 ± 0.11	6	-7.56 ± 0.04	6	1.23
83b	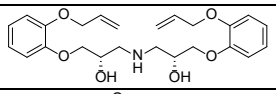	-7.77 ± 0.05	5	-9.32 ± 0.06	5	1.55
48a	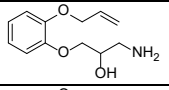	-6.41 ± 0.01	6	-7.07 ± 0.02	5	0.66
77b	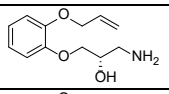	-6.93 ± 0.05	7	-7.63 ± 0.03	7	0.70
81b	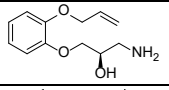	-6.23 ± 0.07	7	-6.94 ± 0.08	6	0.71
49b	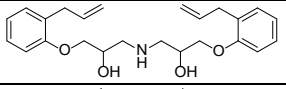	-7.12 ± 0.02	6	-8.16 ± 0.04	6	1.04
78a	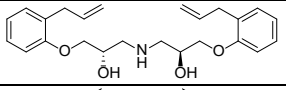	-7.31 ± 0.04	4	-8.22 ± 0.08	5	0.91
82a	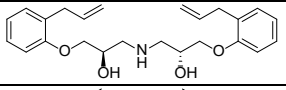	-6.45 ± 0.07	5	-6.98 ± 0.02	5	0.53
83a	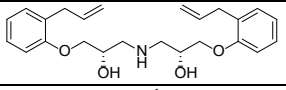	-7.41 ± 0.04	5	-8.08 ± 0.07	5	0.67
48b	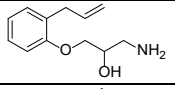	-6.56 ± 0.03	6	-7.18 ± 0.03	6	0.62
81a	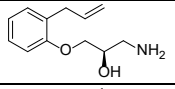	-5.61 ± 0.08	5	-6.54 ± 0.07	5	0.93
77a	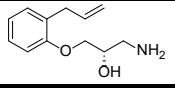	-6.80 ± 0.06	5	-7.58 ± 0.04	5	0.78

TABLE 5.1: Binding affinities for human β_1- and β_2-AR assessed using [^{3}H]-CGP12177 whole cell binding assays. Values represent mean and ± the standard error of the mean (s.e.m) for n separate experiments.

(figure 5.3). Similarly, *(S,S')* bis alprenolol ligand **78a** and meso bis alprenolol ligand **83a** showed similar affinities for both receptors, which were higher than the affinity values obtained for the *(R,R')*-enantiomer **82a**. Non-substituted *(S)*-enantiomers **77a** and **77b** also required a lower concentration to bind to both receptors than the counterpart *(R)*-enantiomers **81a** and **81b**.

Removal of the second hydroxyl (analogue **90**) resulted in a marginal increase in affinity

	Structure	$LogK_D\beta_1$	n	$LogK_D\beta_2$	n	$LogK_D(\beta_2/\beta_1)$
47g	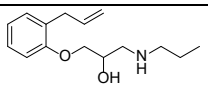	-7.07 ± 0.04	6	-8.09 ± 0.11	5	1.02
47h	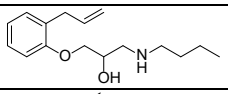	-6.86 ± 0.02	6	-7.75 ± 0.04	6	0.89
94a	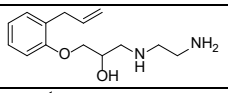	-6.84 ± 0.08	5	-7.46 ± 0.04	5	0.62
95a	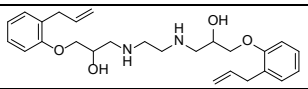	-7.29 ± 0.05	6	-7.86 ± 0.08	7	0.57
95b	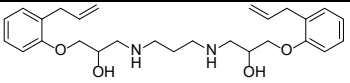	-6.90 ± 0.02	6	-7.64 ± 0.07	6	0.74
90	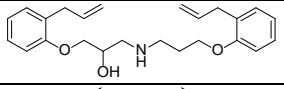	-7.22 ± 0.04	7	-8.41 ± 0.03	7	1.19
86	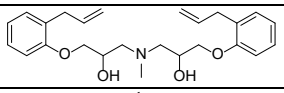	-6.66 ± 0.05	5	-7.19 ± 0.06	5	0.53
85	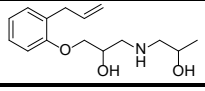	-6.74 ± 0.08	5	-7.46 ± 0.03	5	0.72

TABLE 5.2: Binding affinities for human β_1- and β_2-AR assessed using [^{3}H]-CGP12177 whole cell binding assays. Values represent mean and ± the standard error of the mean (s.e.m) for n separate experiments.

for both receptors, while alkylation of the central amine functional group (analogue **86**) decreased the affinity for both β_1- and β_2-AR. Removal of the 2-allylphenoxy group seen in analogue **85** resulted in a decrease in affinity for both receptors. This ligand also showed lower affinity than the *N*-butylamino alprenolol analogue discussed in chapter 3. Introduction of a linear ethyl linker between two aryloxypropanolamine alprenolol units (**95a**) led to an increase in affinity for β_1-AR ($logK_D\beta_1 = -7.29 \pm 0.05$, n=6, table 5.2) but decreased the affinity for the β_2-AR when compared with the alprenolol bis ligand **49b**. Increasing the length of this linker by one carbon (**95b**) decreased the affinity for both receptors. Compound **94a** containing the two linear carbon linker and a terminal primary amine yielded a lower affinity for both receptors than the *N*-butylamine analogue described in chapter 3.

Overall, *(R,R')*-enantiomer of the bis alprenolol and oxprenolol compounds exhibited much lower affinity for the primary conformation of β_1-AR and for the β_2-AR than both the *(S,S')*-enantiomer and meso compounds which supports the importance of a *(S)* chirality centre in that position. The second chirality centre present in these compounds does not seem to contribute to the affinity observed as meso and *(S,S')*-enantiomers exhibited similar affinities and the removal of the hydroxyl group (**90**) even increased slightly the affinity for both receptors. The 2-allylphenoxy moiety seems to contribute to

the affinity observed in the alprenolol bis analogue **49b** while introduction of a two linear carbon linker between two aryloxypropanolamine alprenolol units increases the affinity for the β_1-AR.

5.2.2.2 CRE-SPAP production

A CRE-SPAP functional assay in CHO cells expressing either the human β_1- or β_2-AR was used to assess the $logEC_{50}$ and $\%isop$ of these compounds.

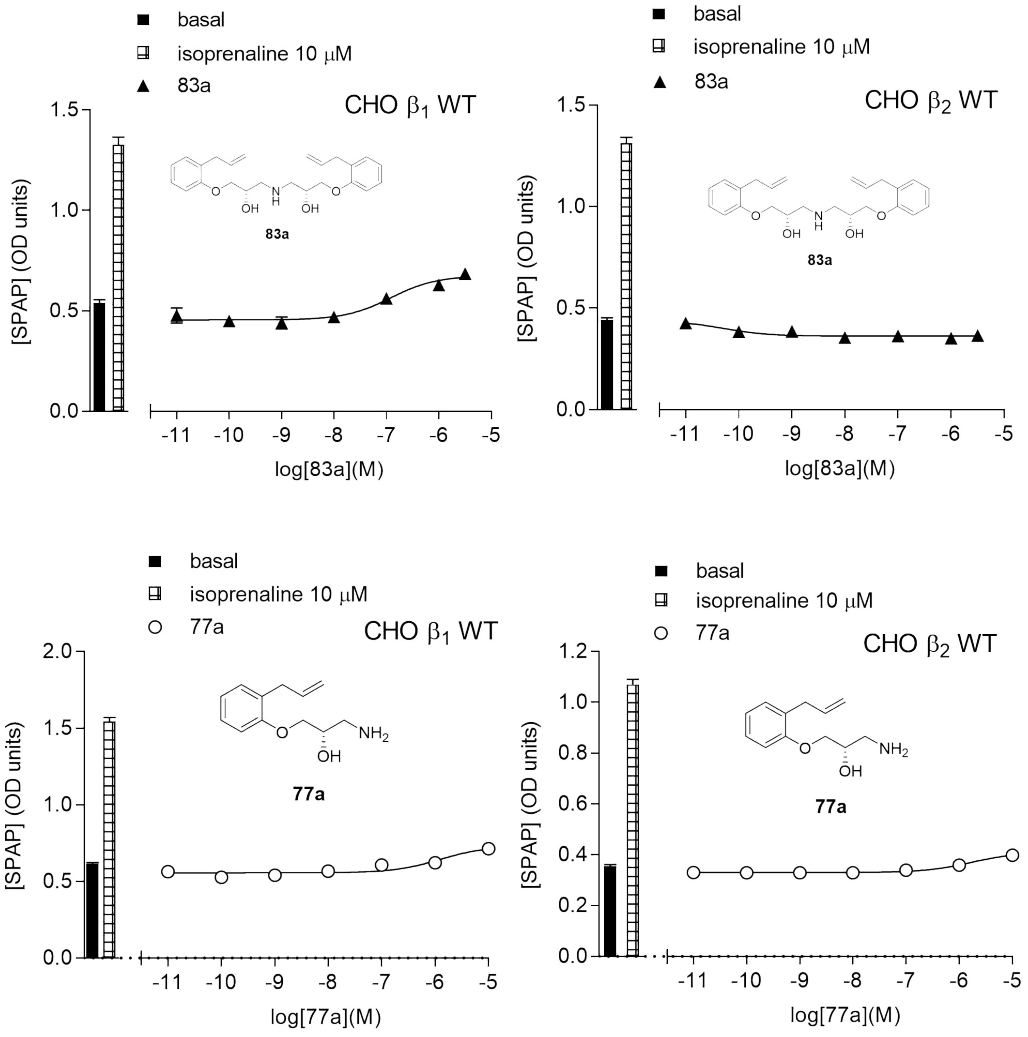

FIGURE 5.4: CRE-SPAP production in response to alprenolol meso bis analogue 83a and non-substituted *(S)*-alprenolol analogue 77a in CHO-β_1 and β_2 cells. Bars represents basal SPAP accumulation and SPAP increase in the presence of 10μM isoprenaline. In bottom right concentration response curve a zoomed in version is also presented for the CRE-SPAP production of 77a in CHO-β_2 cells. Data points represent mean ± s.e.m. of triplicate determinations.

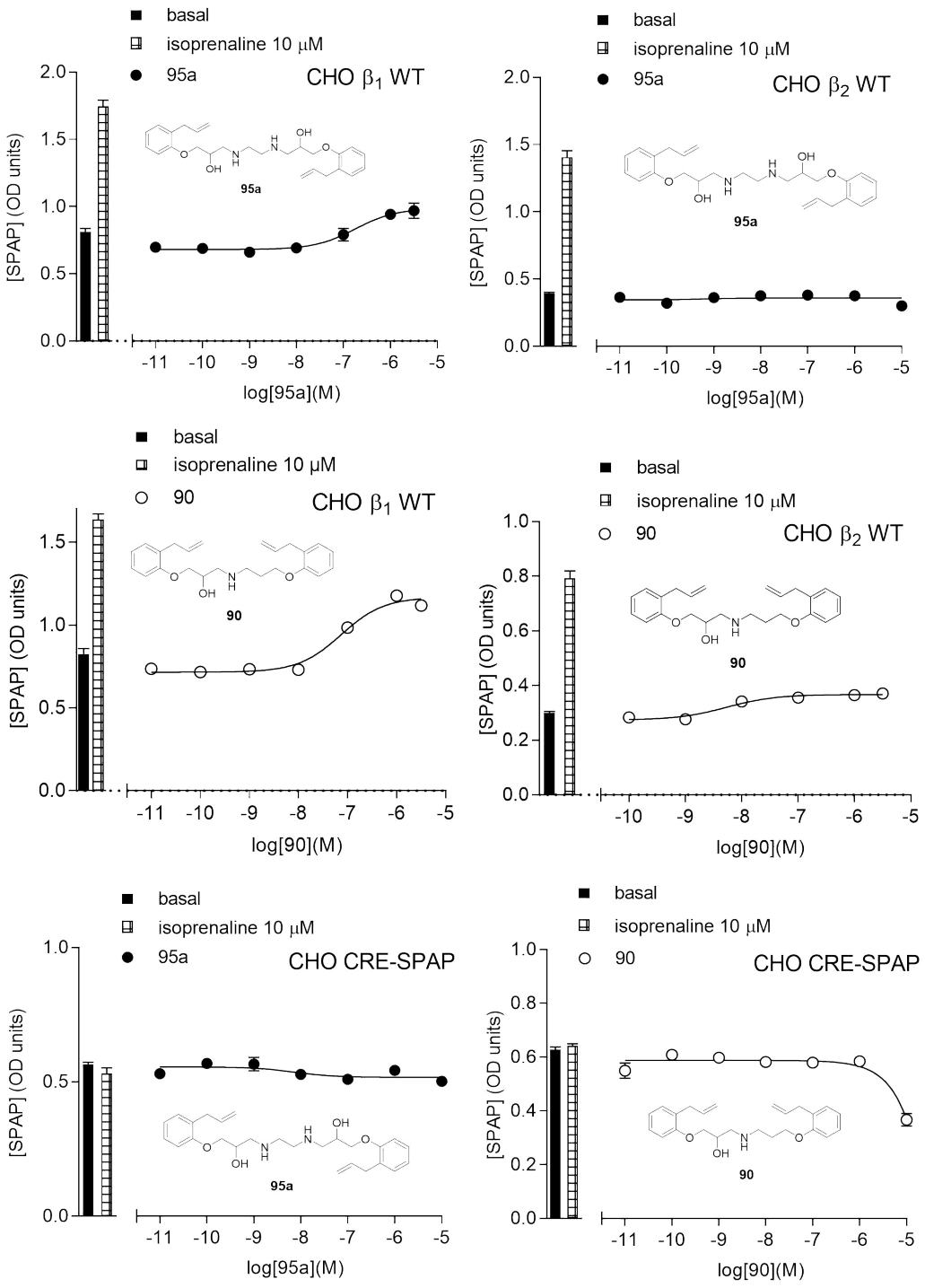

FIGURE 5.5: CRE-SPAP production in response to analogue 95a and 90 in CHO-β_1, CHO-β_2 and CHO CRE-SPAP (without receptor expression) cells. Bars represents basal SPAP accumulation and SPAP increase in the presence of 10μM isoprenaline. Data points represent mean $\pm$ s.e.m. of triplicate determinations.

Generally, most analogues were able to increase CRE-SPAP production in CHO-β_1 cells contrary to what was observed in CHO-β_2 cells. . Both enantiomers of alprenolol and oxprenolol non-substituted analogues **48a-b** were only able to stimulate a very weak response inferior to 10% of isoprenaline maximum response at both receptors as observed for the racemic mixture in chapter 3 (figure 5.4). This can be observed in figure 5.4 for *(S)* enantiomer **77a** which is able to elicit a very weak response in CHO-β_2 cells which is zoomed in the figure. *(R,R')* bis alprenolol and oxprenolol (**82a** and **82b**) were able to mediate a single component response in CHO-β_1 cells with a potency $logEC_{50}\beta_1$ value identical to $logK_D\beta_1$ value derived from radioligand binding assays (-6.36 vs -6.45 for 82a, respectively; -6.35 vs -6.33 for 82b, respectively).

Meso compound **83a** CRE-SPAP production was best described as a monophasic response curve with a $logEC_{50}\beta_1$ of -7.06 ± 0.13 and an E_{max} of $38.92\% \pm 4.90$ (n=7, table 5.3) of the maximal isoprenaline response in CHO-β_1 cells (figure 5.4). This compound requires a slighly higher concentration to mediate half of the maximal response than to bind to half of the receptors ($logEC_{50}\beta_1 = -7.06$, $logK_D\beta_1 = -7.41$) which indicates that this response might be mediated through the secondary conformation of the β_1-AR (table 5.3-5.6). In CHO-β_2 cells, analogue behaves as an antagonist, failing to elicit an increase in SPAP concentration (figure 5.4).

Similarly to analogue **83a**, analogue **83b** and *(S,S')*-enantiomers **78a** and **78b** also show an anomalous behaviour in CHO-β_1 cells with $logEC_{50}\beta_1$ values higher than the $logK_D$ obtained from radioligand binding assays, suggesting that these responses may be mediated through the secondary conformation of the β_1-AR. Interestingly, both *(R,R')* enantiomers exhibited higher %isoprenaline maximum than the *(S,S')* and meso counterparts. These analogues behaved as antagonists failing to mediate a CRE-SPAP increase in CHO-β_2 cells, except *(R,R')* bis oxprenolol **82b** which behaved as a weak partial agonist with a $logEC_{50}\beta_2 = logK_D\beta_2$. ($logEC_{50}\beta_2 = -7.84 \pm 0.10$, $\%isop = 19 \pm 3$, n=6, table 5.5).

Deoxy analogue **90** elicited a response in CHO-β_1 cells with a $logEC_{50}\beta_1$ of -6.70 ± 0.20 and a $\%isop$ of $42\% \pm 4$ (n=6, table 5.4, figure 5.5) of the maximal isoprenaline response, a similar $\%isop$ to the parent compound **49b** but higher $logEC_{50}\beta_1$. Similarly to several other bis ligands from this set, the deoxy analogue required higher concentration to mediate half of the maximal response ($logEC_{50}$) than to bind to half of the receptors ($logK_D$) in CHO-β_1 cells which points to a response mediated through the secondary conformation of the β_1-AR. This compound also mediated a response through the β_2-AR and behaved as a very weak partial agonist with a $logEC_{50}\beta_2$ identical to the $logK_D\beta_2$ derived from the competitive binding assays (-7.84 vs -7.56) (figure 5.5).

	Structure	$LogK_D\beta_1$	n	$LogEC_{50}\beta_1 1$	$LogEC_{50}\beta_1 2$	% 1st component	n	% isop	n	CGP20712A $LogK_D$	n
49a	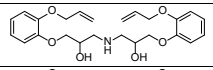	-7.42 ± 0.01	6	-7.50 ± 0.15	-	-	6	32 ± 3	6	-8.03 ± 0.23	3
78b	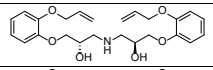	-7.68 ± 0.06	5	-6.88 ± 0.12	-	-	7	24 ± 3	7	-7.85 ± 0.10	3
82b	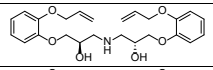	-6.33 ± 0.11	6	-6.35 ± 0.11	-	-	10	33 ± 3	10	-8.31 ± 0.02	4
83b	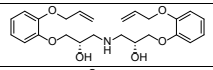	-7.77 ± 0.05	5	-7.20 ± 0.23	-	-	8	27 ± 3	8	-7.83 ± 0.20	4
77b	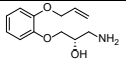	-6.93 ± 0.05	7	-	-	-	-	< 10	3	-	-
81b	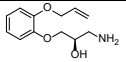	-6.23 ± 0.07	7	-	-	-	-	< 10	3	-	-
49b	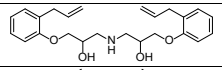	-7.12 ± 0.02	6	-7.13 ± 0.12	-	-	5	47 ± 6	5	-7.93 ± 0.15	3
78a	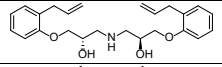	-7.31 ± 0.04	4	-6.93 ± 0.15	-	-	8	35 ± 4	8	-7.37 ± 0.12	3
82a	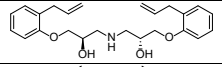	-6.45 ± 0.07	5	-6.36 ± 0.15	-	-	5	51 ± 4	5	-7.81 ± 0.13	3
83a	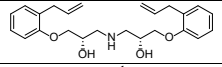	-7.41 ± 0.04	5	-7.06 ± 0.13	-	-	7	39 ± 5	7	-7.44 ± 0.07	4
81a	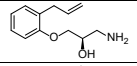	-5.61 ± 0.08	5	-	-	-	-	< 10	3	-	-
77a	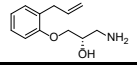	-6.80 ± 0.06	5	-	-	-	-	< 10	3	-	-

TABLE 5.3: $LogK_D$, $logEC_{50}$ and $\%isop$ maximum responses are presented in the table for β_1-AR. $LogK_D$ values were derived from IC_{50} values obtained through radioligand competitive binding assays (figure 5.3, table 5.1 and 5.2). $LogEC_{50}$ were obtained from CRE-SPAP functional assays (figure 5.4 and 5.5) and $\%isop$ represents the percentage of total response generated by 10μM isoprenaline elicited by the ligand. $LogEC_{50}\beta_1 1$ represents the $logEC_{50}$ determined for the first component of a biphasic response curve while $LogEC_{50}\beta_1 2$ represents the value for the second component. $\%site1$ represents the percentage of total response accounted for the first component of a biphasic response curve. CGP20712A $logK_D$ represents the affinity derived from the inhibition of the ligand CRE-SPAP production using fixed concentrations of CGP20712A in whole cell assays. Values represent mean of data obtained and ± the standard error of the mean (s.e.m) for n separate experiments.

	Structure	$LogK_D\beta_1$	n	$LogEC_{50}\beta_1 1$	$LogEC_{50}\beta_1 2$	% 1st component	n	% isop	n	CGP20712A $LogK_D$	n
47g	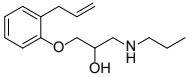	-7.07 ± 0.04	6	-7.40 ± 0.21	-	-	6	29 ± 4	6	-9.26 ± 0.11	3
47h	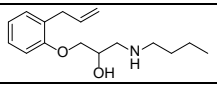	-6.86 ± 0.02	6	-7.22 ± 0.06	-*	-	3	55 ± 4	3	-8.90 ± 0.09	3
94a	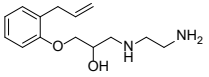	-6.84 ± 0.08	5	-6.76 ± 0.12	-*	-	7	24 ± 3	7	-9.04 ± 0.08	3
95a	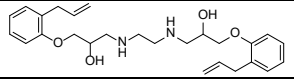	-7.29 ± 0.05	6	-7.11 ± 0.22	-	-	6	36 ± 4	4	-7.59 ± 0.22	3
95b	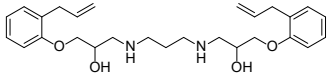	-6.90 ± 0.02	6	-6.49 ± 0.17	-	-	6	32 ± 3	6	-7.48 ± 0.11	3
90	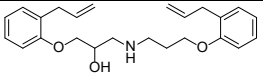	-7.22 ± 0.04	7	-6.70 ± 0.20	-	-	6	42 ± 4	6	-7.49 ± 0.15	4
86	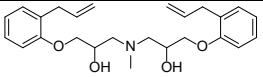	-6.66 ± 0.05	5	-6.77 ± 0.09	-	-	7	47 ± 6	7	-7.90 ± 0.17	3
85	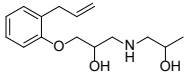	-6.74 ± 0.08	5	-6.93 ± 0.09	-	-	7	29 ± 5	8	-8.63 ± 0.20	4

TABLE 5.4: $LogK_D$, $logEC_{50}$ and $\%isop$ maximum responses are presented in the table for β_1-AR. $LogK_D$ values were derived from IC_{50} values obtained through radioligand competitive binding assays (figure 5.3, table 5.1 and 5.2). $LogEC_{50}$ were obtained from CRE-SPAP functional assays (figure 5.4 and 5.5) and $\%isop$ represents the percentage of total response generated by 10μM isoprenaline elicited by the ligand. $LogEC_{50}\beta_1 1$ represents the $logEC_{50}$ determined for the first component of a biphasic response curve while $LogEC_{50}\beta_1 2$ represents the value for the second component. $\%site1$ represents the percentage of total response accounted for the first component of a biphasic response curve. CGP20712A $logK_D$ represents the affinity derived from the inhibition of the ligand CRE-SPAP production using fixed concentrations of CGP20712A in whole cell assays. Values represent mean of data obtained and ± the standard error of the mean (s.e.m) for n separate experiments. *ligand seems to elicit a biphasic dose response curve but $logEC_{50}\beta_1$ could not be obtained for the second component as it lays on the limit of the assay.

	Structure	$LogK_D\beta_2$	n	$LogEC_{50}\beta_2$	% isop	n	ICI118551 $LogK_D$	n
49a	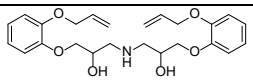	-9.01 ± 0.08	5	-	No response	3	-	-
78b	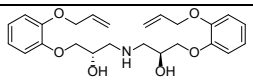	-9.30 ± 0.04	4	-	No response	4	-	-
82b	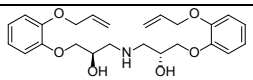	-7.56 ± 0.04	6	-7.84 ± 0.10	19 ± 3	6	-9.62 ± 0.08	3
83b	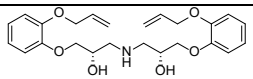	-9.32 ± 0.06	5	-	No response	4	-	-
48a	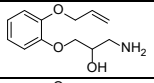	-7.07 ± 0.02	5	-	< 10	3	-	-
77b	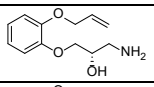	-7.63 ± 0.03	7	-	< 10	3	-	-
81b	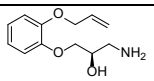	-6.94 ± 0.08	6	-	< 10	3	-	-
49b	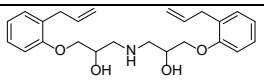	-8.16 ± 0.04	6	-	No response	3	-	-
78a	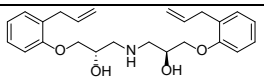	-8.22 ± 0.08	5	-	No response	4	-	-
82a	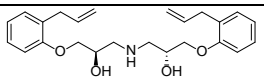	-6.98 ± 0.02	5	-	No response	3	-	-
83a	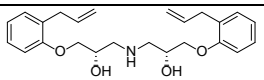	-8.08 ± 0.07	5	-	No response	3	-	-
48b	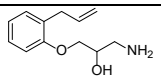	-7.18 ± 0.03	6	-	< 10	3	-	-
81a	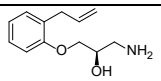	-6.54 ± 0.07	5	-	< 10	4	-	-
77a	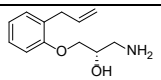	-7.58 ± 0.04	5	-	< 10	4	-	-

TABLE 5.5: $LogK_D$, $logEC_{50}$ and $\%isop$ maximum responses are presented in the table for β_1-AR. $LogK_D$ values were derived from IC_{50} values obtained through radioligand competitive binding assays (figure 5.3, table 5.1 and 5.2). $LogEC_{50}$ were obtained from CRE-SPAP functional assays (figure 5.4 and 5.5) and $\%isop$ represents the percentage of total response generated by 10μM isoprenaline elicited by the ligand. ICI118551 $logK_D$ represents the affinity derived from the inhibition of the ligand CRE-SPAP production using fixed concentrations of ICI118551 in whole cell assays. Values represent mean of data obtained and ± the standard error of the mean (s.e.m) for n separate experiments.

Alkylation of the central amine group (**86**) reduced the potency as expected ($logEC_{50}\beta_1 = -6.77 \pm 0.09$, n=7) to a value similar to the affinity obtained through binding assays ($logK_D\beta_1 = -6.66$) with a $\%isop = 47\% \pm 6$.

Analogues **95a** and **95b**, bearing a 2 and 3 linear carbon linker, respectively, between two alprenolol aryloxypropanolamine units, showed similar values of $\%isop$, even though

	Structure	$LogK_D\beta_2$	n	$LogEC_{50}\beta_2$	% isop	n	ICI118551 $LogK_D$	n
47g	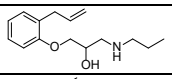	-8.09 ± 0.11	5	-8.44 ± 0.11	28 ± 2	8	-9.67 ± 0.10	3
47h	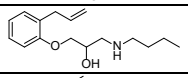	-7.75 ± 0.04	6	-8.29 ± 0.09	30 ± 3	10	-10.00 ± 0.15	3
94a	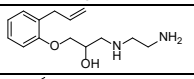	-7.46 ± 0.04	5	-7.55 ± 0.12	23 ± 3	7	-9.71 ± 0.08	3
95a	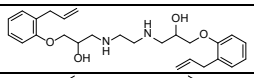	-7.86 ± 0.08	7	-	No response	3	-	-
95b	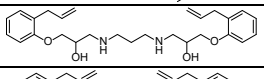	-7.64 ± 0.07	6	-	No response	3	-	-
90	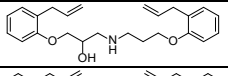	-8.41 ± 0.03	7	-8.05 ± 0.13	13 ± 1	7	-9.59 ± 0.11	4
86	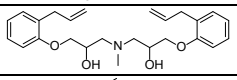	-7.19 ± 0.06	5	-	No response	3	-	-
85	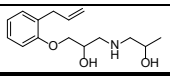	-7.46 ± 0.03	5	-7.89 ± 0.05	22 ± 3	4	-9.75 ± 0.02	3

TABLE 5.6: $LogK_D$, $logEC_{50}$ and $\%isop$ maximum responses are presented in the table for β_1-AR. $LogK_D$ values were derived from IC_{50} values obtained through radioligand competitive binding assays (figure 5.3, table 5.1 and 5.2). $LogEC_{50}$ were obtained from CRE-SPAP functional assays (figure 5.4 and 5.5) and $\%isop$ represents the percentage of total response generated by 10μM isoprenaline elicited by the ligand. ICI118551 $logK_D$ represents the affinity derived from the inhibition of the ligand CRE-SPAP production using fixed concentrations of ICI118551 in whole cell assays. Values represent mean of data obtained and ± the standard error of the mean (s.e.m) for n separate experiments.

analogue **95a** displayed lower $logEC_{50}$ values than analogue **95b**. Analogue **95a** concentration response curve is displayed in figure 5.5 for both β_1 and β_2-AR. This analogue elicits a response in CHO-β_1 cells with a $logEC_{50}\beta_1$ of -7.11 ± 0.22 and a $\%isop$ of 36%±4 (n=6, table 5.4, figure 5.5) but behaves as an antagonist in CHO-β_2 cells. Analogue **94a**, bearing the 2 carbon linear linker, seems to elicit a biphasic concentration-response curve in CHO-β_1 cells even though the $logEC_{50}$ of the second component of this response could not be obtain as it is too close to the limit of the assay as seen for some compounds described in the previous chapters.$LogEC_{50}$ values obtained for the first component of this response at β_1-AR and for the single component at β_2-AR where identical to the $logK_D$ values obtained from competitive binding assays for each receptor. Analogue **94a** behaves therefore as a partial agonist in both receptors.

Removal of the 2-allylphenoxy group (**85**) resulted in a decrease both in potency (higher $logEC_{50}$ value) and in % of isoprenaline maximum response in CHO-β_1 cells. However, contrary to the parent compound **49b**, analogue **85** mediated a response through the β_2-AR, behaving as a partial agonist at this receptor.

It is noteworthy to mention that several ligands containing a bis alprenolol ligand backbone (analogues **49b**, **78a**, **82a**, **83a**, **95a**, **95b** and **86**), but not bis oxprenolol, reduced CRE-SPAP production at high concentrations in CHO-β_1, CHO-β_2 and CHO CRE-SPAP cells lacking expression of any of the receptors which limits the maximal concentration used in several assays (figure 5.5). This is highlighted in figure 5.5 where compound **90** is able to stimulate a response in CHO-β_1 cells up to 3μM but decreases CRE-SPAP production at 10μM in CHO CRE-SPAP cells without receptor expression suggesting a possible cytotoxic effect in these cell lines.

Altogether, several ligands showed an anomalous behaviour in CHO-β_1 cells similarly to parent compound **49b** with a higher $logEC50\beta_1$ value than the $logK_D$ obtained from radioligand competitive binding assays pointing to a response mediated through the secondary conformation of the β_1-AR. The ability of CGP20712A to inhibit these response will be discussed in a later subsection, while a resistance to antagonism by these responses may provide further evidences that these responses are mediated through the secondary conformation. Affinites for the primary ($logK_D\beta_{1cim}$ using cimaterol as agonist) and secondary ($logK_D\beta_{1CGP}$ using CGP12177 as agonist) conformation of the β_1 are discussed in the next subsection.

5.2.2.3 Affinity at primary and secondary conformation of the β_1-AR

Similarly to the other sets of compounds described in the previous chapters, a CRE-SPAP assay was used to determine the affinities of this set of ligands at the primary and secondary conformation of the β_1-AR. Affinity for the primary conformation of the β_1-AR ($logK_D\beta_{1cim}$) was derived from the capacity of a fixed concentration of ligand to parallel rightward shift the concentration-response curve of cimaterol, a primary conformation agonist. Affinity for the secondary conformation of the β_1-AR ($logK_D\beta_{1CGP}$) was derived from the ability to shift CGP12177 mediated response, a secondary conformation agonist. Likewise, cimaterol and CGP12177 were used to mediate a response in CHO-β_2 cells in the presence and absence of a fixed concentration of ligand. $LogK_D$ values obtained through this method are presented in tables 5.7 and 5.8 for the β_1-AR and 4.9 and 4.10 for the β_2-AR. $LogK_D\beta_{1CGP}$ values were not obtained for some compounds as no shift of CGP12177 concentration-response curve was observed in the presence of the maximal concentration (10 μM) of compound. As mentioned in the previous subsection, several analogues decreased CRE-SPAP production at 10μM in a non-receptor related fashion, therefore a maximal concentration of 3 μM was used for these ligands. This complicates the determination of an accurate affinity value for several low affinity analogues (eg. **82a**), increasing the error values obtained. $LogK_D\beta_{2CGP}$ values were also not obtained

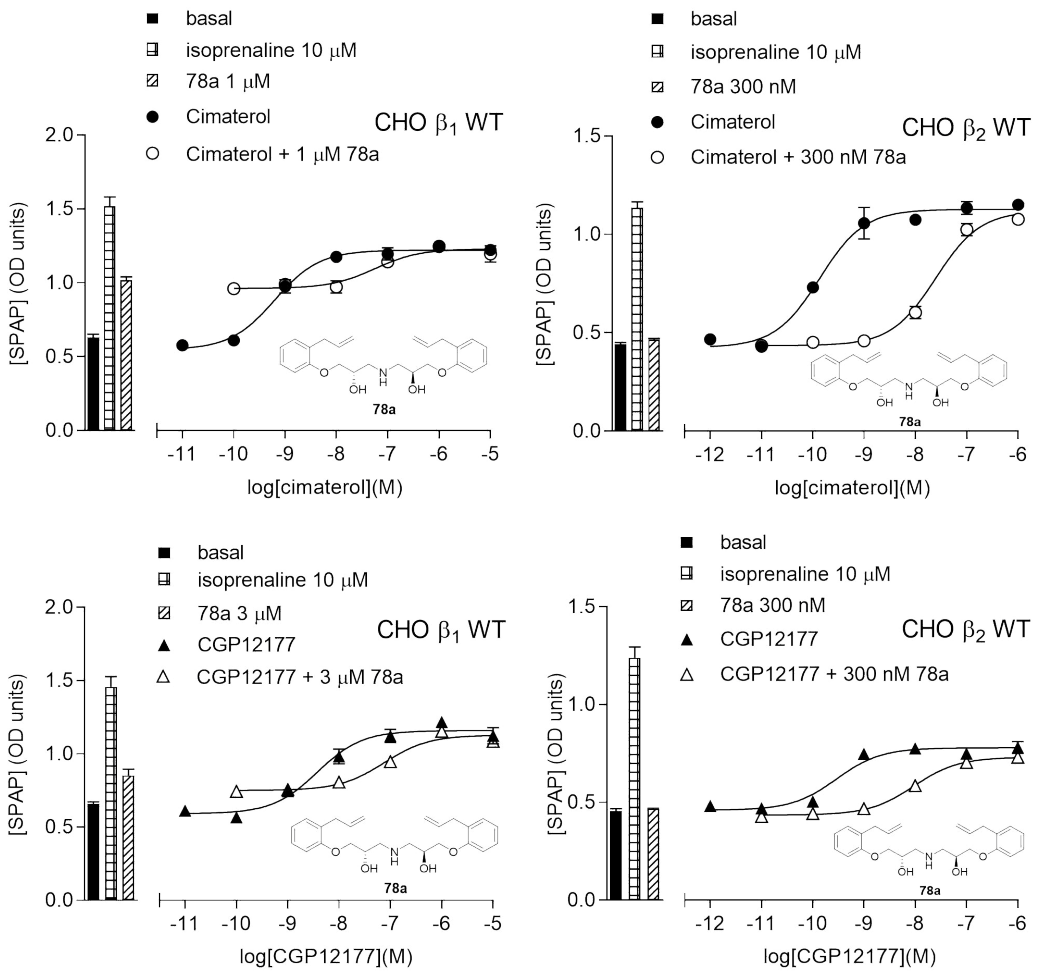

FIGURE 5.6: Left: CRE-SPAP production in response to cimaterol in the absence and presence of **78a** in CHO-β_1 and -β_2 cells; Right: CRE-SPAP production in response to CGP12177 in the absence and presence of **78a** in CHO-β_1 and -β_2 cells. Data points represent mean ± s.e.m. of triplicate determinations.

for some analogues as these ligands elicited a maximum response superior to CGP12177 maximum response at this receptor.

Effect of individual alprenolol and oxprenolol bis isomers in the affinity for primary and secondary conformation of the β_1-AR: Alprenolol *(S,S')* bis isomer **78a** was able to rightshift the response curve of cimaterol and CGP12177 in both CHO-β_1 and β_2 cells (figure 5.6). Addition of a fixed concentration of **78a** increased basal levels of the responses consistently with its agonistic activity. In CHO-β_1 cells, analogue **78a** was able to inhibit CGP12177 in a manner consistent with its agonist effect ($logK_D\beta_{1CGP} = -6.86 \pm 0.11$; $logEC_{50}\beta_1 = -6.93$). This gives strength to the idea that these responses are mediated through the secondary conformation of the β_1-AR. $LogK_D\beta_{1cim}$ obtained

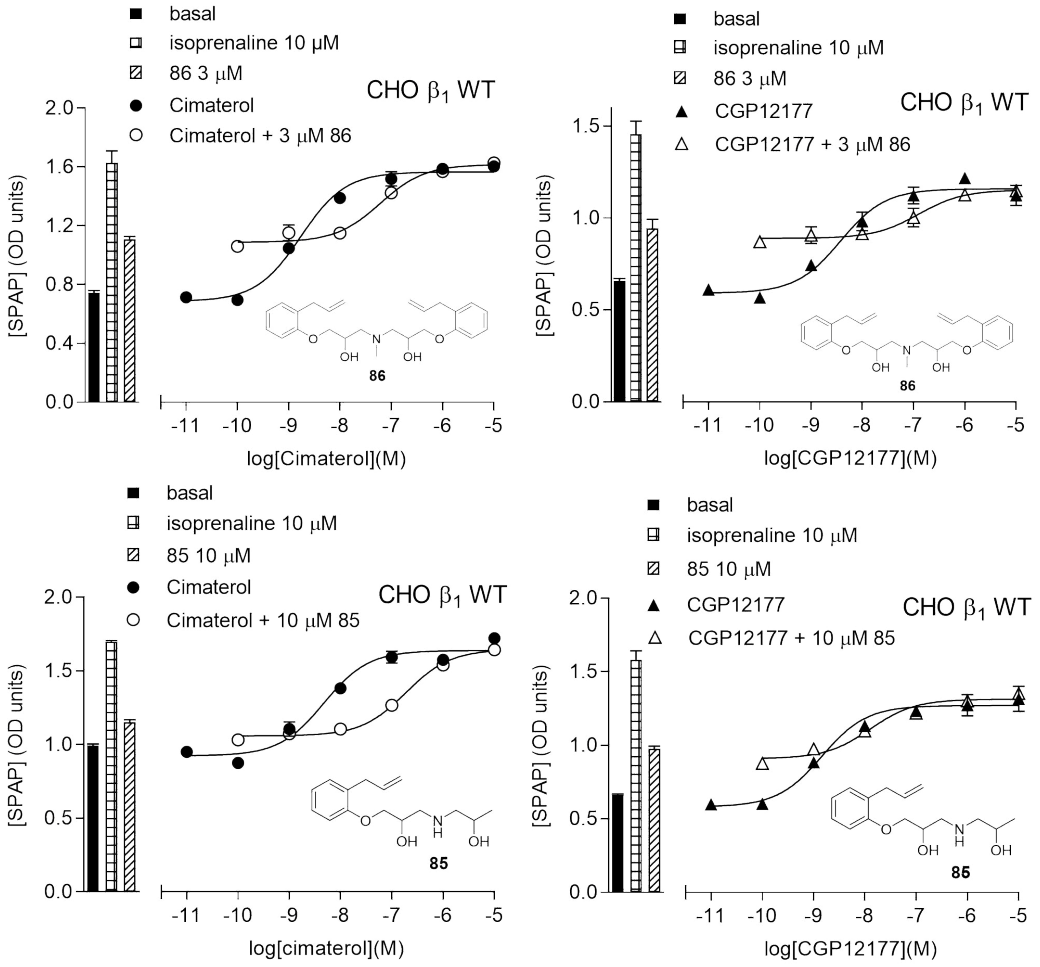

FIGURE 5.7: Left: CRE-SPAP production in response to cimaterol in the absence and presence of **86** or **85** in CHO-β_1 cells; Right: CRE-SPAP production in response to CGP12177 in the absence and presence of **86** or **85** in CHO-β_1 cells. Data points represent mean s.e.m. of triplicate determinations.

for this analogue using cimaterol as an agonist ($logK_D\beta_{1cim} = -7.42 \pm 0.14$) was consistent with the $logK_D\beta_1$ obtained from binding ($logK_D\beta_1 = -7.31$) and slightly lower than the value obtained using CGP12177 as agonist, similarly to what was observed for **49b**. Alprenolol *(R,R')* bis isomer **82a** and meso compound **83a** were also able to inhibit cimaterol and CGP12177 with similar affinities ($logK_D\beta_{1cim} - logK_D\beta_{1CGP} = 0.57$ for 82a and $= 0.41$ for 83a, table 5.7) suggesting that these compounds might have a similar affinity for the primary and secondary conformation of the β_1-AR. Similarly, only a small difference between the $logK_D$ values obtained with cimaterol and CGP12177 as agonists was observed in CHO-β_2 cells ($logK_D\beta_{2cim} - logK_D\beta_{2CGP} = 0.70$ for 82a and $= 0.53$ for 83a, table 5.9). Likewise, oxprenolol bis ligand individual isomers **78b**, **82b** and **83b** seem to retain the small difference in affinities ($logK_D\beta_{1cim} - logK_D\beta_{1CGP}$) between the

	Compound	$LogK_D$ β_1	n	$LogK_D$ β_{1cim}	n	$LogK_D$ β_{1CGP}	n	$LogK_{Dcim} - LogK_{DCGP}$
49a	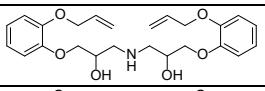	-7.42 ± 0.01	6	-7.73 ± 0.07	3	-6.86 ± 0.09	3	0.87
78b	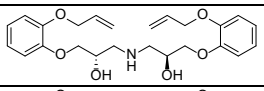	-7.68 ± 0.06	5	-7.62 ± 0.05	5	-6.98 ± 0.09	5	0.64
82b	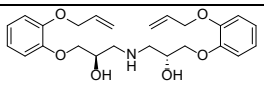	-6.33 ± 0.11	6	-6.31 ± 0.09	3	-5.71 ± 0.07	3	0.60
83b	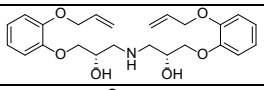	-7.77 ± 0.05	5	-7.63 ± 0.17	5	-6.85 ± 0.04	5	0.78
48a	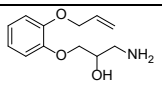	-6.41 ± 0.01	6	-6.56 ± 0.08	3	> -5	3	-
77b	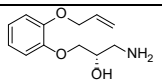	-6.93 ± 0.05	7	-6.89 ± 0.05	7	-5.48 ± 0.06	4	1.41
81b	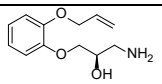	-6.23 ± 0.07	7	-6.18 ± 0.05	6	> -5	3	-
49b	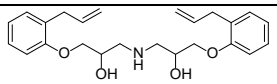	-7.12 ± 0.02	6	-7.45 ± 0.11	4	-7.11 ± 0.03	5	0.34
78a	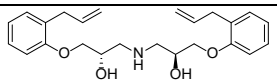	-7.31 ± 0.04	4	-7.42 ± 0.14	5	-6.86 ± 0.11	5	0.56
82a	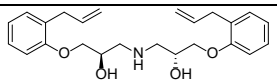	-6.45 ± 0.07	5	-6.15 ± 0.03	3	-5.78 ± 0.16	3	0.57
83a	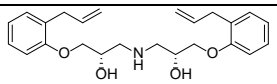	-7.41 ± 0.04	5	-7.47 ± 0.09	3	-7.06 ± 0.09	4	0.41
48b	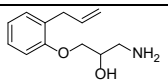	-6.56 ± 0.03	6	-6.52 ± 0.11	3	-5.60 ± 0.02	3	0.92
81a	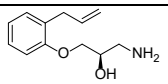	-5.61 ± 0.08	5	-5.76 ± 0.12	4	-5.26 ± 0.07	3	0.50
77a	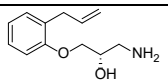	-6.80 ± 0.06	5	-6.93 ± 0.08	3	-5.48 ± 0.09	3	1.45

TABLE 5.7: $LogK_D$ values are presented here for the β_1-AR. $LogK_D\beta_1$ were previously derived from radioligand competitive binding assays (table 5.1). $LogK_D\beta_{1cim}$ were determined through the inhibition of cimaterol CRE-SPAP production using fixed concentrations of ligand, while $logK_D\beta_{1CGP}$ were determined through the inhibition of CGP12177 mediated response in whole cell assays (figure 5.6). Values represent mean of data ± the standard error of the mean (s.e.m) for n separate experiments.

primary and secondary conformation of the β_1-AR observed for the mixture **49a** (table 5.7). *(R,R')*-enantiomer **82b** decrease in affinity for the primary conformation was accompanied by a similar decrease for the secondary conformation retaining the slight selectivity towards the primary conformation of the β_1. Non-substituted *(S)*-enantiomers

	Compound	$LogK_D$ β_1	n	$LogK_D$ β_{1cim}	n	$LogK_D$ β_{1CGP}	n	$LogK_{Dcim}$ - $LogK_{DCGP}$
47g	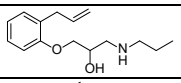	-7.07 ± 0.04	6	-7.53 ± 0.05	4	-5.49 ± 0.08	4	2.04
47h	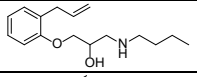	-6.86 ± 0.02	6	-7.06 ± 0.08	4	-5.23 ± 0.00	3	1.83
94a	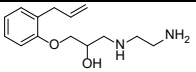	-6.84 ± 0.08	5	-6.68 ± 0.05	4	-5.25 ± 0.04	3	1.43
95a	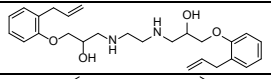	-7.29 ± 0.05	6	-7.36 ± 0.14	6	-7.45 ± 0.11	6	- 0.09
95b	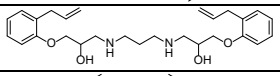	-6.90 ± 0.02	6	-7.07 ± 0.06	4	-6.50 ± 0.05	4	0.57
90	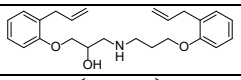	-7.22 ± 0.04	7	-7.28 ± 0.10	6	-6.79 ± 0.18	6	0.49
86	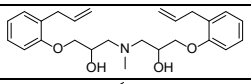	-6.66 ± 0.05	5	-6.43 ± 0.09	5	-6.43 ± 0.16	3	0
85	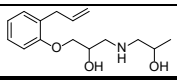	-6.74 ± 0.08	5	-6.71 ± 0.07	5	-5.48 ± 0.08	3	1.23

TABLE 5.8: $LogK_D$ values are presented here for the β_1-AR. $LogK_D\beta_1$ were previously derived from radioligand competitive binding assays (table 5.2). $LogK_D\beta_{1cim}$ were determined through the inhibition of cimaterol CRE-SPAP production using fixed concentrations of ligand, while $logK_D\beta_{1CGP}$ were determined through the inhibition of CGP12177 mediated response in whole cell assays (figure 5.7). Values represent mean of data ± the standard error of the mean (s.e.m) for n separate experiments.

for both alprenolol and oxprenolol exhibited identical selectivity for the primary conformation of the β_1-AR (ca. 1.4 log units), whilst surprisingly, *(R)*-enantiomer **81a** showed a difference between affinities of only 0.5 log units.

Effect of the second hydroxyl and 2-allylphenoxy moiety in the affinity for primary and secondary conformation of the β_1-AR: Removal of the second hydroxyl group (analogue **90**) resulted in a low difference in affinities ($logK_D\beta_{1cim} - logK_D\beta_{1CGP} = 0.49$) similar to the difference observed for parent compound **49b** (table 5.8). The affinity for the secondary conformation obtained for this analogue is also in accordance with the potency obtained for the response mediated at the β_1-AR ($logK_D\beta_{1CGP} = -6.79$ vs $logEC_{50}\beta_1 = -6.70$). Interestingly, removal of the 2-allylphenoxy moiety (analogue **85**) increased selectivity for the primary conformation of the β_1-AR ($LogK_D\beta_{1cim} - LogK_D\beta_{1CGP} = 1.23$). This can be observed in figure 5.7 where analogue **85** is able to produce a much larger shift to cimaterol mediated response than to CGP12177 mediated response at the same fixed concentration of 10μM. Comparison of analogue **85** and **47g** $logK_D$ values suggests that the introduction of the second hydroxyl group seems to lower the affinity for the primary conformation ($logK_D\beta_{1cim}$

	Compound	LogK$_D$ β_2	n	LogK$_D$ $\beta_{2\ Cim}$	n	LogK$_D$ $\beta_{2\ CGP}$	n	LogK$_{DCim}$ – LogK$_{DCGP}$
49a	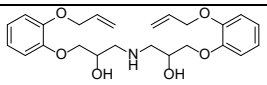	-9.01 ± 0.08	5	-9.49 ± 0.10	6	-9.16 ± 0.11	4	0.33
78b	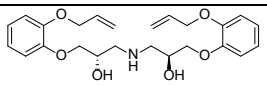	-9.30 ± 0.04	4	-9.51 ± 0.19	5	-9.15 ± 0.08	5	0.36
82b	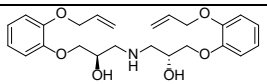	-7.56 ± 0.04	6	-7.57 ± 0.15	3	-7.12 ± 0.14	3	0.45
83b	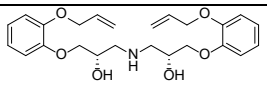	-9.32 ± 0.06	5	-9.33 ± 0.10	4	-9.22 ± 0.04	5	0.11
48a	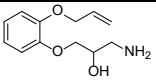	-7.07 ± 0.02	5	-7.49 ± 0.08	4	-7.07 ± 0.06	4	0.42
77b	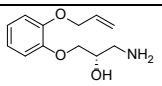	-7.63 ± 0.03	7	-7.77 ± 0.07	8	-7.56 ± 0.06	7	0.21
81b	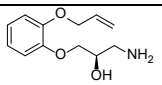	-6.94 ± 0.08	6	-7.07 ± 0.06	5	-6.80 ± 0.18	4	0.27
49b	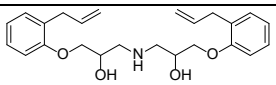	-8.16 ± 0.04	6	-8.39 ± 0.14	7	-7.87 ± 0.12	3	0.52
78a	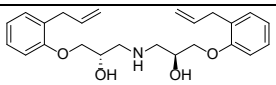	-8.22 ± 0.08	5	-8.64 ± 0.10	4	-8.14 ± 0.14	4	0.50
82a	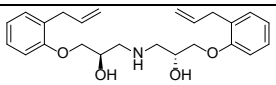	-6.98 ± 0.02	5	-7.30 ± 0.12	3	-6.60 ± 0.02	3	0.70
83a	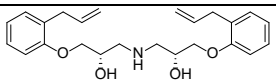	-8.08 ± 0.07	5	-8.35 ± 0.15	4	-7.82 ± 0.12	5	0.53
48b	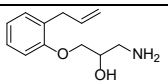	-7.18 ± 0.03	6	-7.46 ± 0.06	4	-7.00 ± 0.15	4	0.46
81a	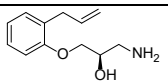	-6.54 ± 0.07	5	-6.72 ± 0.11	3	-6.27 ± 0.10	3	0.45
77a	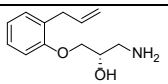	-7.58 ± 0.04	5	-7.80 ± 0.10	3	-7.27 ± 0.03	3	0.53

TABLE 5.9: $LogK_D$ values are presented here for the β_2-AR. $LogK_D\beta_2$ were previously derived from radioligand competitive binding assays (table 5.1). $LogK_D\beta_{2cim}$ were determined through the inhibition of cimaterol CRE-SPAP production using fixed concentrations of ligand, while $logK_D\beta_{2CGP}$ were determined through the inhibition of CGP12177 mediated response in whole cell assays (figure 5.6). Values represent mean of data ± the standard error of the mean (s.e.m) for n separate experiments.

-6.71 for **85** and -7.53 for **47g**) whilst maintaining the affinity for the secondary conformation of the β_1-AR ($logK_D\beta_{1CGP}$ -5.48 for **85** and -5.49 for **47g**).

Effect of the presence of a linker between two alprenolol aryloxypropanolamine units in the affinity for primary and secondary conformation of the β_1-AR:

	Compound	LogK$_D$ β_2	n	LogK$_D$ β_{2Cim}	n	LogK$_D$ β_{2CGP}	n	LogK$_{DCim}$ – LogK$_{DCGP}$
47g	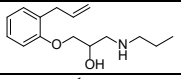	-8.09 ± 0.11	5	-8.72 ± 0.10	3	-	-	-
47h	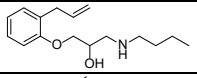	-7.75 ± 0.04	6	-8.43 ± 0.11	3	-	-	-
94a	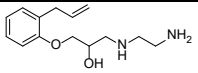	-7.46 ± 0.04	5	-7.68 ± 0.07	3	-7.37 ± 0.12	4	0.31
95a	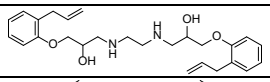	-7.86 ± 0.08	7	-8.61 ± 0.07	8	-8.49 ± 0.09	8	0.12
95b	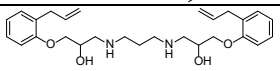	-7.64 ± 0.07	6	-8.18 ± 0.15	4	-7.77 ± 0.11	4	0.41
90	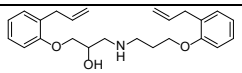	-8.41 ± 0.03	7	-8.72 ± 0.16	7	-8.29 ± 0.23	5	0.43
86	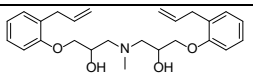	-7.19 ± 0.06	5	-7.69 ± 0.10	7	-7.29 ± 0.07	6	0.40
85	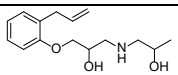	-7.46 ± 0.03	5	-7.73 ± 0.05	3	-	-	-

TABLE 5.10: $LogK_D$ values are presented here for the β_1-AR. $LogK_D\beta_2$ were previously derived from radioligand competitive binding assays (table 5.2). $LogK_D\beta_{2cim}$ were determined through the inhibition of cimaterol CRE-SPAP production using fixed concentrations of ligand, while $logK_D\beta_{2CGP}$ were determined through the inhibition of CGP12177 mediated response in whole cell assays. Values represent mean of data ± the standard error of the mean (s.e.m) for n separate experiments.

Analogue **94a**, containing a two carbon linker with a terminal amino moiety, was able to differentiate between the primary and secondary conformation of the β_1 and required a higher concentration to shift the response mediated by CGP12177 than cimaterol-mediated response at this receptor ($logK_D\beta_{2cim} - logK_D\beta_{2CGP} = 1.43$, table 5.7). In CHO-$\beta_2$ cells, $logK_D$ values obtained were independent of the ligand used as agonist in the experiment, as expected ($logK_D\beta_{2cim} = -7.68$ and $logK_D\beta_{2CGP} = -7.37$, table 5.10). Two alprenolol aryloxypropanolamine units connected by this two carbon linear linker **95a** yielded identical affinities for the primary and secondary conformations of the β_1-AR ($logK_D\beta_{1cim} = -7.36$, $logK_D\beta_{1CGP} = -7.45$, table 5.8). This suggests that the presence of a second alprenolol aryloxypropanolamine unit has a quite striking effect on the affinity for the secondary conformation of the β_1 in comparison with analogue **94a** (2.20 log units decrease in $logK_D\beta_{1CGP}$) accompanied by a much smaller increase in affinity for the primary conformation (0.68 log units decrease in $logK_D\beta_{1cim}$). Extension the length of the linker by one carbon (**95b**) decreased the affinity for both conformations.

Effect of methylation of the central amino group of bis alprenolol ligand in the affinity for primary and secondary conformation of the β_1-AR: *N*-methylated

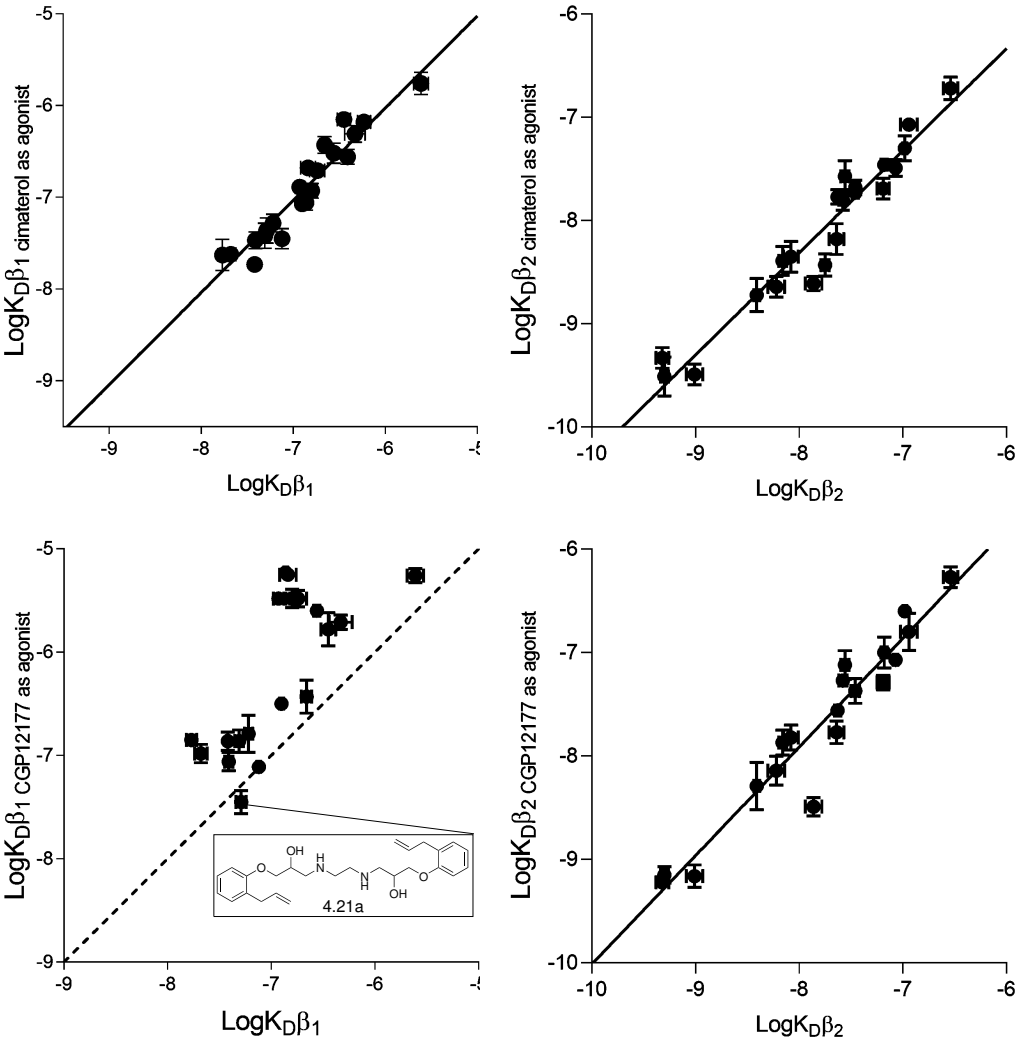

FIGURE 5.8: Left: Correlation between $logK_D\beta_1$ derived from radioligand binding assays and $logK_D\beta_{1cim}$ obtained from inhibition of cimaterol SPAP response (top) or $logK_D\beta_{1CGP}$ obtained by inhibition of CGP12177 response (bottom); Right: Correlation between $logK_D\beta_2$ derived from radioligand binding assays and $logK_D\beta_{2cim}$ obtained from inhibition of cimaterol SPAP response (top) or $logK_D\beta_{2CGP}$ obtained by inhibition of CGP12177 response (bottom). Analogue **95a** is highlighted as it is shows similar $logK_D\beta_{1CGP}$ and $logK_D\beta_1$.

analogue **86** behaved as a non-selective compound and did not differentiate between cimaterol and CGP12177 responses in CHO-β_1 cells, even though it yielded overall lower affinities than parent compound **49b** as expected from radioligand binding assays (figure 5.7). This analogue was able to increase SPAP accumulation therefore increased the basal level of both cimaterol and CGP12177 response curves but was able to rightshift these curves a similar lenght at a fixed concentration of 3μM. In CHO-β_2 cells a small difference of $logK_D\beta_{2cim} - logK_D\beta_{2CGP} = 0.4$ was observed (table 5.10).

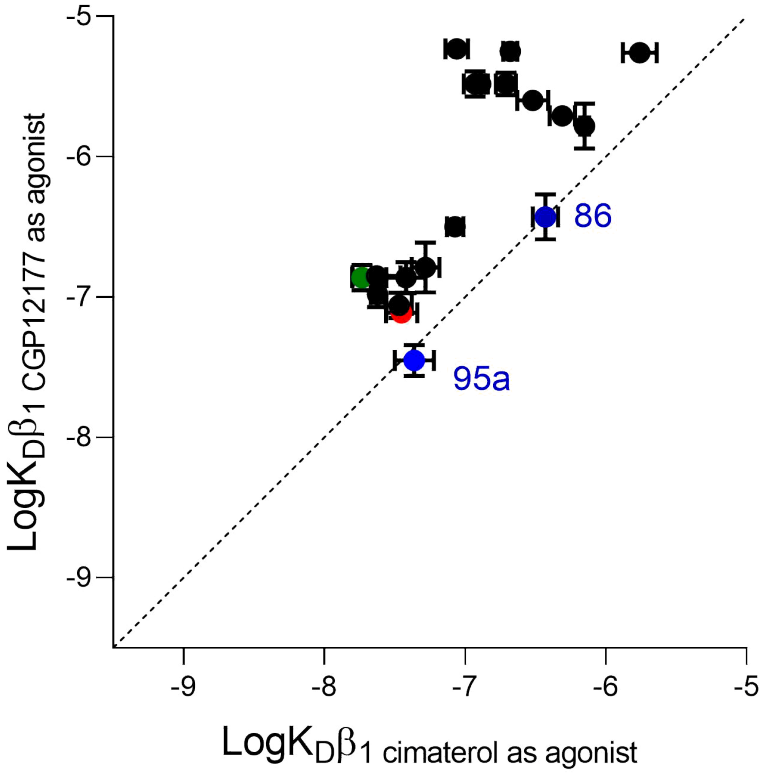

FIGURE 5.9: Selectivity between $logK_D\beta_{1cim}$, obtained from inhibition of cimaterol SPAP response (represents affinity for the primary conformation) and $logK_D\beta_{1CGP}$ obtained by inhibition of CGP12177 response (represents affinity for the secondary conformation). Parent compound alprenolol bis ligand **49b** is highlighted in red, while oxprenolol bis ligand **49a** is highlighted in green. Analogues **95a** and **86** are highlighted in blue and behaved as non-selective compounds.

Overall, the affinity values derived from the rightshift of cimaterol concentration response curve ($logK_D\beta_{1cim}$) in CHO-β_1 cells correlate well and were identical to the values obtained from competitive ligand binding ($logK_D\beta_1$) ($r^2 = 0.916$, figure 5.8 top left). This is expected as, in radioligand binding assays, [^{3}H]-CGP12177 is added in a concentration such that only occupies the primary conformation of the β_1-AR. $LogK_{DCGP}\beta_1$ values obtained by inhibition of CGP12177-mediated response do not seem to correlate with $logK_D\beta_1$ derived from radioligand binding experiments. In this figure a identation line is presented showing that the majority of compounds possess an anomalous behaviour with a much lower affinity determined by inhibition of CGP12177 response than determined from radioligand binding assays. Analogue **95a** is highlighted as it was the only compound to obtain a higher affinity for the secondary conformation of the β_1-AR than the $logK_D\beta_1$ obtained from binding (figure 5.8 bottom left). In CHO-β_2 cells both the affinity derived from the inhibition of cimaterol ($logK_D\beta_{2cim}$) and CGP12177 ($logK_D\beta_{2CGP}$)

seem to correlate well with the values obtained from radioligand binding ($r^2 = 0.936$ for the first and $r^2 = 0.925$ for the later) (figure 5.8 right). Affinity values obtained through the rightshift of cimaterol response at β_2-AR seem to be overestimated in around 0.5 log units when compared with the $logK_D\beta_2$ values obtained from radioligand binding assays as previously seen for the other sets of ligands.

$LogK_D\beta_{1cim}$ values obtained from the righshift of cimaterol response curve in SPAP functional assays were also plotted against the $logK_D\beta_{1CGP}$ values obtained from inhibition of CGP12177 response (figure 5.9). Parent compounds **49a** and **49b** are highlighted in green and red respectively. Analogues **86** and **95a** stand out as the only compounds with exactly the same affinity for both conformations, even though **95a** has an overall higher affinity than **86**.

5.2.2.4 CGP20712A affinity

As seen in the previous chapters, a fixed concentration of the antagonist CGP20712A was added to increasing concentrations of agonists from this set in CHO-β_1 cells (figure 5.10). CGP20712A is able to differentiate between responses mediated by cimaterol, a primary conformation agonist, and CGP12177, a secondary conformation agonist, requiring a higher concentration to inhibit CGP12177 mediated response ($logK_D\beta_{1cim} = -9.23$ and $logK_D\beta_{1CGP} = -7.23$, table 2.5). Likewise, ICI118551, a β_2 antagonist was added to increasing concentrations of ligand in CHO-β_2 cells as a control assay ($logK_D = -9.24$, obtained from competitive binding assays, $logK_D\beta_{2cim} = -9.84$ and $logK_D\beta_{2CGP} = -9.48$). $LogK_D$ values for CGP20712A derived from the parallel rightshift of the responses mediated by the agonists in this set are presented in tables 5.3 and 5.4, while $logK_D$ for ICI118551 are displayed in tables 5.5 and 5.6.

Response mediated by the meso alprenolol bis compound **83b** at the β_1-AR is more resistant to antagonism by CGP20712A yielding a $logK_D$ value for this antagonist of -7.44 ± 0.07, similar to the $logK_D$ obtained when inhibiting CGP12177 response. This can be observed in figure 5.10, in which the addition of 100 nM of CGP20712A barely shifts the response curve of **83b**. This resistance to antagonism together with the discrepancy observed in $logK_D\beta_1$ vs $logEC50\beta_1$ and the similarity between the obtained $logEC50\beta_1$ and $logK_{DCGP}\beta_1$ values strongly indicates that the response is mediated via the secondary conformation of the β_1-AR. Likewise, the response mediated by the *(S,S')*-bis alprenolol enantiomer **78a** is more resistant to antagonism resulting in a $logK_D = -7.37 \pm 0.12$ for CGP20712A. Interestingly, the *(R,R')*-enantiomer **82a** gave a $logK_D = -7.81 \pm 0.13$ for CGP20712A, slightly lower than the value

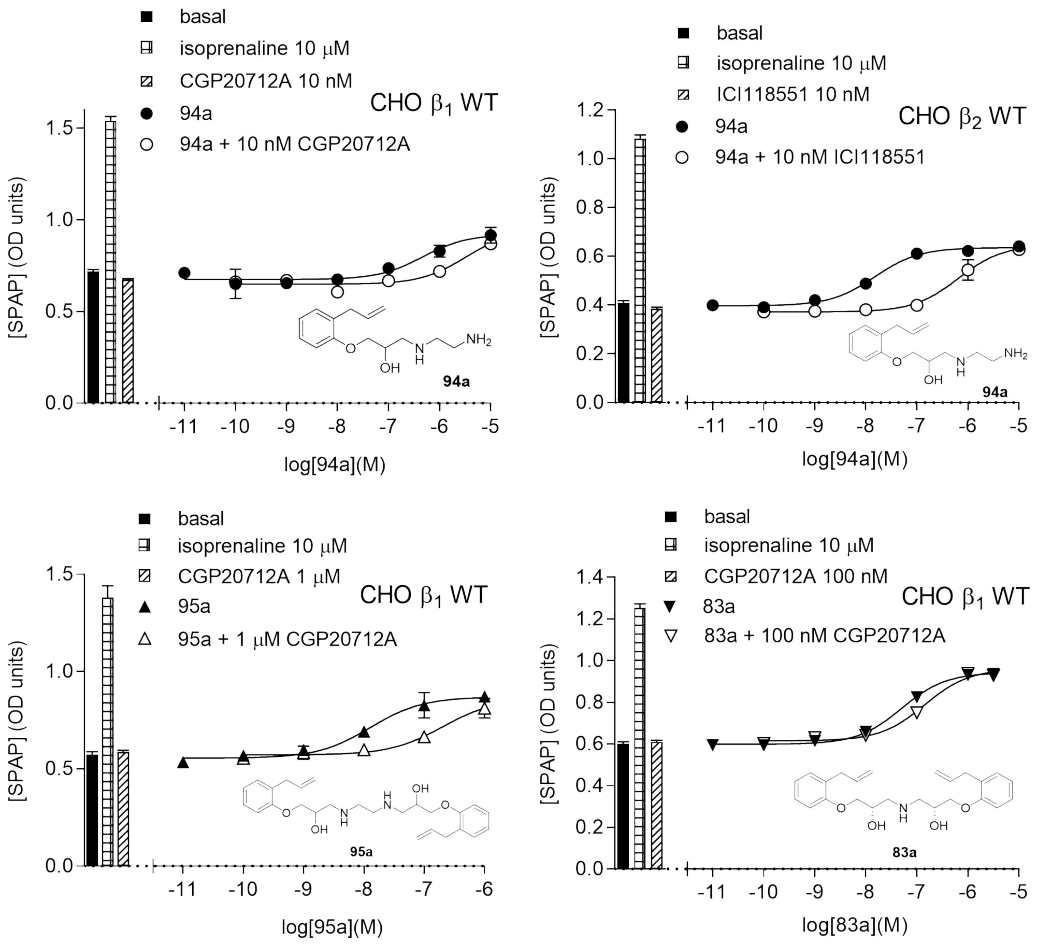

FIGURE 5.10: Top: CRE-SPAP activity in response to analogue **94a** in the presence and absence of a fixed concentration of CGP20712A in CHO-β_1 cells and in the presence and absence of a fixed concentration of ICI118551 in CHO-β_2 cells; Bottom: CRE-SPAP activity in response to analogue **95a** (left) or **83a** (right) in the presence and absence of a fixed concentration of CGP20712A in CHO-β_1 cells; Bars show basal SPAP activity in response to 10μM isoprenaline and in response to a fixed concentration of either CGP20712A or ICI118551. Data points are mean ± s.e.m. of three determinations in a single experiment. These individuals experiments are representative of three or more separate experiments.

obtained by inhibition of the other isomers. Similarly, the *(R,R')*-enantiomer of oxprenolol bis compound **82b** also yielded a $logK_D$ for CGP20712A lower than the other isomer counterparts but still lower than the $logK_D$ obtained through inhibition of cimaterol response ($logK_D\beta_{1cim} = -9.23$ for CGP20712A). This suggests that *(R,R')*-enantiomers of alprenolol and oxprenolol bis ligands might be able to activate to activate both conformations of the β_1-AR. Even though activation of both conformations usually results in a biphasic concentration response curve, the close proximity of the affinity obtained for both conformations might hinder the obtention of a biphasic response

curve. In CHO-β_2 cells, ihibition of compound **82b** mediated response by ICI118551 yielded a $logK_D = -9.62 \pm 0.08$ for this antagonist, similar to the values obtained through inhibition of cimaterol ($logK_D\beta_{2cim} = -9.84$ for ICI118551) and CGP12177 ($logK_D\beta_{2CGP} = -9.48$ for ICI118551) responses at this receptor.

Response mediated by the desoxy analogue **90** at the β_1-AR also showed resistance to antagonism by CGP20712A, suggesting that **90** is a secondary conformation agonist. Likewise, compounds **94a** and **95a** were resistant to antagonism by CGP20712A yielding $logK_D$ values for the antagonist similar to those obtained using CGP12177 as agonist (table 5.4, figure 5.10). A concentration of 1μM of CGP20712A was required to rightshift **95a** response curve while the response mediated by **94a**, an analogue containing the linker used for **95a**, was rightshifted by a concentration as low as 10 nM of CGP20712A, 100 fold lower. A $logK_D = -9.04 \pm 0.08$ was obtained from CGP20712A when inhibiting **94a** response, consistent with a response mediated by the primary conformation of the β_1-AR. Compound **85** was easily antagonised by CGP20712A, resulting in a $logK_D$ value consistent with a response mediated via primary conformation of the β_1-AR.

In CHO-β_2 cells, analogues **94a**, **90** and **85** mediated a response easily antagonised by ICI118551, resulting in $logK_D$ values for this antagonist similar to the values obtained from radioligand binding and inhibition of both cimaterol and CGP12177 responses previously presented in table 2.5.

5.3 Conclusion

In this chapter, the enantioselective synthesis of alprenolol **49b** and oxprenolol **49a** bis individual isomers was attempted. Even though the derised enantiopurity was not achieved and only enriched fractions with the desired isomer were obtained, this aided the identification of the isomers during chiral separation by chiral HPLC. In order to understand which chemical feature was responsible for the interesting behaviour observed in ligand **49b** several analogues of these compound were synthesised. Analogues lacking the 2-allylaryloxy moiety (**85**) and the second hydroxyl (**90**; and therefore lacking the second chiral centre) were successfully synthesised. Analogues containing a linear carbon spacer between two aryloxypropanolamine alprenolol units (**95a-b**) together with an analogue only containing the two carbon linker **94a** were also synthesised. An analogue of **49b** containing a tertiary, methylated, amine was also obtained.

All of **49b** and **49a** individual isomers retaining the selectivity between the primary and secondary conformation observed in the mixture. *(R,R')*-enantiomers of both the compounds showed overall lower affinity for both conformation than the other isomers while

(S,S')-enantiomers and meso compounds showed similar affinities between themselves suggesting that the second chiral centre does not have a major impact in affinity for either of the conformations. In fact, removal of that hydroxyl group (**90**) only reduced slightly the affinity for both primary and secondary conformation but retaining the low selectivity towards the primary conformation. Besides showing a very small difference in affinities between primary and secondary conformation, analogues **78a**, **83a** and **90** mediated a response via the secondary conformation with a $logEC_{50}$ consistent with the affinity obtained for the secondary conformation that were also resistant to antagonism by CGP20712A. Both *(R,R')*-enantiomers yielded a lower affinity for CGP20712A than the isomer counterparts, suggesting that their response might be partially also mediated via the primary conformation.

Methylated analogue **86** showed reduced affinity for both conformations of the β_1 but behaved as a non-selective compound with similar affinities for both conformations. This compound was also able to elicit a response with a $logEC_{50}$ similar to the $logK_D$ that was somewhat resistant to antagonism by CGP20712A suggesting a response mediated via both conformation but mainly through the secondary conformation.

Introduction of a two carbon linker between the two alprenolol moieties was ideal and introduction of an extra carbon in the linker reduced affinity for both conformations of the β_1-AR. Both analogues **95a** and **95b** behaved as non-selective secondary conformation partial agonists eliciting a response highly resistant to antagonism by CGP20712A, similarly to CGP12177.

85 and **94a** behave as primary conformation partial agonist at the β_1 stimulating responses that are easily inhibited by CGP20712A which suggest that the presence of a second 2-allylaryloxy moiety increases the affinity for the secondary conformation and might also contribute to its activation.

Chapter 6

Synthesis of a potential photoactivable covalent antagonist ligand based on betaxolol

6.1 Introduction

In this chapter, the synthesis of a potential photoactivable covalent antagonist for the β_1-adrenergic receptor is reported. Covalent probes, also referred to as affinity or irreversible probes, are powerful pharmacological tools which target a specific binding site within a protein and bind covalently to it near the binding site. Covalent probes are ligands which usually contain a pharmacophore that targets and displays high affinity for a certain receptor connected to either a chemoreactive or photoreactive tag by a linker. Photoactivable covalent probes contain a photoreactive chemically inert group which produces a highly reactive species upon photolysis that react covalently with the protein and chemoreactive probes bear an eletrophilic group able to react with nucleophilic residues within the protein.[92, 93]

As previously mentioned, probing the primary conformation of the β_1-AR with an irreversible antagonist could be a successful strategy to study the secondary conformation in more detail. In the hypothetical case that the phenomenon seen is dependent on two related binding events across a homodimer as proposed by Hill et al, having a fixed probe in the orthostaric binding site would be useful as these phenomenon are usually probe dependent.[34, 73] This strategy would be particularly useful as compounds with higher affinity for the secondary conformation than the primary conformation of the β_1-AR have not been described yet. The desired ligand would be a compound that: 1) binds

covalently with a high affinity to the primary conformation of the β_1-AR in order to decrease non-specific binding; 2) binds with high selectivity and high efficiency of incorporation to the primary conformation over the secondary conformation of the β_1-AR allowing control of the concentration over a broad range; 3) lacks intrinsic activity, in order to allow the better study of the secondary conformation; 4) allows the study of the receptor in whole living cells.

Covalent ligands have been popular for decades as a way to gain more information regarding the receptor structure and function. Covalent probes have been used as important pharmacological tools to map protein's binding sites, determine receptor reserves and receptor turnover, study receptor dimerisation or even to stabilise receptor structures and obtain X-ray crystal structures.[94, 93, 92, 95, 96] The β-adrenergic receptors have been the focus of several studies using either photoactivable covalent probes or chemoreactive probes. [97, 98, 99, 100, 101, 102]

6.1.1 Chemoreactive probes targeting β-ARs

A plethora of electrophilic halomethylketone-containing ligands but also isothiocyanate-containing compounds have been used to probe the β-adrenergic receptors either in tissues or cells (figure 6.1). These irreversible ligands have been based on several pharmacophores such as alprenolol (BAAM, **96**), betaxolol (**97**), carazolol (pBABC **98**), carbostyril moiety of indacaterol (DCITC **99**), pindolol, noradrenaline, among others. [97, 98, 103, 104, 95, 94, 105]

BAAM (**96**), bromoacetyl alprenolol menthane, containing a chemoreactive halomethylketone, was used in several *in vivo* and *in vitro* studies to study receptor function by selective destruction of the β-adrenergic receptors in living cells and animals.[106] This compound requires a relatively high concentration ($1 - 10\mu M$) to reduce the number of [^{3}H] dihydroalprenolol binding sites, a ligand able to radiolabel the β-ARs, in frog erythrocyte membranes, which has been associated with some nonspecific effect and therefore limits its usefulness.[98, 95] Betaxolol chemoreactive analogue **97** exhibited a much lower affinity than betaxolol ($pA_2 = 7.66$ in guinea pig atria; $pA_2 = 5.28$ in guinea pig trachea; determined through the rightward shift of isoprenaline chronotropic dose-effect curve). This compound was able to reduce the number of [^{125}I] cyanopindolol binding sites, a radioiodinated ligand which probes the β-ARs, by only 60% at $10\mu M$ in rat cortical membranes.[103] *para*-(Bromoacetamidyl)benzylcarazolol (pBABC **98**) contains the same linker and chemoreactive group as betaxolol analogue **97**.[107, 94] This chemoreactive probe displayed high affinity ($\mathrm{Log}K_D = -9.40$) for both frog (mostly β_2-AR) and turkey erythrocytes (mostly β_1-AR) and was able to inactivate 88% of the sites occupied

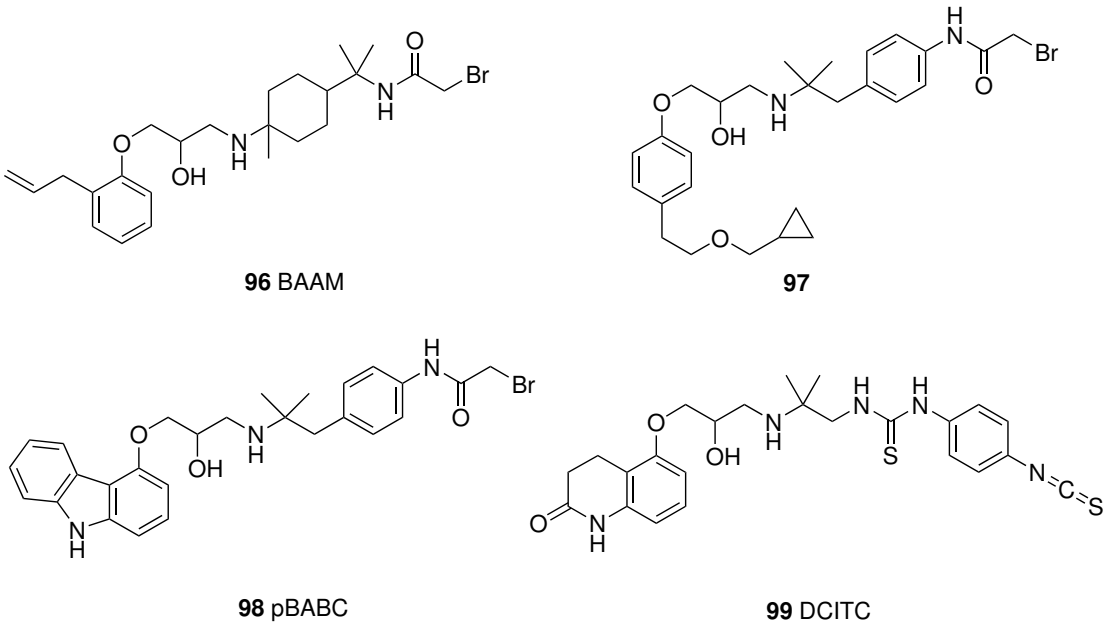

FIGURE 6.1: Chemoreactive probes described in the literature to target the β adrenergic receptors.

by [^{125}I] cyanopindolol at 10 nM. Interestingly, a radioiodinated version of this probe was later successfully used to map the β_2-AR orthosteric binding site even though the specific labeled residue was not identified. An isothiocyanate-containing probe (DCITC **99**) was also used to irreversibly bind to the β-ARs in DDT cells. Preincubation of DDT cell membranes with 5 nM of DCITC followed by several washes resuted in a 75% decrease in [^{125}I] cyanopindolol binding. This ligand also demonstrated an irreversible antagonistic effect in rat isolated aorta (containing predominantly β_2-AR subtype) when preincubation with 100 nM reduced irreversibly the maximal relaxation caused by isoprenaline by 88%. [95].

Recently, Gmeiner et al, designed and synthesised several chemoreactive probes targeting both the β_1 and β_2-AR (figure 6.2).[99] FAUC50 (**100**) has been used to obtain the first crystal structure of the β_2-AR bound to an agonist. A cysteine anchor mutation was introduced in the receptor, replacing $His^{2.64}$ in the upper part of TM2, in a suitable position to form a disulfide bond with FAUC50. This covalent bond prevented dissociation of the ligand turning its agonistic response resistant to antagonism by ICI118551 in the $\beta_2AR^{H2.64C}$.[96] A similar strategy was adopted for the β_1-AR, a cysteine mutation was introduced in the same position (murine $\beta_1AR^{I2.64C}$) and several ligands with different pharmacophores and linkers were tested.[99] Compounds **101** and **102** were designed to target this mutated β_1-AR with a structure based on the β_1-selective antagonist CGP20712A. Both of these ligand were able to bind covalently with high affinity to the mutated receptor, in HEK293T cells transiently expressing the receptor. Compound

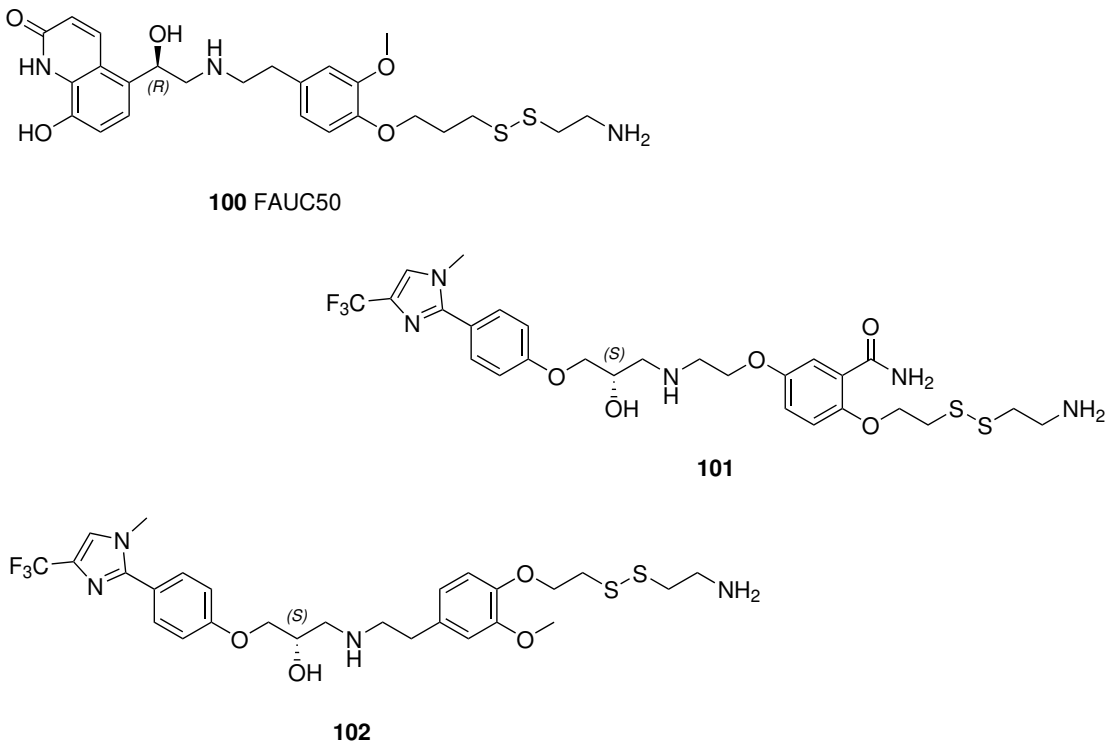

FIGURE 6.2: Chemoreactive probes based on indacaterol and and CGP20712A pharmacophore units designed and synthesised by Gmeiner et al, targeting a nucleophilic cysteine residue in mutated murine $\beta_1 AR^{I2.64C}$ and human $\beta_2 AR^{H2.64C}$.

101 displaced [^{3}H] CGP12177 in a biphasic manner with K_D values of 0.56 nM and 280 nM for the murine $\beta_1 AR^{I2.64C}$ and was able to block covalently 76% of the receptors at 50 nM. This biphasic displacement of radiolabeled [^{3}H] CGP12177 was also observed for the human $\beta_2 AR^{H2.64C}$ and might have been caused by a mixture of covalent cross-linking and non-covalent ligand binding. [99] Similarly, compound **102** displaced [^{3}H] CGP12177 in a biphasic manner with K_D values of 0.071 nM and 270 nM and was able to block covalently 79% of the receptors at 1μM.

While these chemoreactive probes can prove to be quite useful, they come with some limitations. Most of these ligands have been studied in tissues before the discovery of β-adrenergic receptor subtypes which complicates the interpretation and evaluation of the results obtained in these studies. The failure to identify any nucleophilic residue within the protein labeled by the chemoreactive group is another major drawback. For this reason, various studies suggested that several chemoreactive probes designed and characterised in the 70-80s might behave as slowly dissociating ligands whereas the apparant irreversible behaviour is due to an extremely slow dissociation from the receptor.[108, 109] Using a mutated receptor could prove an attractive alternative approach to deal with

this issue and would allow characterisation of the ligand in the wildtype receptor in equilibrium assays, however a thorough validation of the mutated receptor would have been required.

6.1.2 Photoactivable probes targeting β-ARs

Photoactivable probes, contrary to chemoreactive probes, possess a chemically inert group which, upon photoactivation, generates a highly reactive species that forms an irreversible bond with the receptor. These highly reactive species generated upon photolysis are able to react and incorporate the probe in non-nucleophilic residues. The fact that these ligands bear an inert group until photoactivation allows their prior characterisation in equilibrium assays before being activated *in situ*. Even though this reduces nonspecific binding to a minimum, UV radiation used to produce the highly reactive species might cause damage to proteins and cells used in the assays. For this reason, the selection of a photoreactive group which requires a low energy wavelength for activation is of high importance.

Several photoactivable irreversible probes have been widely used to label β adrenergic receptors.[110, 93] Azide-containing probes have been the most popular to target β-AR, even though some diazirine-containing probes have also been described.[110] Azide groups generate reactive nitrenes upon photoactivation but require high energy wavelengths ($<$300 nm) for activation. Acetobutolol azide **103**, *para*-azido-benzylcarazolol **104** and ICYP-azide **105** are some of the described azide-containing photoactivable probes designed to target the β-ARs (figure 6.3). Introduction of an azido group in the aromatic core of acetobutolol (**103**) resulted in a slight decrease in affinity ($logK_D = -6.41$) in rat reticulocytes (mainly a β_2-AR model).[111] Photoactivation of this ligand resulted in a 50% non-competitive blockade of catecholamines response.[111] *para*-Azidobenzylcarazolol **104** was characterised in frog erythrocyte membranes (also containing mostly the β_2-AR subtype) and was able to bind with high affinity ($\mathrm{Log}K_D = -9.62$) to the receptors.[112] Addition of the ligand to these membranes, followed by photoactivation, led to the blockade of 60% of the receptor binding sites.[112] Interestingly, the addition of this probe without photolysis resulted in a 35% apparent irreversible loss of observable sites.[112] This highlights the importance of characterising the probe before photolysis, as the ligand might slowly dissociate from the receptor and appear irreversible even after several washes. An azido-containing iodocyanopindolol probe (**105**) has also been described.[113] Introduction of the amide linker and the aromatic azido group retained the high affinity ($\mathrm{Log}K_D = -10.03$) seen for iodocyanopindolol in turkey erythrocyte membranes (containing mostly the β_1-AR subtype). Addition of 2 nM of this ligand to the membranes followed by photoactivation resulted in a decrease of 80% the

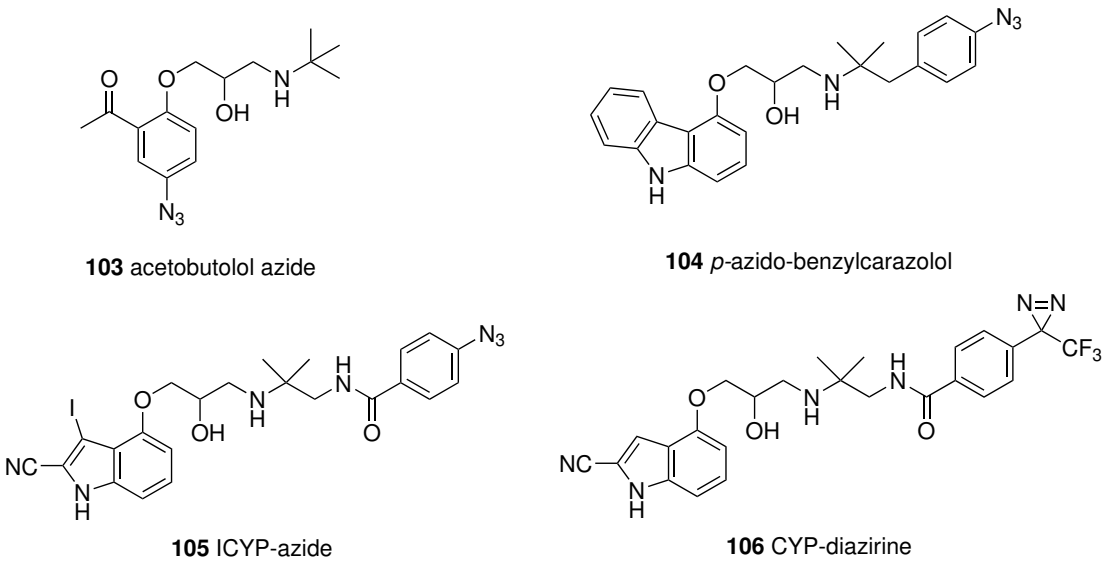

FIGURE 6.3: Photoactivable probes described in the literature to target the β adrenergic receptors.

number of detectable binding sites. As a high energy wavelength (268 nm) was required to photoactivate this ligand, which could result in tissue damage, a new probe based on cyanopindolol containing the same linker and a diazirine photoreactive group (**106**) was synthesised (figure 6.3).[114] Aromatic trifluoromethyl diazirines are able to generate a highly reactive carbene upon photolysis under mild condition (350-380 nm), shorter activation times and efficiently insert into an aminoacid residue within the protein. CYP-diazirine **106** was able to bind the β-ARs in turkey erythrocyte membranes with high affinity ($K_D = 0.38$ nM) and covalently label these receptors after photolysis under mild conditions (366 nm UV wavelength). This CYP-diazirine **106** probe was later radioiodinated and used in several experiments to label the β_1-AR for the study of receptor phosphorylation and desensitisation but also to map β_1-AR binding site.[100, 101, 102]

Similarly to the chemoreactive probes most of these ligands have been tested previously to the discovery of the β_1 and β_2 receptor subtypes and tested in tissues containing both receptor subtypes.

6.1.3 Design of a potential photoactivable ligand based on betaxolol

As mentioned before, the ideal compound to probe the primary conformation of the β_1-AR would possess a high selectivity for the primary over the secondary conformation, allowing the use of broad window of concentrations in the cell assays. Preparation of compound **107** (figure 6.4) using betaxolol, a known β_1-AR antagonist, most active *(S)*-configuration as pharmacophore seems ideal as betaxolol exhibited a 3.14 log units

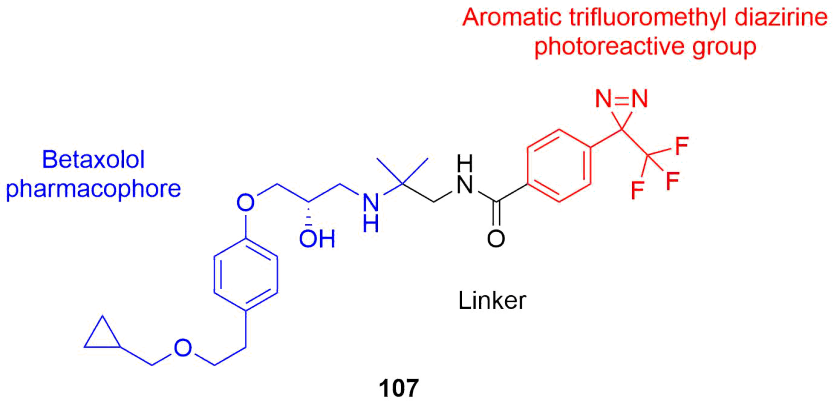

FIGURE 6.4: Potential photoactivable covalent antagonist ligand based on betaxolol containing an aromatic trifluoromethyl diazirine group.

difference in affinities for these conformations (around 1400 fold selectivity for the primary conformation) while retaining a high affinity for the primary conformation of the β_1-AR ($logK_D\beta_1 = -8.21$). [35] The linker and aromatic trifluoromethyl diazirine group present in CYP-diazirine **106** were chosen. The linker used retained the high affinity of cyanopindolol for the β_1-AR and the diazirine group was able to covalently label the receptor upon activation under mild conditions, which should therefore allow the study of the receptor in living cells without little or no damage.

6.2 Results and discussion

6.2.1 Chemistry

Herein, the synthesis of the potential covalent antagonist **107** is described (Scheme 6.1). Protection of the phenol **108** was performed with the addition of benzyl bromide to a solution of 4-hydroxyphenethyl alcohol and potassium carbonate in DMF at 60 °C. Resulting protected phenol **109** was alkylated through the addition of a slight excess of cyclopropylmethyl bromide (**110**) to a solution of **109** and sodium hydride in DMF at 60 °C yielding compound **111** in 76% yield. Compound **111** was then deprotected to completion to the corresponding phenol **112** through an hydrogenation using palladium on carbon as a catalyst in methanol. Deprotection was followed by alkylation of the phenol with the chiral reagent *(S)*-glycidyl nosylate in DMF in the presence of sodium hydride yielding oxirane **113**. In parallel, 2.1 equivalents of diamine **91** were added to boc anhydride in DMF in the presence of triethylamine which led to the selective boc protection of the less hindered amine (**114**). Initially, amine **114** was reacted with oxirane **113** in hexafluoroisopropanol (HFIP) under microwave irradiation at 60 °C, a method

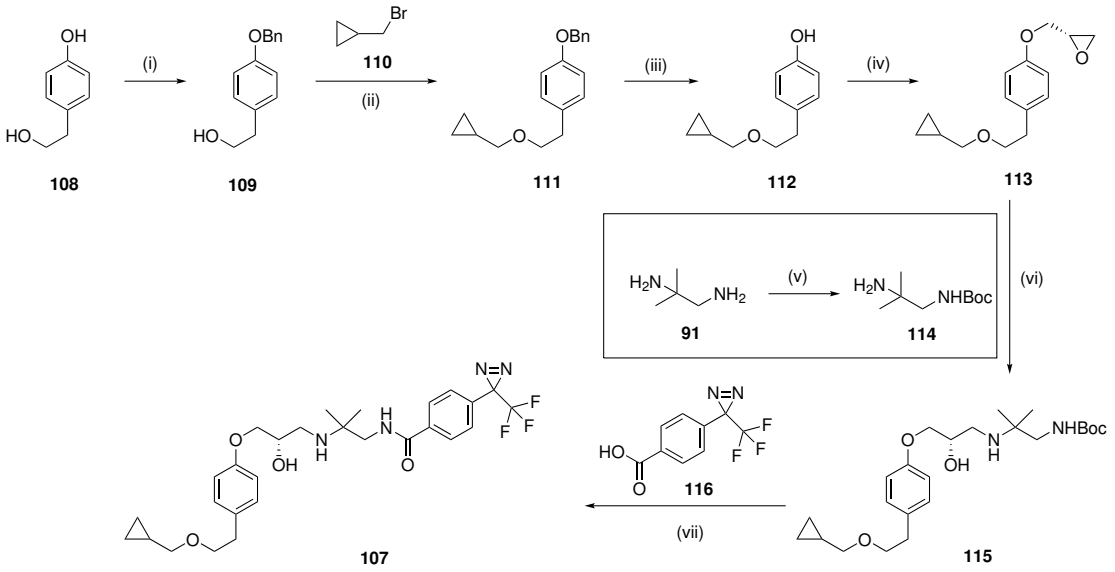

SCHEME 6.1: Synthesis of *(S)-N*-(2-((3-(4-(2-(cyclopropylmethoxy)ethyl)phenoxy)-2-hydroxypropyl)amino)-2-methylpropyl)-4-(3-(trifluoromethyl)-3H-diazirin-3-yl)benzamide **107**. Conditions and reagents: (i) Benzyl bromide, K_2CO_3, DMF, 60 °C, 24 h., 92%; (ii) **110**, NaH, DMF, 60 °C, 48 h., 76%; (iii) H_2, Pd/C, MeOH, r.t., 5 h., 84%; (iv) *(S)*-glycidyl nosylate, NaH, DMF, 60 °C, 14 h, 64%; (v) Di-tert-butyl dicarbonate, Et_3N, DCM, r.t., 24 h., 85%; (vi) **114**, DMF:H_2O (9:1), r.t., 48 h., 45%; (vii) 1. TFA, DCM, r.t., 2 h.; 2. **116** HATU, Et_3N, ACN, r.t., 18 h.

used for several epoxide openings described in the previous chapters. This method led to the removal of the *tert*-butyloxycarbonyl protecting group due to HFIP acidity ($pKa = 9.3$) and therefore resulted in an undesirable mixture of regioisomers. Alternatively, a mixture of DMF:H_2O (9:1) was used as a solvent and the addition of amine **114** to oxirane **113** resulted in the desired analogue **115** which was then purified through flash column chromatography. Boc deprotection of this compound was performed by stirring compound **115** in the presence of trifluoroacetic acid (TFA) in dichloromethane for two hours. Resulting salt was free based and then coupled with carboxylic acid **116** using HATU coupling agent in the presence of triethylamine yielding the aromatic trifluoromethyl diazirine **107** which was purified through HPLC.

6.2.2 Pharmacology

Potential photoactivable covalent antagonist **107** has not been photophysically and pharmacologically characterised yet. Nevertheless, intermediate **115** has been pharmacologically characterised in CHO-cells expressing either the human β_1 or β_2-AR together with a CRE-SPAP. Figure 6.5 represents the amount of radioactivity bound to the CHO-β_1 and CHO-β_2 cells at different concentrations of **115** when a fixed concentration of radiolabeled (−)[^{3}H] CGP12177 is added. Total binding and non-specific binding in the

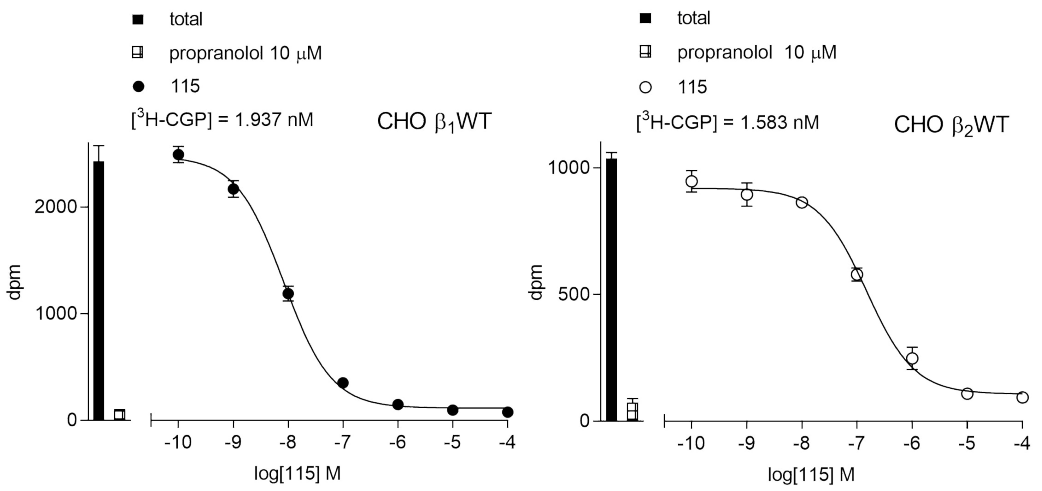

FIGURE 6.5: Inhibition of [^{3}H] CGP12177 binding to whole cells in CHO-β_1 and -β_2 cells by compound **115**. Left bar represents total [^{3}H] CGP12177 binding and the right one non-specific binding which was determined in the presence of 10 μM propranolol. Data points are triplicate determinations from a single experiment and represent mean ± S.E.M. .

presence of a $10\mu M$ of propranolol are also represented. IC_{50} values taken from the displacement curve were then converted into K_D values using the Cheng-Prusoff equation presented in the experimental section. Compound **115** displaced the radioligand (−)[^{3}H] CGP12177 both in CHO-β_1 with a $logK_D\beta_1 = -8.93 \pm 0.04$, n=5 and in CHO-$\beta_2$ cells with a $logK_D\beta_2 = -7.93 \pm 0.04$, n=5. This analogue shows higher affinity for both receptor subtypes than racemic betaxolol which displayed $logK_D\beta_1 = -8.21$ and $logK_D\beta_2 = -7.38$ (literature values obtained by displacing (−)[^{3}H] CGP12177 in CHO-cells). [35] K_D values for racemic mixtures are given by the harmonic mean of the K_D values of the pure enantiomers which means the most active enantiomer of betaxolol racemic mixture could only have a maximal $logK_D\beta_1 \approx -8.51$ still inferior to the β_1 affinity obtained for the enantiomerically pure analogue **115**. This analogue also exhibited similar β_1-selectivity to that observed for the parent compound betaxolol.

The ability of analogue **115** to increase CRE-SPAP accumulation was evaluated in CHO-β_1 and CHO-β_2 cells. Figure 6.6 shows CRE-SPAP activity in response to analogue **115**. This analogue mediated a very weak response at β_1-AR ($<$ 5% of isoprenaline maximal response) and did not increase SPAP accumulation at β_2-AR. Similarly, betaxolol behaves as an antagonist at both β_1- and β_2-subtypes.[81]

$LogK_D$ values for the primary conformation were also obtained through the parallel rightward shift of cimaterol (an agonist at the primary conformation of the β_1-AR) concentration-response curve, while affinity for the secondary conformation was obtained

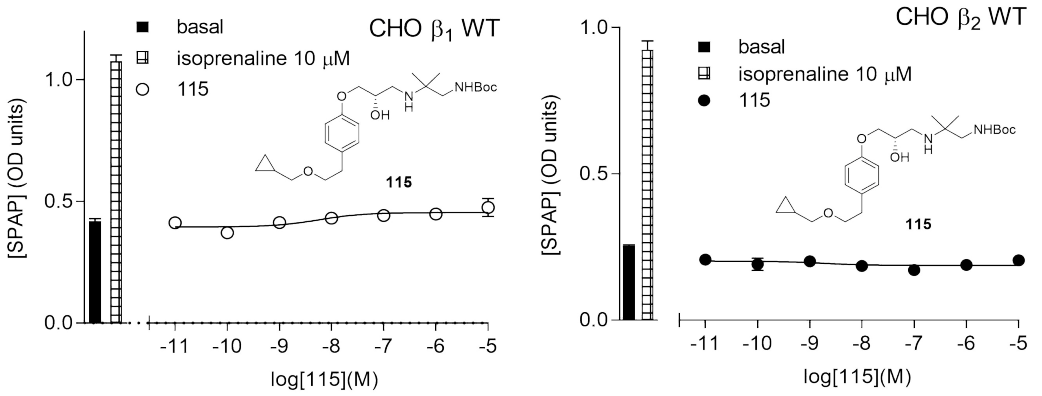

FIGURE 6.6: CRE-SPAP production in response to compound **115** in CHO-β_1 and -β_2 cells. Data points were obtained in triplicate and represent mean ± S.E.M. from a single experiment.

through the shift of CGP12177 (an agonist at the secondary conformation of the β_1-AR) response curve. Figure 6.7 shows CRE-SPAP production in response to either cimaterol or CGP12177 in the presence and absence of a fixed concentration of **115** in both CHO-β_1 and CHO-β_2 cells. A $logK_D = -8.82 \pm 0.08$, n=5 was obtained for analogue **115** using cimaterol as an agonist at β_1-AR. This value is consistent with the value obtained from radioligand binding assays and previously mentioned ($logK_D\beta_1 = -8.93$). Analogue **115** required a higher concentration to rightshift CGP12177 response at β_1 as observed in figure 6.7 where a fixed concentration of 100 nM of **115** produced a lower shift to CGP12177 response than 30 nM of **115** to cimaterol response. Therefore, a $logK_D = -7.26 \pm 0.12$, n=5 was obtained for **115** using CGP12177 as an agonist for the secondary conformation of the β_1-AR. At β_2-AR, $logK_D$ values obtained for **115** using cimaterol as an agonist ($logK_D = -8.19 \pm 0.03$, n=4) and CGP12177 as an agonist ($logK_D = -7.90 \pm 0.14$, n=5) were identical. These values were also in agreement with the $logK_D$ value obtained from radioligand competitive binding ($logK_D\beta_2 = -7.93$).

$LogK_D$ values for racemic betaxolol obtained by the righshift of cimaterol and CGP12177 responses in CHO-cells expressing the human β_1-AR have been described in the literature by Baker et al.[35] In that article a system expressing a luciferase cAMP reporter gene was used instead of a SPAP cAMP reporter gene to determine these $logK_D$ values. That system yielded similar values to those obtained by the CRE-SPAP system as can also be seen in the article mentioned: a $logK_D = -9.61$ was obtained for CGP20712A using cimaterol as an agonist in CHO-β_1-luciferase cells while a $logK_D = -9.82$ was obtained for CGP20712A using cimaterol as an agonist in CHO-β_1-SPAP cells; a $logK_D = -7.09$ was obtained for CGP20712A using CGP12177 as an agonist in CHO-β_1-luciferase cells while a $logK_D = -7.66$ was obtained for CGP20712A using CGP12177 as an agonist in

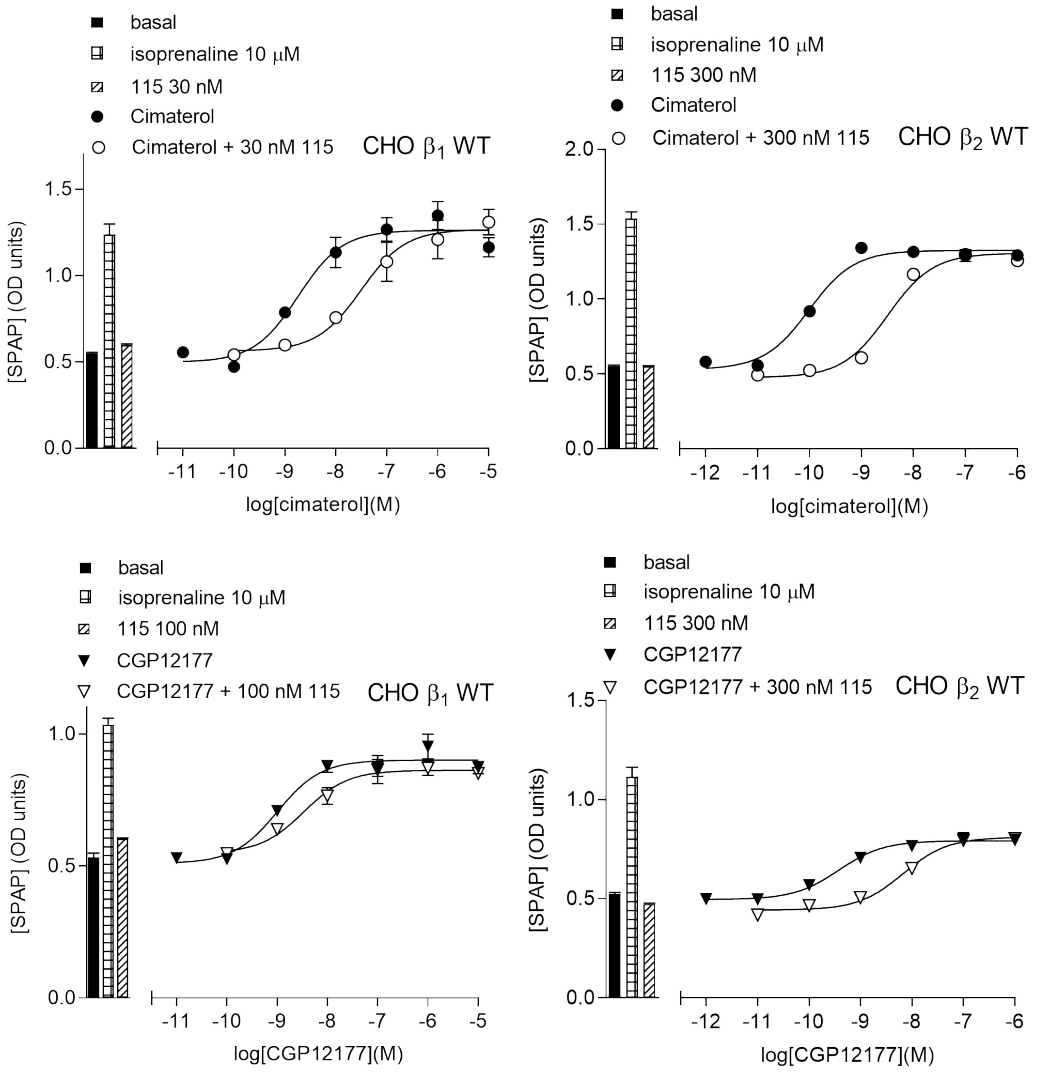

FIGURE 6.7: (Left) CRE-SPAP production in response to increasing concentrations of CGP12177, an agonist at the secondary conformation of the β_1-AR, in the absence and presence of a fixed concentration of **115** in CHO-β_1 and -β_2 cells. (Right) CRE-SPAP production in response to increasing concentrations of cimaterol, an agonist at the primary conformation of the β_1-AR, in the absence and presence of a fixed concentration of **115** in CHO-β_1 and -β_2 cells. Data points were obtained in triplicate and represent mean ± S.E.M. from a single experiment.

CHO-β_1-SPAP cells. [35] It is therefore reasonable to compare the affinity of betaxolol obtained from CRE-luciferase system to that obtained here in the CRE-SPAP system. A $logK_D = -8.87$ was described for betaxolol in CHO-β_1-luciferase cells using cimaterol as an agonist, while a $logK_D = -5.73$ was obtained using CGP12177 as an agonist in the same system. [35]

Betaxolol showed a difference between affinities of 3.14 log units while analogue **115**

exhibited a much lower difference of 1.56 log units. This is mainly due to an increase in affinity for the secondary conformation of the β_1 for **115** when compared to the affinity obtained for betaxolol ($logK_D$ of -7.90 vs -5.73 using CGP12177 as agonist). This decrease in selectivity towards the primary conformation of the β_1-AR is undesirable and might indicate that the linker chosen increases the affinity for the secondary conformation of the β_1-AR and, therefore, reduces the difference between affinities for the primary and secondary conformation.

6.3 Conclusion

A potential photocovalent antagonist probe has been synthesised. This probe was based on betaxolol most active *(S)*-configuration and contains a diazirine photoreactive moiety connected to the pharmacophore by a linker. Preliminary pharmacological characterisation of intermediate **115** containing betaxolol pharmacophore and the linker was also described. **115** was able to bind with higher affinity than betaxolol to the primary conformation of the β_1-AR in radioligand competitive binding assays, showing some selectivity for β_1 over β_2-AR. This ligand exhibited a negligible increase in CRE-SPAP accumulation at the β_1-AR as desired. Compound **115** rightshifted cimaterol mediated response with a K_D value similar to that obtained through radioligand competitive bindind assays and required higher concentration to rightshift CGP12177 mediated response at β_1-AR, as expected. However, the K_D value obtained through the inhibition of CGP12177 for the secondary conformation of the β_1-AR was significantly higher than that obtained for betaxolol. A significantly lower difference in affinities between conformations for **115** was observed (1.56 vs 3.14 log units for betaxolol) which might indicate that the linker chosen increases the affinity for the secondary conformation. This might translate in an undesirable reduction of concentration assay window for the final analogue **107** caused by the linker moiety. Future work will include the photophysical and pharmacological characterisation of **107** and will be discussed in further detail in the next chapter.

Chapter 7

General discussion, conclusions and future work

7.1 General discussion

Endogenous catecholamine agonists adrenaline (**1**) and noradrenaline (**2**) bind to the endogenous orthosteric binding site and mediate a response through the β_1-AR thus causing cardiostimulation. Blockade of these responses with β-blockers (eg. propranolol) is an essential clinical treatment in several heart diseases (eg. myocardial infarction, hypertension). [115] Propranolol, bisoprolol, atenolol and a plethora of β-blockers are able to bind to the orthosteric binding site and antagonise the response mediated by these endogenous catecholamines at low concentrations. Other ligands (eg. CGP12177 **16**, carvedilol **13**), while able to antagonise the catecholamine response at low concentrations also stimulated partial agonist effects at higher concentrations that they required to bind the receptor. These ligands which are able to stimulate a response at much higher concentrations than they require to bind the receptor have been referred in the literature as non-conventional partial agonist.[36] Further investigation of this phenomenon led to the confirmation that this non-conventional partial agonism was mediated through the β_1-AR.[116] Therefore, the existance of two agonist conformations of the β_1-AR was proposed: a primary conformation where the endogenous catecholamines adrenaline (**1**) and noradrenaline (**2**) bind to the endogenous orthosteric binding site and activate the receptor; and a secondary conformation through which CGP12177 is able to stimulate a response which is more resistant to antagonism by the conventional β-blockers. [36] Several ligands other than CGP12177 were found to stimulate a response through this conformation. Alprenolol, oxprenolol and pindolol were able to mediate a response through both of the conformations, even though they required much higher concentration

to mediate a response through the secondary conformation, while carvedilol, similarly to CGP12177, behaved as an antagonist at lower concentration and as an agonist (through the secondary conformation) at higher concentrations. Further studies of this conformation were described using the radiolabelled [^3H] CGP12177 and the fluorescent analog of CGP12177 (BODIPY-TMR-CGP, **22**) to probe this conformation which precise nature is still unknown.[65, 74] Baker *et al* studied the effect of TM swap with the β_2-AR (which does not show this phenomenon of non-conventional agonists) and point mutations across the receptor.[64, 66] This study led to the identification of key residues for this secondary conformation (Val$^{4.56}$, Leu$^{4.62}$ and Trp$^{4.66}$) even though it is not known how they influence or abolish this agonist secondary conformation of the β_1-AR.[66] Mutation of key residues for binding to the orthosteric site (Asp$^{3.32}$, Asn$^{7.39}$) also showed a major influence in the affinity to the secondary conformation.[64] Thus, in order to better understand this conformation, several analogues of alprenolol and oxprenolol were synthesised and pharmacologically characterised in CHO cells to identify which chemical features of these ligands influence their affinity and are able to activate the secondary conformation of the β_1-AR.

During this work, the CHO-β_1 and CHO-β_2 expressing either the human β_1-AR or the human β_2-AR together with a CRE-SPAP reporter gene were used. These cells lines were validated and it was clearly demonstrated that this phenomenon can be observed in these cell lines (Chapter 2). β_1-selective ligands (eg. CGP20712A **19**) showed higher affinity in CHO-β_1 cells, while β_2-selective ligands (eg. ICI118551 **21**) showed higher affinity in CHO-β_2 cells.

Cimaterol was able to mediate a response through both receptors, as expected, and these responses were easily inhibited by either the β_1-selective antagonist CGP20712A in CHO-β_1 cells or by the β_2- selective antagonist ICI118551 in CHO-β_2 cells.[35] The logK_D values derived for both CGP20712A and ICI118551 from inhibition of cimaterol response in CRE-SPAP functional assays were similar to the values derived from the radioligand competitive binding assays for both β_1 and β_2-AR, which suggests that cimaterol response at the β_1-AR is mediated through the primary conformation.

CGP12177 (**16**) behaved as a non-conventional partial agonist, showing a higher affinity for the β_1-AR but requiring a much higher concentration to stimulate a response in CRE-SPAP functional assays (logEC_{50} > logK_D). The response stimulated by CGP12177 in this receptor was also more resistant to antagonism by CGP20712A (**19**), suggesting that this response is mediated through the secondary conformation as described in the literature.[36, 35, 64] At the β_2-AR, CGP12177 (**16**) behaved as a partial agonist stimulating a response with a logEC_{50} similar to the logK_D derived from the binding studies, thus showing that this behaviour is specific for the CHO-β_1 cells.

Alprenolol (**6**) and oxprenolol (**7**) stimulated a response best described by a biphasic concentration-response curve with two components in CHO-β_1 cells. The first component of this response, with a logEC_{50} similar to the logK_D derived from binding studies, was easily inhibited by CGP20712A suggesting that this response is mediated through the primary conformation of the β_1-AR. The second component of the response, which required a much higher concentration of ligand, was more resistant to antagonism by CGP20712A, suggesting that both ligands are able to stimulate a response through both the primary and secondary conformation of the β_1-AR.

The chemical features of alprenolol and oxprenolol responsible for their affinity and stimulation of the secondary conformation were investigated to complement an ongoing study on the chemical features of CGP12177 (**16**) and pindolol responsible for stimulation of a response through this conformation. Initially, several ligands containing different substituents in the *N*-end of the ligand (other than the *N-iso*-propyl seen in the parent compounds alprenolol and oxprenolol) were synthesised and pharmacologically characterised (Chapter 3). Most of the substituents introduced in the amine end of oxprenolol and alprenolol structures led to a decrease in affinity for both receptors, with the exception of *tert*-butylamino (**44b, 47b**) and (3,4-dimethoxyphenethyl)amino groups (**44k, 47k**). While most of compounds retained the 10-fold selectivity for β_2-AR seen in the parent compounds, the (3,4-dimethoxyphenethyl)amino analogues increased β_1 affinity turning these compounds non-selective ligands as described in the literature. [86] Interestingly, oxprenolol *bis* analogue (**49a**) showed an increase in selectivity for the β_2-AR. Evaluation of the individual isomers **78b** and **82b** and meso isomer **83b** of **49a** shows that this increase in β_2-selectivity is only observed for the ligands containing a *(S)*-chiral centre. Recently, Geiser *et al* probed a metastable binding site, previously identified on computational studies with alprenolol, on the β_2-AR.[**?** 117] In this work, Geiser synthesised symmetric homobivalent bitopic ligands based on alprenolol and identified the second aromatic core as a key moiety to increase the affinity for this receptor.[118] While unlikely due to the proximity of the two aromatic cores units, this would explain the increase in affinity seen for the β_2-AR for oxprenolol *bis* ligand **49a**.

tert-Butylated alprenolol and oxprenolol (**47b, 44b**) analogue, (3,4-dimethoxyphenethyl) amino alprenolol analogue (**47k**) and the *N*-cyclopentyl alprenolol analogue (**47i**) were able to clearly mediate a response best described by a biphasic concentration-response curve with a first component easily inhibited by CGP20712A. Similarly to alprenolol and oxprenolol, these ligands seem to stimulate a response at both conformation of the β_1-AR. In order to determine the affinity of all these compounds for both conformations of the β_1-AR, their capacity to inhibit a response mediated through the primary conformation (cimaterol mediated response) versus a response mediated through the secondary conformation (CGP12177 mediated response) was evaluated. The logK_D obtained from

cimaterol response inhibition was similar to the logEC_{50} obtained for the first component of the biphasic response (and to the logK_D obtained from radioligand competitive binding), while the logEC_{50} obtained for the second component of the response was similar to the logK_D derived from the rightshifting of CGP12177 mediated response, once again suggesting that they are able to activate both conformations. Overall, most ligands showed similar selectivity for the primary conformation to the parent compounds. Several ligands showed a quite low affinity for the secondary conformation suggesting that, even if they were able to stimulate a response through the secondary conformation, this response might not be detected in the CRE-SPAP functional assays as a maximum concentration of 10 μM was used. Interestingly, both alprenolol and oxprenolol *N*-benzyl analogues (**44j, 47j**) showed a much lower selectivity for the primary conformation than the parent compounds. Alprenolol *N*-benzyl analogue (**47j**), but not oxprenolol *N*-benzyl analogue (**44j**) was even able to mediate a response resistant to antagonism by CGP20712A, suggesting that this response is mediated through the secondary conformation. Similarly, alprenolol and oxprenolol *bis* analogues **49b** and **49a** showed an increase in affinity for the secondary conformation compared to the parent compounds while their affinity for the primary conformation decreased, thus leading to a marginal selectivity towards the primary conformation of the β_1-AR. It is noteworthy to mention that the 0.34 log units difference (Table 3.6) in affinities observed for the alprenolol *bis* analogue **49b** may suggest that this ligand is not able to differentiate between CGP12177 and several conventional agonists. LogK_D values obtained through the inhibition of cimaterol response have been shown to be 0.1-0.5 log units off the value obtained through the inhibition of other conventional agonist responses (eg. isoprenaline, adrenaline) both in CHO-β_1-SPAP and CHO-β_1-luciferase cells.[35] Interestingly, the chirality of the second chiral centre does not seem to have a major influence on the affinity for either the primary conformation or secondary conformation, while both alprenolol and oxprenolol *(R,R') bis* enantiomers showed a similar decrease in affinities for both conformations, retaining the small difference in affinities between conformations.

Further *N-tert*-butylated alprenolol analogues containing either a fluoro, chloro, methoxy and methyl substituent in the aromatic core were synthesised and pharmacologically characterised (Chapter 4). Interestingly, the introduction of a substituent at the 6-position of the aromatic ring (except 6-fluoro) led to a marked decrease in affinity for both conformations of the β_1-AR and for the β_2-AR. Fluoro analogues behaved in a similar manner to the parent compound and elicited a biphasic response with a first component easily inhibited by CGP20712A mediated through the primary conformation and a second component. at higher concentrations, more resistant to antagonism. Most of the other ligands from this set behaved as antagonists at both conformations of the β_1-AR. Interestingly, affinities for the primary and secondary conformation seem to correlate

for this set, the affinity obtained from the secondary conformation through the inhibition of CGP12177 response decreases or increases in agreement with the changes observed for the affinity obtained for the primary conformation.

bis Alprenolol ligand **49b** was identified as the most interesting ligand from the previous sets (mediated a response presumably through the secondary conformation, more resistant to antagonism, and showed similar affinities for both conformations), thus further modifications to this compound were made to identify the chemical feature responsible for this behaviour (Chapter 5). The second phenoxy moiety of these analogues was identified as a key feature to increase the affinity for the secondary conformation of the β_1-AR, while removal of the second hydroxyl group did not have a major influence.

A potential irreversible antagonist based on betaxolol was also synthesised in an attempt to use this probe to block the primary conformation and study its impact on the secondary conformation of the β_1-AR.

7.2 Conclusions and future work

Several sets of alprenolol and oxprenolol analogues were synthesised and pharmacologically tested in CHO-β_1 and CHO-β_2 cells. The influence of the chemical moieties on their behaviour was assessed. Ligands with distinct behaviours were identified. Several compounds (eg. fluoro analogues **62b** and **70d**) behaved as agonists at both the primary and secondary conformation of the β_1-AR, similarly to the parent compounds (alprenolol and oxprenolol), eliciting biphasic response with a second component more resistant to antagonism. Other ligands (eg. methyl analogues **62e**, **68c**, **70c**) behaved as antagonists at both conformations, similarly to CGP20712A, even though all required a higher concentration to inhibit CGP12177 response mediated through the secondary conformation. Compounds that behave similarly to CGP12177 were also identified. *bis* Alprenolol ligands (**86**, **95a**) were able to mediate a response through the secondary conformation, more resistant to antagonism by CGP20712A. However, contrary to CGP12177, these analogues showed similar affinities for both conformations. The second 2-allylphenoxy moiety of these analogues was identified as a key feature to increase the affinity but also to activate this secondary conformation. Interestingly, a very small structural difference as seen for alprenolol *N*-benzyl analogue **47j** versus oxprenolol *N*-benzyl analogue **44j** can have a major influence in the behaviour of these ligands. Even though CRE-SPAP assays correlate quite well with direct cAMP assays, this should be confirmed in the direct measurement of cAMP in [^{3}H]cAMP accumulation assays, while a kinetic study could also be useful.

Further studies are necessary to understand why these *bis* analogues did not differentiate between the primary and secondary conformation of the β_1-AR. While it is not quite clear if the mutations in the thermostabilised turkey receptor used for x-ray structure determination are able to abolish this secondary conformation, a ligand-bound x-ray structure, even though unrealistic, would shed some light on the extra interactions made by these ligands. Nevertheless, molecular dynamic studies could also be useful. It would also be of interest to study the pharmacology of these *bis* ligands at the mutated receptors, previously identified, known to impact the secondary conformation and abolish CGP12177 non-conventional response.

A reduced number of *bis* compounds analogues were synthesised therefore, synthesis of several analogues with different modifications in the second aromatic core may help shed some light on the importance of the phenoxy moiety. Currently, *bis* ligands with distinct aromatic cores based on propranolol and pindolol are also being evaluated for the secondary conformation of the β_1-AR.

Several possible explanations for this secondary conformation have been described in the literature, from an extended binding pocket upon a first ligand binding event to a negative cooperativity effect across two receptor units in an homodimer.[119, 74] As most of these events could show probe-dependence, the use of an irreversible antagonist with a high selectivity for the primary conformation over the secondary could prove useful.

Chapter 8

Experimental

8.1 Pharmacology

8.1.1 Materials

CHO-CRE SPAP cells, CHO-β_1-SPAP and CHO-β_2-SPAP cells were a kind gift from Dr Jillian G. Baker. Cell culture hardware was purchased from Fisher Scientific (Loughborough, UK) and all medium reagents, including phosphate-buffered saline (PBS), were from Sigma Aldrich (Gillingham, UK). Fetal calf serum (FCS) was from PAA Laboratories (Teddington, Middlesex, UK). [^{3}H] CGP12177 was obtained from GE Healthcare (Chalfont St. Giles, Buckinghamshire, UK). Isoprenaline, cimaterol, ICI118551, CGP20712A and bisoprolol were purchased from Tocris Life Sciences (Avonmouth, UK). Propranolol, CGP12177, the remaining ligands, reagents using during assays (eg. diethanolamine, *para*-nitrophenylphosphate) and other cell culture reagents were from Sigma Chemicals (Poole, Dorset, UK). Racemic ligands were used throughout.

8.1.2 Cell culture

Chinese hamster ovary (CHO) cells lines were used throughout this thesis. Chinese hamster ovary (CHO) cells stably expressing the human recombinant β_1-AR (CHO-β_1 WT) and a reporter gene, Secreted Placental Alkaline Phosphatase (SPAP) under the transcriptional control of a six cAMP response element (CRE) were used. CHO cells expressing the human recombinant β_2-AR (CHO-β_2 WT) together with CRE-SPAP or the reporter gene alone (CHO CRE-SPAP) were also used in this study. [83, 66] Cell culture techniques were perfomed in class II laminar flow cell culture hoods. Cells were maintained in 75 cm^2 tissue culture treated flasks (T75s) in Dulbecco's modified Eagle's

medium nutrient mix F12 (DMEM/F12) containing 10% fetal calf serum (FCS) and 2 mM L-glutamine in cell culture incubators in a 5 % CO2/ 95 % air atmosphere. To avoid strees to the cells, cell culture solutions and medium were pre-warmed to 37 °C in a water bath. Cells were returned to the cell culture incubator (37 °C, 5 % CO2/95 % air atmosphere) after each experimentation, allowing cells to grow and adhere to the T75s until next experimentation.

8.1.2.1 Passaging of cells

The media was removed from 75 cm^2 tissue culture treated flasks (T75s) where the cells used in these experiments were generally maintained. 5-10 ml of phosphate buffered saline (PBS) were added to wash the cells and remove any serum still remaining in T75s and then removed. Next, 1 ml of trypsin was added in a manner that covered completely the cells in the flask and was incubated for 4 minutes at 37 °C in a 5% CO2 atmosphere to dislodge the cells from the bottom of the flask. Trypsin, a serine protease, hydrolyses proteins that facilitate the adherence of the cells to the flasks. 10 ml of media were added to universals (2 for each cell line used) and 7 ml of media were added from one of the universals to T75s. The walls of the T75s were washed until all cells were in the media and then the media was transferred back into the universal. Then, cells were pelleted through centrifugation at 1000 rpm for 4 minutes. The media was removed from the universal leaving the pellet of cells behind. Around 1 ml of media from the other universal was used to break down the pellet of cells into the media and transferred back into the universal. Cells were resuspended in the 10 ml and mixed resulting in a 1:10 dilution. The required number of T75 flasks were set up and 20 ml of media were added to each of them. 1 ml of the cell resuspension was added to each of the flasks previously set up which were used for experiments in the following week.

8.1.2.2 Seeding cells into 96-well plates

The media was removed from T75 and the cells were washed with 5 ml of PBS and then removed. Then, 1 ml of trypsin was added and cells were incubated for 4 minutes at 37 °C in a 5% CO2 atmosphere . Two universals were used for each cell line used, one with 10 ml of media and the other with 6 ml. 7 ml were removed from the universal containing 10 ml and added to the T75s until the cells were suspended in the media. Then, the media was transferred back into the universal and cells were pelleted through centrifugation at 1000 rpm for 4 minutes. The media was removed from the universal leaving the pellet behind and the cells were resuspended in 6 ml of media resulting in a

1:6 dilution. 1 ml of the suspension was added to 10 ml of media (per plate) and 100 μM of that were added into each well of a 96-well plate.

8.1.3 Radioligand experiments

During the day before the experiment, cells were plated into white 96-well plates and were allowed to grow to confluence. Propranolol, ICI118551, CGP12177, cimaterol, salmeterol, CGP20712A, salbutamol, bisoprolol and bucindolol were commercially available. Compounds described in chapter 3-6 were synthesised and concentrations used were made up from a stock solution of 10^{-2}M dissolved in DMSO (and stored this way).

8.1.3.1 Saturation binding assays

Immediately before the experiment, the media was removed from each well. For saturation binding assays, 100 μL of serum-free media (DMEM/F12 with 2 mM L-glutamine) were added to the upper half of the plate, while 100 μL of a 20 μM solution (10 μM in the plate as this method requires a 1:2 dilution) of propranolol in serum-free media were added to the bottom half of the plate. 12 solutions with increasing concentrations of [^3H] CGP12177 in serum-free media were prepared, one for each row of the plate (quadriplicate determinations). Then, 100 μL of serum-free media containing [^3H] CGP12177 were added to each row of wells, starting with the lowest concentrated solution in the far left row. The plates were incubated for 2 hours at 37 °C in a 5% CO2 atmosphere. After that, the media was removed from each well, the wells were washed twice with 200 μL of cold PBS/well that was then removed. 100 μL of Microscint 20 were added to each well and a sealant film was placed over the wells. The plates were counted on the next day on a Topcount (PerkinElmer) 2 min/well. The concentration of each used solution of [^3H] CGP12177 in serum-free media was determined by adding 50 μL of the solution, 500 μL of imidazole and 5 ml of scintillation fluid to 3 scintillation vials. These vials were counted on Packard scintillation counter with single 3H count, 3 minutes per vial. The disintegrations per minute obtained were then converted to concentration values (ranging from 0.012 to 36 nM).

8.1.3.2 Radioligand competitive binding experiments

For competitive binding studies, the media was also removed previously from each well. 100 μL of the competing ligand solution in serum-free media (each concentration of competing ligand solution was made in triplicate) were added followed by addition of 100 μL [^3H] CGP12177 solution in serum-free media. The first row of each plate was used to

measure total and non specific binding by adding 100 μL of serum-free media or a 10 μM solution of propranolol in serum-free media, respectively. The plates were incubated for 2 hours at 37 °C in a 5% CO2 atmosphere. As described in the saturation binding, the media was removed and each well was washed twice with cold PBS. 100 μL of scintillation fluid were added to each well and the plated were counted the following day on Topcount. The concentration of the $[^3H]$ CGP12177 solution in serum-free media was determined by the protocol described in the saturation binding subsection. Concentrations of $[^3H]$ CGP12177 ranging from 0.10 and 2 nM were used during the radioligand competitive binding experiments. These concentrations prevent binding of $[^3H]$ CGP12177 to the secondary conformation of the β_1-AR.

8.1.4 CRE-mediated SPAP transcription assay

Chinese hamster ovary (CHO) cells stably expressing a CRE-SPAP reporter gene construct alone, or together with either the human recombinant β_1-AR or the human recombinant β_2-AR were used. In the cells used throughout the experiments, the SPAP gene was under the control of a cAMP response element, thus increasing SPAP transcription in the presence of cAMP.[83] This assay have been previously used in the study of β-ARs by Baker *et al* as a downstream measurement of cAMP production upon receptor activation. [34]

Initially, two days before the experiment, cells were platted in 96-well plates and allowed to grow to confluence (as described in *Seeding cells into 96-well plates*, one T75 was used to plate around six 96-well plate). In the following day, the growth medium was removed from the wells using a sterile pipette tip connected to a vacuum pump in the laminar flow cell culture hood. Serum-free media (100 μL of media DMEM/F12 supplemented only with 2 mM L-glutamine but not with FCS) were added to the wells and the plates were returned to the cell culture incubator. This process of serum starving minimises cAMP production which is stimulated by the growth medium containing FCS, thus reducing interference in the SPAP gene transcription assay.

8.1.4.1 Agonist mode

On the day of the experiment, all agonist drugs were made up in serum-free media to 10 times final required concentrations from the 10^{-2}M stock solution in DMSO as the experimentation uses a 1:10 dilution in well (10 μL addition to 100 μL in well). Serum-free medium was removed from each well and replaced with 100 μL of serum-free medium and then 10 μL of increasing concentrations of agonist were added to the wells (triplicate determinations for each concentration). Six wells were used as negative control

(only containing serum-free medium), while six wells were used as a positive control (10 μL of a 100 μM isoprenaline solution were added to give a final concentration of 10 μM). Following the addition of the agonist to the wells, the plates were incubated for 5 hours in a humidified atmosphere of 5 % CO2/95 % air at 37 °C. After 5 hours, the media was removed from every well and replaced by 40 μL of previously warmed fresh serum-free media and incubated again for a further hour to collect the secreted placental alkaline phosphatase, which is heat resistant. After one hour, the plates were placed for 30 minutes in a pre-heated open air oven at 65 °C to denature any undesirable endogenous alkaline phosphatases. After 30 minutes the plates were then cooled to 37 °C and the phosphatase activity was measure through addition of 100 μL of 5 mM *para*-nitrophenylphosphate (p-NPP) in diethanolamine (DEA) buffer (280 mM NaCl, 0.5 mM $MgCl_26H_2O$, 100 mM DEA, pH 9.85) to each well. Under alkaline conditions, SPAP, a phosphatase, hydrolyses the phosphate group of p-NPP yielding a yellow *para*-nitrophenol. The plates were placed in a normal atmosphere incubator until the colour change from pink to yellow was observed (approximately 20 minutes). Once the yellow colour developed, absorbance was read at 405 nm using an MRX plate reader (Dynatech Labs, Chantilly, VA) to quantify the CRE-SPAP activity. Activity was measured as optical density (OD) readings with higher readings corresponding to higher levels of *para*-nitrophenol and therefore higher concentration of SPAP resulting from higher concentrations of cAMP.

8.1.4.2 Antagonist mode

The antagonist mode allows the determination of the affinity of antagonist and partial agonists. Agonist concentration-response curves were obtained in the presence and absence of a fixed concentration of antagonist or partial agonist. Solutions of a fixed concentration of antagonists or partial agonists were made up in serum-free media to the final concentration from a 10^{-2}M stock solution in DMSO and the increasing concentrations of agonist drugs were made up in serum-free media with 10 times the final required concentration (1:10 dilution in the well). Initially, on the day of the experiment, serum-free media was removed from the wells and replaced by either 100 μL of serum-free media (agonist alone wells and control) or 100 μL of a fixed concentration of an antagonist or a partial agonist (agonist + antagonist; agonist + partial agonist; antagonist/partial agonist control). The plates were incubated for 1 hour at 37 °C in a 5 % CO2/95 % air atmosphere. Then, 10 μL of 100 μM isoprenaline was added to six wells (positive control) and 10 μL of increasing agonist concentrations (1:10 dilution) were added to wells containing only 100 μL (agonist response alone, triplicate determinations for each concentration) and wells containing 100 μL of a fixed concentration of antagonist/partial agonist (agonist response + fixed concentration of antagonist/partial agonist, triplicate

determinations for each concentration). Increasing concentrations of agonist were not added to several wells (six negative controls, serum-free media without agonist; three fixed concentration of antagonist/partial agonist controls without agonist). Following the addition of agonist drug concentrations, the procedure for the *Agonist mode* previously described was used.

8.1.5 Data analysis

8.1.5.1 Radioligand experiments

Curves of the specific binding (SB) of $[^3H]$ CGP12177 at different concentrations of the $[^3H]$ ligand were fitted using the nonlinear regression program Graphdpad prism 8 to the equation:

$$SB = \frac{[A] \times B_{max}}{[A] + K_D} \tag{8.1}$$

where [A] is the concentration of $[^3H]$ CGP12177, B_{max} is the maximal specific binding, and K_D is the dissociation constant of $[^3H]$ CGP12177. All data are presented as mean ± S.E.M. The n number refers to the number of separate experiments.

In radioligand competitive binding experiments, the concentration required to inhibit 50% of the specific binding (IC_{50}) was determined by fitting the data obtained to the following equation:

$$\%uninhibitedbinding = \frac{(100 - NS)}{([A]/IC_{50} + 1)} \tag{8.2}$$

, where [A] is the concentration of the ligand, NS is the nonspecific binding, IC_{50} is the concentration at which half of the specific binding of $[^3H]$ CGP12177 was inhibited.

The K_D value for the competing ligand can then be obtained through the Cheng-Prusoff equation using the IC_{50} value determined by the previous equation and the fixed concentration of $[^3H]$ CGP12177 used in the experiment:

$$K_D = \frac{IC_{50}}{1 + \frac{[[^3H]CGP12177]}{K_D[^3H]CGP12177}} \tag{8.3}$$

8.1.5.2 CRE-mediated SPAP transcription assay

Agonist mode

Monophasic agonist concentration-response curves were fitted to the equation showed here:

$$Response = \frac{E_{max} \times [agonist]}{[agonist] + EC_{50}} \tag{8.4}$$

E_{max} represents the maximal system response, while [agonist] is the concentration of agonist and EC_{50} represents the concentration that stimulates half of the maximal system response.

Biphasic concentration-response curves were fitted in Graphpad Prism 8 using the following equation:

$$\%maximalstimulation = \frac{[A] \times N}{[A] + EC_{50}1} + \frac{[A] \times (100 - N)}{[A] + EC_{50}2} \tag{8.5}$$

where N is the percentage of the first component response, [A] is the concentration of agonist, and $EC_{50}1$ and $EC_{50}1$ are the concentration which stimulate half of the maximal response for each component.

When increasing concentration of agonist C were added to a fixed concentration of full agonist A (eg. fig. 4.3, chapter 4, cimaterol used as full agonist) the following equation was used to fit the data:

$$Response = Basal + (A_R - Basal)[1 - \frac{[C]}{[C] + IC_{50}}] + C_{max}[\frac{[C]}{[C] + EC_{50}}] \tag{8.6}$$

where Basal is the response produced in the absence of agonist, A_R is the measured response to the fixed concentration of full agonist, [C] is the concentration of agonist C, IC_{50} is the concentration of agonist C required to inhibit the stimulated SPAP production by full agonist A by 50%, C_{max} is the maximal stimulation of SPAP production produced by agonist C, and EC_{50} is the concentration of agonist C required to produce 50% of the maximal stimulation of SPAP secretion produced by C.

Antagonist mode

Agonists in the absence of a fixed concentration of antagonist/partial agonist were fitted either to equation 8.4 or 8.5. The K_D values for the antagonists were determined by the shift observed in the agonists dose-response curves in the absence and presence of a fixed concentration of antagonist, using the following equation (which assumes equilibrium conditions and competitive antagonism):

$$DR = 1 + \frac{[B]}{K_D} \tag{8.7}$$

where DR (dose-ratio) is the dose ratio of concentrations required to stimulate the same response in the absence and presence of a fixed concentration of antagonist [B] and K_D is the equilibrium dissociation constant (figure 8.1, DR = curve 2 EC_{50} / curve 1 EC_{50}). [120]

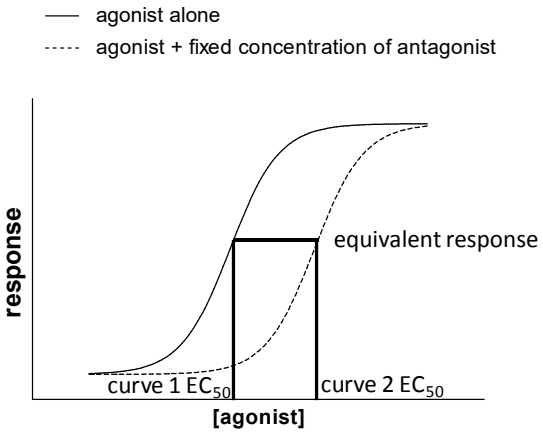

FIGURE 8.1: Schematic representation of two concentration-response curves: curve 1 (agonist concentration-response curve alone, in the absence of a fixed concentration of antagonist) and curve 2 (agonist concentration-response curve alone in the presence of a fixed concentration of antagonist). Modified from Gherbi *et al.* [121]

The K_D values for partial agonists used to rightshift the concentration-response of full(er) agonists were determined by the method of Stephenson *et al.* [85] The data obtained was fitted to the following equation:

$$K_D = \frac{Y \times [P]}{1 - Y} \tag{8.8}$$

, where

$$Y = \frac{[A_2] - [A_1]}{[A_3]} \tag{8.9}$$

[P] is the concentration of partial agonist, $[A_1]$ is the concentration of the full(er) agonist at which the concentration-response curve of the full(er) agonist in the presence and absence of the partial agonist (P) causes the same response, $[A_2]$ is the concentration of the full(er) agonist causing a certain response and $[A_3]$ is the concentration of the full(er) agonist in the presence of a fixed concentration of the partial agonist which causes the same response as $[A_2]$ (Figure 8.2).

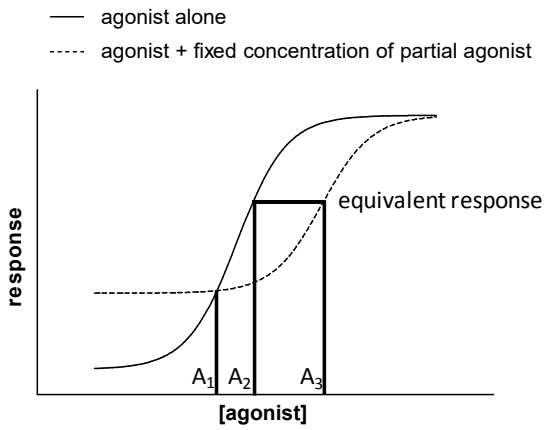

FIGURE 8.2: Schematic representation of two concentration-response curves: curve 1 (agonist concentration-response curve alone, in the absence of a fixed concentration of partial agonist) and curve 2 (agonist concentration-response curve alone in the presence of a fixed concentration of partial agonist). Modified from Gherbi *et al.* [121]

8.2 General chemistry

Chemicals and solvents were purchased from standard suppliers and used without further purification. Merck Kieselgel 60, 230-400 mesh, for flash column chromatography (FCC), was supplied by Merck KgaA (Darmstadt, Germany), and deuterated solvents were purchased from Goss International Limited (England) and Sigma-Aldrich Co. Ltd. (England). Unless otherwise stated, reactions were carried out at ambient temperature. Reactions were monitored by thin layer chromatography on commercially available precoated aluminum-backed plates (Merck Kieselgel 60 F254). Visualization was by examination under UV light (254 and 366 nm). General staining was carried out with $KMnO_4$ or ninhydrin in ethanol for the primary and secondary amines. All organic extracts collected after aqueous workup procedures were dried over anhydrous $MgSO_4$ or Na_2SO_4 before gravity filtration and evaporation to dryness. Organic solvents were evaporated in vacuo at 40 °C (water bath temperature). Purification using preparative layer chromatography (PLC) was carried out using Fluka silica gel 60 PF254 containing gypsum (200 mm x 200 mm x 1 mm). Flash chromatography was performed using Merck Kieselgel 60 (0.040-0.063 mm).

^{1}H NMR spectra were recorded on a Bruker-AV 400 at 400.13 MHz. ^{13}C NMR spectra were recorded at 101.62 MHz. Chemical shifts (δ) are recorded in parts per million (ppm) with reference to the chemical shift of the deuterated solvent/an internal tetramethylsilane (TMS) standard. Coupling constants (J) are recorded in hertz.

LC-MS spectra were recorded on a Shimadzu UFLCXR system coupled to an Applied

Biosystems API2000 and visualised at 254 nm (channel 1) and 220 nm (channel 2). LC-MS was carried out using a Phenomenex Gemini-NX C18 110A column (50 mm x 2 mm x 3 μm) at a flow rate of 0.5 mL/min over a 5 min period (Method A). Analytical reverse-phase high-performance liquid chromatography (RP-HPLC) was performed on a Waters Millenium 995 LC using both system 1 and system 2 described below and was used to confirm that all final products were >95% pure. System 1: Phenomenex Onyx Monolithic reverse phase C18 column (100 x 4.6 mm), a flow rate of 3.00 mL/min and UV detection at 287 nm. Linear gradient 5-95% solvent B over 10 min. Solvent A, 0.1% formic acid (FA) in water; solvent B, 0.1% FA in MeCN. Analytical and semi-prep chiral HPLC was performed using a Phenomenex lux cellulose-1 eluted with a mixture of Hexane:Ethanol:0.2% DEA.

8.2.1 Chapter 3 synthesis

2-allyloxyphenol (40)

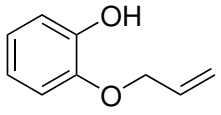

Potassium carbonate (0.044 mol) was added to a solution of pyrocatechol (0.045 mol) in dry acetone (20 mL) in portions for 30 minutes. Then the reaction mixture was left stirring for 1 hour and allyl bromide (0.045 mol) was added over 30 minutes. The potassium carbonate was filtered after completion of the reaction and the filtrate was extracted with chloroform (3 x 75 mL), washed with brine (1 x 50 mL) and dried with anhydrous sodium sulfate. The crude was purified by flash column chromatography over silica gel using eluants of 10% chloroform in petroleum ether.

Yield: 78 % (colorless liquid)

^{1}H NMR (400 MHz, $CDCl_3$) δ 4.64 (dt, J = 5.5, 1.4 Hz, 2H), 5.36 (ddd, J= 10.5, 2.5, 1.2 Hz, 1H), 5.45 (ddd, J = 17.3, 3.0, 1.5 Hz, 1H), 5.71 (s, 1H), 6.11 (ddt, J = 17.2, 10.7, 5.5 Hz, 1H), 6.82 - 6.96 (m, 3H), 6.96 - 7.03 (m, 1H).

2-[[2-(2-propen-1-yloxy)phenoxy]methyl]-oxirane (42)

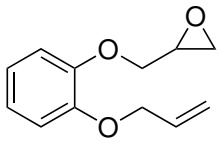

To a solution of 2-allyloxyphenol (0.012 mol) in 40 mL DMF was added sodium hydride (0.018 mol, 1.5eq) (60% in mineral oil) at 0 °C. The reaction mixture was warmed to room temperature and epichlorhydrin (0.060 mol, 5 eq) was added dropwise over 2 minutes. The reaction was monitored

by TLC and reacted during the weekend. After starting material was consumed, the mixture was poured into ice water (50 mL) and extracted with diethyl ether (3 x 75 mL). The reaction mixture was concentrated and it was purified by column chromatography with 12% ethyl acetate in petroleum ether.

Yield: 89 % (colorless liquid)

^{1}H NMR (400 MHz, $CDCl_3$) δ 2.75 (dd, J = 5.0, 2.7 Hz, 1H), 2.83 - 2.94 (m, 1H), 3.33 - 3.47 (m, 1H), 4.04 (dd, J = 11.4, 5.4 Hz, 1H), 4.25 (dd, J = 11.4, 3.4 Hz, 1H), 4.56 - 4.65 (m, 2H), 5.27 (dd, J = 10.5, 1.5 Hz, 1H), 5.42 (dd, J = 17.3, 1.6 Hz, 1H), 6.08 (tdd, J = 15.8, 10.5, 5.3 Hz, 1H), 6.82 - 7.00 (m, 4H).

2-[[2-(2-propen-1-yl)phenoxy]methyl]-oxirane (46)

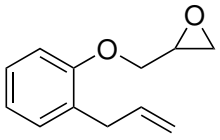

To a stirred solution of 2-allylphenol (0.022 mol, 1 eq) and potassium carbonate (0.033, 1.5 eq) in dry acetone, epichlorohydrin (0.033, 1.5 eq) was added and the reaction mixture was allowed to reflux until all the phenol was consumed. As after 48 hours the phenol was not fully consumed, 1 equivalent of epichlorhydrin and potassium carbonate were added to the mixture. The reaction was controlled by TLC after 5 days and the phenol was consumed. The reaction mixture was filtered, concentrated under vacuo and purified by column chromatography with 8% ethyl acetate in petroleum ether. Yield: 62 % (colorless liquid)

^{1}H NMR (400 MHz, $CDCl_3$) δ 2.78 (dd, J = 5.0, 2.7 Hz, 1H), 2.91 (dd, J = 4.9, 4.2 Hz, 1H), 3.33-3.39 (m, 1H), 3.43 (d, J = 6.6 Hz, 2H), 4.00 (dd, J = 11.1, 5.4 Hz, 1H), 4.24 (dd, J = 11.0, 3.1 Hz, 1H), 5.01-5.12 (m, 2H), 5.93-6.07 (m, 1H), 6.80-6.96 (m, 2H), 7.14-7.24 (m, 2H).

General procedures for epoxide opening:

a) A solution of the respective oxirane (**42** for oxprenolol and **46** for alprenolol analogues) in 1 mL of the respective amine was heated in the microwave at 60 °C (for oxprenolol analogues) or at 70 °C (for alprenolol analogues) for 1 hour. The reaction mixture was checked by TLC. The reaction mixture was purified by column chromatography with percentages ranging from 2% to 6% of 1N ammonia in methanol in dichloromethane as indicated in each compound in the experimental section.

b) A solution of the respective oxirane (**42** for oxprenolol and **46** for alprenolol analogues) in 1 mL of the respective amine was left stirring at room temperature for 72 hours. The reaction mixture was checked by TLC and after the oxirane was consumed it was purified

by column chromatohraphy with eluents of 2% to 6% of 1N ammonia in methanol in dichloromethane as indicated for each case in the experimental section.

c) A solution of the respective oxirane (**42** for oxprenolol and **46** for alprenolol analogues) and the respective amine (2 eq) in 1 mL of hexafluoroisopropanol was heated in the microwave at 70 °C for 1 hour. The reaction mixture was checked by TLC. The reaction mixture was purified by column chromatography with percentages ranging from 2% to 6% of 1N ammonia in methanol in dichloromethane as indicated in each compound in the experimental section.

1-(2-(allyloxy)phenoxy)-3-(isopropylamino)propan-2-ol (Oxprenolol, 7)

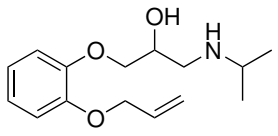

Eluent: 5% 1M ammonia in MeOH in DCM; Method a) Yield: 90 % (colorless oil)

^{1}H NMR (400 MHz, $CDCl_3$) δ 1.12 (d, J = 6.3 Hz, 6H), 2.81 (dd, J = 12.1, 7.1 Hz, 1H), 2.85 - 2.95 (m, 2H), 3.35 (s, 2H), 3.99 - 4.07 (m, 2H), 4.10 (ddt, J = 11.1, 7.0, 4.2 Hz, 1H), 4.57 (dt, J= 5.3, 1.4 Hz, 2H), 5.27 (dd, J = 10.5, 1.4 Hz, 1H), 5.41 (dd,J = 17.3, 1.6 Hz, 1H), 6.07 (ddt, J = 17.2, 10.6, 5.3 Hz, 1H), 6.86 - 6.97 (m, 4H).

^{13}C NMR (101 MHz, $CDCl_3$) δ 22.65, 22.71, 49.33, 68.25, 70.04, 73.06, 114.40, 115.57, 117.85, 121.65, 122.14, 133.50, 148.82, 149.04.

m/z MS (TOF ES+) $C_{15}H_{23}NO_3$[MH]+ calcd 266.17; found 266.2. tR: 2.02 (method A)

1-(2-(allyloxy)phenoxy)-3-(tert-butylamino)propan-2-ol (44b)

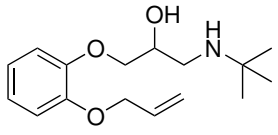

Eluent: 6% 1M ammonia in MeOH in DCM; Method a) Yield: 79 % (yellow oil)

^{1}H NMR (400 MHz, $CDCl_3$) δ 1.13 (s, 9H), 2.76 (dd, J = 11.9, 6.3 Hz, 1H), 2.86 (broad s, 2H, exchangeable protons), 2.87 (dd, J = 11.7, 3.6 Hz, 1H), 3.92 - 4.13 (m, 3H), 4.57 (dt, J = 5.2, 1.5 Hz, 2H), 5.27 (dd, J = 10.5, 1.4 Hz, 1H), 5.41 (dd, J = 17.3, 1.6 Hz, 1H), 6.07 (ddt, J = 17.2, 10.5, 5.3 Hz, 1H), 6.78 - 7.08 (m, 4H).

^{13}C NMR (101 MHz, $CDCl_3$) δ 29.04, 44.84, 50.83, 68.56, 70.05, 72.99, 114.47, 115.37, 117.75, 121.64, 121.99, 133.56, 148.95, 149.01.

m/z MS (TOF ES+) $C_{16}H_{25}NO_3$[MH]+ calcd 280.18; found 280.0. tR: 2.12 (method A)

1-(2-(allyloxy)phenoxy)-3-(cyclopropylamino)propan-2-ol (44c)

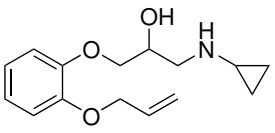

Eluent: 5% 1M ammonia in MeOH in DCM; Method a) Yield: 92 % (yellow oil)

^{1}H NMR (400 MHz, $CDCl_3$) δ 0.36 - 0.43 (m, 2H), 0.43 - 0.49 (m, 2H), 2.16 - 2.24 (m, 1H), 2.90 (dd, J = 12.3, 6.7 Hz, 1H), 2.92 (s, 2H, exchangeable protons), 2.97 (dd, J = 12.3, 4.3 Hz, 1H), 3.98 (dd, J = 9.5, 5.8 Hz, 1H), 4.08 (ddd, J = 13.2, 8.4, 4.0 Hz, 2H), 4.57 (d, J = 5.3 Hz, 2H), 5.28 (dd, J = 10.5, 1.3 Hz, 1H), 5.42 (dd, J = 17.3, 1.5 Hz, 1H), 6.08 (ddt, J = 17.0, 10.6, 5.3 Hz, 1H), 6.92 (qd, J= 7.1, 3.9 Hz, 4H).

^{13}C NMR (101 MHz, $CDCl_3$) δ 6.37, 6.65, 30.59, 51.82, 68.21, 70.02, 73.25, 114.30, 115.53, 117.87, 121.62, 122.10, 133.46, 148.86, 149.05.

m/z MS (TOF ES+) $C_{15}H_{21}NO_3$[MH]+ calcd 264.33; found 264.1. tR: 2.00 (method A)

1-(2-(allyloxy)phenoxy)-3-((cyclopropylmethyl)amino)propan-2-ol (44d)

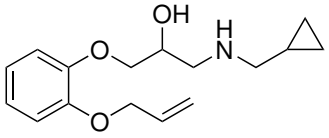

Eluent: 5% 1M ammonia in MeOH in DCM; Method a) Yield: 65 % (yellow oil)

^{1}H NMR (400 MHz, $CDCl_3$) δ 0.19 (q, J= 4.4 Hz, 2H), 0.52 (q, J = 4.4 Hz, 2H), 0.94 - 1.09 (m, 1H), 2.50 - 2.71 (m, 2H), 2.91 (dd, J = 12.2, 7.3 Hz, 1H), 3.00 (dd, J = 12.2, 4.1 Hz, 1H), 3.60 (s, 2H), 4.00 - 4.11 (m, 2H), 4.15 - 4.21 (m, 1H), 4.57 (dt, J = 5.3, 1.4 Hz, 2H), 5.28 (dd, J = 10.5, 1.4 Hz, 1H), 5.41 (dd, J = 17.3, 1.6 Hz, 1H), 6.07 (ddt, J = 17.2, 10.6, 5.3 Hz, 1H), 6.84 - 7.00 (m, 4H).

^{13}C NMR (101 MHz, $CDCl_3$) δ 3.63, 3.71, 10.69, 51.63, 54.81, 68.10, 70.04, 72.96, 114.38, 115.52, 117.87, 121.65, 122.13, 133.48, 148.78, 148.89.

m/z MS (TOF ES+) $C_{16}H_{23}NO_3$[MH]+ calcd 278.36; found 278.1. tR: 2.10 (method A)

1-(2-(allyloxy)phenoxy)-3-(methylamino)propan-2-ol (44e)

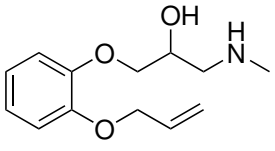

Eluent: 8% 1M ammonia in MeOH in DCM; Method b) Yield: 38 % (yellow oil)

^{1}H NMR (400 MHz, $CDCl_3$) δ 2.52 (s, 3H), 2.88 (t,J = 5.4 Hz, 2H), 3.95 (s, 2H), 4.04 (qd, J = 9.8, 5.1 Hz, 2H), 4.13 - 4.25 (m, 1H), 4.55 (dt, J = 5.3, 1.4 Hz, 2H), 5.28 (dd, J = 10.5, 1.4 Hz, 1H), 5.41 (dd, J = 17.3, 1.6 Hz, 1H), 6.07 (ddt, J = 17.2, 10.6, 5.4 Hz, 1H), 6.91 (qd, J = 7.1, 4.2 Hz, 4H)

^{13}C NMR (101 MHz, $CDCl_3$) δ 36.10, 54.00, 67.77, 70.01, 72.97, 114.25, 115.47, 117.99, 121.65, 122.17, 133.44, 148.70, 148.96.

m/z MS (TOF ES+) $C_{13}H_{19}NO_3$[MH]+ calcd 238.29; found 237.9. tR: 1.88 (method A)

1-(2-(allyloxy)phenoxy)-3-(ethylamino)propan-2-ol (44f)

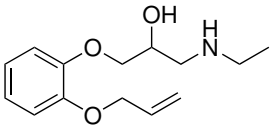

Eluent: 6% 1M ammonia in MeOH in DCM; Method b) Yield: 75 % (colorless oil)

^{1}H NMR (400 MHz, $CDCl_3$) δ 1.14 (t, J =7.1 Hz, 3H), 2.72 (qd, J = 7.1, 1.3 Hz, 2H), 2.85 (qd, J = 12.1, 5.6 Hz, 2H), 3.13 (s, 2H), 4.03 (qd, J = 9.7, 5.1 Hz, 2H), 4.12 (tt, J = 6.9, 4.2 Hz, 1H), 4.57 (d, J= 5.2 Hz, 2H), 5.28 (dd, J = 10.4, 1.0 Hz, 1H), 5.42 (dd, J = 17.2, 1.4 Hz, 1H), 6.07 (ddt, J = 17.1, 10.6, 5.3 Hz, 1H), 6.86 - 7.00 (m, 4H)

^{13}C NMR (101 MHz, $CDCl_3$) δ 15.10, 44.25, 51.73, 68.25, 70.04, 73.12, 114.35, 115.55, 117.89, 121.65, 122.13, 133.46, 148.81, 149.02.

m/z MS (TOF ES+) $C_{14}H_{21}NO_3$[MH]+ calcd 252.15; found 252.0. tR: 1.98 (method A)

1-(2-(allyloxy)phenoxy)-3-(propylamino)propan-2-ol (44g)

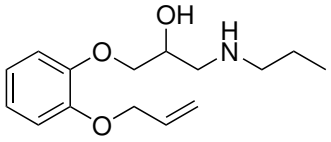

Eluent: 6% 1M ammonia in MeOH in DCM; Method a) Yield: 64 % (yellow oil)

^{1}H NMR (400 MHz, $CDCl_3$) δ 0.92 (t, J = 7.4 Hz, 3H), 1.46 - 1.61 (m, 2H), 2.63 (t, J = 7.1 Hz, 2H), 2.84 (qd, J = 12.2, 5.5 Hz, 2H), 2.95 (s, 2H), 3.89 - 4.21 (m, 3H), 4.57 (dt, J= 5.2, 1.3 Hz, 2H), 5.28 (dd, J = 10.5, 1.4 Hz, 1H), 5.41 (dd, J = 17.3, 1.6 Hz, 1H), 6.07 (ddt, J = 17.2, 10.6, 5.3 Hz, 1H), 6.80 - 7.03 (m, 4H).

^{13}C NMR (101 MHz, $CDCl_3$) δ 11.67, 22.97, 29.71, 51.74, 68.12, 69.92, 73.00, 114.26, 115.44, 117.71, 121.52, 121.99, 133.37, 148.74, 148.92.

m/z MS (TOF ES+) $C_{15}H_{23}NO_3$[MH]+ calcd 266.17; found 266.0. tR: 2.06 (method A)

1-(2-(allyloxy)phenoxy)-3-(butylamino)propan-2-ol (44h)

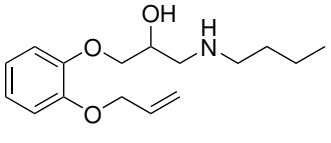

Eluent: 5% 1M ammonia in MeOH in DCM; Method a) Yield: 82 % (yellow oil)

^{1}H NMR (400 MHz, $CDCl_3$) δ 0.91 (t, J = 7.3 Hz, 3H), 1.35 (dq, J = 14.2, 7.1 Hz, 2H), 1.49 (ddd, J = 12.2, 9.0, 7.0 Hz, 2H), 2.65 (td,J = 7.1, 1.4 Hz, 2H), 2.78 (s, 2H), 2.79 - 2.88 (m, 2H), 4.00 (dd, J = 9.5, 6.1 Hz, 1H), 4.05 (t,J = 4.9 Hz, 1H), 4.06 - 4.12 (m, 1H), 4.57 (dt, J = 5.3, 1.4 Hz, 2H), 5.28 (dq, J = 10.5, 1.3 Hz, 1H), 5.41 (dq, J = 17.3, 1.6 Hz, 1H), 6.07 (ddt, J = 17.2, 10.6, 5.3 Hz, 1H), 6.87 - 6.97 (m, 4H).

^{13}C NMR (101 MHz, $CDCl_3$) δ 14.12, 20.53, 32.38, 49.80, 51.95, 68.34, 70.05, 73.18, 114.41, 115.60, 117.81, 121.64, 122.11, 133.51, 148.90, 149.07.

m/z MS (TOF ES+) $C_{16}H_{25}NO_3$[MH]+ calcd 280.18; found 280.2. tR: 2.16 (method A)

1-(2-(allyloxy)phenoxy)-3-(cyclopentylamino)propan-2-ol (44i)

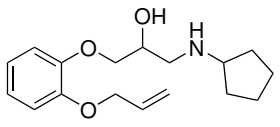

Eluent: 6% 1M ammonia in MeOH in DCM; Method a) Yield: 82 % (colorless oil)

^{1}H NMR (400 MHz, DMSO) δ 1.22 - 1.37 (m, 2H), 1.38 - 1.51 (m, 2H), 1.53 - 1.65 (m, 2H), 1.72 (dt, J = 12.0, 5.9 Hz, 2H), 2.59 (dd, J = 11.8, 6.4 Hz, 1H), 2.73 (dd, J = 11.7, 4.1 Hz, 1H), 2.97 - 3.08 (m, 1H), 3.34 (s, 2H), 3.83 - 3.94 (m, 3H), 4.54 (dt, J = 5.1, 1.5 Hz, 2H), 5.23 (dd, J = 10.5, 1.7 Hz, 1H), 5.40 (dd, J = 17.3, 1.8 Hz, 1H), 6.03 (ddt, J = 17.2, 10.4, 5.1 Hz, 1H), 6.83 - 6.90 (m, 2H), 6.93 - 7.00 (m, 2H).

^{13}C NMR (101 MHz, DMSO) δ 23.55, 32.32, 51.18, 59.23, 68.02, 69.02, 71.61, 114.09, 114.44, 116.98, 120.97, 121.23, 134.01, 148.00, 148.66.

m/z MS (TOF ES+) $C_{17}H_{25}NO_3$[MH]+ calcd 292.39; found 292.2. tR: 2.12 (method A)

1-(2-(allyloxy)phenoxy)-3-(benzylamino)propan-2-ol (44j)

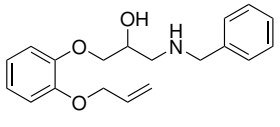

Eluent: 5% 1M ammonia in MeOH in DCM; Method c) Yield: 76 % (yellow oil)

^{1}H NMR (400 MHz, $CDCl_3$) δ 2.78 (s, 2H), 2.85 (qd, J= 12.1, 5.3 Hz, 2H), 3.80 - 3.92 (m, 2H), 4.00 (dd, J = 10.5, 7.0 Hz, 1H), 4.09 (ddd, J = 10.5, 6.2, 3.9 Hz, 2H), 4.54 (dt, J= 5.3, 1.4 Hz, 2H), 5.26 (dd, J = 10.5, 1.4 Hz, 1H), 5.39 (dd, J = 17.3, 1.6 Hz, 1H), 6.03 (ddt, J = 17.2, 10.6, 5.3 Hz, 1H), 6.86 - 6.97 (m, 4H), 7.22 - 7.29 (m, 1H), 7.30 - 7.37 (m, 4H).

^{13}C NMR (101 MHz, $CDCl_3$) δ 51.33, 54.00, 68.50, 69.99, 73.26, 114.32, 115.57, 117.86, 121.62, 122.13, 127.19, 128.27, 128.57, 133.46, 140.07, 148.84, 149.06

m/z MS (TOF ES+) $C_{19}H_{23}NO_3$[MH]+ calcd 314.17; found 314.3. tR: 2.19 (method A)

1-(2-(allyloxy)phenoxy)-3-((3,4-dimethoxyphenethyl)amino)propan-2-ol (44k)

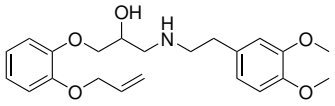

Eluent: 6% 1M ammonia in MeOH in DCM; Method c) Yield: 61 % (yellow oil)

^{1}H NMR (400 MHz, $CDCl_3$) δ 2.72 - 2.82 (m, 4H), 2.86 (dd, J = 8.7, 5.5 Hz, 2H), 2.88 - 2.95 (m, 2H), 3.85 (d, J= 4.4 Hz, 6H), 3.99 (dd,J= 9.5, 6.1 Hz, 1H), 4.04 (t, J = 5.3 Hz, 1H), 4.06 - 4.11 (m, 1H), 4.55 (dt, J = 5.3, 1.4 Hz, 2H), 5.27 (dd, J = 10.5, 1.4 Hz, 1H), 5.40 (dd, J = 17.3, 1.6 Hz, 1H), 6.06 (ddt, J = 17.2, 10.6, 5.3 Hz, 1H), 6.70 - 6.75 (m, 2H), 6.78 (d, J = 8.7 Hz, 1H), 6.86 - 6.96 (m, 4H)

^{13}C NMR (101 MHz, $CDCl_3$) δ 36.00, 51.45, 51.77, 55.96, 56.04, 68.37, 69.99, 73.08, 111.44, 112.10, 114.34, 115.65, 117.81, 120.70, 121.62, 122.18, 132.48, 133.48, 147.59, 148.80, 149.05, 149.07.

m/z MS (TOF ES+) $C_{22}H_{29}NO_5$[MH]+ calcd 388.20; found 388.1. tR: 2.20 (method A)

1-(2-allylphenoxy)-3-(isopropylamino)propan-2-ol (Alprenolol, 6)

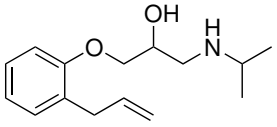

Eluent: 5% 1M ammonia in MeOH in DCM; Method a) Yield: 96 % (colorless oil)

^{1}H NMR (400 MHz, $CDCl_3$) δ 1.11 (d, J = 6.3 Hz, 6H), 2.78 (s, 1H), 2.78 (dd, J = 12.1, 7.6 Hz, 2H), 2.86 (dd,J = 12.6, 6.3 Hz, 1H), 2.92 (dd, J = 12.1, 3.9 Hz, 1H), 3.40 (d, J= 6.4 Hz, 2H), 3.94 - 4.03 (m, 2H), 4.07 (dt, J = 9.0, 5.1 Hz, 1H), 5.03 (dt, J = 16.3, 1.5 Hz, 1H), 5.04 (dt,J = 11.1, 1.3 Hz, 1H), 5.99 (ddt, J = 17.8, 9.1, 6.4 Hz, 1H), 6.85 (d, J = 8.1 Hz, 1H), 6.91 (td, J = 7.4, 0.8 Hz, 1H), 7.15 (d, J= 7.4 Hz, 1H), 7.18 (td,J = 8.0, 1.6 Hz, 1H).

^{13}C NMR (101 MHz, $CDCl_3$) δ 22.80, 22.90, 34.67, 49.08, 49.38, 68.50, 70.52, 111.36, 115.28, 120.95, 127.49, 128.51, 130.06, 137.23, 156.33.

m/z MS (TOF ES+) $C_{15}H_{23}NO_2$[MH]+ calcd 250.17; found 249.9. tR: 2.13 (method A)

1-(2-allylphenoxy)-3-(*tert*-butylamino)propan-2-ol (47b)

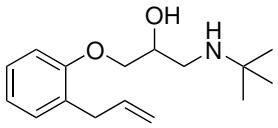

Eluent: 5% 1M ammonia in MeOH in DCM; Method a) Yield: 93 % (yellow oil)

^{1}H NMR (400 MHz, $CDCl_3$) δ 1.16 (s, 9H), 2.77 (dd, J = 11.9, 7.2 Hz, 1H), 2.91 (dd, J = 11.9, 3.7 Hz, 1H), 2.92 (s, 2H, exchangeable protons) 3.40 (d, J = 6.4 Hz, 2H), 3.90 - 4.12 (m, 3H), 5.02 (dd, J = 5.4, 1.7 Hz, 1H), 5.05 (s, 1H), 5.99 (ddt, J = 18.3, 9.4, 6.4 Hz, 1H), 6.85 (d, J = 8.1 Hz, 1H), 6.91 (td, J = 7.4, 0.9 Hz, 1H), 7.14 (dd, J = 7.4, 1.5 Hz, 1H), 7.19 (td, J = 8.0, 1.7 Hz, 1H).

^{13}C NMR (101 MHz, $CDCl_3$) δ 28.90, 34.78, 45.02, 51.26, 68.59, 70.58, 111.48, 115.40, 121.06, 127.61, 128.66, 130.18, 137.33, 156.48

m/z MS (TOF ES+) $C_{16}H_{25}NO_2$[MH]+ calcd 264.19; found 264.2. tR: 2.18 (method A)

1-(2-allylphenoxy)-3-(cyclopropylamino)propan-2-ol (47c)

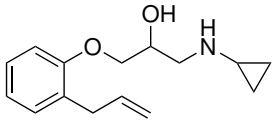

Eluent: 5% 1M ammonia in MeOH in DCM; Method b) Yield: 12 % (colorless oil)

^{1}H NMR (400 MHz, $CDCl_3$) δ 0.33 - 0.43 (m, 2H), 0.43 - 0.52 (m, 2H), 2.16 - 2.24 (m, 1H), 2.59 (s, 2H), 2.88 (dd, J = 12.3, 7.7 Hz, 1H), 2.98 (dd, J = 12.3, 4.0 Hz, 1H), 3.40 (dd,J = 6.3, 1.1 Hz, 2H), 3.98 (d, J = 5.1 Hz, 2H), 4.09 (dt,J = 8.8, 4.9 Hz, 1H), 5.04 (dt, J = 16.4, 1.6 Hz, 1H), 5.05 (dt, J = 11.0, 1.4 Hz, 1H), 5.99 (ddt, J = 15.5, 11.4, 6.4 Hz, 1H), 6.84 (d, J = 8.1 Hz, 1H), 6.92 (td, J = 7.4, 0.9 Hz, 1H), 7.15 (d, J = 7.4 Hz, 1H), 7.18 (td, J= 8.0, 1.7 Hz, 1H).

^{13}C NMR (101 MHz, $CDCl_3$) δ 6.30, 6.76, 30.63, 34.82, 52.01, 68.43, 70.64, 111.51, 115.39, 121.09, 127.61, 128.65, 130.20, 137.39, 156.47.

1-(2-allylphenoxy)-3-((cyclopropylmethyl)amino)propan-2-ol (47d)

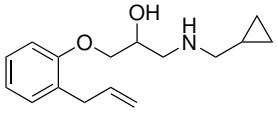

Eluent: 5% 1M ammonia in MeOH in DCM; Method a) Yield: 88 % (colorless oil)

^{1}H NMR (400 MHz, $CDCl_3$) δ 0.15 (q, J = 4.7 Hz, 2H), 0.46 - 0.55 (m, 2H), 0.84 - 1.13 (m, 1H), 2.55 (ddd, J = 26.2, 12.2, 6.9 Hz, 2H), 2.66 (s, 2H), 2.84 (dd,J = 12.2, 7.7 Hz, 1H), 2.94 (dd, J = 12.2, 4.0 Hz, 1H), 3.40 (d, J = 6.3 Hz, 2H), 4.00 (d, J = 5.0 Hz, 2H), 4.12 (td, J = 9.2, 5.1 Hz, 1H), 5.03 (dd, J = 17.9, 1.5 Hz, 1H), 5.04 (dd, J =

10.1, 1.4 Hz, 1H), 5.99 (ddt, J = 18.1, 9.3, 6.4 Hz, 1H), 6.85 (d, J = 8.1 Hz, 1H), 6.92 (td, J = 7.4, 0.7 Hz, 1H), 7.14 (dd, J = 7.6, 1.2 Hz, 1H), 7.19 (td, J= 8.0, 1.6 Hz, 1H).

^{13}C NMR (101 MHz, $CDCl_3$) δ 3.52, 3.59, 11.19, 34.75, 51.90, 55.04, 68.51, 70.67, 111.50, 115.40, 121.07, 127.59, 128.64, 130.15, 137.34, 156.44

1-(2-allylphenoxy)-3-(methylamino)propan-2-ol (47e)

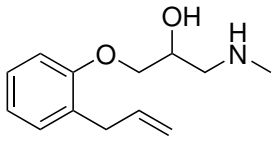

Eluent: 6% 1M ammonia in MeOH in DCM; Method b) Yield: 77 % (yellow oil)

^{1}H NMR (400 MHz, $CDCl_3$) δ 2.49 (s, 3H), 2.59 (s, 2H, exchangeable protons), 2.81 (qd, J = 12.2, 5.8 Hz, 2H), 3.40 (dd, J = 6.2, 1.0 Hz, 2H), 3.99 (d, J= 5.2 Hz, 2H), 4.12 (dq, J = 7.4, 5.0 Hz, 1H), 5.04 (d, J = 10.4 Hz, 1H), 5.04 (d, J = 16.7 Hz, 1H), 5.99 (ddt, J = 14.8, 10.8, 6.4 Hz, 1H), 6.85 (d, J= 8.1 Hz, 1H), 6.92 (t, J = 7.4 Hz, 1H), 7.15 (d, J = 7.4 Hz, 1H), 7.18 (t, J = 7.8 Hz, 1H).

^{13}C NMR (101 MHz, $CDCl_3$) δ 34.71, 36.46, 54.34, 68.30, 70.67, 111.48, 115.37, 121.05, 127.57, 128.58, 130.14, 137.32, 156.40

m/z MS (TOF ES+) $C_{13}H_{19}NO_2$[MH]+ calcd 222.14; found 222.0. tR: 2.00 (method A)

1-(2-allylphenoxy)-3-(ethylamino)propan-2-ol (47f)

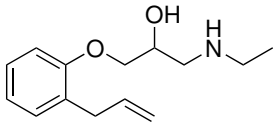

Eluent: 5% 1M ammonia in MeOH in DCM; Method b) Yield: 55 % (yellow oil)

^{1}H NMR (400 MHz, $CDCl_3$) δ 1.18 (t, J = 7.1 Hz, 3H), 2.40 (s, 2H, exchangeable protons), 2.76 (dd, J = 7.1, 4.4 Hz, 2H), 2.84 (dd, J = 12.2, 7.8 Hz, 1H), 2.93 (dd, J = 12.2, 3.9 Hz, 1H), , 3.40 (d,J= 6.4 Hz, 2H), 4.00 (d, J = 5.2 Hz, 2H), 4.14 (td,J = 9.1, 5.0 Hz, 1H), 5.03 (dd, J = 17.3, 1.5 Hz, 2H), 5.04 (dd, J = 10.4, 1.5 Hz, 1H), 5.98 (ddt, J = 17.2, 11.1, 6.4 Hz, 1H), 6.85 (d, J = 8.1 Hz, 1H), 6.92 (t, J = 7.3 Hz, 1H), 7.15 (d, J = 7.4 Hz, 1H), 7.19 (t, J = 7.6, 1H).

^{13}C NMR (101 MHz, $CDCl_3$) δ 15.30, 34.77, 44.28, 51.92, 68.49, 70.66, 111.48, 115.38, 121.07, 127.60, 128.61, 130.17, 137.36, 156.44

m/z MS (TOF ES+) $C_{14}H_{21}NO_2$[MH]+ calcd 236.16; found 236.0. tR: 2.10 (method A)

1-(2-allylphenoxy)-3-(propylamino)propan-2-ol (47g)

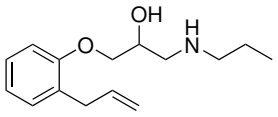

Eluent: 5% 1M ammonia in MeOH in DCM; Method a) Yield: 59 % (yellow oil)

^{1}H NMR (400 MHz, $CDCl_3$) δ 0.94 (t, J = 7.4 Hz, 3H), 1.55 (sx, J = 7.3 Hz, 2H), 2.46 (s, 2H, exchangeable protons), 2.65 (td, J = 7.0, 4.0 Hz, 2H), 2.81 (dd, J = 12.2, 7.7 Hz, 1H), 2.90 (dd, J = 12.2, 4.0 Hz, 1H), 3.40 (d, J = 6.3 Hz, 2H), 3.99 (dd,J = 5.2, 0.9 Hz, 2H), 4.10 (td, J = 9.2, 5.0 Hz, 1H), 5.03 (dd, J = 18.0, 1.2 Hz, 1H), 5.04 (dd, J = 9.6, 1.5 Hz, 1H), 5.99 (ddt, J = 17.8, 9.1, 6.4 Hz, 1H), 6.85 (d, J= 8.1 Hz, 1H), 6.92 (t,J = 7.4 Hz, 1H), 7.15 (d, J = 7.4 Hz, 1H), 7.18 (t, J = 7.8 Hz, 1H).

^{13}C NMR (101 MHz, $CDCl_3$) δ 11.75, 23.12, 34.65, 51.84, 52.13, 68.34, 70.67, 111.43, 115.34, 120.96, 127.50, 128.57, 130.05, 137.25, 156.39.

m/z MS (TOF ES+) $C_{15}H_{23}NO_2$[MH]+ calcd 250.17; found 250.2. tR: 2.16 (method A)

1-(2-allylphenoxy)-3-(butylamino)propan-2-ol (47h)

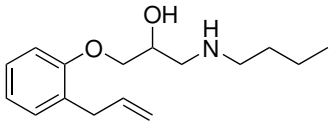

Eluent: 5% 1M ammonia in MeOH in DCM; Method a) Yield: 78 % (colorless oil)

^{1}H NMR (400 MHz, $CDCl_3$) δ 0.93 (t, J = 7.3 Hz, 3H), 1.36 (sx, J= 7.1 Hz, 2H), 1.51 (q, J = 7.2 Hz, 2H), 2.50 (s, 2H, exchangeable protons), 2.60 - 2.73 (m, 2H), 2.80 (dd, J = 12.2, 7.6 Hz, 1H), 2.88 (dd, J = 12.2, 4.0 Hz, 1H), 3.40 (d, J = 5.7 Hz, 2H), 3.99 (dd, J = 5.2, 1.1 Hz, 2H), 4.08 (ddd,J = 9.2, 7.7, 5.1 Hz, 1H), 5.03 (dd, J = 17.2, 1.5 Hz, 1H), 5.04 (dd, J = 9.8, 1.6 Hz, 1H), 5.99 (ddt, J = 18.0, 9.3, 6.4 Hz, 1H), 6.85 (d, J = 8.2 Hz, 1H), 6.91 (td, J = 7.4, 0.9 Hz, 1H), 7.14 (dd, J = 7.4, 1.5 Hz, 1H), 7.18 (td, J = 8.0, 1.7 Hz, 1H).

^{13}C NMR (101 MHz, $CDCl_3$) δ 14.13, 20.53, 32.33, 34.80, 49.78, 52.07, 68.47, 70.66, 111.51, 115.41, 121.08, 127.61, 128.66, 130.18, 137.38, 156.47.

m/z MS (TOF ES+) $C_{16}H_{25}NO_2$[MH]+ calcd 264.19; found 264.2. tR: 2.24 (method A)

1-(2-allylphenoxy)-3-(cyclopentylamino)propan-2-ol (47i)

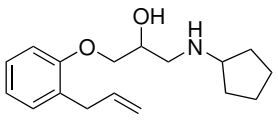

Eluent: 5% 1M ammonia in MeOH in DCM; Method a) Yield: 50 % (yellow oil)

^{1}H NMR (400 MHz, $CDCl_3$) δ

1.40 (s, 2H), 1.56 (s, 2H), 1.71 (s, 2H), 1.88 (s, 2H), 2.66 (s, 2H), 2.80 (dd,J =

12.0, 7.7 Hz, 1H), 2.87 - 2.97 (m, 1H), 3.09 - 3.19 (m, 1H), 3.39 (d, J = 5.7 Hz, 2H), 3.99 (s, 2H), 4.09 (s, 1H), 4.98 - 5.11 (m, 2H), 5.91 - 6.07 (m, 1H), 6.85 (d, J= 8.1 Hz, 1H), 6.91 (t, J = 7.4 Hz, 1H), 7.14 (d, J = 7.5 Hz, 1H), 7.18 (t, J = 7.6 Hz, 1H).

^{13}C NMR (101 MHz, $CDCl_3$) δ 23.98, 24.01, 32.94, 33.05, 50.97, 59.95, 68.40, 70.67, 111.36, 115.29, 120.88, 127.44, 128.51, 129.98, 137.17, 156.34.

m/z MS (TOF ES+) $C_{17}H_{25}NO_2$[MH]+ calcd 276.19; found 276.2. tR: 2.21 (method A)

1-(2-allylphenoxy)-3-(benzylamino)propan-2-ol (47j)

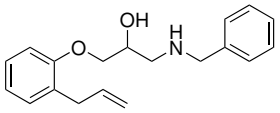

Eluent: 4% 1M ammonia in MeOH in DCM; Method c) Yield: 70 % (yellow oil)

^{1}H NMR (400 MHz, $CDCl_3$) δ 2.48 (s, 2H), 2.83 (dd, J = 12.2, 7.4 Hz, 1H), 2.91 (dd, J = 12.2, 4.1 Hz, 1H), 3.37 (dd, J = 6.4, 1.4 Hz, 2H), 3.85 (d, J = 4.9 Hz, 2H), 4.00 (d, J = 5.2 Hz, 2H), , 4.10 (ddd, J = 9.2, 7.4, 5.1 Hz, 1H), 5.00 (dq, J = 11.1, 1.6 Hz, 1H), 5.01 (dq, J = 18.7, 1.6 Hz, 1H), 5.96 (ddt, J = 16.7, 10.3, 6.4 Hz, 1H), 6.84 (d, J = 8.1 Hz, 1H), 6.92 (td, J = 7.4, 1.0 Hz, 1H), 7.10 - 7.23 (m, 2H), 7.24 - 7.30 (m, 1H), 7.34 (d, J= 4.4 Hz, 4H).

^{13}C NMR (101 MHz, $CDCl_3$) δ 34.80, 51.42, 53.97, 68.68, 70.58, 111.48, 115.39, 121.10, 127.31, 127.61, 128.30, 130.20, 137.36, 139.89, 156.43.

m/z MS (TOF ES+) $C_{19}H_{23}NO_2$[MH]+ calcd 298.17; found 298.2. tR: 2.26 (method A)

1-(2-allylphenoxy)-3-((3,4-dimethoxyphenethyl)amino)propan-2-ol (47k)

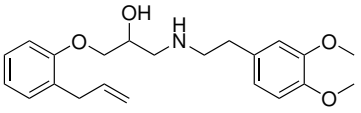

Eluent: 5% 1M ammonia in MeOH in DCM; Method c) Yield: 78 % (yellow oil)

^{1}H NMR (400 MHz, $CDCl_3$) δ 2.43 (s, 2H), 2.77 (dd, J = 11.0, 4.5 Hz, 2H), 2.83 (dd, J = 14.1, 6.6 Hz, 1H), 2.88 (d, J = 4.3 Hz, 1H), 2.90 - 2.99 (m, 2H), 3.38 (d, J = 6.3 Hz, 2H), 3.86 (d,J = 6.0 Hz, 6H), 3.98 (d, J= 5.0 Hz, 2H), 4.07 (td, J= 9.2, 5.0 Hz, 1H), 5.03 (dd, J = 9.7, 1.5 Hz, 1H), 5.04 (dd, J = 18.0, 1.6 Hz, 1H), 5.98 (ddt, J= 17.9, 9.2, 6.4 Hz, 1H), 6.71 - 6.77 (m, 2H), 6.81 (dd, J = 16.8, 8.0 Hz, 2H), 6.91 (td, J= 7.4, 0.7 Hz, 1H), 7.14 (d, J = 7.4 Hz, 1H), 7.18 (t, J= 7.8 Hz, 1H).

^{13}C NMR (101 MHz, $CDCl_3$) δ 34.65, 35.93, 51.26, 51.78, 55.86, 55.94, 68.39, 70.43, 111.37, 111.98, 115.29, 120.60, 120.99, 127.49, 128.51, 130.06, 132.28, 137.23, 147.53, 148.98, 156.29.

m/z MS (TOF ES+) $C_{22}H_{29}NO_4$[MH]+ calcd 372.21; found 372.3. tR: 2.25 (method A)

1-(2-(allyloxy)phenoxy)-3-aminopropan-2-ol (48a)

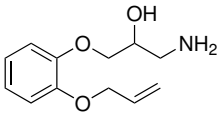

Eluent: 3% to 5% 1M ammonia in MeOH in DCM; Method b) Yield: 31% (colorless liquid)

^{1}H NMR (400 MHz, $CDCl_3$) δ 2.38 (s, 3H), 2.90 (tdd, J = 13.1, 9.6, 3.4 Hz, 2H), 3.98 (p, J = 6.1 Hz, 2H), 4.05 (q, J = 6.9 Hz, 1H), 4.59 (dt, J = 5.4, 1.3 Hz, 2H), 5.31 (dd, J = 10.5, 1.3 Hz, 1H), 5.43 (dd, J = 17.3, 1.5 Hz, 1H), 6.09 (ddt, J = 17.0, 10.7, 5.4 Hz, 1H), 6.89 - 6.97 (m, 4H).

^{13}C NMR (101 MHz, $CDCl_3$) δ 44.28, 70.05, 70.55, 72.61, 114.12, 115.03, 118.14, 121.68, 122.00, 133.25, 148.65, 148.72.

m/z MS (TOF ES+) $C_{12}H_{17}NO_3$[MH]+ calcd 224.12; found 224.0. tR: 1.80 (method A)

1-(2-allylphenoxy)-3-aminopropan-2-ol (48b)

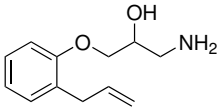

Eluent: 3% to 6% 1M ammonia in MeOH in DCM; Method b) Yield: 42% (colorless liquid)

^{1}H NMR (400 MHz, $CDCl_3$) δ 2.35 (s, 3H), 2.90 (d, J = 9.1 Hz, 1H), 2.99 (d, J = 11.4 Hz, 1H), 3.39 (d, J = 5.5 Hz, 2H), 3.98 (s, 3H), 5.03 (dd, J = 16.9, 1.8 Hz, 1H), 5.04 (dd, J = 10.1, 1.5 Hz, 1H), 5.98 (ddt, J= 16.7, 10.4, 6.4 Hz, 1H), 6.84 (d, J = 8.1 Hz, 1H), 6.92 (td, J= 7.4, 0.8 Hz, 1H), 7.14 (dd, J = 7.4, 1.4 Hz, 1H), 7.18 (td, J = 8.0, 1.7 Hz, 1H).

^{13}C NMR (101 MHz, $CDCl_3$) δ 34.72, 44.19, 70.02, 70.67, 111.32, 115.27, 121.02, 127.54, 128.45, 130.15, 137.30, 156.31.

m/z MS (TOF ES+) $C_{12}H_{17}NO_2$[MH]+ calcd 208.13; found 208.0. tR: 2.00 (method A)

3,3'-azanediylbis(1-(2-(allyloxy)phenoxy)propan-2-ol) (49a)

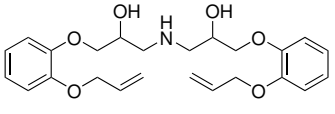

Eluent: 3% to 5% 1M ammonia in MeOH in DCM; Method b) Yield: 45% (white solid)

^{1}H NMR (400 MHz, $CDCl_3$) δ 2.29 (s, 3H), 2.77 - 2.94 (m, 4H), 3.96 (ddd, J = 9.5, 6.5, 2.7 Hz, 2H), 4.01 (ddd, J = 9.6, 3.8, 1.7 Hz, 2H), 4.06 - 4.19 (m, 2H), 4.56 (dt, J = 5.4, 1.3 Hz, 4H), 5.27 (dd, J = 10.5, 1.0 Hz, 2H), 5.39 (dd, J = 17.2, 1.5 Hz, 2H), 6.05 (ddt,J = 16.9, 10.7, 5.4 Hz, 2H), 6.89 (s, J = 2.9 Hz, 8H)

^{13}C NMR (101 MHz, $CDCl_3$) δ 50.64, 51.94, 52.08, 68.38, 68.52, 70.13, 72.56, 114.15, 114.72, 118.22, 121.74, 121.89, 133.22, 148.51, 148.58.

m/z MS (TOF ES+) $C_{24}H_{31}NO_6$[MH]+ calcd 430.22; found 430.0. tR: 2.32 (method A)

3,3'-azanediylbis(1-(2-allylphenoxy)propan-2-ol) (49b)

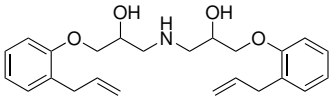

Eluent: 3% to 6% 1M ammonia in MeOH in DCM; Method b) Yield: 56% (white solid)

^{1}H NMR (400 MHz, $CDCl_3$) δ 2.74 (s, 3H), 2.82 - 3.02 (m, 4H), 3.40 (dd, J = 6.3, 1.0 Hz, 4H), 3.95 - 4.05 (m, 4H), 4.09 - 4.19 (m, 2H), 5.02 (d, J = 8.4 Hz, 2H), 5.06 (s, 2H), 5.99 (ddt, J= 16.8, 10.4, 6.4 Hz, 2H), 6.85 (d, J = 8.1 Hz, 2H), 6.93 (t, J= 7.4 Hz, 2H), 7.15 (d, J = 7.4 Hz, 2H), 7.19 (td, J = 8.0, 1.7 Hz, 2H)

^{13}C NMR (101 MHz, $CDCl_3$) δ 34.83, 52.20, 52.28, 68.94, 68.98, 70.49, 111.51, 115.41, 121.20, 127.66, 128.59, 130.28, 137.42, 156.38.

m/z MS (TOF ES+) $C_{24}H_{31}NO_4$[MH]+ calcd 398.23; found 398.2. tR: 2.43 (method A)

8.2.2 Chapter 4 synthesis

General procedure for the allylation of phenols

The phenol (1 eq, 1g) was dissolved in DMF (10 mL) and potassium carbonate (2 eq) and allyl bromide (1.5 eq) were added. The reaction was stirred at room temperature for 24h. Water (100 mL) was added to the reaction mixture and then extracted with diethyl ether. The organic phase was washed with water and brine and concentrated under vacuum.

1-(allyloxy)naphthalene (51)

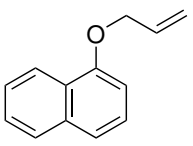

Yield: 85% (colorless oil)

^{1}H NMR (400 MHz, $CDCl_3$) δ 4.75 (dt, J= 5.1, 1.5 Hz, 2H), 5.39 (dd, J= 10.6, 1.5 Hz, 1H), 5.58 (dd, J= 17.3,

1.6 Hz, 1H), 6.23 (ddt, J= 17.3, 10.4, 5.1 Hz, 1H), 6.85 (dd, J= 7.5, 0.5 Hz, 1H), 7.38 - 7.45 (m, 1H), 7.49 (d, J= 8.3 Hz, 1H), 7.51 - 7.58 (m, 2H), 7.82 - 7.90 (m, 1H), 8.37 - 8.42 (m, 1H)

1-(allyloxy)-2-chlorobenzene (58d)

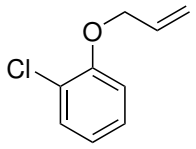

Yield: 88% (yellow liquid)

^{1}H NMR (400 MHz, $CDCl_3$) δ 4.61 (dt, J = 5.1, 1.6 Hz, 2H), 5.31 (dd, J = 10.6, 1.5 Hz, 1H), 5.47 (dd, J = 17.3, 1.6 Hz, 1H), 6.07 (ddt, J = 17.2, 10.4, 5.1 Hz, 1H), 6.89 (td, J = 7.6, 1.4 Hz, 1H) 6.93 (dd, J = 8.1, 1.5 Hz, 1H), 7.19 (ddd, J = 8.3, 7.4, 1.7 Hz, 1H), 7.36 (dd, J = 7.8, 1.6 Hz, 1H).

^{13}C NMR (101 MHz, $CDCl_3$) δ 69.72, 113.88, 117.89, 121.60, 123.11, 127.70, 130.41, 132.78, 154.19.

1-(allyloxy)-3-chlorobenzene (64a)

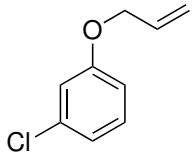

Yield: 93% (yellow liquid)

^{1}H NMR (400 MHz, $CDCl_3$) δ 4.52 (dt, J = 5.3, 1.5 Hz, 2H), 5.30 (dd, J = 10.5, 1.4 Hz, 1H), 5.41 (dd, J = 17.3, 1.5 Hz, 1H), 6.04 (ddt, J = 17.3, 10.5, 5.3 Hz, 1H), 6.81 (ddd, J = 8.4, 2.4, 1.0 Hz, 1H), 6.90 - 6.96 (m, 2H), 7.15 - 7.23 (m, 1H).

^{13}C NMR (101 MHz, $CDCl_3$) δ 69.10, 113.40, 115.27, 118.09, 121.14, 130.31, 132.87, 134.95, 159.44.

1-(allyloxy)-4-chlorobenzene (58c)

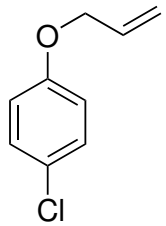

Yield: 91% (yellow liquid)

^{1}H NMR (400 MHz, $CDCl_3$) δ 4.51 (dt, J = 5.3, 1.5 Hz, 2H), 5.30 (dd, J = 10.5, 1.4 Hz, 1H), 5.41 (dd, J = 17.3, 1.6 Hz, 1H), 6.04 (ddt, J = 17.2, 10.5, 5.3 Hz, 1H), 6.80 - 6.88 (m, 2H), 7.21 - 7.25 (m, 2H).

^{13}C NMR (101 MHz, $CDCl_3$) δ 69.18, 116.15, 117.99, 125.81, 129.42, 133.05, 157.31.

1-(allyloxy)-2-methylbenzene (58f)

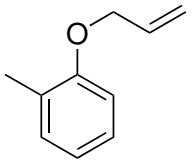

Yield: 80% (colorless liquid)

^{1}H NMR (400 MHz, $CDCl_3$) δ 2.34 (s, 3H), 4.57 - 4.64 (m, 2H), 5.34 (ddd, J = 10.6, 2.0, 1.1 Hz, 1H), 5.51 (ddd, J = 17.3, 2.5, 1.2 Hz, 1H), 6.08 - 6.20 (m, 1H), 6.88 (d, J = 8.4 Hz, 1H), 6.94 (t, J = 7.4 Hz, 1H), 7.21 (ddd, J = 8.4, 1.3, 0.6 Hz, 2H).

^{13}C NMR (101 MHz, $CDCl_3$) δ 16.39, 68.73, 111.39, 116.93, 120.57, 126.80, 127.05, 130.81, 133.77, 156.84.

tR: 3.638 (Method B)

1-(allyloxy)-3-methylbenzene (64c)

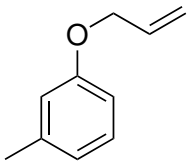

Yield: 84% (colorless liquid)

^{1}H NMR (400 MHz, $CDCl_3$) δ 2.34 (s, 3H), 4.53 (d, J = 5.3 Hz, 2H), 5.29 (d, J = 10.5 Hz, 1H), 5.42 (d, J = 17.2 Hz, 1H), 6.07 (ddd, J = 16.8, 10.5, 5.3 Hz, 1H), 6.74 (d, J = 8.5 Hz, 1H), 6.76 (d, J = 0.5 Hz, 1H), 6.78 (dd, J = 9.1, 0.6 Hz, 1H), 7.17 (t, J = 7.7 Hz, 1H)

1-(allyloxy)-4-methylbenzene (58e)

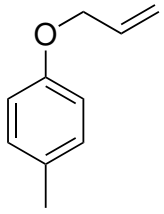

Yield: 86% (colorless liquid)

^{1}H NMR (400 MHz, $CDCl_3$) δ 2.31 (s, 3H), 4.53 (dt, J = 5.3, 1.5 Hz, 2H), 5.30 (dd, J = 10.5, 1.4 Hz, 1H), 5.43 (dd, J = 17.3, 1.6 Hz, 1H), 6.08 (ddt, J = 17.2, 10.5, 5.3 Hz, 1H), 6.85 (d, J = 8.6 Hz, 2H), 7.10 (d, J = 8.6 Hz, 2H).

^{13}C NMR (101 MHz, $CDCl_3$) δ 20.58, 69.00, 114.72, 117.58, 129.99, 130.15, 133.67, 156.60.

1-(allyloxy)-2-methoxybenzene (58h)

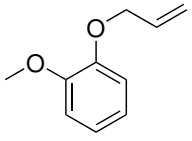

Yield: 85% (colorless liquid)

^{1}H NMR (400 MHz, $CDCl_3$) δ 3.88 (s, 3H), 4.62 (dt, J = 5.4, 1.5 Hz, 2H), 5.28 (dq, J = 10.5, 1.4 Hz, 1H), 5.41 (dq, J = 17.3, 1.6 Hz, 1H), 6.10 (ddt, J = 17.3, 10.7, 5.4 Hz, 1H), 6.84 - 6.99 (m, 4H).

^{13}C NMR (101 MHz, $CDCl_3$) δ 55.98, 69.96, 111.89, 113.73, 117.98, 120.84, 121.35, 133.55, 148.13, 149.62.

1-(allyloxy)-3-methoxybenzene (64b)

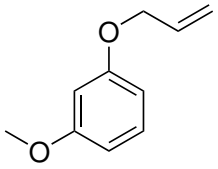

Yield: 93% (colorless liquid)

^{1}H NMR (400 MHz, $CDCl_3$) δ 3.79 (s, 3H), 4.53 (dt, J = 5.3, 1.5 Hz, 2H), 5.30 (dd, J = 10.5, 1.4 Hz, 1H), 5.43 (dd, J = 17.3, 1.6 Hz, 1H), 6.07 (ddt, J = 17.2, 10.6, 5.3 Hz, 1H), 6.49 - 6.57 (m, 3H), 7.19 (t, J = 8.1 Hz, 1H)

^{13}C NMR (101 MHz, $CDCl_3$) δ 55.32, 68.90, 101.33, 106.52, 106.97, 117.73, 129.94, 133.37, 159.95, 160.92.

1-(allyloxy)-4-methoxybenzene (58g)

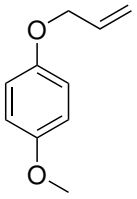

Yield: 93% (colorless liquid)

^{1}H NMR (400 MHz, $CDCl_3$) δ 3.77 (s, 3H), 4.50 (dt, J = 5.3, 1.5 Hz, 2H), 5.28 (dd, J = 10.5, 1.4 Hz, 1H), 5.41 (dd, J = 17.3, 1.6 Hz, 1H), 6.06 (ddt, J = 17.2, 10.6, 5.3 Hz, 1H), 6.79 - 6.92 (m, 4H).

^{13}C NMR (101 MHz, $CDCl_3$) δ 55.80, 69.62, 114.72, 115.83, 117.57, 133.75, 152.87, 154.02.

1-(allyloxy)-2-fluorobenzene (58b)

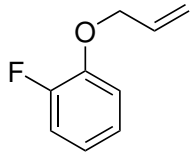

Yield: 88% (yellow liquid)

^{1}H NMR (400 MHz, $CDCl_3$) δ 4.61 (dt, J = 5.4, 1.5 Hz, 2H), 5.31 (dd, J = 10.5, 1.4 Hz, 1H), 5.43 (dd, J = 17.3, 1.5 Hz, 1H), 6.07 (ddt, J = 17.2, 10.6, 5.4 Hz, 1H), 6.87 - 6.94 (m, 1H), 6.97 (td, J = 8.2, 1.7 Hz, 1H), 7.02 - 7.07 (m, 1H), 7.06 - 7.12 (m, 1H).

1-(allyloxy)-3-fluorobenzene (64d)

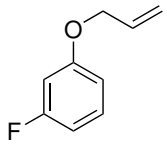

Yield: 82% (yellow liquid)

^{1}H NMR (400 MHz, $CDCl_3$) δ 4.53 (d, J = 6.1 Hz, 2H), 5.30 (dq, J = 10.1, 1.7 Hz, 1H), 5.32 (dq, J = 17.0, 1.6 Hz, 1H), 5.97 (ddt, J = 17.2, 10.4, 6.2 Hz, 1H), 6.55 - 6.70 (m, 3H), 7.10 - 7.25 (m, 1H).

1-(allyloxy)-4-fluorobenzene (58a)

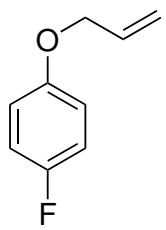

Yield: 92% (yellow liquid)

^{1}H NMR (400 MHz, $CDCl_3$) δ 4.50 (dt, J = 5.3, 1.5 Hz, 2H), 5.29 (dd, J = 10.5, 1.4 Hz, 1H), 5.41 (dd, J = 17.3, 1.6 Hz, 1H), 6.05 (ddt, J = 17.2, 10.5, 5.3 Hz, 1H), 6.81 - 6.90 (m, 2H), 6.93 - 7.02 (m, 2H).

^{13}C NMR (101 MHz, $CDCl_3$) δ 69.57, 115.88 (d, J = 8.0 Hz), 115.90 (d, J = 23.1 Hz), 117.86, 133.32, 154.83 (d, J = 2.0 Hz), 156.25, 157.43 (d, J = 238.3 Hz).

General procedure for the claisen rearrangement of allylated phenols

The allylated phenol (200 mg) was dissolved in DMF (1.5 mL) and heated in the microwave at 200 °C for 40 or 50 min. The crude was concentrated under vacuum and the product was isolated by flash column chromatography (Ethyl Acetate: Petroleum ether 1:6 to 1:11).

2-allyl-1-naphthol (52)

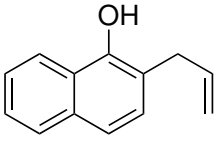

Yield: 66% (yellow liquid)

^{1}H NMR (400 MHz, $CDCl_3$) δ 3.74 (d, J = 6.2 Hz, 2H), 5.40 (dq, J = 3.1, 1.6 Hz, 1H), 5.44 (dq, J = 9.7, 1.6 Hz, 1H), 6.25 (ddt, J = 17.0, 10.1, 6.2 Hz, 1H), 7.40 (d, J = 8.4 Hz, 1H), 7.60 (d, J = 8.3 Hz, 1H), 7.61 - 7.69 (m, 2H), 7.92 - 8.02 (m, 1H), 8.35 - 8.40 (m, 1H).

2-allyl-3-chlorophenol (65a)

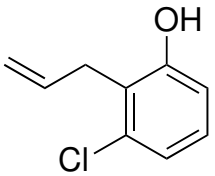

Yield: 32% (yellow oil)

^{1}H NMR (400 MHz, $CDCl_3$) δ 3.60 (dt, J = 6.0, 1.6 Hz, 2H), 5.10 (dq, J = 8.1, 1.7 Hz, 1H), 5.13 (t, J = 1.7 Hz, 1H), 5.20 (s, 1H), 5.98 (ddt, J = 14.7, 10.8, 6.0 Hz, 1H), 6.73 (dd, J = 7.9, 1.3 Hz, 1H), 6.98 (dd, J = 8.0, 1.3 Hz, 1H), 7.04 (t, J = 8.0 Hz, 1H)

^{13}C NMR (101 MHz, $CDCl_3$) δ 31.61, 114.45, 116.34, 122.13, 124.05, 128.01, 134.75, 135.18, 155.21.

2-allyl-4-chlorophenol (59c)

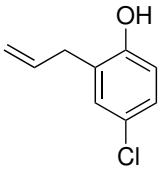

Yield: 57% (yellow oil)

^{1}H NMR (400 MHz, $CDCl_3$) δ 3.38 (d, J = 6.4 Hz, 2H), 4.93 (s, 1H), 5.16 (dq, J = 11.6, 1.6 Hz, 1H), 5.19 (dq, J = 5.0, 1.6 Hz, 1H), 5.99 (ddt, J = 16.7, 10.3, 6.4 Hz, 1H), 6.75 (dd, J = 8.6, 4.7 Hz, 1H), 6.79 - 6.87 (m, 2H)

^{13}C NMR (101 MHz, $CDCl_3$) δ 34.95, 117.15, 117.27, 127.30, 125.70, 127.72, 130.22, 135.63, 152.81.

2-allyl-5-chlorophenol (66a)

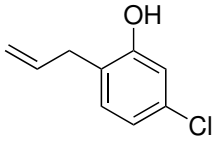

Yield: 47% (orange oil)

^{1}H NMR (400 MHz, $CDCl_3$) δ 3.37 (d, J = 6.3 Hz, 2H), 5.10 (s, 1H), 5.15 (dq, J = 10.8, 1.6 Hz, 1H), 5.18 (dq, J = 3.4, 1.6 Hz, 1H), 5.98 (ddt, J = 16.7, 10.3, 6.3 Hz, 1H), 6.84 (d, J = 2.0 Hz, 1H), 6.87 (dd, J = 8.0, 2.1 Hz, 1H), 7.03 (d, J = 8.0 Hz, 1H)

^{13}C NMR (101 MHz, $CDCl_3$) δ 34.74, 116.32, 117.06, 121.20, 124.00, 131.37, 132.97, 135.94, 154.85.

2-allyl-6-chlorophenol (59d)

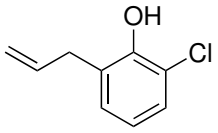

Yield: 41% (yellow liquid)

^{1}H NMR (400 MHz, $CDCl_3$) δ 3.44 (d, J = 6.6 Hz, 2H), 5.07 - 5.10 (m, 1H), 5.10 - 5.14 (m, 1H), 5.59 (s, 1H), 6.01 (ddt, J = 17.7, 9.5, 6.6 Hz, 1H), 6.82 (t, J = 7.8 Hz, 1H), 7.05 (dd, J = 7.6, 1.2 Hz, 1H), 7.20 (dd, J = 8.0, 1.5 Hz, 1H).

^{13}C NMR (101 MHz, $CDCl_3$) δ 34.68, 116.20, 120.02, 120.97, 127.00, 127.94, 129.01, 136.13, 149.36.

tR 3.443 (method B)

2-allyl-3-methylphenol and 2-allyl-5-methylphenol (65c and 66c)

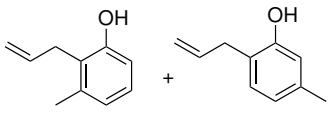

Yield: 82% (obtained as a mixture of X:Y) X 5-methyl, Y 3-methyl (46:54) (colorless liquid)

^{1}H NMR (400 MHz, $CDCl_3$) δ 2.28 (s, 3H, X), 2.29 (s, 3H, Y),

3.38 (d, J = 6.3 Hz, 2H, X), 3.43 (d, J = 5.8 Hz, 2H, Y), 5.02 (dq, J = 17.1, 1.8 Hz, 1H, Y), 5.07 (dq, J = 9.9, 1.6 Hz, 1H, Y), 5.14 (dd, J = 8.9, 1.2 Hz, 1H, X), 5.16 (dd, J = 17.6, 1.3 Hz, 1H, X), 5.97 (ddt, J = 16.9, 10.2, 6.2 Hz, 1H, Y), 6.01 (ddt, J = 17.2, 10.1, 6.4 Hz, 1H, X), 6.65 (s, 1H, X), 6.67 (d, J = 7.7 Hz, 1H, Y), 6.70 (d, J = 6.8 Hz, 1H, X) 6.77 (d, J = 7.5 Hz, 1H, Y), 6.99 (d, J = 6.3 Hz, 1H, X), 7.01 (t, J = 7.2 Hz, 1H, Y)

2-allyl-4-methylphenol(59e)

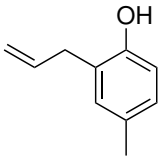

Yield: 89% (colorless liquid)

^{1}H NMR (400 MHz, $CDCl_3$) δ 2.28 (s, 3H), 3.40 (d, J = 6.4 Hz, 2H), 5.04 (broad s, OH, 1H), 5.16 (dd, J = 10.2, 1.7 Hz, 1H), 5.17 (dd, J = 17.1, 1.7 Hz, 1H), 6.04 (ddt, J = 16.8, 10.3, 6.4 Hz, 1H), 6.73 (d, J = 8.7 Hz, 1H), 6.94 (s, 1H), 6.94 (d, J = 6.5 Hz, 1H).

2-allyl-6-methylphenol(59f)

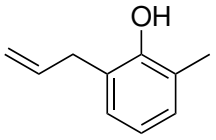

Yield: 62% (colorless liquid)

^{1}H NMR (400 MHz, $CDCl_3$) δ 2.30 (s, 3H), 3.46 (d, J = 6.4 Hz, 2H), 5.02 (s, 1H), 5.21 (dt, J = 3.0, 1.6 Hz, 1H), 5.21 (dq, J = 3.0, 1.6 Hz, 1H), 5.25 (dq, J = 4.6, 1.7 Hz, 1H), 5.25 (dq, J = 4.6, 1.7 Hz, 1H), 6.07 (ddt, J = 16.8, 10.1, 6.4 Hz, 1H), 6.85 (t, J = 7.5 Hz, 1H), 7.02 (d, J = 7.5 Hz, 1H), 7.08 (d, J = 7.4 Hz, 1H).

^{13}C NMR (101 MHz, $CDCl_3$) δ 15.96, 35.63, 116.65, 120.52, 124.30, 124.69, 128.14, 129.45, 136.66, 152.64.

tR 3.340 (method B)

4-allyl-2-methylphenol (60f)

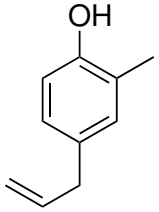

Yield: 25% (colorless liquid)

^{1}H NMR (400 MHz, $CDCl_3$) δ 2.25 (s, 3H), 3.31 (d, J = 6.7 Hz, 2H), 4.53 (s, 1H), 5.03 - 5.11 (m, 2H), 5.96 (ddt, J = 16.8, 10.1, 6.7 Hz, 1H), 6.72 (d, J = 8.1 Hz, 1H), 6.91 (dd, J = 8.1, 2.1 Hz, 1H), 6.96 (s, 1H).

^{13}C NMR (101 MHz, $CDCl_3$) δ 15.87, 39.51, 115.00, 115.45, 123.81, 127.16, 131.30, 132.32, 138.13, 152.17.

2-allyl-3-methoxyphenol (65b)

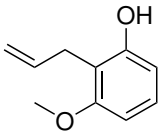

Yield: 42% (yellow liquid)

^{1}H NMR (400 MHz, $CDCl_3$) δ 3.49 (d, J = 6.0 Hz, 2H), 3.82 (s, 3H), 5.10 (dd, J = 3.5, 2.0 Hz, 1H), 5.11 (dq, J = 26.4, 1.7 Hz, 1H), 6.01 (ddt, J = 12.1, 10.1, 5.8 Hz, 1H), 6.50 (d, J = 8.1 Hz, 1H), 6.52 (d, J = 8.2 Hz, 1H), 7.09 (t, J = 8.2 Hz, 1H).

^{13}C NMR (101 MHz, $CDCl_3$) δ 27.44, 55.93, 103.47, 108.91, 113.84, 115.39, 127.61, 136.46, 155.23, 158.37.

2-allyl-4-methoxyphenol (59g)

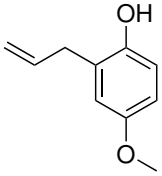

Yield: 68% (colorless liquid)

^{1}H NMR (400 MHz, $CDCl_3$) δ 3.40 (d, J = 6.3 Hz, 2H), 3.78 (s, 3H), 4.87 (s, 1H), 5.15 (dd, J = 14.8, 1.2 Hz. 1H), 5.16 (dd, J = 10.1, 1.3 Hz, 1H), 6.02 (dt, J = 16.1, 6.5 Hz, 1H), 6.69 (dd, J = 8.6, 2.9 Hz, 1H), 6.74 (dd, J = 10.5, 5.9 Hz, 2H).

^{13}C NMR (101 MHz, $CDCl_3$) δ 35.14, 55.88, 112.67, 116.08, 116.44, 116.47, 127.00, 136.33, 148.03, 153.08.

2-allyl-5-methoxyphenol (66b)

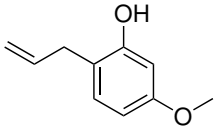

Yield: 23% (yellow liquid)

^{1}H NMR (400 MHz, $CDCl_3$) δ 3.35 (d, J = 6.3 Hz, 2H), 3.75 (s, 3H), 5.11 (dd, J = 10.1, 1.3 Hz, 1H), 5.13 (dd, J = 17.1, 1.6 Hz, 1H), 5.30 (s, 1H, OH) 6.01 (ddt, J = 16.7, 10.3, 6.3 Hz, 1H), 6.43 (d, J = 2.4 Hz, 1H), 6.46 (dd, J = 8.2, 2.5 Hz, 1H), 7.00 (d, J = 8.2 Hz, 1H).

^{13}C NMR (101 MHz, $CDCl_3$) δ 34.29, 55.35, 102.06, 106.08, 115.95, 117.96, 130.84, 137.01, 155.08, 159.45.

2-allyl-6-methoxyphenol (59h)

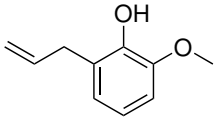

Yield: 45% (colorless liquid)

^{1}H NMR (400 MHz, $CDCl_3$) δ 3.92 (3H, s), 4.63 (td, J = 5.6, 1.7 Hz, 2H), 5.34 (ddd, J = 10.8, 2.8,

1.6 Hz, 1H), 5.39 (ddd, J = 17.1, 2.9, 1.6 Hz, 1H), 6.13 (tdd, J = 17.2, 10.7, 5.5 Hz, 1H), 6.86 - 6.93 (m, 4H)

^{13}C NMR (101 MHz, $CDCl_3$) δ 55.92, 69.82, 111.72, 113.41, 117.94, 120.72, 121.25, 133.42, 148.09, 149.42.

2-allyl-4-fluorophenol (59a)

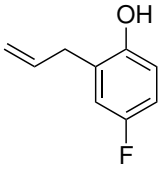

Yield: 55% (colorless liquid)

^{1}H NMR (400 MHz, $CDCl_3$) δ 3.38 (d, J = 6.4 Hz, 2H), 4.93 (broad s, 1H), 5.16 (dq, J = 17.0, 1.6 Hz, 1H), 5.18 (dq, J = 10.3, 1.5 Hz, 1H), 5.99 (ddt, J = 16.7, 10.3, 6.4 Hz, 1H), 6.75 (dd, J = 8.6, 4.7 Hz, 1H), 6.79 - 6.87 (m, 2H).

^{13}C NMR (101 MHz, $CDCl_3$) δ 35.05 (d, J = 1.1 Hz), 114.02 (d, J = 23.0 Hz), 116.64 (d, J = 5.4 Hz), 116.79 (d, J = 20.3 Hz), 117.14, 127.16 (d, J = 7.2 Hz), 135.68, 150.04 (d, J = 2.2 Hz), 157.29 (d, J = 238.0 Hz).

2-allyl-5-fluorophenol (66d

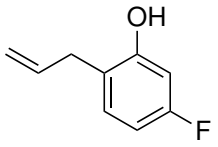

Yield: 25% (yellow liquid)

^{1}H NMR (400 MHz, $CDCl_3$) δ 3.37 (d, J = 6.3 Hz, 2H), 5.16 (dd, J = 18.0, 1.2 Hz, 1H), 5.17 (dd, J = 9.3, 1.1 Hz, 1H), 5.99 (ddt, J = 16.8, 10.5, 6.3 Hz, 1H), 6.57 (dd, J = 9.8, 2.6 Hz, 1H), 6.60 (td, J = 8.3, 2.6 Hz, 1H), 7.04 (dd, J = 8.2, 6.7 Hz, 1H).

^{13}C NMR (101 MHz, $CDCl_3$) δ 34.72, 103.66 (d, J = 24.5 Hz), 107.67 (d, J = 21.0 Hz), 116.90, 120.99 (d, J = 3.2 Hz), 131.20 (d, J = 9.7 Hz), 136.31, 155.27 (d, J = 11.3 Hz), 162.49 (d, J = 244.0 Hz).

2-allyl-6-fluorophenol (59b)

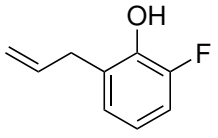

Yield: 54% (orange liquid)

^{1}H NMR (400 MHz, $CDCl_3$) δ 3.29 (d, J = 6.2 Hz, 2H), 4.98 (dd, J = 10.2, 1.5 Hz, 1H), 5.04 (dd, J = 17.2, 1.3 Hz, 1H), 5.92 (ddt, J = 16.9, 10.1, 5.9 Hz, 1H), 6.83 - 6.86 (m, 1H), 6.95 - 7.02 (m, 2H).

1-(tert-butylamino)-3-((2-(prop-1-en-1-yl)naphthalen-1-yl)oxy)propan-2-ol (53)

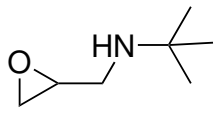

To a solution of *tert*-butylamine (1.1 eq) at 0 C in isopropylalcohol was added epichlorohydrin (1 eq) and stirred for 24 at room temperature. The reaction mixture was concentrated under vacuo, re-dissolved in ether and filtered. The crude was stirred for 90 minutes with KOH in diethyl ether. The ether layer was concentrated under vacuo and the crude was purified by FCC (ether:triethylamine 100:1) to afford a colorless liquid. Yield: 56 %

^{1}H NMR (400 MHz, $CDCl_3$) δ 1.07 (s, 9H), 1.31 (broad s, 1H), 2.53 - 2.61 (m, 2H), 2.75 (ddd, J = 5.0, 3.9, 1.0 Hz, 1H), 2.82 (ddd, J = 12.2, 3.8, 0.9 Hz, 1H), 3.06 (dtdd, J = 6.4, 3.8, 2.6, 1.0 Hz, 1H).

^{13}C NMR (101 MHz, $CDCl_3$) δ 29.03, 45.08, 45.95, 50.29, 52.40.

General procedure for the epichlorohydrin coupling

Epichlorohydrin (2 mL) was added to a phenol (0.0012 mol, 1 eq.) and then sodium hydroxide (1,05 eq) was added. The reaction mixture was heated in the microwave at 120 C for 30 min. Water (20 mL) was added to the reaction mixture and then extracted with DCM (3 x 20 mL). The crude was concentrated under vacuum and purified by flash column chromatography (Ethyl acetate : hexane, 1:5 to 1:9).

2-(((2-allylnaphthalen-1-yl)oxy)methyl)oxirane (52)

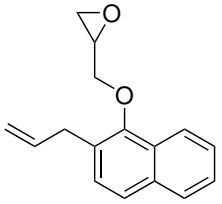

Yield: 60 % (yellow liquid)

^{1}H NMR (400 MHz, $CDCl_3$) δ 2.79 (dd, J = 5.0, 2.7 Hz, 1H), 2.94 (t, J = 4.6 Hz, 1H), 3.49 (td, J = 6.5, 2.8 Hz, 1H), 3.64 (dd, J = 6.4, 0.8 Hz, 2H), 3.95 (dd, J = 11.1, 6.1 Hz, 1H), 4.27 (dd, J = 11.1, 2.9 Hz, 1H), 5.10 (dd, J = 3.6, 1.6 Hz, 1H), 5.14 (s, 1H), 6.05 (ddtd, J = 9.5, 7.6, 6.4, 1.2 Hz, 1H), 7.33 (d, J = 8.4 Hz, 1H), 7.49 (dt, J = 14.8, 6.9 Hz, 2H), 7.61 (d, J = 8.4 Hz, 1H), 7.83 (d, J = 8.1 Hz, 1H), 8.16 (d, J = 8.3 Hz, 1H).

2-((2-allyl-3-chlorophenoxy)methyl)oxirane (67a)

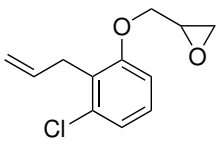

Yield: 56 % (colorless liquid)

^{1}H NMR (400 MHz, $CDCl_3$) δ 2.77 (dd, J = 4.9, 2.6 Hz, 1H), 2.90 (dd, J = 4.9, 4.2 Hz, 1H), 3.35 (ddt, J = 5.6, 4.1, 2.8 Hz, 1H), 3.58 (d, J = 6.3 Hz, 2H), 3.98 (dd, J = 11.1, 5.4 Hz, 1H), 4.23 (dd,

J = 11.1, 3.0 Hz, 1H), 5.02 (dt, J = 3.6, 1.6 Hz, 1H), 5.02 (dq, J = 24.8, 1.6 Hz, 1H), 5.93 (ddt, J = 17.0, 10.1, 6.2 Hz, 1H), 6.76 (dd, J = 8.2, 0.9 Hz, 1H), 7.01 (dd, J = 8.1, 1.1 Hz, 1H), 7.10 (t, J = 8.1 Hz, 1H).

^{13}C NMR (101 MHz, $CDCl_3$) δ 31.42, 44.69, 50.27, 69.41, 110.33, 115.46, 122.48, 127.30, 127.66, 135.07, 135.31, 157.37.

2-((2-allyl-4-chlorophenoxy)methyl)oxirane (61c)

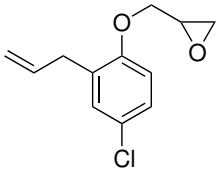

Yield: 67 % (yellow liquid)

^{1}H NMR (400 MHz, $CDCl_3$) δ 2.76 (dd, J = 5.0, 2.6 Hz, 1H), 2.89 (dd, J = 4.9, 4.2 Hz, 1H), 3.32 - 3.36 (m, 1H), 3.37 (d, J = 6.7 Hz, 2H), 3.92 (dd, J = 11.1, 5.6 Hz, 1H), 4.22 (dd, J = 11.1, 2.9 Hz, 1H), 5.08 (dq, J = 11.6, 1.4 Hz, 2H), 5.08 (dq, J = 15.9, 1.7 Hz, 2H) 5.95 (ddt, J = 17.5, 9.6, 6.7 Hz, 1H), 6.75 (d, J = 9.4 Hz, 1H), 7.12 (dq, J = 5.1, 2.7 Hz, 2H).

^{13}C NMR (101 MHz, $CDCl_3$) δ 34.19, 44.63, 50.27, 69.26, 112.88, 116.40, 126.12, 127.04, 129.90, 131.07, 136.03, 154.88.

2-((2-allyl-5-chlorophenoxy)methyl)oxirane (69a)

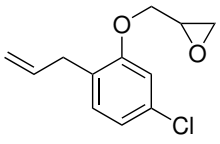

Yield: 68 % (yellow liquid)

^{1}H NMR (400 MHz, $CDCl_3$) δ 2.77 (dd, J = 4.9, 2.6 Hz, 1H), 2.91 (dd, J = 4.9, 4.2 Hz, 1H), 3.36 (d, J = 6.8 Hz, 3H), 3.94 (dd, J = 11.0, 5.6 Hz, 1H), 4.24 (dd, J = 11.0, 2.9 Hz, 1H), 5.05 (dq, J = 11.2, 1.5 Hz, 1H), 5.05 (dq, J = 17.4, 1.7 Hz, 1H) 5.94 (ddt, J = 17.5, 9.5, 6.6 Hz, 1H), 6.82 (s, 1H), 6.90 (dd, J = 8.0, 2.0 Hz, 1H), 7.06 (d, J = 8.0 Hz, 1H).

^{13}C NMR (101 MHz, $CDCl_3$) δ 33.98, 44.62, 50.18, 69.14, 112.33, 116.00, 121.21, 127.70, 130.80, 132.56, 136.40, 156.75.

2-((2-allyl-6-chlorophenoxy)methyl)oxirane(61d)

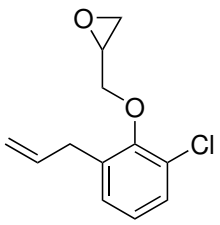

Yield: 75 % (yellow liquid)

^{1}H NMR (400 MHz, $CDCl_3$) δ 2.73 (dd, J = 5.0, 2.6 Hz, 1H), 2.89 (dd, J = 4.9, 4.2 Hz, 1H), 3.40 (dddd, J = 6.0, 4.1, 3.3, 2.7 Hz, 1H), 3.48 (d, J = 6.5 Hz, 2H), 3.93 (dd, J = 10.9, 6.0 Hz, 1H), 4.21

(dd, J = 10.9, 3.3 Hz, 1H), 5.07 (dq, J = 16.2, 1.7 Hz, 1H), 5.09 (dq, J = 10.2, 1.5 Hz, 1H), 5.96 (ddt, J = 16.7, 10.2, 6.5 Hz, 1H), 7.01 (t, J = 7.8 Hz, 1H), 7.10 (dd, J = 7.7, 1.7 Hz, 1H), 7.24 (dd, J = 7.9, 1.7 Hz, 2H).

^{13}C NMR (101 MHz, $CDCl_3$) δ 34.23, 44.71, 50.44, 74.20, 116.47, 125.15, 127.89, 128.65, 129.07, 135.47, 136.64, 152.78.

2-((2-allyl-4-methylphenoxy)methyl)oxirane(61e)

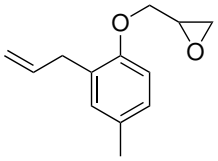

Yield: 55 % (colorless liquid)

^{1}H NMR (400 MHz, $CDCl_3$) δ 2.31 (s, 3H), 3.23 (d, J = 6.4 Hz, 2H), 3.20 - 3.40 (m, 3H), 4.02 - 4.12 (m, 2H), 5.16 (dd, J = 10.1, 1.7 Hz, 1H), 5.19 (dd, J = 17.2, 1.2 Hz, 1H), 5.90 (ddt, J = 16.9, 10.1, 6.4 Hz, 1H), 6.71 (d, J = 6.7 Hz, 1H), 6.95 (s, 1H), 6.94 (d, J = 6.5 Hz, 1H).

^{13}C NMR (101 MHz, $CDCl_3$) δ 20.86, 33.94, 44.20, 49.58, 68.44, 113.49, 115.85, 127.14, 128.27, 129.55, 134.35, 136.66, 154.07.

2-((2-allyl-6-methylphenoxy)methyl)oxirane(61f)

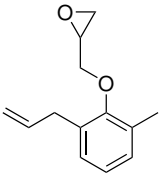

Yield: 43 % (colorless liquid)

^{1}H NMR (400 MHz, $CDCl_3$) δ 2.35 (s, 3H), 3.27 (d, J = 6.2 Hz, 2H), 3.40 - 3.50 (m, 3H), 4.12 - 4.22 (m, 2H), 5.17 (dd, J = 10.2, 1.5 Hz, 1H), 5.19 (dd, J = 17.0, 1.3 Hz, 1H), 5.96 (ddt, J = 16.9, 10.0, 6.3 Hz, 1H), 6.90 (t, J = 7.5 Hz, 1H), 7.04 (d, J = 7.2 Hz, 1H), 7.06 (d, J = 7.3 Hz, 1H).

rt. 6.407 (method B)

2-((2-allyl-3-methoxyphenoxy)methyl)oxirane (67b)

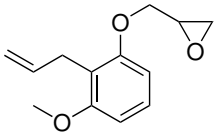

Yield: 47 % (colorless liquid)

^{1}H NMR (400 MHz, $CDCl_3$) δ 2.77 (dd, J = 5.0, 2.7 Hz, 1H), 2.89 (dd, J = 5.0, 4.2 Hz, 1H), 3.31 - 3.38 (m, 1H), 3.44 (d, J = 6.3 Hz, 2H), 3.82 (s, 3H), 4.00 (dd, J = 11.1, 5.3 Hz, 1H), 4.20 (dd, J = 11.1, 3.2 Hz, 1H), 4.93 (ddt, J = 10.0, 2.1, 1.5 Hz, 1H), 4.99 (ddd, J = 17.1, 3.8, 1.7

Hz, 1H), 5.95 (ddt, J = 17.0, 10.0, 6.2 Hz, 1H), 6.53 (d, J = 8.3 Hz, 1H), 6.57 (d, J = 8.2 Hz, 1H), 7.13 (t, J = 8.3 Hz, 1H).

^{13}C NMR (101 MHz, $CDCl_3$) δ 27.49, 44.80, 50.46, 55.97, 69.23, 104.51, 105.21, 114.27, 117.29, 127.27, 136.94, 157.24, 158.47.

2-((2-allyl-4-methoxyphenoxy)methyl)oxirane (59g)

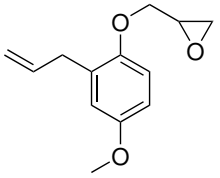

Yield: 51 % (colorless liquid)

^{1}H NMR (400 MHz, $CDCl_3$) δ 2.76 (dd, J = 5.0, 2.7 Hz, 1H), 2.89 (dd, J = 5.0, 4.2 Hz, 1H), 3.34 (ddt, J = 5.7, 4.1, 2.9 Hz, 1H), 3.39 (d, J = 6.6 Hz, 2H), 3.76 (s, 3H), 3.93 (dd, J = 11.1, 5.4 Hz, 1H), 4.17 (dd, J = 11.1, 3.1 Hz, 1H), 5.03 - 5.11 (m, 2H), 5.97 (ddt, J = 16.8, 10.1, 6.6 Hz, 1H), 6.69 (dd, J = 8.7, 3.1 Hz, 1H), 6.74 (d, J = 2.9 Hz, 1H), 6.79 (d, J = 8.8 Hz, 1H).

^{13}C NMR (101 MHz, $CDCl_3$) δ 34.57, 44.79, 50.54, 55.77, 69.96, 111.58, 113.40, 115.89, 116.25, 130.66, 136.81, 150.58, 154.23.

2-((2-allyl-5-methoxyphenoxy)methyl)oxirane (69b)

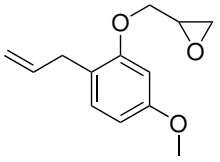

Yield: 55 % (colorless liquid)

^{1}H NMR (400 MHz, $CDCl_3$) δ 2.77 (dd, J = 5.0, 2.7 Hz, 1H), 2.90 (dd, J = 4.9, 4.2 Hz, 1H), 3.31 - 3.39 (m, 2H), 3.78 (s, 2H), 3.96 (dd, J = 11.0, 5.4 Hz, 1H), 4.20 (dd, J = 11.1, 3.1 Hz, 1H), 5.02 (dq, J = 9.9, 1.3 Hz, 1H), 5.04 (dq, J = 17.0, 1.6 Hz, 1H), 5.97 (ddt, J = 16.7, 10.1, 6.6 Hz, 1H), 6.45 (dd, J = 5.7, 2.4 Hz, 1H), 6.47 (d, J = 2.4 Hz, 1H), 7.04 (d, J = 8.2 Hz, 1H)

^{13}C NMR (101 MHz, $CDCl_3$) δ 33.84, 44.76, 50.35, 55.51, 68.91, 99.77, 104.97, 115.22, 121.47, 130.31, 137.45, 157.05, 159.38.

2-((2-allyl-4-fluorophenoxy)methyl)oxirane (61a)

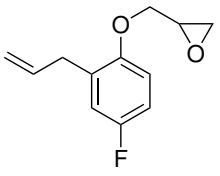

Yield: 46 % (yellow liquid)

^{1}H NMR (400 MHz, $CDCl_3$) δ 2.76 (dd, J = 5.0, 2.7 Hz, 1H), 2.90 (dd, J = 4.9, 4.2 Hz, 1H), 3.34 (ddt, J = 5.6, 4.1, 2.8 Hz, 1H), 3.39 (d, J = 6.7 Hz, 2H), 3.93 (dd, J = 11.1, 5.5 Hz, 1H), 4.21 (dd,

J = 11.0, 3.0 Hz, 1H), 5.09 - 5.12 (m, 2H), 5.89 - 6.01 (m, 1H), 6.77 (dd, J = 8.8, 4.6 Hz, 1H), 6.83 (dd, J = 8.0, 3.1 Hz, 1H), 6.87 (dt, J = 8.7, 3.0 Hz, 1H).

^{13}C NMR (101 MHz, $CDCl_3$) δ 34.30 (d, J = 1.1 Hz), 44.70, 50.50, 69.77, 112.92 (d, J = 8.4 Hz), 113.16 (d, J = 22.9 Hz), 116.39, 116.78 (d, J = 23.2 Hz), 131.19 (d, J = 7.2 Hz), 136.15, 152.41 (d, J = 2.2 Hz), 157.54 (d, J = 239.0 Hz).

2-((2-allyl-5-fluorophenoxy)methyl)oxirane (69d)

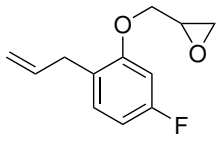

Yield: 49 % (yellow liquid)

^{1}H NMR (400 MHz, $CDCl_3$) δ 2.78 (dd, J = 4.9, 2.6 Hz, 1H), 2.91 (dd, J = 4.9, 4.2 Hz, 1H), 3.31 - 3.40 (m, 1H), 3.35 (d, J = 5.7 Hz, 2H), 3.93 (dd, J = 11.0, 5.5 Hz, 1H), 4.22 (dd, J = 11.0, 2.9 Hz, 1H), 5.04 (dd, J = 10.1, 1.4 Hz, 1H), 5.05 (dd, J = 17.2, 1.6 Hz, 1H), 5.95 (ddt, J = 18.2, 9.4, 6.6 Hz, 1H), 6.50 (dd, J = 8.9, 2.5 Hz, 1H), 6.62 (td, J = 8.3, 2.5 Hz, 1H), 7.07 (dd, J = 8.3, 6.8 Hz, 1H).

2-((2-allyl-6-fluorophenoxy)methyl)oxirane (61b)

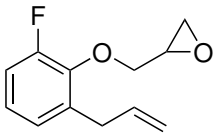

Yield: 39 % (yellow liquid)

^{1}H NMR (400 MHz, $CDCl_3$) δ 2.70 (dd, J = 5.0, 2.6 Hz, 1H), 2.87 (t, J = 5.0, 1H), 3.34 (dtd, J = 6.7, 3.3, 0.7 Hz, 1H), 3.46 (d, J = 6.5 Hz, 2H), 4.01 (ddd, J = 11.3, 6.0, 1.1 Hz, 1H), 4.28 (ddd, J = 11.3, 3.2, 1.1 Hz, 1H), 5.05 (dq, J = 9.6, 1.6 Hz, 1H), 5.08 (dd, J = 16.7, 1.5 Hz, 1H), 5.96 (ddt, J = 16.8, 10.4, 6.5 Hz, 1H), 6.90 - 7.00 (m, 3H).

^{13}C NMR (101 MHz, $CDCl_3$) δ 34.11 (d, J = 2.6 Hz), 44.64, 50.56 (d, J = 1.2 Hz), 74.52 (d, J = 5.7 Hz), 114.90 (d, J = 19.3 Hz), 116.17, 123.94 (d, J = 8.0 Hz), 125.44 (d, J = 3.0 Hz), 135.07 (d, J = 1.8 Hz), 136.72, 144.36 (d, J = 10.6 Hz), 155.55 (d, J = 246.1 Hz).

General procedure for epoxide opening with *tert*-butylamine A solution of the respective oxirane in 1 mL of *tert*-butylamine was heated in the microwave at 70 °C (for alprenolol analogues) for 1 hour. The reaction mixture was checked by TLC. The reaction mixture was purified by column chromatography with percentages ranging from 4% to 6% of 1N ammonia in methanol in dichloromethane.

1-(tert-butylamino)-3-((2-(prop-1-en-1-yl)naphthalen-1-yl)oxy)propan-2-ol (54)

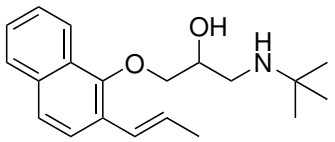

To a stirring solution of 2-allyl-1-naphthol (**52**, 0.69 mmol, 1 eq.) in isopropyl alcohol, sodium hydroxide (0.83 mmol, 1.2 eq.) was added and left stirring for 30 minutes at room temperature. 1-(*tert*-butylamino)-3-((2-(prop-1-en-1-yl)naphthalen-1-yl)oxy)propan-2-ol (**53**, 1.38 mmol, 2 eq.) was added to the reaction mixture and left stirring at 90 °C for 9h. Reaction mixture was washed with water (x2) and extracted with DCM (x2). The organic fraction was collected, dried with anhydrous sodium sulfate and concentrated under vacuum. The crude was purified by FCC over silica gel using 2 % of 1N ammonia in methanol in dichloromethane. Yield: 4 %

^{1}H NMR (400 MHz, $CDCl_3$) δ 1.29 (s, 9H), 1.96 (dd, J = 6.7, 1.7 Hz, 3H), 2.99 (dd, J = 11.8, 8.7 Hz, 1H), 3.11 (dd, J = 11.8, 3.3 Hz, 1H), 4.01 (dd, J = 4.9, 1.4 Hz, 2H), 4.07 (s, 2H), 4.35 (td, J = 8.4, 4.8 Hz, 1H), 6.34 (dq, J = 15.9, 6.6 Hz, 1H), 6.88 (dd, J = 15.9, 1.7 Hz, 1H), 7.43 (dddd, J = 21.6, 8.1, 6.9, 1.3 Hz, 2H), 7.56 (q, J = 8.7 Hz, 2H), 7.77 (d, J = 7.3 Hz, 1H), 8.11 - 8.19 (m, 1H).

1-((2-allylnaphthalen-1-yl)oxy)-3-(tert-butylamino)propan-2-ol (56)

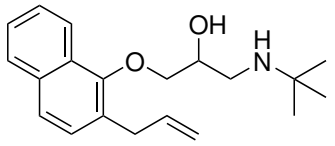

General procedure for epoxide opening (method A). Yield: 72%

^{1}H NMR (400 MHz, DMSO) δ 1.15 (s, 9H), 2.72 - 2.88 (m, 2H), 3.60 (dd, J = 6.6, 1.2 Hz, 2H), 3.89 (dd, J = 9.4, 6.1 Hz, 1H), 3.96 (dd, J = 9.4, 4.2 Hz, 1H), 4.08 (s, 1H), 5.11 (ddd, J = 14.6, 8.1, 1.8 Hz, 2H), 6.03 (ddt, J = 16.7, 10.0, 6.6 Hz, 1H), 7.35 (d, J = 8.4 Hz, 1H), 7.44 - 7.57 (m, 2H), 7.66 (d, J = 8.4 Hz, 1H), 7.85 - 7.95 (m, 1H), 8.21 (d, J = 8.1 Hz, 1H).

1-(2-allyl-3-chlorophenoxy)-3-(tert-butylamino)propan-2-ol (68a)

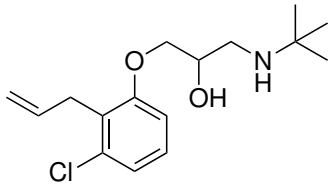

General procedure for epoxide opening (method A). Yield: 89%

^{1}H NMR (400 MHz, DMSO) δ 1.07 (s, 9H), 2.60 - 2.85 (m, 2H), 3.48 (d, J = 6.2 Hz, 2H), 3.83 - 4.07 (m, 3H), 4.96 (dd, J = 13.6, 1.9 Hz, 2H), 5.78 - 5.94 (m, 1H), 6.96 (d, J = 8.3 Hz, 1H), 7.01 (d, J = 8.0 Hz, 1H), 7.20 (t, J = 8.2 Hz, 1H).

^{13}C NMR (101 MHz, $CDCl_3$) δ 28.09, 31.43, 45.25, 53.18, 67.64, 70.76, 109.98, 115.24, 122.29, 126.73, 127.80, 135.27, 125.41, 157.42.

1-(2-allyl-4-chlorophenoxy)-3-(tert-butylamino)propan-2-ol (62c)

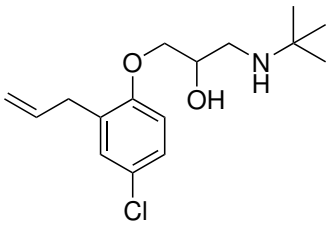

General procedure for epoxide opening (method A). Yield: 86%

^{1}H NMR (400 MHz, $CDCl_3$) δ 1.17 (s, 9H), 2.37 (s, 2H), 2.76 (dd, J = 12.0, 7.7 Hz, 1H), 2.92 (dd, J = 12.0, 3.8 Hz, 1H), 3.35 (d, J = 6.4 Hz, 2H), 3.91-4.00 (m, 3H), 5.04 (dd, J = 10.0, 1.6 Hz, 1H), 5.07 (dd, J = 17.0, 1.7 Hz, 1H), 5.94 (ddt, J = 16.7, 10.2, 6.5 Hz, 1H), 6.77 (d, J = 8.5 Hz, 1H), 7.11 (d, J = 2.5 Hz, 1H), 7.13 (dd, J = 8.5, 2.6 Hz, 1H).

^{13}C NMR (101 MHz, $CDCl_3$) δ 29.15, 34.46, 44.80, 50.71, 68.67, 71.06, 112.63, 116.18, 125.81, 127.16, 129.94, 130.55, 136.33, 155.15.

1-(2-allyl-5-chlorophenoxy)-3-(tert-butylamino)propan-2-ol (70a)

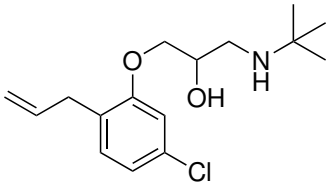

General procedure for epoxide opening (method A). Yield: 88%

^{1}H NMR (400 MHz, DMSO) δ 1.03 (s, 9H), 2.58 (dd, J = 11.3, 6.7 Hz, 1H), 2.67 (dd, J = 11.2, 5.0 Hz, 1H), 3.31 (d, J = 8.3 Hz, 2H), 3.81 (dd, J = 11.0, 5.4 Hz, 1H), 3.92 (dd, J = 9.8, 5.4 Hz, 1H), 3.99 (dd, J = 9.8, 5.0 Hz, 1H), 5.00 (dd, J = 10.2, 2.0 Hz, 1H), 5.03 (dd, J = 17.2, 1.9 Hz, 1H), 5.93 (ddt, J = 16.7, 10.0, 6.7 Hz, 1H), 6.92 (dd, J = 8.0, 2.0 Hz, 1H), 7.03 (d, J = 2.0 Hz, 1H), 7.11 (d, J = 8.0 Hz, 1H).

^{13}C NMR (101 MHz, $CDCl_3$) δ 28.53, 34.22, 45.00, 52.17, 68.02, 70.74, 112.17, 115.79, 121.02, 127.20, 130.89, 132.75, 136.72, 156.95.

1-(2-allyl-6-chlorophenoxy)-3-(tert-butylamino)propan-2-ol (62d)

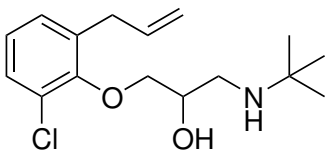

General procedure for epoxide opening (method A). Yield: 86%

^{1}H NMR (400 MHz, $CDCl_3$) δ 1.15 (s, 9H), 2.80 (s, 2H, interchangeable protons), 2.81 (dd, J = 11.8, 7.1 Hz, 1H), 2.90 (dd, J = 11.8, 4.0 Hz, 1H), 3.47 (d, J = 6.4 Hz, 2H), 3.96 (dd, J = 4.9, 2.2 Hz, 2H), 4.02 (ddd, J = 9.0, 7.1, 4.6 Hz, 1H), 5.08 (ddq, J = 16.8, 13.8, 1.6 Hz, 2H), 5.95 (ddt, J = 16.7, 10.2, 6.5 Hz, 1H), 7.00 (t, J = 7.8 Hz, 1H), 7.09 (dd, J = 7.7, 1.7 Hz, 1H), 7.24 (dd, J = 7.9, 1.7 Hz, 1H).

^{13}C NMR (101 MHz, $CDCl_3$) δ 29.09, 34.28, 44.70, 50.89, 69.16, 75.75, 116.50, 125.05, 127.98, 128.64, 129.17, 135.44, 136.70, 152.76.

1-(2-allyl-3-methylphenoxy)-3-(*tert*-butylamino)propan-2-ol (68c)

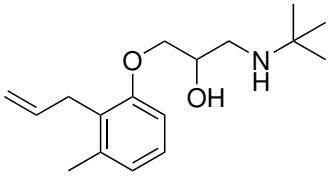

Purified by semi-preparative HPLC.

^{1}H NMR (401 MHz, $CDCl_3$) δ 1.14 (s, 9H), 2.28 (s, 3H), 2.52 (broad s, 2H, interchangeable protons), 2.75 (dd, J = 11.9, 6.7 Hz, 1H), 2.87 (dd, J = 11.9, 3.7 Hz, 1H), 3.42 (dd, J = 5.8, 1.5 Hz, 2H), 3.91 - 4.03 (m, 3H), 4.96 (dq, J = 10.1, 1.7 Hz, 1H), 4.90 (dq, J = 17.1, 1.8 Hz, 1H), 5.92 (ddt, J = 17.0, 10.1, 5.8 Hz, 1H), 6.73 (d, J = 8.2 Hz, 1H), 6.80 (d, J = 7.5 Hz, 1H), 7.08 (t, J = 7.9 Hz, 1H).

^{13}C NMR (101 MHz, $CDCl_3$) δ 19.54, 29.03, 30.66, 44.94, 50.93, 68.75, 70.82, 109.32, 114.53, 123.11, 126.65, 126.91, 136.48, 138.20, 156.64.

1-(2-allyl-4-methylphenoxy)-3-(*tert*-butylamino)propan-2-ol (62e)

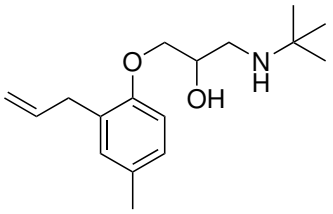

General procedure for epoxide opening (method A). Yield: 80%

^{1}H NMR (401 MHz, DMSO) δ 1.03 (s, 9H), 2.20 (s, 3H), 2.57 (dd, J = 11.3, 6.8 Hz, 1H), 2.69 (dd, J = 11.3, 4.6 Hz, 1H), 3.29 (d, J = 6.7 Hz, 2H), 3.80 (dt, J = 10.5, 5.2 Hz, 1H), 3.83 - 3.93 (m, 2H), 4.98 (ddt, J = 10.0, 2.3, 1.2 Hz, 1H), 5.03 (ddd, J = 17.1, 3.7, 1.6 Hz, 1H), 5.94 (ddt, J = 16.8, 10.0, 6.7 Hz, 1H), 6.82 (d, J = 8.2 Hz, 1H), 6.90 (d, J = 2.0 Hz, 1H), 6.96 (dd, J = 8.3, 1.8 Hz, 1H).

^{13}C NMR (101 MHz, DMSO) δ 20.12, 28.65, 33.96, 45.26, 49.89, 68.92, 70.65, 111.59, 115.28, 127.54, 127.71, 128.84, 130.14, 137.18, 154.12.

tR: 5.358 r.t. (method B)

tR: 2.906 (method A)

1-(2-allyl-6-methylphenoxy)-3-(*tert*-butylamino)propan-2-ol (62f)

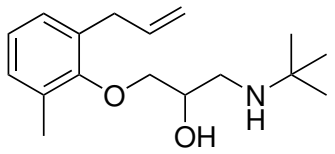

General procedure for epoxide opening (method A). Yield: 90%

^{1}H NMR (401 MHz, DMSO) δ 1.04 (s, 9H), 2.24 (s, 3H), 2.60 (dd, J = 11.1, 6.8 Hz, 1H), 2.69 (dd, J = 11.2, 4.8 Hz, 1H), 3.40 (d, J = 6.7 Hz, 2H), 3.65 (dd, J = 9.2, 5.8 Hz, 1H), 3.74 (dd, J = 9.2, 4.8 Hz, 1H), 3.77 - 3.88 (m, 1H), 5.00 - 5.10 (m, 2H), 5.95 (ddt, J = 16.7, 10.0, 6.7 Hz, 1H), 6.95 (t, J = 7.2 Hz, 1H), 6.99 (dd, J = 7.6, 1.9 Hz, 1H), 7.04 (dd, J = 7.1, 1.6 Hz, 1H).

^{13}C NMR (101 MHz, DMSO) δ 16.08, 28.70, 33.39, 45.11, 49.81, 69.52, 75.43, 115.64, 123.73, 127.78, 129.14, 130.65, 132.58, 137.65, 155.01

rT 5.210 (method B)

1-(2-allyl-3-methoxyphenoxy)-3-(tert-butylamino)propan-2-ol (68b)

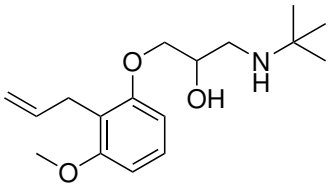

General procedure for epoxide opening (method A). Yield: 91%

^{1}H NMR (401 MHz, DMSO) δ 1.21 (s, 9H), 2.82 (dd, J = 11.9, 7.7 Hz, 1H), 2.96 (dd, J = 12.0, 3.7 Hz, 1H), 3.45 (d, J = 6.0 Hz, 2H), 3.84 (s, 3H), 3.98 (dd, J = 9.4, 5.4 Hz, 1H), 4.05 (dd, J = 9.4, 5.0 Hz, 1H), 4.07 - 4.16 (m, 1H), 4.96 (dq, J = 16.8, 1.7 Hz, 1H) 4.98 (dq, J = 10.1, 1.7 Hz, 1H), 5.97 (ddt, J = 17.1, 10.1, 6.0 Hz, 1H), 6.56 (dd, J = 8.3, 0.9 Hz, 1H), 6.59 (dd, J = 8.4, 0.9 Hz, 1H), 7.16 (t, J = 8.3 Hz, 1H).

^{13}C NMR (101 MHz, DMSO) δ 27.50, 28.91, 45.11, 50.93, 55.99, 69.07, 71.83, 106.22, 107.84, 115.87, 116.95, 129.36, 137.28, 158.68, 159.09.

1-(2-allyl-4-methoxyphenoxy)-3-(tert-butylamino)propan-2-ol (62g)

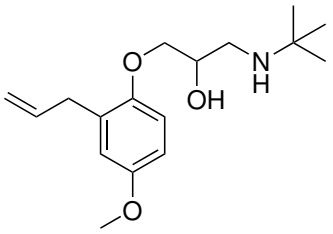

General procedure for epoxide opening (method A). Yield: 83%

^{1}H NMR (401 MHz, DMSO) δ 1.31 (s, 9H), 2.89 (dd, J = 12.0, 8.7 Hz, 1H), 3.09 (d, J = 10.4 Hz, 1H), 3.36 (d, J = 6.4 Hz, 2H), 3.75 (s, 3H), 3.92 (dd, J = 9.5, 5.6 Hz, 1H), 4.01 (dd, J = 9.5, 4.9 Hz, 1H), 4.27 (s, 2H), 4.99 - 5.09 (m, 2H), 5.88 - 6.03 (m, 1H), 6.70 (dt, J = 8.7, 3.0 Hz, 2H), 6.77 (d, J = 8.7 Hz, 1H).

^{13}C NMR (101 MHz, DMSO) δ 28.90, 34.11, 44.88, 51.03, 55.60, 69.07, 72.09, 114.00, 114.50, 114.82, 116.23, 129.45, 136.81, 151.77, 154.34

1-(2-allyl-5-methoxyphenoxy)-3-(tert-butylamino)propan-2-ol (70b)

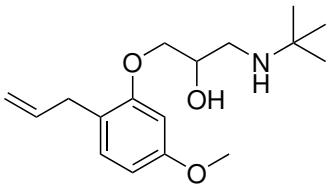

General procedure for epoxide opening (method A). Yield: 80%

^{1}H NMR (401 MHz, DMSO) δ 1.06 (s, 9H), 2.56 - 2.83 (m, 2H), 3.25 (d, J = 6.6 Hz, 2H), 3.72 (s, 3H), 3.78 - 3.99 (m, 3H), 4.88 - 5.07 (m, 2H), 5.92 (ddt, J = 16.7, 10.0, 6.6 Hz, 1H), 6.45 (dd, J = 8.2, 2.4 Hz, 1H), 6.51 (d, J = 2.4 Hz, 1H), 6.99 (d, J = 8.3 Hz, 1H).

^{13}C NMR (101 MHz, DMSO) δ 29.79, 33.80, 44.92, 50.89, 55.74, 69.06, 72.10, 102.5, 107.50, 116.22, 123.48, 129.40, 137.10, 158.27, 160.11.

1-(2-allyl-6-methoxyphenoxy)-3-(tert-butylamino)propan-2-ol (62h)

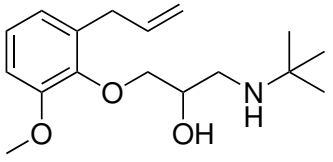

General procedure for epoxide opening (method A). Yield: 78%

^{1}H NMR (401 MHz, $CDCl_3$) δ 1.14 (s, 9H), 2.69 - 2.94 (m, 2H), 2.80 (broad s, 2H, interchangeable protons), 3.43 (d, J = 6.4 Hz, 2H), 3.84 (s, 3H), 3.88 - 4.03 (m, 3H), 5.04 (dd, J = 15.8, 1.5 Hz, 1H), 5.05 (dd, J = 10.1, 1.4 Hz, 1H), 5.96 (ddt, J = 18.1, 9.4, 6.4 Hz, 1H), 6.78 (d, J = 8.1 Hz, 2H), 7.00 (t, J = 8.1 Hz, 1H).

^{13}C NMR (101 MHz, $CDCl_3$) δ 28.99, 34.15, 44.80, 50.79, 55.86, 69.59, 76.05, 110.46, 115.85, 122.38, 124.20, 134.09, 137.22, 145.94, 152.52.

1-(2-allyl-4-fluorophenoxy)-3-(tert-butylamino)propan-2-ol (62a)

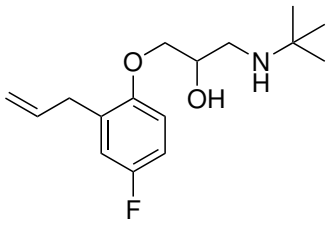

General procedure for epoxide opening (method A). Yield: 85%

^{1}H NMR (401 MHz, $CDCl_3$) δ 1.22 (s, 9H), 2.75 - 2.86 (m, 1H), 2.98 (ddd, J = 12.0, 5.3, 3.6 Hz, 1H), 3.36 (d, J = 6.4 Hz, 2H), 3.79 (d, J = 14.1 Hz, 2H), 3.93 (dd, J = 9.4, 5.3 Hz, 1H), 3.99 (dd, J = 9.4, 5.0 Hz, 1H), 4.13 (dt, J = 8.4, 4.5 Hz, 1H), 5.05 (dq, J = 16.9, 1.6 Hz, 1H), 5.06 (dt, J = 10.3, 1.5 Hz, 1H), 5.94 (ddt, J = 16.7, 10.2, 6.4 Hz, 1H), 6.74 - 6.80 (m, 1H), 6.81 - 6.90 (m, 2H).

^{13}C NMR (101 MHz, $CDCl_3$) δ 28.35, 34.48, 45.15, 52.53, 68.00, 71.21, 112.48 (d, J = 8.3 Hz), 113.25 (d, J = 22.8 Hz), 116.18, 116.87 (d, J = 23.2 Hz), 130.58 (d, J = 7.2 Hz), 136.38, 152.51 (d, J = 2.1 Hz), 157.38 (d, J = 238.6 Hz).

1-(2-allyl-5-fluorophenoxy)-3-(tert-butylamino)propan-2-ol (70d)

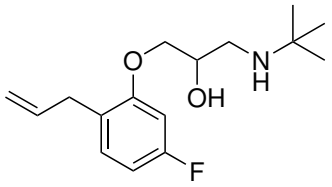

General procedure for epoxide opening (method A). Yield: 84%

^{1}H NMR (401 MHz, $CDCl_3$) δ 1.12 (s, 9H), 2.12 (broad s, 2H, exchangeable protons), 2.68 - 2.76 (m, 1H), 2.82 - 2.91 (m, 1H), 3.34 (d, J = 6.3 Hz, 2H), 3.87 - 4.03 (m, 3H), 5.01 (ddd, J = 17.0, 3.5, 1.7 Hz, 1H), 5.04 (ddd, J = 10.1, 3.3, 1.6 Hz, 1H), 5.95 (ddt, J = 16.7, 10.2, 6.4 Hz, 1H), 6.60 (d, J = 8.0 Hz, 1H), 6.65 (t, J = 7.4 Hz, 1H), 7.06 (t, J = 7.4 Hz, 1H).

^{13}C NMR (101 MHz, $CDCl_3$) δ 29.21, 34.18, 44.74, 50.62, 68.65, 70.93, 99.81 (d, J = 25.7 Hz), 107.05 (d, J = 20.7 Hz), 115.51, 124.16 (d, J = 3.2 Hz), 130.55 (d, J = 9.8 Hz), 137.13, 157.36 (d, J = 9.7 Hz), 162.39 (d, J = 243.7 Hz).

1-(2-allyl-6-fluorophenoxy)-3-(tert-butylamino)propan-2-ol (62b)

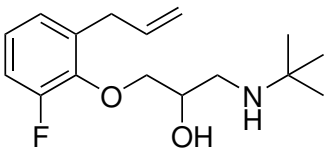

General procedure for epoxide opening (method A). Yield: 90%

^{1}H NMR (401 MHz, $CDCl_3$) δ 1.22 (s, 9H), 2.83 (dd, J = 11.9, 7.0 Hz, 1H), 2.97 (dd, J = 12.2, 2.2 Hz, 1H), 3.44 (dd, J = 6.4, 1.4 Hz, 2H), 3.55 (s, 2H, exchangeable protons), 4.01-4.12 (m, 3H), 5.04 (dd, J = 16.9, 1.8 Hz, 1H), 5.07 (dd, J = 9.9, 1.8 Hz, 1H), 5.96 (ddt, J = 16.6, 10.2, 6.4 Hz, 1H), 6.90-6.98 (m, 3H).

^{13}C NMR (101 MHz, $CDCl_3$) δ 28.45, 34.11 (d, J = 2.5 Hz), 44.86, 52.30, 68.57, 76.10 (d, J = 5.2 Hz), 114.93 (d, J = 19.3 Hz), 116.17, 123.84 (d, J = 8.0 Hz), 125.50 (d, J = 3.0 Hz), 134.93 (d, J = 1.8 Hz), 136.81, 144.49 (d, J = 10.5 Hz), 155.59 (d, J = 246.0 Hz).

2-bromo-5-methylphenyl acetate (72)

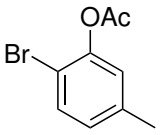

2-Bromo-5-methylphenol (1 g, 53 mmol) was dissolved in pyridine (4 mL) and acetic anhydride was added (1.01 mL, 106 mmol, 2 eq). Reaction mixture was left stirring at room temperature for 24 h. The mixture dispersed in water (40 mL). The aqueous slurry was extracted with DCM (3 x 20 mL), and the combined organic extracts were washed with brine (20 mL). After drying over anhydrous $MgSO_4$, the organic extracts were concentrated under reduced pressure. Heptane, which forms an azeotropic mixture with pyridine, was added in small portions to facilitate the removal of pyridine traces. A colorless liquid was afforded (0.956 g, 79 %). Adapted from [90].

^{1}H NMR (400 MHz, $CDCl_3$) δ 2.32 (s, 3H), 2.35 (s, 3H), 6.94 (d, J = 7.9 Hz, 1H), 6.95 (s, 1H), 7.46 (d, J = 8.3 Hz, 1H).

^{13}C NMR (101 MHz, $CDCl_3$) δ 20.94, 21.05, 112.79, 124.46, 128.40, 132.98, 139.10, 148.09, 168.80.

2-allyl-5-methylphenol (74)

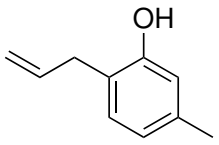

To a solution of 2-bromo-5-methylphenyl acetate (100 mg, 0.44 mmol) in THF (2 mL), allylboronic acid pinacol ester (246 μL, 1.31 mmol, 3 eq.) and K_2CO_3 (180 mg, 1.31 mmol, 3 eq.) were added in a microwave vial. Solution was left stirring in ultrasonic bath for 10 min. and N_2 was purged through the vial. $Pd(PPh_3)_4$ catalyst (26 mg,0.022 mmol, 0.05 eq.) was added and the reaction vial was heated for 50 min at 100 °C under microwave irradiation. The

reaction mixture was filtered through Celite 535RVS and concentrated under reduced pressure. The crude residue was dissolved in anhydrous THF (25 mL) and $LiAlH_4$ (100 mg, 26 mmol) was added at 0 °C. The reaction was quenched with a aqueous solution of potassium sodium tartrate, extracted with EtOAc, dried over $MgSO_4$ and concentrated under vacuo. The residue obtained was purified by SiO_2 column chromatography using a mixture of EtOAc:hexane (1:8) as eluent to afford 2-allyl-5-methylphenol (55 mg, 0.37 mmol, 85 %) as a colorless liquid.

^{1}H NMR (400 MHz, $CDCl_3$) δ 2.30 (s, 3H), 3.39 (d, J = 6.4 Hz, 2H), 4.98 (s, OH, 1H), 5.16 (dd, J = 9.8, 1.5 Hz, 1H) 5.17 (dd, J = 18.9, 1.6 Hz, 1H), 6.03 (ddt, J = 16.7, 10.2, 6.4 Hz, 1H), 6.66 (d, J = 1.7 Hz, 1H), 6.72 (dd, J = 7.6, 1.7 Hz, 1H), 7.01 (d, J = 7.6 Hz, 1H).

^{13}C NMR (101 MHz, $CDCl_3$) δ 21.12, 34.92, 116.38, 116.65, 121.79, 122.26, 130.35, 136.81, 138.05, 154.04.

1-(2-allyl-5-methylphenoxy)-3-(*tert*-butylamino)propan-2-ol (70c)

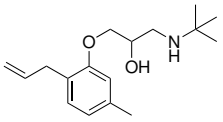

To 2-allyl-5-methylphenol (35 mg, 0.24 mmol) and K_2CO_3 (49 mg, 1.5 eq), epichlorohydrin (1 mL) was added. The reaction mixture was heated under microwave irradiation for 30 min at 120 °C. Reaction crude was then dispersed in water (20 mL) and extracted with EtOAc (3 x 10 mL). Combined organic fraction were washed with 1M aqueous solution of NaOH to remove unreacted phenol. Organic fractions were washed with brine (20 mL), dried over $MgSO_4$ and concentrated under vacuo. Resulting crude was reacted with *tert*-butyl amine (1 mL) under microwave irradiation for 1h at 70 °C. The resulting mixture was concentrated under reduced pressure and purified through flash column chromatography eluted with 3% 1N ammonia in methanol solution in DCM to afford a colorless oil (40 mg, 0.14 mmol, 60 % over two steps).

^{1}H NMR (400 MHz, $CDCl_3$) δ 1.12 (s, 9H), 2.20 (broad s, exchangeable protons, 2H) 2.32 (s, 3H), 2.73 (dd, J = 11.7, 6.5 Hz, 1H), 2.85 (dd, J = 11.8, 3.7 Hz, 1H), 3.35 (d, J = 6.4 Hz, 1H), 3.89 - 4.04 (m, 3H), 5.01 (dd, J = 11.5, 1.7 Hz, 1H), 5.02 (dd, J = 17.3, 1.7 Hz, 1H), 5.97 (ddt, J = 17.7, 9.5, 6.4 Hz, 1H), 6.68 (s, 1H), 6.73 (d, J = 7.6 Hz, 1H), 7.01 (d, J = 7.5 Hz, 1H).

^{13}C NMR (101 MHz, $CDCl_3$) δ 21.43, 29.10, 34.37, 44.72, 50.36, 68.79, 70.50, 112.37, 115.03, 121.44, 125.43, 129.81, 137.38, 137.53, 156.26.

Characterisation of chapter 5 compounds:

***(2S,2'S)*-3,3'-azanediylbis(1-(2-(allyloxy)phenoxy)propan-2-ol) (78b)**

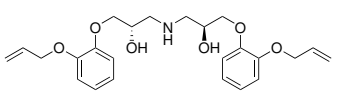

^{1}H NMR (400 MHz, $CDCl_3$) δ 2.59 (broad s, exchangeable protons, 3H), 2.81 - 2.94 (m, 4H), 3.98 - 4.12 (m, 6H), 4.57 (d, J = 5.4 Hz, 4H), 5.28 (dd, J = 10.5, 1.4 Hz, 2H), 5.41 (dd, J = 17.2, 1.6 Hz, 2H), 6.07 (ddt, J = 17.3, 10.5, 5.3 Hz, 2H), 6.86 - 6.98 (m, 8H).

^{13}C NMR (101 MHz, $CDCl_3$) δ 52.03, 68.78, 70.03, 73.16, 114.37, 115.93, 117.95, 121.66, 122.32, 133.47, 148.81, 149.17.

_(S)_-1-(2-(allyloxy)phenoxy)-3-((_(R)_-3-(2-(allyloxy)phenoxy)-2-hydroxypropyl)amino)propan-2-ol (83b)

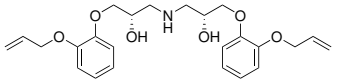

^{1}H NMR (400 MHz, $CDCl_3$) δ 2.79 (broad s, exchangeable protons, 3H), 2.80 - 2.94 (m, 4H), 3.97 - 4.14 (m, 6H), 4.57 (d, J = 5.3 Hz, 4H), 5.28 (dd, J = 10.5, 1.4 Hz, 2H), 5.41 (dd, J = 17.2, 1.6 Hz, 2H), 6.07 (ddt, J = 17.3, 10.6, 5.4 Hz, 2H), 6.88 - 6.97 (m, 8H).

^{13}C NMR (101 MHz, $CDCl_3$) δ 52.09, 68.70, 70.04, 73.10, 114.36, 115.87, 117.99, 121.68, 122.31, 133.45, 148.77, 149.13.

_(2R,2'R)_-3,3'-azanediylbis(1-(2-(allyloxy)phenoxy)propan-2-ol) (82b)

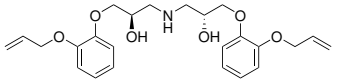

^{1}H NMR (400 MHz, $CDCl_3$) δ 2.66 (broad s, exchangeable protons, 3H), 2.79 - 2.94 (m, 4H), 3.97 - 4.14 (m, 6H), 4.57 (d, J = 5.3 Hz, 4H), 5.28 (dd, J = 10.5, 1.5 Hz, 2H), 5.41 (dd, J = 17.3, 1.6 Hz, 2H), 6.07 (ddt, J = 17.4, 10.6, 5.3 Hz, 2H), 6.87 - 6.98 (m, 8H).

^{13}C NMR (101 MHz, $CDCl_3$) δ 52.04, 68.79, 70.03, 73.16, 114.37, 115.92, 117.94, 121.66, 122.31, 133.46, 148.81, 149.17.

_(2S,2'S)_-3,3'-azanediylbis(1-(2-allylphenoxy)propan-2-ol) (78a)

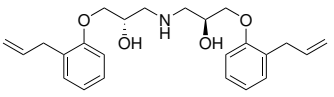

^{1}H NMR (400 MHz, $CDCl_3$) δ 2.78 (broad s, exchangeable protons, 3H), 2.89 (dd, J = 12.3, 7.2 Hz, 2H), 2.95 (dd, J = 12.3, 4.1 Hz, 2H), 3.40 (dd, J = 6.4, 2.0 Hz, 4H), 4.01 (d, J = 5.8 Hz, 4H), 4.10 - 4.18 (m, 2H), 5.03 (dd, J = 18.7, 1.8 Hz, 2H), 5.04 (dd, J = 8.5, 1.7 Hz, 2H), 5.98 (ddt, J = 16.7,

10.3, 6.3 Hz, 2H), 6.84 (dd, J = 8.2, 1.1 Hz, 2H), 6.92 (td, J = 7.4, 1.1 Hz, 2H), 7.15 (dd, J = 7.4, 1.7 Hz, 2H), 7.19 (td, J = 7.8, 1.8 Hz, 2H).

^{13}C NMR (101 MHz, $CDCl_3$) δ 34.84, 52.16, 68.85, 70.44, 111.50, 115.42, 121.22, 127.68, 128.58, 130.30, 137.43, 156.38.

(*S*)-1-(2-allylphenoxy)-3-(((*R*)-3-(2-allylphenoxy)-2-hydroxypropyl)amino)-propan-2-ol (83a)

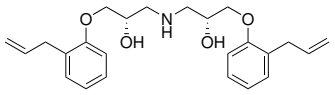

^{1}H NMR (400 MHz, $CDCl_3$) δ 2.62 (broad s, exchangeable protons, 3H), 2.86 (dd, J = 12.2, 7.5 Hz, 2H), 2.93 (dd, J = 12.2, 4.1 Hz, 2H), 3.40 (dd, J = 6.4, 1.8 Hz, 4H), 4.00 (d, J = 5.8 Hz, 2H), 4.01 (d, J = 4.0 Hz, 2H), 4.08 - 4.16 (m, 2H), 5.04 (dd, J = 18.6, 1.7 Hz, 2H), 5.05 (dd, J = 8.7, 1.6 Hz, 2H), 5.99 (ddt, J = 16.7, 10.4, 6.4 Hz, 2H), 6.84 (dd, J = 8.2, 1.1 Hz, 2H), 6.93 (td, J = 7.5, 1.1 Hz, 2H), 7.15 (dd, J = 7.4, 1.7 Hz, 2H), 7.19 (td, J = 7.8, 1.8 Hz, 2H).

^{13}C NMR (101 MHz, $CDCl_3$) δ 34.85, 52.24, 69.03, 70.50, 111.49, 115.41, 121.20, 127.68, 128.59, 130.29, 137.45, 156.40.

***(2R,2'R)*-3,3'-azanediylbis(1-(2-allylphenoxy)propan-2-ol) (82a)**

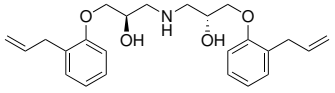

^{1}H NMR (400 MHz, $CDCl_3$) δ 2.65 (broad s, exchangeable protons, 3H), 2.88 (dd, J = 12.3, 7.1 Hz, 2H), 2.94 (dd, J = 12.3, 4.0 Hz, 2H), 3.40 (dd, J = 6.4, 2.0 Hz, 4H), 4.01 (d, J = 4.2 Hz, 2H), 4.01 (d, J = 6.0 Hz, 2H), 4.13 (q, J = 6.0 Hz, 2H), 5.03 (dd, J = 18.7, 1.8 Hz, 2H), 5.04 (dd, J = 8.4, 1.7 Hz, 2H), 5.98 (ddt, J = 16.7, 10.3, 6.4 Hz, 2H), 6.84 (dd, J = 8.2, 1.1 Hz, 2H), 6.92 (td, J = 7.4, 1.1 Hz, 2H), 7.15 (dd, J = 7.4, 1.7 Hz, 2H), 7.19 (td, J = 7.8, 1.8 Hz, 2H).

^{13}C NMR (101 MHz, $CDCl_3$) δ 34.85, 52.16, 68.87, 70.45, 111.50, 115.42, 121.22, 127.68, 128.59, 130.30, 137.44, 156.39.

***(R)*-1-(2-(allyloxy)phenoxy)-3-aminopropan-2-ol (81b)**

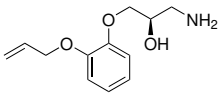

^{1}H NMR (400 MHz, $CDCl_3$) δ 2.19 (broad s, exchangeable protons, 3H), 2.87 (dd, J = 12.8, 6.0 Hz, 1H), 2.94 (dd, J = 12.9, 4.1 Hz, 1H), 3.91 - 4.02 (m, 2H), 4.02 - 4.10 (m, 1H), 4.56 (dt, J = 5.3, 1.5 Hz, 2H), 5.28 (dd, J = 10.5, 1.4 Hz, 1H), 5.41 (dd, J = 17.3, 1.6 Hz, 1H), 6.07 (ddt, J = 17.3, 10.6, 5.3 Hz, 1H), 6.86 - 6.97 (m, 4H).

^{13}C NMR (101 MHz, $CDCl_3$) δ 44.26, 70.01, 70.53, 72.89, 114.30, 115.68, 117.95, 121.66, 122.22, 133.43, 148.84, 149.11.

(S)-1-(2-(allyloxy)phenoxy)-3-aminopropan-2-ol (77b)

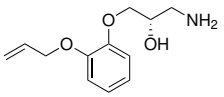

^{1}H NMR (400 MHz, $CDCl_3$) δ 2.17 (broad s, exchangeable protons, 3H), 2.87 (dd, J = 12.9, 5.9 Hz, 1H), 2.94 (dd, J = 12.9, 3.9 Hz, 1H), 3.91 - 4.02 (m, 2H), 4.03 - 4.10 (m, 1H), 4.57 (dt, J = 5.4, 1.5 Hz, 2H), 5.28 (dd, J = 10.5, 1.4 Hz, 1H), 5.42 (dd, J = 17.3, 1.6 Hz, 1H), 6.07 (ddt, J = 17.3, 10.6, 5.3 Hz, 1H), 6.87 - 6.97 (m, 4H).

^{13}C NMR (101 MHz, $CDCl_3$) δ 44.24, 70.00, 70.51, 72.86, 114.25, 115.60, 118.00, 121.66, 122.20, 133.40, 148.79, 149.05.

(R)-1-(2-allylphenoxy)-3-aminopropan-2-ol (81a)

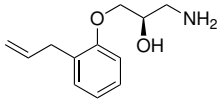

^{1}H NMR (400 MHz, $CDCl_3$) δ 2.05 (broad s, exchangeable protons, 3H), 2.88 (dd, J = 13.0, 6.1 Hz, 1H), 2.98 (dd, J = 12.9, 3.5 Hz, 1H), 3.39 (dd, J = 6.3, 1.7 Hz, 2H), 3.89 - 4.06 (m, 3H), 5.02 (dd, J = 10.6, 1.8 Hz, 1H), 5.03 (dd, J = 18.8, 1.8 Hz, 1H), 5.99 (ddt, J = 16.7, 10.3, 6.4 Hz, 1H), 6.85 (dd, J = 8.2, 1.1 Hz, 1H), 6.92 (td, J = 7.4, 1.1 Hz, 1H), 7.15 (dd, J = 7.4, 1.7 Hz, 1H), 7.19 (td, J = 7.8, 1.8 Hz, 1H).

^{13}C NMR (101 MHz, $CDCl_3$) δ 34.85, 44.31, 70.14, 70.80, 111.45, 115.39, 121.15, 127.66, 128.58, 130.27, 137.43, 156.44.

(S)-1-(2-allylphenoxy)-3-aminopropan-2-ol (77a)

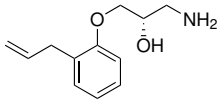

^{1}H NMR (400 MHz, $CDCl_3$) δ 2.08 (broad s, exchangeable protons, 3H), 2.88 (dd, J = 13.0, 6.1 Hz, 1H), 2.98 (dd, J = 12.8, 3.4 Hz, 1H), 3.39 (dd, J = 6.4, 1.7 Hz, 2H), 3.90 - 4.09 (m, 3H), 5.02 (dd, J = 10.5, 1.8 Hz, 1H), 5.03 (dd, J = 18.8, 1.8 Hz, 1H), 5.99 (ddt, J = 16.7, 10.4, 6.4 Hz, 1H), 6.85 (dd, J = 8.1, 1.1 Hz, 1H), 6.92 (td, J = 7.4, 1.1 Hz, 1H), 7.15 (dd, J = 7.5, 1.7 Hz, 1H), 7.19 (td, J = 7.8, 1.8 Hz, 1H).

^{13}C NMR (101 MHz, $CDCl_3$) δ 34.84, 44.31, 70.15, 70.78, 111.44, 115.39, 121.14, 127.66, 128.58, 130.27, 137.42, 156.44.

1-(2-allylphenoxy)-3-((2-hydroxypropyl)amino)propan-2-ol (85)

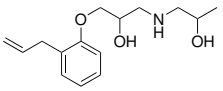

General procedure for epoxide opening (method C). Yield: 45 %

^{1}H NMR (401 MHz, $CDCl_3$) δ 1.18 (d, J = 6.2 Hz, 3H), 2.28 (s, 3H), 2.50 (ddd, J = 12.1, 9.2, 2.9 Hz, 1H), 2.75 (ddd, J = 12.1, 3.0, 1.7 Hz, 1H), 2.79 - 2.94 (m, 2H), 3.40 (d, J = 5.2 Hz, 2H), 3.83 (dqd, J = 9.2, 6.1, 3.1 Hz, 1H), 3.95 - 4.04 (m, 2H), 4.11 (ttt, J = 6.0, 4.0, 1.7 Hz, 1H), 5.02 (dq, J = 10.2, 1.6 Hz, 1H), 5.03 (dq, J = 17.0, 1.7 Hz, 1H), 5.98 (ddt, J = 16.7, 10.2, 6.3 Hz, 1H), 6.84 (d, J = 8.2 Hz, 1H), 6.92 (td, J = 7.3, 1.1 Hz, 1H), 7.15 (dd, J = 7.4, 1.7 Hz, 1H), 7.19 (td, J = 7.8, 1.8 Hz, 1H).

^{13}C NMR (101 MHz, $CDCl_3$) δ 20.70, 34.88, 51.97, 57.10, 66.10, 69.14, 70.52, 111.50, 115.39, 121.24, 127.70, 128.55, 130.33, 137.49, 156.39.

3,3'-(methylazanediyl)bis(1-(2-allylphenoxy)propan-2-ol) (86)

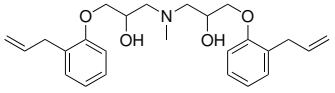

General procedure for epoxide opening (method C). Yield: 72 %

^{1}H NMR (401 MHz, $CDCl_3$) δ 2.44 (d, J = 7.2 Hz, 3H), 2.60 - 2.80 (m, 4H), 3.40 (d, J = 5.5 Hz, 2H), 3.94 - 4.06 (m, 4H), 4.14 (dq, J = 8.9, 4.5 Hz, 2H), 5.04 (dq, J = 15.8, 1.7 Hz, 2H), 5.05 (dq,J = 10.0, 1.7 Hz, 2H), 5.99 (ddt, J = 18.0, 9.3, 6.4 Hz, 2H), 6.84 (d, J = 8.2 Hz, 2H), 6.92 (t, J = 7.4 Hz, 2H), 7.15 (dd, J = 7.5, 1.5 Hz, 2H), 7.19 (td, J = 8.0, 1.7 Hz, 2H)

^{13}C NMR (101 MHz, $CDCl_3$) δ 34.79, 34.81, 43.71, 60.81, 61.26, 67.48, 67.77, 70.29, 70.31, 111.46, 111.49, 115.44, 121.14, 127.63, 127.64, 128.66, 130.23, 137.39, 137.41, 156.41.

***tert*-butyl (3-bromopropyl)carbamate (88)**

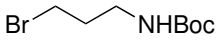

To a mixture of boc anhydride (2.74 mmol, 1.2 eq), 3-bromopropylamine hydrobromide (2.28 mmol, 1 eq) in dichloromethane (20 mL), triethylamine (9.14 mmol, 4 eq) was added dropwise and left stirring for 24h at room temperature. The reaction mixture was then washed with 1M HCl (2 x 5 mL) and water (2 x 5 mL). The organic phase was dried over anhydrous $MgSO_4$ and concentrated under vacuo to afford compound 88 as a yellow oil in 93 % yield.

^{1}H NMR (401 MHz, $CDCl_3$) δ 1.43 (s, 9H), 2.04 (p, J = 6.6 Hz, 2H), 3.26 (t, J = 6.4 Hz, 2H), 3.43 (t, J = 6.5 Hz, 2H), 4.67 (s, 1H).

^{13}C NMR (101 MHz, $CDCl_3$) δ 28.49, 30.90, 32.82, 39.10, 79.52, 156.08.

3-(2-allylphenoxy)propan-1-amine (89)

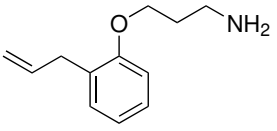

2-Allylphenol (1.26 mmol, 1.5 eq) was dissolved in DMF (2 mL) and potassium carbonate (1.51 mmol, 1.8 eq) and *tert*-butyl (3-bromopropyl)carbamate (88, 0.84 mmol, 1 eq) were added. The reaction was stirred at room temperature for 24h. Water (100 mL) was added to the reaction mixture and then extracted with diethyl ether. The organic phase was washed with 5% sodium hydroxide solution and brine and concentrated under vacuum. Without further purification the crude was dissolved in dichloromethane (2 mL), TFA was added dropwise and the reaction mixture was left stirring at room temperature for 4h. The reaction mixture was poured into a solution of ethyl acetate: 1M sodium hydroxide (1:1, 20 mL) and then extracted with further ethyl acetate (10 mL x 2). Combined organic fractions were washed with brine, dried over anhydrous $MgSO_4$ and concentrated under vacuo to give compound **89** as a colorless oil (82 % over two steps).

^{1}H NMR (401 MHz, $CDCl_3$) δ 1.96 (dt, J = 12.8, 6.4 Hz, 2H), 2.02 (s, 2H), 2.94 (t, J = 6.8 Hz, 2H), 3.39 (d, J = 6.6 Hz, 2H), 4.05 (t, J = 6.0 Hz, 2H), 5.03 (ddd, J = 10.1, 3.2, 1.6 Hz, 1H), 5.04 (dq, J = 18.2, 1.5 Hz, 1H), 5.99 (ddt, J = 16.8, 10.1, 6.6 Hz, 1H), 6.85 (d, J = 8.2 Hz, 1H), 6.89 (t, J = 7.4 Hz, 1H), 7.14 (d, J = 8.0 Hz, 1H), 7.18 (t, J = 7.8 Hz, 1H).

^{13}C NMR (101 MHz, $CDCl_3$) δ 32.98, 34.53, 39.33, 65.77, 111.20, 115.42, 120.60, 127.40, 128.74, 129.91, 137.13, 156.65.

1-(2-allylphenoxy)-3-((3-(2-allylphenoxy)propyl)amino)propan-2-ol (90)

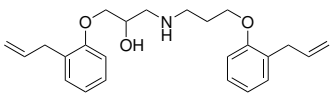

General procedure for epoxide opening (method C). Yield: 51 %

^{1}H NMR (401 MHz, $CDCl_3$) δ 2.02 (p, J = 6.5 Hz, 2H), 2.39 (broad s, 2H), 2.80 - 2.95 (m, 4H), 3.39 (d, J = 6.3 Hz, 4H), 4.00 (d, J = 5.2 Hz, 2H), 4.06 (t, J = 6.0 Hz, 2H), 4.06 - 4.13 (m, 1H), 5.00 - 5-08 (m, 4H), 5.99 (ddt, J = 16.9, 10.2, 6.5 Hz, 2H), 6.85 (d, J = 8.2 Hz, 2H), 6.91 (td, J = 7.5, 1.0 Hz, 2H), 7.15 (d, J = 7.7 Hz, 2H), 7.19 (td, J = 7.9, 1.7 Hz, 2H).

^{13}C NMR (101 MHz, $CDCl_3$) δ 29.98, 34.56, 34.81, 47.19, 52.12, 66.19, 68.59, 70.59, 111.28, 111.50, 115.41, 115.47, 120.69, 121.11, 127.46, 127.64, 128.61, 128.77, 129.98, 130.22, 137.16, 137.39, 156.45, 156.65.

1-(2-allylphenoxy)-3-((2-aminoethyl)amino)propan-2-ol (94a)

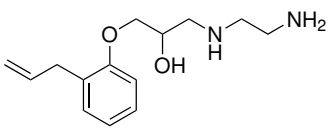

General procedure for epoxide opening (method B). Purification by HPLC.

^{1}H NMR (401 MHz, DMSO) δ 2.56 – 2.66 (m, 6H), 3.33 (d, J = 6.7 Hz, 2H), 3.82 – 3.96 (m, 3H), 4.99 (dd, J = 10.3, 1.9 Hz, 1H), 5.04 (dd, J = 17.1, 1.9 Hz, 1H), 5.96 (ddt, J = 16.9, 10.0, 6.7 Hz, 1H), 6.86 (td, J = 7.4, 1.1 Hz, 1H), 6.89 – 7.02 (m, 1H), 7.10 (dd, J = 7.5, 1.7 Hz, 1H), 7.16 (td, J = 7.8, 1.8 Hz, 1H).

^{13}C NMR (101 MHz, $CDCl_3$) δ 33.95, 41.48, 52.45, 52.60, 68.29, 70.61, 111.58, 115.41, 120.28, 127.40, 128.00, 129.43, 137.08, 156.22.

3,3'-(ethane-1,2-diylbis(azanediyl))bis(1-(2-allylphenoxy)propan-2-ol) (95a)

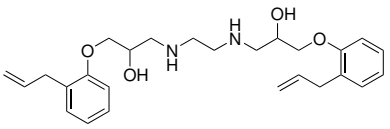

General procedure for epoxide opening (method B). Purification by HPLC.

^{1}H NMR (401 MHz, $CDCl_3$) δ 2.78 - 2.94 (m, 12H), 3.39 (d, J = 6.2 Hz, 4H), 3.98 (dd, J = 5.3, 1.9 Hz, 4H), 4.10 (dq, J = 9.1, 5.1 Hz, 2H), 4.99 - 5.07 (m, 4H), 5.98 (ddt, J = 18.1, 9.3, 6.4 Hz, 2H), 6.84 (d, J = 8.1 Hz, 2H), 6.91 (td, J = 7.4, 0.9 Hz, 2H), 7.14 (dd, J = 7.4, 1.6 Hz, 2H), 7.18 (td, J = 8.0, 1.7 Hz, 2H).

^{13}C NMR (101 MHz, $CDCl_3$) δ 34.77, 49.24, 52.04, 68.77, 68.81, 70.49, 111.50, 115.42, 121.09, 127.62, 128.60, 130.18, 137.38, 156.42. tR 5.431 (method B)

3,3'-(propane-1,3-diylbis(azanediyl))bis(1-(2-allylphenoxy)propan-2-ol) (95b)

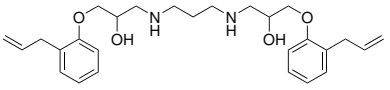

General procedure for epoxide opening (method B). Purification by HPLC.

1.75 - 1.87 (m, 2H), 2.69 - 3.07 (m, 8H), 3.39 (d, J = 6.2 Hz, 4H), 3.80 (broad s, 4H), 3.96 (dd, J = 9.5, 5.4 Hz, 4H), 4.02 (dd, J = 9.4, 5.3 Hz, 2H), 4.11 - 4.20 (m, 2H), 5.02 (d, J = 16.4 Hz, 2H), 5.03 (d, J = 10.7 Hz, 2H), 5.97 (ddt, J = 17.5, 9.2, 6.4 Hz, 2H), 6.84 (d, J = 8.1 Hz, 2H), 6.91 (t, J = 7.4 Hz, 2H), 7.13 (d, J = 7.4 Hz, 2H), 7.17 (t, J = 7.8 Hz, 2H)

^{13}C NMR (101 MHz, $CDCl_3$) δ 27.49, 34.66, 49.15, 49.19, 51.93, 52.08, 67.91, 68.10, 70.05, 70.29, 111.50, 111.52, 115.44, 115.48, 121.15, 121.18, 127.63, 127.65, 128.57, 128.62, 130.14, 130.20, 137.33, 137.34, 156.30.

8.2.3 Chapter 6 synthesis

2-(4-(benzyloxy)phenyl)ethan-1-ol (109)

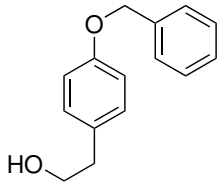

Potassium carbonate (7.96 mmol, 1.1 eq) was added to a round bottom flask containing *p*-Hydroxyphenethyl alcohol (7.24 mmol, 1 eq) in 20 mL DMF and left stirring for 30 min at room temperature. Benzyl bromide (7.96 mmol, 1.1 eq) was added dropwise and the reaction mixture was left sitting at 60 °C for 24h. After monitoring completion by TLC, the reaction was quenched with water (100 mL) and extracted with ethyl acetate (50 mL x 3). The combined organic layers were washed with water (50 mL), brine (30 mL), dried over anhydrous $MgSO_4$ and concentrated under vacuo to afford compound 109 as a white solid in 92 % yield.

^{1}H NMR (401 MHz, $CDCl_3$) δ 1.50 (s, 1H), 2.82 (t, J= 6.5 Hz, 2H), 3.83 (t, J= 6.5 Hz, 2H), 5.06 (s, 2H), 6.91-6.96 (m, 2H), 7.12-7.18 (m, 2H), 7.30-7.35 (m, 1H), 7.36-7.41 (m, 2H), 7.42-7.46 (m, 2H).

^{13}C NMR (101 MHz, $CDCl_3$) δ 38.42, 63.94, 70.19, 115.15, 127.59, 128.07, 128.72, 130.14, 130.85, 137.23, 157.67.

1-(benzyloxy)-4-(2-(cyclopropylmethoxy)ethyl)benzene (111)

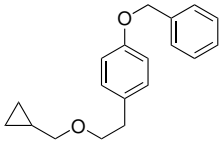

To suspension of 60% sodium hydride in mineral oil (14.46 mmol, 1.1 eq) in 40 mL of DMF under inert atmosphere 2-(4-(benzyloxy)phenyl)ethan-1-ol (109, 13.14 mmol, 1 eq) was added and left stirring for 15 minutes. Cyclopropylmethyl bromide (110, 14.46 mmol, 1.1 eq) was then added to the reaction mixture and heated at 60 °C for 48h. The reaction mixture was then poured into cold water (100 mL) and extracted with ether. The combined organic layers were then washed with water, dried with anhydrous $MgSO_4$ and concentrated under vacuo. The residue was stirred for 30 minutes in petroleum ether, filtered and evaporated to dryness to afford 1-(benzyloxy)-4-(2-(cyclopropylmethoxy)ethyl)benzene (111) in 76 % yield.

^{1}H NMR (401 MHz, $CDCl_3$) δ 0.22 (q, J = 5.1 Hz, 2H), 0.55 (q, J = 5.1 Hz, 2H), 1.01-1.14 (m, 1H), 2.87 (t, J = 7.4 Hz, 2H), 3.30 (d, J = 6.8 Hz, 2H), 3.64 (t, J = 7.4 Hz, 2H), 5.06 (s, 2H), 6.92 (d, J = 8.3 Hz, 2H), 7.16 (d, J = 8.5 Hz, 2H), 7.33 (t, J = 7.1 Hz, 1H), 7.39 (t, J = 7.4 Hz, 2H), 7.44 (d, J = 7.4 Hz, 2H).

^{13}C NMR (101 MHz, $CDCl_3$) δ 3.11, 10.75, 35.62, 70.14, 71.94, 75.74, 114.87, 127.56, 128.00, 128.67, 129.96, 131.47, 137.30, 157.40.

4-(2-(cyclopropylmethoxy)ethyl)phenol (112)

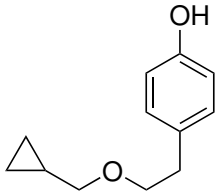

1-(benzyloxy)-4-(2-(cyclopropylmethoxy)ethyl) benzene (111, 4.15 mmol, 1 eq), 10% Pd/C (catalytical, 0.01 eq) were stirred in methanol (10 mL) under hydrogen atmosphere using an hydrogen balloon at room temperature for 5h. Completion of the reaction was checked by TLC and once complete the catalyst was filtered and the filtrate concentrated under vacuum to yield 4-(2-(cyclopropylmethoxy)ethyl)phenol (112) in 84 %.

^{1}H NMR (401 MHz, $CDCl_3$) δ 0.20 (q, J= 4.6 Hz 2H), 0.53 (td, J= 5.9, 4.5 Hz, 2H), 0.98-1.13 (m, 1H), 2.84 (t, J= 7.4 Hz, 2H), 3.31 (d, J= 6.9 Hz, 2H), 3.64 (t, J= 7.4 Hz, 2H), 5.61 (s, 1H), 6.74 (d, J= 8.5 Hz, 2H), 7.07 (d, J= 8,4 Hz, 2H).

^{13}C NMR (101 MHz, $CDCl_3$) δ 3.19, 10.68, 35.48, 72.00, 75.85, 115.39, 130.06, 130.78, 154.37.

(S)-2-((4-(2-(cyclopropylmethoxy)ethyl)phenoxy)methyl)oxirane (113)

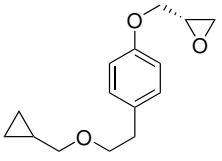

To suspension of 60% sodium hydride in mineral oil (3.12 mmol, 1.2 eq) in 20 mL of DMF under inert atmosphere 4-(2-(cyclopropyl methoxy)ethyl)phenol (112, 2.6 mmol, 1 eq) was added and left stirring for 30 minutes at room temperature. *S*-Glycidyl nosylate was then added and heated at 60 °C for 14h. The reaction mixture was poured into cold water and extracted with ether. The combined organic layers were dried with anhydrous $MgSO_4$ and concentrated under vacuo. The crude was purified by FCC using petroleum ether: ethyl acetate (95:5) as eluent to yield (S)-2-((4-(2-(cyclopropylmethoxy)ethyl)phenoxy)methyl)oxirane (113) in 64 % yield.

^{1}H NMR (401 MHz, $CDCl_3$) δ 0.19 (q, J = 4.5 Hz, 2H), 0.52 (td, J = 5.9, 4.5 Hz, 2H), 0.97 - 1.11 (m, 1H), 2.75 (dd, J = 4.9, 2.7 Hz, 1H), 2.84 (t, J = 7.4 Hz, 2H), 2.89 (t, J = 4.7 Hz, 1H), 3.28 (d, J = 6.9 Hz, 2H), 3.34 (ddt, J = 5.8, 4.0, 3.0 Hz, 1H), 3.61 (t, J = 7.4 Hz, 2H), 3.95 (dd, J = 11.0, 5.6 Hz, 1H), 4.19 (dd, J = 11.0, 3.3 Hz, 1H), 6.85 (d, J = 8.7 Hz, 2H), 7.14 (d, J = 8.7 Hz, 2H).

***tert*-butyl (2-amino-2-methylpropyl)carbamate (114)**

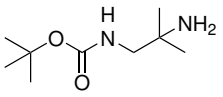

A mixture of boc anhydride (2.70 mmol, 1 eq), 1,2-diamino-2-methylpropane (91, 5.67 mmol, 2.1 eq) and triethylamine (5.67 mmol, 2.1 eq) in dichloromethane (5 mL) were stirred for 24h at room temperature. The reaction mixture was then concentrated to dryness and the crude was purified by FCC using methanol : dichloromethane (10:1) to afford *tert*-butyl (2-amino-2-methylpropyl)carbamate (114) as a white solid in 85 % yield.

^{1}H NMR (401 MHz, $CDCl_3$) δ 1.04 (s, 6H), 1.22 (s, 2H), 1.39 (s, 9H), 2.95 (d, J = 6.2 Hz, 2H), 5.05 (s, 1H).

^{13}C NMR (101 MHz, $CDCl_3$) δ 28.26, 28.46, 50.26, 52.19, 79.11, 156.54.

tert-butyl (S)-(2-((3-(4-(2-(cyclopropylmethoxy)ethyl)phenoxy)-2-hydroxypropyl)-amino)-2-methylpropyl)carbamate (115)

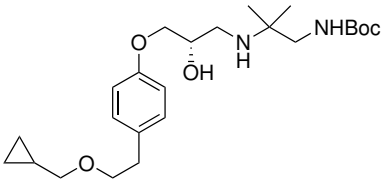

Amine **114** was added to a solution of epoxide **113** in DMF:water (9:1) and left stirring at room temperature for 48h. The reaction mixture was concentrated to dryness and purified by FCC using 6% 1N ammonia in methanol in DCM to afford *tert*-butyl (S)-(2-((3-(4-(2-(cyclopropylmethoxy)ethyl)phenoxy)-2-hydroxy propyl)amino)-2-methylpropyl)carbamate in 45 % yield.

^{1}H NMR (401 MHz, $CDCl_3$) δ 0.19 (dt, J = 6.0, 4.5 Hz, 2H), 0.53 (dq, J = 8.1, 6.0 Hz 2H), 1.02 - 1.08 (m, 1H), 1.10 (s, 6H), 1.44 (s, 9H), 2.52 (broad s, exchangeable protons, 2H), 2.73 (d, J = 7.5 Hz, 2H), 2.84 (t, J = 7.4 Hz, 2H), 3.05 - 3.15 (m, 2H), 3.28 (d, J = 6.8 Hz, 2H), 3.61 (t, J = 7.4 Hz, 2H), 3.97 (dd, J = 5.1, 2.9 Hz, 2H), 3.99 - 4.10 (m, 1H), 4.98 (s, 1H, N-H amide), 6.84 (d, J = 8.6 Hz, 2H), 7.13 (d, J = 8.6 Hz, 1H).

^{13}C NMR (101 MHz, $CDCl_3$) δ 3.12, 10.77, 24.96, 25.15, 28.55, 35.62, 44.61, 48.43, 53.67, 69.13, 70.65, 71.95, 75.78, 79.51, 114.63, 130.00, 131.72, 156.64, 157.22.

tR: 5.748 (method B)

(S)-N-(2-((3-(4-(2-(cyclopropylmethoxy)ethyl)phenoxy)-2-hydroxypropyl)amino)-2-methylpropyl)-4-(3-(trifluoromethyl)-3H-diazirin-3-yl)benzamide (107)

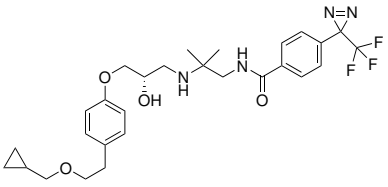

Compound **115** was dissolved in dichloromethane (2 mL) and TFA was

added dropwise. The reaction mixture was left stirring at room temperature for 2h. The reaction mixture was poured into a solution of ethyl acetate: 1M sodium hydroxide (1:1, 20 mL) and then extracted with further ethyl acetate (10 mL x 2). Combined organic fractions were washed with brine, dried over anhydrous $MgSO_4$ and concentrated under vacuo. Without further purification, the crude was dissolved in 10 mL of acetonitrile and the carboxylic acid (**116**, 1.1 eq) and triethylamine (2 eq) were added and left stirring for 10 minutes. HATU (1.2 eq) was then added and the reaction mixture was controlled by TLC and left stirring at room temperature for 18h. The reaction mixture was then washed with water (1 x 5 mL), extracted with DCM, and the crude product was purified by HPLC.

^{1}H NMR (401 MHz, $CDCl_3$) δ 0.19 (q, J = 4.7 Hz, 2H), 0.52 (q, J = 4.7 Hz, 2H), 0.97 - 1.11 (m, 1H), 1.17 (s, 6H), 2.44 (broad s, exchangeable protons, 2H), 2.76 (dd, J = 12.0, 7.2 Hz, 1H), 2.85 (t, J = 7.3 Hz, 2H), 2.87 (dd, J = 7.8, 4.1 Hz, 1H), 3.28 (d, J = 6.8 Hz, 2H), 3.41 (t, J = 5.2 Hz, 2H), 3.61 (t, J = 7.3 Hz, 2H), 3.98 (dd, J = 5.2, 3.3 Hz, 2H), 4.07 (dt, J = 7.1, 3.2 Hz, 1H), 6.80 (d, J = 8.6 Hz, 2H), 7.02 (s, 1H), 7.13 (d, J = 8.6 Hz, 2H), 7.20 (d, J = 8.2 Hz, 2H), 7.81 (d, J = 8.5 Hz, 2H).

^{13}C NMR (101 MHz, $CDCl_3$) δ 3.12, 10.75, 25.53, 25.59, 35.58, 44.36, 46.92, 53.42, 69.54, 70.47, 71.85, 75.77, 114.54, 121.93 (q, J = 274.8 Hz), 126.72, 127.57, 130.08, 132.09, 132.31, 135.78, 156.98, 166.48.

Appendix A

Sequence of turkey and human β_1 receptors

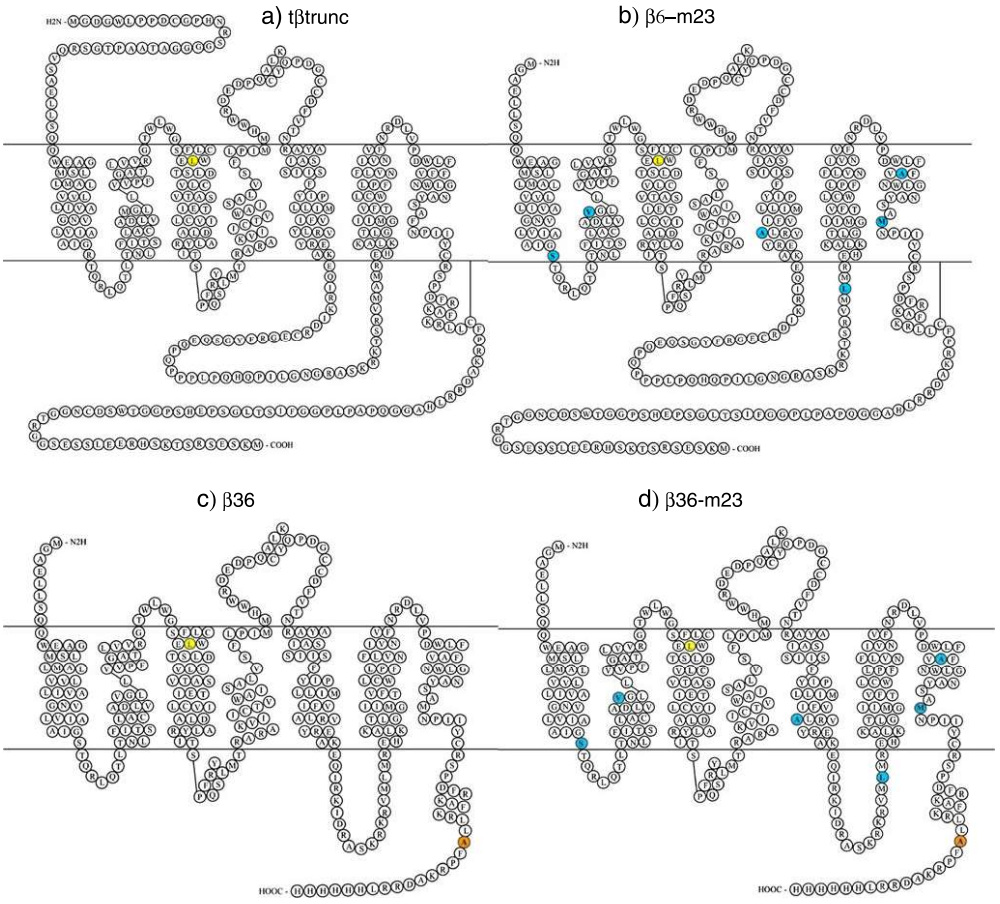

FIGURE A.1: Amino acid sequence of the turkey tβtrunc), β6–m23, β36 and β36–m23, taken from Baker *et al.*[54]

```
humanβ1  1    MGAGVLVLGASEPGNLSSAAP---LPDGAATAARLLVPASPPASLLPPASE--SPEPLSQQWTAGMGLLMALIVLLIVAG  75
humanβ2  1    ---------MGQPGN---GSAFLLAPNGSHAP-----------DHDVTQQR-------DEVWVVGMGIVMSLIVLAIVFG  50
humanβ3  1    M--------APWPHENSSLAPWPDLPTLAPNTAN--------TSGLPGVPW---EAALA-----GA--LLALAVLATVGG  54
tβtrunc  1    MGDGWLPPDCG-PHNRSGG--------GGATAA------------PTGSRQVSAELLSQQWEAGMSLLMALVVLLIVAG  58
tβ3C     1    ---------MGVAGT---E-----LPGGNVSANQ--------SDADPTVSR-------D-VWVVGMGILMSLIVLVIVFG  47
tβ4C     1    M--------TPLPAGNGSV---------------------------PNCSW---AAVLSRQWAVGA--ALSITILVIVAG  40

humanβ1  76   NVLVIVAIAKTPRLQTLTNLFIMSLASADLVMGLLVVPFGATIVVWGRWEYGSFFCELWTSVDVLCVTASIETLCVIALD  155
humanβ2  51   NVLVITAIAKFERLQTVTNYFITSLACADLVMGLAVVPFGAAHILMKMWTFGNFWCEFWTSIDVLCVTASIETLCVIAVD  130
humanβ3  55   NLLVIVAIAWTPRLQTMTNVFVTSLAAADLVMGLLVVPPAATLALTGHWPLGATGCELWTSVDVLCVTASIETLCALAVD  134
tβtrunc  59   NVLVIAAIGRTQRLQTLTNLFITSLACADLVMGLLVVPFGATLVVRGTWLWGSFLCECWTSLDVLCVTASIETLCVIAID  138
tβ3C     48   NVLVITAIARFQRLQTVTNYFITSLACADLVMGLGVVPFGACHIIMEMWKFGNFWCEFWTSLDVLCVTASIETLCVIAVD  127
tβ4C     41   NLLVIVAIAKTPRLQTMTNVFVTSLACADLVMGLLVVPPGATILLSGHWPYGTVVCELWTSLDVLCVTASIETLCAIAVD  120

humanβ1  156  RYLAITSPFRYQSLLTRARARGLVCTVWAISALVSFLPILMHWWRA-ESDEARRCYNDPKCCDFVTNRAYAIASSVVSFY  234
humanβ2  131  RYFAITSPFKYQSLLTKNKARVIILMVWIVSGLTSFLPIQMHWYRA-THQEAINCYANETCCDFFTNQAYAIASSIVSFY  209
humanβ3  135  RYLAVTNPLRYGALVTKRCARTAVVLVWVVSAAVSFAPIMSQWWRVGADAEAQRCHSNPRCCAFASNMPYVLLSSSVSFY  214
tβtrunc  139  RYLAITSPFRYQSLMTRARAKVIICTVWAISALVSFLPIMMHWWRD-EDPQALKCYQDPGCCDFVTNRAYAIASSIISFY  217
tβ3C     128  RYFAITSPFKYQSLLTKSKARVVILVVWAISALTSFLPIQMHWYRA-DRDEAILCYEKDTCCDFFTNQAYAIASSIISFY  206
tβ4C     121  RYLAITAPLQYEALVTKGRAWAVVCMVWAISAFISFLPIMNHWWRDGADEQAVRCYDDPRCCDFVTNMTYAIVSSTVSFY  200

humanβ1  235  VPLCIMAFVYLRVFREAQKQVKKIDSCERRFLGGPARPPSPSPSPVPAPAPPPGPPRPAAAAATAPLANGRAGK-RRPSR  313
humanβ2  210  VPLVIMVFVYSRVFQEAKRQLQKIDKSEGRFHVQNLSQ---------------------------VEQDGRTGHGLRRSS  262
humanβ3  215  LPLLVMLFVYARVFVVATRQLRLLRGELGRFPPEESPP-APSRSLAPAPVGTCAPPEGVPAC------------GRRPAR  281
tβtrunc  218  IPLLIMIFVYLRVYREAKEQIRKIDRCEGRFYGSQEQ---PQPPPLPQHQP--------------ILGNGRASK-RKTSR  279
tβ3C     207  LPLVVMVFVYARVFQVAKKQLQKIDRSEGRFHIQNKEQ----------------------------DQNGKAGH--RRSS  256
tβ4C     201  VPLLVMIFVYVRVFAVATRHVQLIGKDKVRFLQENPSL-SSRGGR----------------------------WRRPSR  250

humanβ1  314  LVALREQKALKTLGIIMGVFTLCWLPFFLANVVKAFHREL-VPDRLFVFFNWLGYANSAFNPIIYCRSPDFRKAFQRLLC  392
humanβ2  263  KFCLKEHKALKTLGIIMGTFTLCWLPFFIVNIVHVIQDNL-IRKEVYILLNWIGYVNSGFNPLIYCRSPDFRIAFQELLC  341
humanβ3  282  LLPLREHRALCTLGLIMGTFTLCWLPFFLANVLRALGGPSLVPGPAFLALNWLGYANSAFNPLIYCRSPDFRSAFRRLLC  361
tβtrunc  280  VMAMREHKALKTLGIIMGVFTLCWLPFFLVNIVNVFNRDL-VPDWLFVFFNWLGYANSAFNPIIYCRSPDFRKAFKRLLC  358
tβ3C     257  KFFLKEHKALKTLGIIMGTFTLCWLPFFIVNIVHVIQDDI-IPKYVYILLNWLGYVNSAFNPLIYCRSPDFRYAFQEL--  333
tβ4C     251  LLAIKEHKALKTLGIIMGTFTLCWLPFFVANIIKVFCRPL-VPDQLFLFLNWLGYVNSAFNPIIYCRSPDFRSAFRKLLC  329

humanβ1  393  CARRAARRRHATHGDRPRASGCLARPGPPP-SPGAASDDDDDDVVGATPPARLLEPWAGCNGGAAADSDSSLDEPCRPGF  471
humanβ2  342  LRRSSLKAYGNGYSSNGNTGEQSGYHVEQEKENKLLCED--------LPGT---EDFVGHQGTVPSDN---IDSPGRNCS  407
humanβ3  362  ---RCGRRL-----P-PEPCAAARPALFPSGVPAARSSPAQ-------P-------------------------------  394
tβtrunc  359  FPRKADRRLHAGGQPAPLPGGFISTLGSPEHSPGGT-------------------WSDCNGGTRGGSESSLEERHSKTS  418
tβ3C     334  ---------SNGRSDYNE--EDNGYPLAPDKACELLCEE------GSFPHP---EDFLHCKGTVPS---------G----  380
tβ4C     330  CPRRADRRLHAAPQD-PQHCSCA---FSPRGDPMEDSKAVD-------PGH-LREDSEVQGSGRREENASSHGGGHQQRP  397

humanβ1  472  ASESKV-------------------------------------------------------------  477
humanβ2  408  TNDSLL-------------------------------------------------------------  413
humanβ3  395  ----------------------------RLCQ-----RLDGASW-----GVS------------  408
tβtrunc  419  RSESKM-------------------------------------------------------------  483
tβ3C          -------------------------------------------------------------
tβ4C     398  LGECWLQ-----------------GMQSMLCE-----QLDEFTSTEMPAGPSV-----------  428
```

FIGURE A.2: Aminoacid sequence of the human and turkey β-adrenoceptors. Taken from Baker *et al.*[39]

Appendix B

Buffer composition

DEA buffer

used to measure SPAP activity

280 mM (16.36 g) NaCl

100 mM (100 mL) Diethanolamine

0.5 mM (0.102 g) MgCl2.6H2O

added distilled water up to 1 litre, used concentrated solution of HCl to achieve pH 9.85, *para*-nitrophenolphosphate was dissolved in DEA buffer to achieve a concentration of 100 mM. 500 μL PNPP were then added to 10 mL DEA buffer to develop the CRE-SPAP assay in 96-well plates.

Bibliography

[1] Edgar Jacoby, Rochdi Bouhelal, Marc Gerspacher, and Klaus Seuwen. The 7TM G-Protein-Coupled Receptor Target Family. *ChemMedChem*, 1(8):760–782, 2006.

[2] Christofer S Tautermann. GPCR structures in drug design, emerging opportunities with new structures. *Bioorg. Med. Chem. Lett.*, 24(17):4073–9, 2014.

[3] Sid Topiol and Michael Sabio. X-ray structure breakthroughs in the GPCR transmembrane region. *Biochem. Pharmacol.*, 78(1):11–20, 2009.

[4] Michael Sabio, Kenneth Jones, and Sid Topiol. Use of the X-ray structure of the beta2-adrenergic receptor for drug discovery. Part 2: Identification of active compounds. *Bioorg. Med. Chem. Lett.*, 18(20):5391–5395, 2008.

[5] Tony Warne, Maria J. Serrano-Vega, Jillian G. Baker, Rouslan Moukhametzianov, Patricia C. Edwards, Richard Henderson, Andrew G. W. Leslie, Christopher G. Tate, and Gebhard F. X. Schertler. Structure of a β1-adrenergic G-protein-coupled receptor. *Nature*, 454(7203):486–491, 2008.

[6] S. Blake Wachter and Edward M. Gilbert. Beta-Adrenergic Receptors, from Their Discovery and Characterization through Their Manipulation to Beneficial Clinical Application. *Cardiology*, 122(2):104–112, 2012.

[7] M P Stapleton. Sir James Black and propranolol. The role of the basic sciences in the history of cardiovascular pharmacology. *Tex. Heart Inst. J.*, 24(4):336–42, 1997.

[8] Steven R Post. Beta-Adrenergic receptors and receptor signaling in heart failure. *Annu. Rev. Pharmacol. Toxicol.*, 39:343–360, 1999.

[9] Aref Najafi, Vasco Sequeira, Diederik WD Kuster, and Jolanda van der Velden. β-adrenergic receptor signalling and its functional consequences in the diseased heart. *Eur. J. Clin. Invest.*, 46(4):362–374, apr 2016.

[10] R Seifert, K Wenzel-Seifert, U Gether, and B K Kobilka. Functional differences between full and partial agonists: evidence for ligand-specific receptor conformations. *J. Pharmacol. Exp. Ther.*, 297(3):1218–1226, 2001.

[11] Gordon S Lynch and James G Ryall. Role of β-Adrenoceptor Signaling in Skeletal Muscle: Implications for Muscle Wasting and Disease. *Physiol. Rev.*, 88(2):729–767, 2008.

[12] R.-P. Xiao, Pavel Avdonin, Y.-Y. Zhou, Heping Cheng, Shahab a Akhter, Thomas Eschenhagen, Robert J Lefkowitz, Walter J Koch, and Edward G Lakatta. Coupling of β2-Adrenoceptor to Gi Proteins and Its Physiological Relevance in Murine Cardiac Myocytes. *Circ. Res.*, 84(1):43–52, jan 1999.

[13] Tarik Hadi, Marina Barrichon, Pascal Mourtialon, Maeva Wendremaire, Carmen Garrido, Paul Sagot, Marc Bardou, and Frédéric Lirussi. Biphasic Erk1/2 activation sequentially involving Gs and Gi signaling is required in beta3-adrenergic receptor-induced primary smooth muscle cell proliferation. *Biochim. Biophys. Acta - Mol. Cell Res.*, 1833(5):1041–1051, 2013.

[14] Michael D. Pak and Peter H. Fishman. Anomalous Behavior of CGP 12177A on β1 -Adrenergic Receptors. *J. Recept. Signal Transduct.*, 16(1-2):1–23, jan 1996.

[15] Anish A Konkar, Zhengxian Zhu, and James G Granneman. Aryloxypropanolamine and catecholamine ligand interactions with the β1-adrenergic receptor: evidence for interaction with distinct conformations of β1-adrenergic receptors. *J. Pharmacol. Exp. Ther.*, 294(3):923–32, 2000.

[16] A R Kompa and R J Summers. Desensitization and resensitization of B1- and putative B4- adrenoceptor mediated responses occur in parallel in a rat model of cardiac failure. *Br. J. Pharmacol.*, 128(7):1399–1406, 1999.

[17] Mohamed Yassine Mallem, Gilles Toumaniantz, Sabrina Serpillon, Freddy Gautier, Marc Gogny, Jean-Claude Desfontis, and Chantal Gauthier. Impairment of the low-affinity state beta1-adrenoceptor-induced relaxation in spontaneously hypertensive rats. *Br. J. Pharmacol.*, 143(5):599–605, 2004.

[18] M L Vargas, J Hernandez, and A J Kaumann. Phosphodiesterase PDE3 blunts the positive inotropic and cyclic AMP enhancing effects of CGP12177 but not of noradrenaline in rat ventricle. *Br. J. Pharmacol.*, 147(2):158–163, 2006.

[19] A Kaumann, A B Semmler, and P Molenaar. The effects of both noradrenaline and CGP12177, mediated through human beta1 -adrenoceptors, are reduced by PDE3 in human atrium but PDE4 in CHO cells. *Naunyn-Schmiedebergs Arch. Pharmacol.*, 375(2):123–131, 2007.

[20] Il-Man Kim, Douglas G Tilley, Juhsien Chen, Natasha C Salazar, Erin J Whalen, Jonathan D Violin, and Howard a Rockman. Beta-blockers alprenolol and carvedilol stimulate beta-arrestin-mediated EGFR transactivation. *Proc. Natl. Acad. Sci. U. S. A.*, 105(38):14555–14560, 2008.

[21] Fadia A. Kamal, Joshua G. Travers, and Burns C. Blaxall. Embracing bias: B1-adrenergic receptor-biased ligands and nuclear mirna processing. *Circ. Res.*, 114(5):742–745, 2014.

[22] Segolene Galandrin and Michel Bouvier. Signaling Profiles of Beta-1 and Beta-2 Adrenergic Receptor Ligands toward Adenylyl Cyclase and Mitogen-Activated Protein Kinase Reveals the Pluridimensionality of Efficacy. *Mol. Pharmacol.*, 70(5):1575–1584, 2006.

[23] S Galandrin, G. Oligny-Longpre, Helene Bonin, K Ogawa, C. Gales, and Michel Bouvier. Conformational Rearrangements and Signaling Cascades Involved in Ligand-Biased Mitogen-Activated Protein Kinase Signaling through the 1-Adrenergic Receptor. *Mol. Pharmacol.*, 74(1):162–172, apr 2008.

[24] M. A. Soriano-Ursúa, J. G. Trujillo-Ferrara, J. A. Arias-Montaño, and R. Villalobos-Molina. Insights into a defined secondary binding region on β-adrenoceptors and putative roles in ligand binding and drug design. *Med. Chem. Commun.*, 6(6):991–1002, 2015.

[25] Yahong Sun, Nan Li, Mingliang Zhang, Wei Zhou, Jinghe Yuan, Rong Zhao, Jimin Wu, Zijian Li, Youyi Zhang, and Xiaohong Fang. Single-molecule imaging reveals the stoichiometry change of β 2 -adrenergic receptors by a pharmacological biased ligand. *Chem. Commun.*, 52(44):7086–7089, 2016.

[26] Roshanak Irannejad, Veronica Pessino, Delphine Mika, Bo Huang, Philip B. Wedegaertner, Marco Conti, and Mark Von Zastrow. Functional selectivity of GPCR-directed drug action through location bias. *Nat. Chem. Biol.*, 2017.

[27] Craig A. Nash, Wenhui Wei, Roshanak Irannejad, and Alan V. Smrcka. Golgi localized βi-adrenergic receptors stimulate golgi PI4P hydrolysis by PLCϵ to regulate cardiac hypertrophy. *Elife*, 8:1–22, 2019.

[28] Shin Isogai, Xavier Deupi, Christian Opitz, Franziska M. Heydenreich, Ching-Ju Tsai, Florian Brueckner, Gebhard F. X. Schertler, Dmitry B. Veprintsev, and Stephan Grzesiek. Backbone NMR reveals allosteric signal transduction networks in the β1-adrenergic receptor. *Nature*, 530(7589):237–241, 2016.

[29] Arthur Christopoulos and Terry Kenakin. G protein-coupled receptor allosterism and complexing. *Pharmacol. Rev.*, 54(2):323–374, 2002.

[30] P. Samama, S. Cotecchia, T. Costa, and R. J. Lefkowitz. A mutation-induced activated state of the β2-adrenergic receptor. Extending the ternary complex model. *J. Biol. Chem.*, 1993.

[31] Jack M. Weiss, Paul H. Morgan, Michael W. Lutz, and Terry P. Kenakin. The cubic ternary complex receptor-occupancy model I. Model description. *J. Theor. Biol.*, 1996.

[32] Jack M. Weiss, Paul H. Morgan, Michael W. Lutz, and Terry P. Kenakin. The cubic ternary complex receptor-occupancy model II. Understanding apparent affinity. *J. Theor. Biol.*, 1996.

[33] Jack M. Weiss, Paul H. Morgan, Michael W. Lutz, and Terry P. Kenakin. The cubic ternary complex receptor-occupancy model. III. Resurrecting efficacy. *J. Theor. Biol.*, 1996.

[34] Jillian G Baker, Ian P Hall, and Stephen J Hill. Agonist actions of "beta-blockers" provide evidence for two agonist activation sites or conformations of the human beta1-adrenoceptor. *Mol. Pharmacol.*, 63(6):1312–1321, 2003.

[35] Jillian G Baker. Evidence for a Secondary State of the Human B3- Adrenoceptor. *Mol. Pharmacol.*, 68(6):1645–1655, 2005.

[36] Alberto J. Kaumann and Peter Molenaar. The low-affinity site of the β1-adrenoceptor and its relevance to cardiovascular pharmacology. *Pharmacol. Ther.*, 118(3):303–336, 2008.

[37] Frauke Gorre and Hans Vandekerckhove. Beta-blockers: Focus on mechanism of action which beta-blocker, when and why? *Acta Cardiol.*, 65(5):565–570, 2010.

[38] James J DiNicolantonio and Daniel G Hackam. Carvedilol: a third-generation β-blocker should be a first-choice β-blocker. *Expert Rev. Cardiovasc. Ther.*, 10(1):13–25, 2012.

[39] Jillian G. Baker. A full pharmacological analysis of the three Turkey β-adrenoceptors and comparison with the human β-adrenoceptors. *PLoS One*, 5(11), 2010.

[40] Jillian G Baker. The selectivity of β-adrenoceptor agonists at human β1-, β2- and β3-adrenoceptors. *Br. J. Pharmacol.*, 160(5):1048–1061, 2010.

[41] Shirin S. Joseph, James A. Lynham, William H. Colledge, and Alberto J. Kaumann. Binding of (-)-[3H]-CGP12177 at two sites in recombinant human B1-adrenoceptors and interaction with B-blockers. *Naunyn. Schmiedebergs. Arch. Pharmacol.*, 369(5):525–532, 2004.

[42] Paul M. Vanhoutte and Yuansheng Gao. Beta blockers, nitric oxide, and cardiovascular disease. *Curr. Opin. Pharmacol.*, 13(2):265–273, 2013.

[43] Vadim Cherezov, Daniel M Rosenbaum, Michael a Hanson, Søren G F Rasmussen, Foon Sun Thian, Tong Sun Kobilka, Hee-jung Choi, Peter Kuhn, William I Weis, Brian K Kobilka, and Raymond C Stevens. High-Resolution Crystal Structure of an Engineered Human b2 -Adrenergic G Protein-Coupled Receptor. *Science (80-.).*, 318(November):1258–1265, 2007.

[44] Michiel J M Niesen, Supriyo Bhattacharya, Reinhard Grisshammer, Christopher G. Tate, and Nagarajan Vaidehi. Thermostabilization of the β1-adrenergic receptor correlates with increased entropy of the inactive state. *J. Phys. Chem. B*, 117(24):7283–7291, 2013.

[45] Rouslan Moukhametzianov, Tony Warne, Patricia C Edwards, Maria J Serrano-Vega, Andrew G W Leslie, Christopher G Tate, and Gebhard F X Schertler. Two distinct conformations of helix 6 observed in antagonist-bound structures of a beta1-adrenergic receptor. *Proc. Natl. Acad. Sci. U. S. A.*, 108(20):8228–32, 2011.

[46] Juan A. Ballesteros and Harel Weinstein. Integrated methods for the construction of three-dimensional models and computational probing of structure-function relations in G protein-coupled receptors. *Methods Neurosci.*, 25(C):366–428, 1995.

[47] Tony Warne, Rouslan Moukhametzianov, Jillian G Baker, Rony Nehmé, Patricia C Edwards, Andrew G W Leslie, Gebhard F X Schertler, and Christopher G Tate. The structural basis for agonist and partial agonist action on a β(1)-adrenergic receptor. *Nature*, 469(7329):241–4, 2011.

[48] Tony Warne, Patricia C. Edwards, Andrew G.W. Leslie, and Christopher G. Tate. Crystal Structures of a Stabilized β1-Adrenoceptor Bound to the Biased Agonists Bucindolol and Carvedilol. *Structure*, 20(5):841–849, may 2012.

[49] Jennifer L. Miller-Gallacher, Rony Nehmé, Tony Warne, Patricia C. Edwards, Gebhard F X Schertler, Andrew G W Leslie, and Christopher G. Tate. The 2.1 Å Resolution Structure of Cyanopindolol-Bound β1-Adrenoceptor Identifies an Intramembrane Na+ Ion that Stabilises the Ligand-Free Receptor. *PLoS One*, 9(3):e92727, mar 2014.

[50] Tony Warne, Patricia C. Edwards, Andrew S. Dorfe, Andrew G.W. Leslie, and Christopher G. Tate. Molecular basis for high-affinity agonist binding in GPCRs. *Science (80-.).*, 778(May):775–778, 2019.

[51] Christoph Maack. Partial agonist activity of Bucindolol is dependent on the activation state of the Human β1-Adrenergic receptor. *Circulation*, 108(3):348–353, jul 2003.

[52] Els Pardon, Cecilia Betti, Toon Laeremans, Florent Chevillard, Karel Guillemyn, Peter Kolb, Steven Ballet, and Jan Steyaert. Nanobody-Enabled Reverse Pharmacology on G-Protein-Coupled Receptors. *Angew. Chemie - Int. Ed.*, 2018.

[53] Layara Akemi Abiko, Anne Grahl, and Stephan Grzesiek. High Pressure Shifts the β1-Adrenergic Receptor to the Active Conformation in the Absence of G Protein. *J. Am. Chem. Soc.*, 141(42):16663–16670, 2019.

[54] Jillian G. Baker, Richard G.W. Proudman, and Christopher G. Tate. The pharmacological effects of the thermostabilising (m23) mutations and intra and extracellular (β36) deletions essential for crystallisation of the turkey β-adrenoceptor. *Naunyn. Schmiedebergs. Arch. Pharmacol.*, 2011.

[55] J R Blinks. Archivesof Pharmacology fi-Adrenoceptor Blocking Agents as Partial Agonists in Isolated Heart Muscle :. 248:237–248, 1980.

[56] M Staehelin, P Simons, K Jaeggi, and N Wigger. CGP-12177. A hydrophilic beta-adrenergic receptor radioligand reveals high affinity binding of agonists to intact cells. *J. Biol. Chem.*, 258(6):3496–502, 1983.

[57] Michael Walter, Horst Lemoine, and Alberto Julio Kaumann. Stimulant and blocking effects of optical isomers of pindolol on the sinoatrial node and trachea of guinea pig. Role of β-adrenoceptor subtypes in the dissociation between blockade and stimulation. *Naunyn. Schmiedebergs. Arch. Pharmacol.*, 327(2):159–175, 1984.

[58] H Lemoine, B Ehle, and A J Kaumann. Direct labelling of beta 2-adrenoceptors. Comparison of binding potency of 3H-ICI 118,551 and blocking potency of ICI 118,551. *Naunyn. Schmiedebergs. Arch. Pharmacol.*, 331(1):40–51, oct 1985.

[59] Anish A Konkar, Zhengxian Zhu, and James G Granneman. Aryloxypropanolamine and catecholamine ligand interactions with the β1-adrenergic receptor: evidence for interaction with distinct conformations of β1-adrenergic receptors. *J. Pharmacol. Exp. Ther.*, 294(3):923–32, 2000.

[60] Jillian G Baker. Site of action of β-ligands at the human β1-adrenoceptor. *J. Pharmacol. Exp. Ther.*, 313(3):1163–1171, 2005.

[61] Barbara Malinowska, Katarzyna Kieć-Kononowicz, Karsten Flau, Grzegorz Godlewski, Hanna Kozłowska, Markus Kathmann, and Eberhard Schlicker. Atypical cardiostimulant beta-adrenoceptor in the rat heart: stereoselective antagonism

by bupranolol but lack of effect by some bupranolol analogues. *Br. J. Pharmacol.*, 139(8):1548–54, 2003.

[62] Agnieszka Zakrzeska, Eberhard Schlicker, Grzegorz Kwolek, Hanna Kozłowska, and Barbara Malinowska. Positive inotropic and lusitropic effects mediated via the low-affinity state of beta1-adrenoceptors in pithed rats. *Br. J. Pharmacol.*, 146(5):760–8, 2005.

[63] Martin D Lowe, James a Lynham, Andrew a Grace, and Alberto J Kaumann. Comparison of the affinity of beta-blockers for two states of the beta 1-adrenoceptor in ferret ventricular myocardium. *Br. J. Pharmacol.*, 135(2):451–61, 2002.

[64] Jillian G Baker, Richard G W Proudman, Nicola C Hawley, Peter M Fischer, and Stephen J Hill. Role of key transmembrane residues in agonist and antagonist actions at the two conformations of the human beta1-adrenoceptor. *Mol. Pharmacol.*, 74(5):1246–60, 2008.

[65] Shirin S Joseph, William H Colledge, and Alberto J Kaumann. Aspartate138 is required for the high-affinity ligand binding site but not for the low-affinity binding site of the beta1-adrenoceptor. *Naunyn. Schmiedebergs. Arch. Pharmacol.*, 370(3):223–6, 2004.

[66] Jillian G Baker, Richard G W Proudman, and Stephen J Hill. Identification of key residues in transmembrane 4 responsible for the secondary, low-affinity conformation of the human β1-adrenoceptor. *Mol. Pharmacol.*, 85(5):811–29, 2014.

[67] Mohammed Amine Abdelkrim, Mohamed Yassine Mallem, Gérard Chatagnon, Marc Gogny, Jean-Claude Desfontis, and Jacques Noireaud. Autoantibodies against cardiac β1 adrenoceptor do not affect the low-affinity state β1 adrenoceptor-mediated inotropy in rat cardiomyocytes. *Can. J. Physiol. Pharmacol.*, 90(4):407–414, 2012.

[68] Mark Soave, Gabriella Cseke, Catherine J. Hutchings, Alastair J.H. Brown, Jeanette Woolard, and Stephen J. Hill. A monoclonal antibody raised against a thermo-stabilised β1-adrenoceptor interacts with extracellular loop 2 and acts as a negative allosteric modulator of a sub-set of β1-adrenoceptors expressed in stable cell lines. *Biochem. Pharmacol.*, 147:38–54, 2018.

[69] Jianyun Huang, Shuai Chen, J Jillian Zhang, and Xin-Yun Huang. Crystal structure of oligomeric β1-adrenergic G protein-coupled receptors in ligand-free basal state. *Nat. Struct. Mol. Biol.*, 20(4):419–25, 2013.

[70] S S Joseph, J a Lynham, a a Grace, W H Colledge, and a J Kaumann. Markedly reduced effects of (-)-isoprenaline but not of (-)-CGP12177 and unchanged affinity

of β-blockers at Gly389-β1-adrenoceptors compared to Arg389-β1-adrenoceptors. *Br. J. Pharmacol.*, 142(1):51–6, 2004.

[71] Jillian G Baker, Richard G W Proudman, and Stephen J Hill. Impact of Polymorphic Variants on the Molecular Pharmacology of the Two-Agonist Conformations of the Human β1-Adrenoceptor. *PLoS One*, 8(11):e77582, 2013.

[72] Ali Salahpour, Stéphane Angers, and Michel Bouvier. Functional Significance of Oligomerization of G-protein-coupled Receptors. *Trends Endocrinol. Metab.*, 11(5):163–168, jul 2000.

[73] K. Gherbi, L. T. May, J. G. Baker, S. J. Briddon, and S. J. Hill. Negative cooperativity across β1-adrenoceptor homodimers provides insights into the nature of the secondary low-affinity CGP 12177 β1-adrenoceptor binding conformation. *FASEB J.*, 29(7):2859–2871, 2015.

[74] K Gherbi, S J Briddon, and S J Hill. Detection of the secondary, low-affinity β 1 -adrenoceptor site in living cells using the fluorescent CGP 12177 derivative BODIPY-TMR-CGP. *Br. J. Pharmacol.*, 171(23):5431–5445, dec 2014.

[75] H. Heithier, D. Hallmann, F. Boege, H. Reilander, C. Dees, K.A. Jaeggi, D. Arndt-Jovin, T.M. Jovin, and E.J.M. Helmreich. Synthesis and properties of fluorescent β-adrenoceptor ligands. *Biochemistry*, 1994.

[76] D Sarsero, P Molenaar, a J Kaumann, and N S Freestone. Putative β4 adrenoceptors in rat ventricle mediate increases in contractile force and cell Ca2+: comparison with atrial receptors and relationship to (-)-[3H]-CGP 12177 binding. *Br. J. Pharmacol.*, 128(7):1445–1460, 1999.

[77] Eberhard Schlicker, Anna Pedzinska-Betiuk, Hanna Kozlowska, Natalia Szkaradek, Dorota Zelaszczyk, Marta Baranowska-Kuczko, Katarzyna Kiec-Kononowicz, Henryk Marona, and Barbara Malinowska. MH-3: Evidence for non-competitive antagonism towards the low-affinity site of beta1-adrenoceptors. *Naunyn. Schmiedebergs. Arch. Pharmacol.*, 387(8):743–752, 2014.

[78] D. Zelaszczyk, H. Kozlowska, U. Baranowska, M. Baranowska, A. Reutelsterz, K. Kiec-Kononowicz, B. Malinowska, and Eberhard Schlicker. Four close bupranolol analogues are antagonists at the low-affinity state of B1-adrenoceptors. *J. Physiol. Pharmacol.*, 60(1):51–60, 2009.

[79] Helen Kiriazis, Niquita Tugiono, Qi Xu, Xiao Ming Gao, Nicole L. Jennings, Ziqui Ming, Yidan Su, Paul Klenowski, Roger J. Summers, Alberto Kaumann, Peter Molenaar, and Xiao Jun Du. Chronic activation of the low affinity site of β1-

adrenoceptors stimulates haemodynamics but exacerbates pressure-overload cardiac remodelling. *Br. J. Pharmacol.*, 170(2):352–365, 2013.

[80] Cheng Yung-Chi and William H. Prusoff. Relationship between the inhibition constant (KI) and the concentration of inhibitor which causes 50 per cent inhibition (I50) of an enzymatic reaction. *Biochem. Pharmacol.*, 1973.

[81] Jillian G Baker. The selectivity of β -adrenoceptor antagonists at the human β 1, β 2 and β 3 adrenoceptors. *Br. J. Pharmacol.*, 2005.

[82] Stephen J. Hill, Jillian G. Baker, and Stephen Rees. Reporter-gene systems for the study of G-protein-coupled receptors, 2001.

[83] J McDonnell, M L Latif, E S Rees, N J Bevan, and S J Hill. Influence of receptor number on the stimulation by salmeterol of gene transcription in CHO-K1 cells transfected with the human beta2-adrenoceptor. *Br. J. Pharmacol.*, 125(4):717–726, 1998.

[84] Jillian G Baker. The selectivity of beta-adrenoceptor agonists at human beta1-, beta2- and beta3-adrenoceptors. *Br. J. Pharmacol.*, 2010.

[85] R. P. Stephenson. A modification of receptor theory. *Br. J. Pharmacol. Chemother.*, 11(4):379–393, 1956.

[86] Milton L Hoefle, Stephen G Hastings, Robert F Meyer, Ruth M Corey, Ann Holmes, and Charlotte D Stratton. Cardioselective beta-Adrenergic Blocking Agents. 1. 1-[(3,4-Dimethoxyphenethyl)amino] -3-aryloxy-2-propanol. *J. Med.*, 18(2):2–6, 1975.

[87] Jeroen Rintjema, Roel Epping, Giulia Fiorani, Eddy Martín, Eduardo C. Escudero-Adán, and Arjan W. Kleij. Substrate-Controlled Product Divergence: Conversion of CO2 into Heterocyclic Products. *Angew. Chemie Int. Ed.*, 55(12):3972–3976, mar 2016.

[88] V R Gaertner. Alkyl-2,3-epoxypropylamines. Cyclodimerization and related eight-membered ring closures. *Tetrahedron Lett.*, 23(3):2123–2136, 1967.

[89] Ana M Martin Castro. Claisen rearrangement over the past nine decades. *Chem. Rev.*, 104(6):2939–3002, 2004.

[90] Kenichi Harada, Chiharu Arioka, Akina Miyakita, Miwa Kubo, and Yoshiyasu Fukuyama. Efficient synthesis of neurotrophic honokiol using Suzuki-Miyaura reactions. *Tetrahedron Lett.*, 55(43):6001–6003, 2014.

[91] T Sato Baker, J., Warne, T., Brown, G.A., Leslie, A.G.W., Congreve, M., Tate, C.G. Pharmacological analysis and structure determination of 7-methylcyanopindolol-bound β1-adrenergic receptor. *Mol. Pharmacol.*, 88:1024–1034, 2015.

[92] Dietmar Weichert and Peter Gmeiner. Covalent Molecular Probes for Class A G Protein-Coupled Receptors: Advances and Applications. *ACS Chem. Biol.*, 10(6):1376–1386, 2015.

[93] Manuela Jörg and Peter J. Scammells. Guidelines for the Synthesis of Small-Molecule Irreversible Probes Targeting G Protein-Coupled Receptors. *ChemMedChem*, 11(14):1488–1498, 2016.

[94] Henrik G. Dohlman, Marc G. Caron, Catherine D. Strader, Nourdine Amlaiky, and Robert J. Lefkowitz. Identification and Sequence of a Binding Site Peptide of The β2-Adrenergic Receptor. *Biochemistry*, 27(6):1813–1817, 1988.

[95] Malgorzata D. Deyrup, Phillip G. Greco, Deborah H. Otero, Donn M. Dennis, Craig H. Gelband, and Stephen P. Baker. Irreversible binding of a carbostyril-based agonist and antagonist to the β-adrenoceptor in DDT1 MF-2 cells and rat aorta. *Br. J. Pharmacol.*, 124(1):165–175, 1998.

[96] Daniel M. Rosenbaum, Cheng Zhang, Joseph A. Lyons, Ralph Holl, David Aragao, Daniel H. Arlow, Saren G.F. Rasmussen, Hee Jung Choi, Brian T. Devree, Roger K. Sunahara, Pil Seok Chae, Samuel H. Gellman, Ron O. Dror, David E. Shaw, William I. Weis, Martin Caffrey, Peter Gmeiner, and Brian K. Kobilka. Structure and function of an irreversible agonist-β2 adrenoceptor complex. *Nature*, 469(7329):236–242, 2011.

[97] J. Pitha, J. Zjawiony, N. Nasrin, R. J. Lefkowitz, and M. G. Caron. Potent beta-adrenergic antagonist possessing chemically reactive group. *Life Sci.*, 27(19):1791–1798, 1980.

[98] J. Pitha, B. A. Hughes, J. W. Kusiak, E. M. Dax, and S. P. Baker. Regeneration of β-adrenergic receptors in senescent rats: A study using an irreversible binding antagonist. *Proc. Natl. Acad. Sci. U. S. A.*, 79(14 I):4424–4427, 1982.

[99] Tobias Schwalbe, Harald Huebner, and Peter Gmeiner. Development of covalent antagonists for β1- and β2-adrenergic receptors. *Bioorganic Med. Chem.*, 27(13):2959–2971, 2019.

[100] Neil J. Freedman, Stephen B. Liggett, Douglas E. Drachman, Gang Pei, Marc G. Caron, and Robert J. Lefkowitz. Phosphorylation and desensitization of the human

β1-adrenergic receptor: Involvement of G protein-coupled receptor kinases and cAMP-dependent protein kinase, 1995.

[101] S. K F Wong, C. Slaughter, A. E. Ruoho, and E. M. Ross. The catecholamine binding site of the beta-adrenergic receptor is formed by juxtaposed membrane-spanning domains. *J. Biol. Chem.*, 263(17):7925–7928, 1988.

[102] Y. Eshdat, M. P. Chapot, and A. D. Strosberg. Chemical characterization of ligand binding site fragments from turkey β-adrenergic receptor. *FEBS Lett.*, 246(1-2):166–170, 1989.

[103] Nourdine Amlaiky and Gerard Leclerc. Synthesis and irreversible β-adrenergic blockade with a bromoacetamido derivative of betaxolol. *J. Pharm. Sci.*, 74(10):1117–1119, 1985.

[104] V. Homburger, H. Gozlan, R. Bouhelal, M. Lucas, and J. Bockaert. Irreversible blockade of β-adrenergic receptors with a bromoacetyl derivative of pindolol. *Naunyn. Schmiedebergs. Arch. Pharmacol.*, 328(3):279–287, 1985.

[105] Stephen P Baker and Andras Liptak. Irreversible Inactivation of the Beta-adrenoreceptor by a Partial Agonist. *J. Biol. Chem.*, 260(24):15820–15828, 1985.

[106] Andras Liptak, John W. Kusiak, and Josef Pitha. Alkylating β-Blockers: Activity of Isomeric Bromoacetyl Alprenolol Menthanes. *J. Med. Chem.*, 28(11):1699–1703, 1985.

[107] K. E.J. Dickinson, S. L. Heald, P. W. Jeffs, R. J. Lefkowitz, and M. G. Caron. Covalent labeling of the β-adrenergic ligand-binding site with para-(bromoacetamidyl)benzylcarazolol. A highly potent β-adrenergic affinity label. *Mol. Pharmacol.*, 27(5):499–506, 1985.

[108] Kelly M. Standifer, Josef Pitha, and Stephen P. Baker. Carbostyril-based beta-adrenergic agonists: evidence for long lasting or apparent irreversible receptor binding and activation of adenylate cyclase activity in vitro. *Naunyn. Schmiedebergs. Arch. Pharmacol.*, 339(1):129–137, 1989.

[109] E. Krstew, G. A. MCPherson, E. Malta, P. Molenaar, and C. Raper. Is Ro 03–7894 an irreversible antagonist at β-adrenoceptor sites? *Br. J. Pharmacol.*, 82(2):501–508, 1984.

[110] Amy Grunbeck and Thomas P. Sakmar. Probing G protein-coupled receptor - Ligand interactions with targeted photoactivatable cross-linkers. *Biochemistry*, 52(48):8625–8632, 2013.

[111] S. M. Wrenn and C. J. Homcy. Photoaffinity label for the β-adrenergic receptor: Synthesis and effects on isoproterenol-stimulated adenylate cyclase. *Proc. Natl. Acad. Sci. U. S. A.*, 77(8):4449–4453, 1980.

[112] T N Lavin, S L Heald, P W Jeffs, R G Shorr, R J Lefkowitz, and M G Caron. Photoaffinity labeling of the beta-adrenergic receptor. *J. Biol. Chem.*, 256(22):11944–50, nov 1981.

[113] W. Burgermeister, M. Hekman, and E. J.M. Helmreich. Photoaffinity labeling of the β-adrenergic receptor with azide derivatives of iodocyanopindolol. *J. Biol. Chem.*, 257(9):5306–5311, 1982.

[114] Wolfgang Burgermeister, Michael Nassal, Theodor Wieland, and Ernst J.M. Helmreich. A carbene-generating photoaffinity probe for beta-adrenergic receptors. *BBA - Biomembr.*, 729(2):219–228, 1983.

[115] Jillian G Baker, Luke a Adams, Karolina Salchow, Shailesh N Mistry, Richard J Middleton, Stephen J Hill, and Barrie Kellam. Synthesis and characterization of high-affinity 4,4-difluoro-4-bora-3a,4a-diaza-s-indacene-labeled fluorescent ligands for human β-adrenoceptors. *J. Med. Chem.*, 54:6874–87, 2011.

[116] Alberto J. Kaumann, Frédéric Preitner, Doreen Sarsero, Peter Molenaar, Jean Pierre Revelli, and Jean Paul Giacobino. (-)-CGP 12177 causes cardiostimulation and binds to cardiac putative β4-adrenoceptors in both wild-type and β3-adrenoceptor knockout mice. *Mol. Pharmacol.*, 53(4):670–675, 1998.

[117] Ron O. Dror, Albert C. Pan, Daniel H. Arlow, David W. Borhani, Paul Maragakis, Yibing Shan, Huafeng Xu, and David E. Shaw. Pathway and mechanism of drug binding to G-protein-coupled receptors. *Proc. Natl. Acad. Sci.*, 108(32):13118–13123, aug 2011.

[118] Birgit I. Gaiser, Mia Danielsen, Emil Marcher-Rørsted, Kira Røpke Jørgensen, Tomasz M. Wróbel, Mikael Frykman, Henrik Johansson, Hans Bräuner-Osborne, David E. Gloriam, Jesper Mosolff Mathiesen, and Daniel Sejer Pedersen. Probing the Existence of a Metastable Binding Site at the β2-Adrenergic Receptor with Homobivalent Bitopic Ligands. *J. Med. Chem.*, 62(17):7806–7839, 2019.

[119] Marvin a. Soriano-Ursúa, José G. Trujillo-Ferrara, José Correa-Basurto, and Santiago Vilar. Recent structural advances of β1 and β2 adrenoceptors yield keys for ligand recognition and drug design. *J. Med. Chem.*, 56(21):8207–8223, 2013.

[120] O. Arunlakshana and H. O. Schild. Some quantitative uses of drug antagonists. *Br. J. Pharmacol. Chemother.*, 14(1):45–58, 1959.

[121] Karolina Gherbi. *Investigating the nature of the secondary binding site of the human β1-adrenoceptor using fluorescent ligands and confocal microscopy.* PhD thesis, 2013.